Czech University of Life Sciences, Prague
Faculty of Forestry and Wood Sciences

Ph.D. Thesis

"Essential Biodiversity Variables (EBVs) for Monitoring Forest Biodiversity Change in Ghana: A Remote Sensing and Field-Based Approach"

Ph.D. Student: Elisha Njomaba, MSc.

Study Program: Applied Geoinformatics and Remote Sensing in Forestry

Department: Forest Management and Remote Sensing

Supervisor: Assoc. Prof. Peter Surový, Ph.D.

Author's Declaration

I hereby declare that this Doctoral Thesis ("Essential Biodiversity Variables (EBVs) for Monitoring Forest Biodiversity Change in Ghana: A remote sensing and Field-Based Approach") is my own work and quoted only according to the references listed within. Neither part of this thesis has been submitted to fulfill the requirements for a degree from any other institution. This thesis was written under the guidance of Assoc. Prof. Peter Surový, Ph.D.

I agree to the publication of the thesis according to Act No. 111/1998 Coll. On universities as amended, regardless of the outcome of their defense.

Prague 2025 Signature.……

Elisha Njomaba

Acknowledgments

Psalm 124:1 "*If it had not been for the Lord on our side, now let Israel say*".

I give all glory, honor, and profound gratitude to God Almighty for His unending favor, grace, and mercy upon my life, and for making this chapter of my journey successful.

I am deeply grateful to my supervisor, Prof. Peter Surový, Ph.D., for the opportunity, trust, and invaluable guidance he provided throughout my doctoral studies. My acknowledgment also extends to the Czech University of Life Sciences, Prague, particularly through the Chist-era, FORESTin3D project, IGA/FLD/A_11_23 (Internal grant number: 43140/1312/3189), and Project TH74010001, funded by the Technological Agency of the Czech Republic, whose financial and material support made my studies and manuscript publications possible.

I am equally grateful to the Food and Agriculture Organization of the United Nations (FAO) and the Geospatial Unit of the Land and Water Division for the collaboration and the opportunity to undertake my internship, which greatly enriched my academic and professional experience.

I sincerely thank my family, the Njomabas, for their unwavering prayers and support.

I also appreciate Mr. James Nana Ofori, Miss Araba Manful Owusu, and Mr. Ben Emunah Aikins for their steadfast encouragement and prayers throughout this journey.

My heartfelt gratitude goes to the Church of Pentecost, Prague Assembly, for their emotional and spiritual support and for providing me with a platform to grow spiritually while pursuing this academic milestone.

Finally, I am grateful to Dr. Reginald Tang Guuroh and the staff of the Bobiri Forest Reserve for their significant contribution to my data collection.

CZECH UNIVERSITY OF LIFE SCIENCES PRAGUE

Faculty of Forestry and Wood Sciences

DISSERTATION THESIS TOPIC

Author of thesis:	Elisha Njomaba, MSc
Study programme:	Applied geoinformatics and remote sensing in forestry
Thesis supervisor:	doc. Ing. Peter Surový, PhD.
Supervising department:	Department of Forest Management and Remote Sensing
Language of a thesis:	English

Thesis title:

Essential Biodiversity Variables (EBVs) for Monitoring Forest Biodiversity Change in Ghana: A Remote Sensing and Field-Based Approach

Objectives of thesis:

The overall objectives of this study are Essential Biodiversity Variables that are key to forest biodiversity changes and their implications for forest management. The specific objectives, however, are;

1. To assess the potential for the adoption of land cover standards by preparing a national legend for Ghana as a pilot study following the standards ISO 19144-2, preparing a land cover dataset of Ghana, and engaging experts in Ghana to document the challenges and the opportunities of the adoption of standards for sustainable resource management.

2. To assess the relationship between spectral variability from PlanetScope imagery and field-measured species diversity indices, with the aim of evaluating spectral variability as a proxy for biodiversity monitoring.

3. To investigate the direct effect of climate change (aridity) on aboveground biomass (AGB), mediated through forest fragmentation.

4. To map the spatial distribution and estimate the population abundance of dominant forest tree species in Ghana.

Methodology:

1. For assessing the potential for the adoption of land cover standards, a combination of stakeholder engagement with national agencies, survey designs to engage experts, and the use of the FAO-developed ISO 19144-2 Land Cover Meta Language (LCML) is adopted. Training and validation data are collected via high-resolution satellite imagery interpretation, supported by local knowledge. A multi-sensor dataset combining Sentinel-2 optical imagery, Sentinel-1 SAR data, and ancillary variables is prepared. Key spectral and texture predictors are derived over a one-year period to capture seasonal variability.
Land cover classification is performed using a Random Forest algorithm with optimized parameters. Model accuracy was assessed using standard metrics on independent test samples. Additionally, a stakeholder survey is used to evaluate the awareness and adoption of land cover standards.

2. For analyzing the relationship between species diversity and spectral variability in Bobiri Forest Reserve, field data were collected from 35 systematically placed plots (20 m × 50 m), spaced at least 200 m apart to avoid overlap. Within each plot, adult trees (DBH ≥ 5 cm) were identified, measured for diameter and height, and geolocated using GPS devices. Species identification was verified with taxonomists and cross-checked using the World Flora Online database. Four diversity indices—Species Richness (S), Shannon-Wiener (H′), Simpson (D2), and Evenness (J′)—were calculated per plot.
High-resolution PlanetScope imagery (3 m) covering May 2023 was accessed under

a research license. Four mosaicked scenes were preprocessed (geometric, radiometric, and atmospheric corrections) and aligned with field sampling. Spectral data were extracted using a 3 × 3-pixel mean window for each plot.
Stepwise linear regression was used to analyze the relationship between spectral data and diversity indices. Predictor variables included PlanetScope bands and vegetation indices (NDVI, EVI, SAVI, SRI, NDRE). Model performance was assessed using AIC, RMSE, and R^2, while Pearson correlation coefficients identified key spectral predictors. Bands 2 (blue) and 6 (red) emerged as the most significant predictors for species richness and the Shannon-Wiener index.

3. To investigate the effects of climate change (aridity) on aboveground biomass (AGB), mediated by forest fragmentation, a multi-source dataset is compiled and analyzed across Ghana. Vegetation occurrence data representing tree species are obtained from the Global Biodiversity Information Facility (GBIF), while plot-level biomass data were derived from ESA's global AGB dataset. The AGB raster was subset using Ghana's national boundary and matched to tree species plots by creating 20 m radius circular buffers around each occurrence point. This buffer-based extraction approach enabled plot-level assessment of AGB values.
Aridity data is acquired from the Global Aridity Index (Global-AI), which provides a ratio of annual precipitation to potential evapotranspiration. Plot-level aridity values are extracted corresponding to each vegetation occurrence location. To quantify forest fragmentation, six landscape metrics—Number of Patches (NP), Largest Patch Index (LSI), Mean Shape Index (MSI), Edge Density (ED), and Mean Patch Area (Area_MN) are computed using the landscapemetrics package in R. These metrics are also extracted at the plot level for each vegetation point. The direct effects of aridity on AGB are assessed using Analysis of Variance (ANOVA), with statistical significance evaluated using p-values and standard performance metrics. To evaluate the indirect effects of aridity on AGB mediated by fragmentation, a Partial Least Squares Structural Equation Modeling (PLS-SEM) approach is employed. Finally, to assess the relative contributions of individual fragmentation metrics to AGB variation, a Generalized Additive Model (GAM) is used, capturing nonlinear relationships and quantifying the influence of each fragmentation factor.

4. To map the spatial distribution and estimate the population abundance of dominant forest tree species in Ghana, species distribution modelling (SDM) techniques are implemented in R using Sentinel-2 derived vegetation indices and environmental variables. Tree occurrence data (species name and GPS coordinates) are combined with environmental predictors, including Sentinel-2 indices (NDVI, NDRE, EVI), climate data (temperature and precipitation from WorldClim), the Global Aridity Index, topographic variables (elevation and slope from SRTM), and land cover data.
All raster layers are reprojected to a common coordinate system, resampled to a common resolution, and cropped to the Ghana boundary. Environmental values are extracted at each tree occurrence point and combined with species presence or abundance to create a modelling dataset.
Modelling is conducted using presence-only and abundance-based methods. Presence-only data are modelled using MaxEnt, while abundance models use Random Forest, Poisson GLM, Negative Binomial, and Boosted Regression Tree algorithms. Model performance is evaluated using AUC, Kappa, and TSS for classification models, and RMSE, MAE, and R^2 for regression models. Spatial predictions are generated across the stacked raster layers to produce maps of species distribution and abundance. Final outputs are visualized.

The proposed extent of the thesis: 80-90

Keywords: remote sensing, Ghana, biodiversity, Essential Biodiversity Variables, land cover

Recommended information sources:

1. Anderson, J.; Hardy, E.; Roach, J.; Witmer, R. A Land Use and Land Cover Classification System for Use with Remote Sensor Data; USGS Publications Warehouse: Washington, DC, USA, 2001; Volume 2001
2. Arantzazu L Luzuriaga, Pablo Ferrandis, Joel Flores, Adrián Escudero, Effect of aridity on species assembly in gypsum drylands: a response mediated by the soil affinity of species, AoB PLANTS, Volume 12, Issue 3, June 2020

3. Arekhi, M.; Yılmaz, O.Y.; Yılmaz, H.; Akyüz, Y.F. Can tree species diversity be assessed with Landsat data in a temperate forest? Environ. Monit. Assess. 2017, 189, 586.
4. Baloloy, A.B.; Blanco, A.C.; Candido, C.G.; Argamosa, R.J.L.; Dumalag, J.B.L.C.; Dimapilis, L.L.C.; Paringit, E.C. Estimation of mangrove forest aboveground biomass using multispectral bands, vegetation indices and biophysical variables derived from optical satellite imageries: Rapideye, planetscope and sentinel-2. ISPRS Ann. Photogramm. Remote Sens. Spat. Inf. Sci. 2018, 4, 29–36.
5. Conchedda, G.; Tubiello, F.N. Land Cover Statistics Global, Regional and Country Trends; FAO: Rome, Italy, 2021
6. Ghana Forestry Commission. Framework for National Forest Monitoring System; Ghana Forestry Commission: Accra, Ghana, 2018.
7. Green, J.M.H., Larosa, C., Burgess, N.D., Balmford, A., Johnston, A., Mbilinyi, B.P., Platts, P.J. and Coad, L. (2013) Deforestation in an African biodiversity hotspot: Extent, variation and the effectiveness of protected areas. Biological Conservation 164, 62-172
8. Chao, A.; Wang, Y.T.; Jost, L. Entropy and the species accumulation curve: A novel entropy estimator via discovery rates of new species. Methods Ecol. Evol. 2013, 4, 1091–1100.
9. John, A.; Ong, J.; Theobald, E.J.; Olden, J.D.; Tan, A.; Hillerislambers, J. Detecting Montane Flowering Phenology with CubeSat Imagery. Remote Sens. 2020
10. Madonsela, S.; Cho, M.A.; Ramoelo, A.; Mutanga, O.; Naidoo, L. Estimating tree species diversity in the savannah using NDVI and woody canopy cover. Int. J. Appl. Earth Obs. Geoinf. 2018, 66, 106–115.
11. Maskell, G.; Chemura, A.; Nguyen, H.; Gornott, C.; Mondal, P. Remote Sensing of Environment Integration of Sentinel Optical and Radar Data for Mapping Smallholder Coffee Production Systems in Vietnam. Remote Sens. Environ. 2021
12. Mutowo, G.; Murwira, A. Relationship between remotely sensed variables and tree species diversity in savanna woodlands of Southern Africa. Int. J. Remote Sens. 2012, 33, 6378–6402.
13. Skidmore, A., Pettonelli, N., Coops, N., Geller, G.N., Hansen, M., Lucas, R., Mucher, C.A., O'connor, B., Paganini, M., Pereira, H.M., Scheepman, M., Turner, W., Wang, T. and Wegmann, M. (2015) Agree on biodiversity metrics to track from space. Nature 523(7561): 403-405
14. Soininen, J.; Passy, S.; Hillebrand, H. The relationship between species richness and evenness: A meta-analysis of studies across aquatic ecosystems. Oecologia 2012, 169, 803–809.
15. Vihervaara, P., Auvinen, A. P., Mononen, L., Törmä, M., Ahlroth, P., Anttila, S., Bottcher, K., Forsius, M., Heino, J., Koskelainen, M., Kuussari, M., Meissner, K., Ojala, O., Tuominen, S., Viitasalo, M. & Virkkala, R. (2017). How Essential Biodiversity Variables and remote sensing can help national biodiversity monitoring. Global Ecology and Conservation, 10, 43-59.

Expected date: 2024/25 SS - FFWS - State Doctoral Examinations

Electronically approved: 20/05/2025
doc. Ing. Peter Surový, PhD.
Head of department

Electronically approved: 20/05/2025
doc. Ing. Peter Surový, PhD.
Chairperson of Field of Study Board

Electronically approved: 30/07/2025
prof. Ing. Róbert Marušák, PhD.
Dean

Annotation

Terrestrial biodiversity has been declining due to the increasing human population, which converts biodiversity areas to agricultural land and settlements, and overexploits plants to obtain medicine, wood for fuel, and building materials. Climate change and the introduction of invasive alien species (IAS) are other factors that threaten biodiversity. Hence, finding effective ways to monitor changes in biodiversity is essential from a forest management perspective.

The Essential Biodiversity Variable (EBV) approach facilitates the easier, more consistent, and efficient detection of ecological change compared to ad hoc indicators. This thesis operationalizes the EBV framework for monitoring forest biodiversity change in Ghana by integrating multi-sensor remote sensing (RS) datasets (Sentinel-2, Sentinel-1, Landsat, and PlanetScope) with field data, and existing vegetation datasets from databases such as the Global Biodiversity Information Facility (GBIF). It links spectral signals from satellite datasets to tree species diversity, assesses the adoption of standardized land-cover datasets for national reporting, quantifies ecosystem extent and fragmentation, and models species distribution, population abundance, and species richness to reveal conservation gaps. The results are a tested approach for detecting and mapping biodiversity change across Ghana's high-forest zones, providing earlier warnings and evidence to prioritize protection, restoration, and sustainable forest management practices.

The organization of this thesis is based on four scientific articles, the first of which assesses forest species diversity in Ghana's tropical forests using PlanetScope data (Njomaba et al., 2024). The second article (Njomaba et al., 2025) focuses on adopting land cover standards for sustainable development in Ghana, considering challenges and opportunities. The third article of the thesis (Njomaba et al., 2025) focuses on mapping the distribution and estimating the population abundance of dominant forest tree species in Ghana, with implications for conservation prioritization. The fourth article, submitted and yet to be published, examines the impact of climate change on aboveground biomass, as modulated by forest fragmentation and biodiversity, in Ghana.

Therefore, the thesis explores the application of an integrative framework that combines RS, field-based observations, and different ecological modeling and geospatial approaches to operationalize EBVs for forest biodiversity monitoring in Ghana. The research advances the approach to tracking biodiversity change in tropical forests. It introduces innovative methods for assessing species diversity, mapping land cover, and analyzing relationships between ecosystem variables.

Keywords: Remote sensing, Ghana, Biodiversity, Essential Biodiversity Variables, Land cover, Species distribution, Tropical forests, Fragmentation.

Table of Contents

List of the Figures

List of Tables

List of abbreviations

AIC: Akaike Information Criterion

AGB: Above-Ground Biomass

AI: Aridity Index

AUC: Area Under the Curve

BFR: Bobiri Forest Reserve

CBD: Convention on Biological Diversity

CCI: Climate Change Initiative

CEO: Collect Earth Online

CERSGIS: Center for Remote Sensing and Geographic Information Services

CGLS: Copernicus Global Land Service

CNN: Convolutional Neural Network

CORINE: Coordination of Information on the Environment

DEM: Digital Elevation Model

DBH: Diameter at Breast Height

EAGLE: European Environment Agency's EAGLE Conceptual Framework

EBV(s): Essential Biodiversity Variables (s)

ECV(s): Essential Climate Variables (s)

ED: Edge Density

EO: Earth Observation

ESA: European Space Agency

EVI: Enhanced Vegetation Index

FAO: Food and Agriculture Organization of the United Nations

FORIG: Forestry and Research Institute of Ghana

FRAGSTATS: Fragmentation Statistics Software

GAM: Generalized Additive Model

GBIF: Global Biodiversity Information Facility

GEE: Google Earth Engine

GEDI: Global Ecosystem Dynamics Investigation

GLCM: Gray-Level Co-Occurrence Matrix

GOFC-GOLD: Global Observation of Forest Cover and Land Dynamics

GPS: Global Positioning System

IPBES: Intergovernmental Science Policy Platform on Biodiversity and Ecosystem Services

ISO: International Organization for Standardization

IUCN: International Union for Conservation of Nature

KNN: K-nearest Neighbor

LCML: Land Cover Meta Language

LCLR: land Cover Legend Registry

LDN: Land Degradation Neutrality

LiDAR: Light Detection and Ranging

LPI: Largest patch index

LSI: Landscape Shape Index

LUSPA: Land Use and Spatial Planning Authority

MaxEnt: Maximum Entropy Model

MODIS: Moderate Resolution Imaging Spectroradiometer

MSI: Mean Shape Index

NDRE: Normalized Difference Red Edge Index

NDBI: Normalized Difference Built-up Index

NDVI: Normalized Difference Vegetation Index

Normalized Difference Water Index

NBSAP: National Biodiversity Strategy and Action Plan

NICFI: Norway's International Climate and Forest Initiative

NP: Number of Patches

NIR: Near infrared

OGC: Open Geospatial Consortium

PA: Protected Area

PCA: Principal Component Analysis

PRISMA: Preferred Items for Systematic Reviews and Meta-Analysis

RF: Random Forest

REDD+: Reducing Emissions from Deforestation and Forest Degradation

RMSE: Root Mean Square Error

ROI: Region of Interest

RS: Remote Sensing

SAVI: Soil Adjusted Vegetation Index

SAR: Synthetic Aperture Radar

SD: Standard Deviation

SDG(s): Sustainable Development Goals

SEM: Structural Equation Model

SRTM: Shuttle Radar Topography Mission

SVM: Support Vector Machine

SWIR: Shortwave Infrared

TSS: True Skill Statistic

USGS: United States Geological Survey

UAV: Unmanned Aerial Vehicle

VIF: Variable Inflation Factor

VIs: Vegetation indices

UNEP: United Nations Environment Program

WALCRS: West African Land Cover Reference System

ZIP: Zero-Inflated Poisson Model

Foreword

Forests are among the most important terrestrial ecosystems, as they provide habitats for a wide range of species, regulate the climate, store carbon, and support human livelihoods. Ghana, one of the countries with rich natural ecosystems and a great wealth of biodiversity, is facing challenges to its habitat quality, species quantity, and diversity. Although steps have been taken to address the challenges related to the loss of essential biodiversity, the country still faces numerous challenges, including anthropogenic activities that threaten biodiversity, such as land use conversion, wildfires, and mining, among others. With a land area of approximately 238,533 km², Ghana hosts a vast and diverse forest ecosystem, ranging from wet evergreen to dry savannah woodlands. Monitoring forest biodiversity change across such an extensive and heterogeneous landscape poses severe challenges. Over the years, field-based approaches have been employed to monitor changes in biodiversity. While the approach has been invaluable, they are labor-intensive, costly, and spatially limited, making it challenging to capture large-scale biodiversity dynamics.

RS has emerged as a powerful complement to field surveys, offering repeatable and cost-effective methods to monitor forest ecosystems at national and regional scales. Despite the advantages presented by RS, limitations still exist, especially in tropical areas, where persistent cloud coverage hinders the acquisition of optical images. In such contexts, combining optical with Synthetic Aperture Radar (SAR) provides structural information that complements spectral data. Additionally, high-resolution optical sources, such as PlanetScope, further enable detailed biodiversity mapping. These constraints raise an essential question: How can biodiversity monitoring be comprehensive and practical for large-scale (country-level) forest ecosystems, such as Ghana?

The concept of EBVs provides a framework that enables a hybrid approach to integrating multi-source remote sensing datasets with field-based observations. By focusing on a core set of EBVs such as species population, community composition, ecosystem structure, and function, biodiversity can be streamlined to capture the most relevant dimensions of change.

Contribution of the thesis

The thesis contributed to original publications and can be summarized as follows:

1. **Paper I:** Assessing Forest Species Diversity in Ghana's Tropical Forest Using PlanetScope Data. https://doi.org/10.3390/rs16030463 (Remote Sensing)
2. **Paper II:** Adopting Land Cover Standards for Sustainable Development in Ghana: Challenges and Opportunities. https://doi.org/10.3390/land14030550 (Land)
3. **Paper III:** Mapping Species Distribution and Estimating Population Abundance of Dominant Forest Tree Species in Ghana: Implications for Conservation Prioritization. https://doi.org/10.1016/j.tfp.2025.101019 (Trees, Forests and People)
4. **Paper IV:** Effect of climate change on aboveground biomass modulated by forest fragmentation and biodiversity in Ghana. (accepted, but not yet pushed in Journal of Forestry Research)

1.0 Introduction

1.1 State of the art and motivation

Biodiversity is the foundation of ecosystem functioning and services. It encompasses the variability among living organisms at genetic, species, and ecosystem levels, and supports essential ecological processes such as nutrient cycling, pollination, soil formation, water regulation, and climate stabilization (Reid et al., 2005; Díaz et al., 2019). Biodiversity provides direct and indirect benefits for humans (such as providing food, medicine, and cultural values) while ensuring ecosystem resilience and the continued delivery of ecosystem services (Hooper et al., 2012; Cardinale et al., 2012). Despite its critical role, global assessments have consistently shown that biodiversity is declining at an unprecedented rate. The Intergovernmental Science-Policy Platform on Biodiversity and Ecosystem Services (IPBES, 2019) estimated that over one million species face extinction due to anthropogenic activities. Land use change, forest habitat degradation, overexploitation, pollution, invasive species, and climate disruptions are among the drivers of species loss across many biomes (Jaureguiberry et al., 2022).

Terrestrial biodiversity is of particular importance and concern among the broad biodiversity domains (IPBES, 2019). According to Gaston. (2010) and Newbold et al. (2015), terrestrial ecosystems support approximately 80% of the known species on Earth and account for most of the global primary productivity. Forests, in particular, represent the most species-rich terrestrial ecosystems, providing habitat for more than 80% of the world's terrestrial biodiversity (FAO, 2020). They are essential in regulating the carbon and water cycles, providing habitat and ecological connectivity, and supporting livelihoods through forest products and ecosystem services (Pan et al., 2011). Despite these advantages, forest ecosystems are among the most threatened (FAO, 2020). According to a global forest assessment report by FAO, 2020, an estimated 420 million hectares of forest were lost globally as a result of their conversion to other land uses, agricultural expansion, logging, infrastructure development, and fires (Hansen et al., 2013; Haddad et al., 2015) Between 1990 and 2020, the net decrease in forest area was approximately 178 million hectares.

In West Africa, forests are part of the Guineo-Congolian biodiversity hotspots (Malhi et al., 2013), noted globally for their species richness and endemism levels. These forests extend across countries such as Côte d'Ivoire, Liberia, Sierra Leone, and Ghana, providing vital ecosystem services including water regulation, soil protection, and carbon storage (Myers et al., 2000). Tropical forests are under severe pressure despite their ecological and economic significance. Between 1990 and 2015, the region lost most of its forest cover, mainly due to agricultural expansion (notably cocoa and oil palm cultivation), timber extraction, fuelwood

harvesting, and mining (Makinde, 2016). The fragmentation of remaining forests has further reduced biodiversity and ecosystem integrity (Laurance et al., 2012).

Within this regional context, Ghana's forests, in the high forest and transitional zones, form part of the upper Guinean forest ecosystem, one of the world's most threatened tropical forest ecosystems. The country's forests are home to an estimated 3,725 species, including trees, mammals, birds, amphibians, and reptiles. (Ministry of Environment, 2016; CBD, 2016). However, Ghana's tropical rainforests are rapidly disappearing. According to Global Forest Watch, Ghana recorded a 60% increase in primary rainforest loss in 2016 compared to 2017 (Figure 1), the highest rate globally (Pandit et al., 2018). This trend underscores the urgent need for effective monitoring and conservation mechanisms.

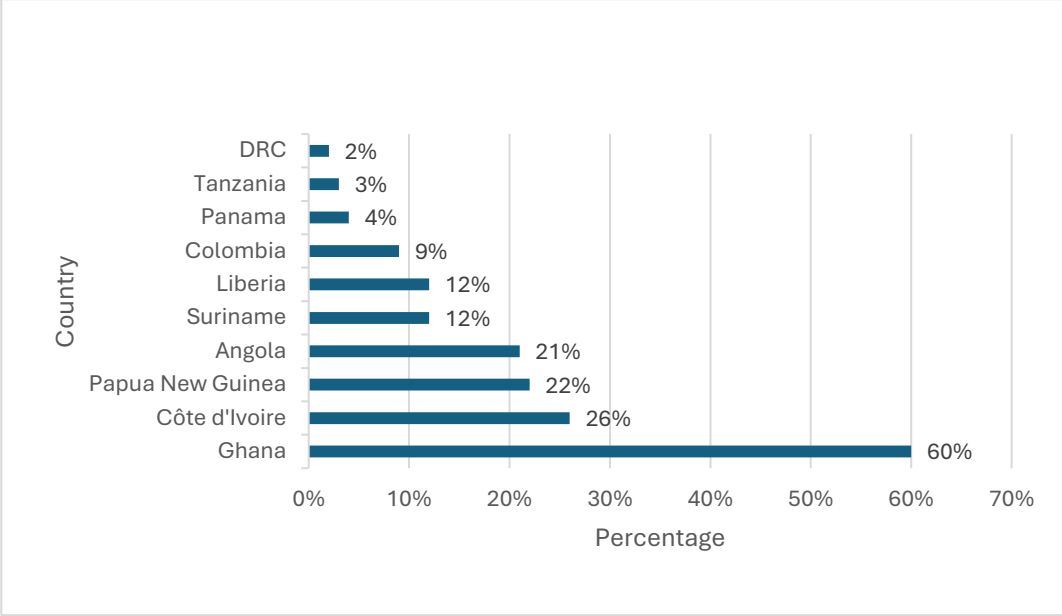

Figure 1: Top 10 countries losing the most tropical primary rainforest in 2018 by percent increase from 2017. Source: (Weisse & Goldman, 2020)

Ghana has signed several international environmental conventions, including the Convention on Biological Diversity (CBD), ratified in 1996. In alignment with this commitment, Ghana developed its National Biodiversity Strategy and Action Plan (NBSAP) as a framework for implementing the Aichi Biodiversity Targets under the Global Strategic Plan for Biodiversity (2011–2020). The NBSAP enhances ecosystem resilience and restoration, promotes sustainable agricultural, aquacultural, and forestry management systems, and maintains ecosystem services and carbon stocks (Ministry of Environment, 2016). Additionally, Ghana participates in other global initiatives, such as the Reducing Emissions from Deforestation and Forest Degradation (REDD+), aimed at reducing deforestation and forest degradation emissions while promoting conservation and sustainable forest management (Gibbs et al., 2007).

Despite these policy-driven efforts, the country still faces substantial challenges, including habitat degradation, unsustainable land use, illegal mining, wildfires, poaching, and the

introduction of invasive species (Ofori et al., 2024). A significant limitation to addressing these issues effectively lies in the lack of consistent and standardized biodiversity monitoring frameworks (Joppa et al., 2016). Current national biodiversity monitoring frameworks and programs are fragmented and rely heavily on field-based observations and datasets, which are time-consuming, spatially limited, and often inconsistent across institutions (Pettorelli, 2016).
To address the global and national challenges, the Group on Earth Observations Biodiversity Observation Network (GEO BON) developed the concept of EBVs, a standardized framework designed to harmonize biodiversity monitoring across scales in 2013. EBVs are a minimum set of complementary measurements that capture key dimensions of biodiversity change, and link primary data collection (RS and in situ) to indicators and policy reporting (Pereira et al., 2013; Haase et al., 2018). The EBV framework organizes variables into six broad classes (Table 1)

Table 1: Essential Biodiversity Variables. Source: Haase et al., 2018

EBV	EBV classes
Co-ancestry	**Genetic composition**
Allelic diversity	
Population genetic differentiation	
Breed and variety diversity	
Species distribution	**Species populations**
Population abundance	
Population structure by age/size class	
Phenology	**Species traits**
Body mass	
Natal dispersal distance	
Migratory behavior	
Demographic traits	
Psychological traits	
Taxonomic diversity	**Community composition**
Species interactions	
Net primary productivity	**Ecosystem function**
Secondary productivity	
Nutrient retention	
Disturbance regime	
Habitat structure	**Ecosystem structure**
Ecosystem extent and fragmentation/land cover	
Ecosystem composition by functional type	

Although the EBV framework has been applied mainly at global or regional scales, its operationalization at the national level remains limited, especially in African countries (Proença et al., 2017). For Ghana, implementing EBVs through integrating RS and field-based observations presents an opportunity to overcome data limitations in biodiversity monitoring and improve and support biodiversity policy and reporting frameworks. In this regard, this study operationalizes a standard set of biodiversity variables under the EBV framework for Ghana, focusing on three key EBV classes: Ecosystem structure, community composition (land cover,

forest fragmentation, and above-ground biomass), and species populations (species diversity, distribution, and abundance).

The study uses multi-source satellite data (PlanetScope, Sentinel-1, Sentinel-2, ESA Biomass, and Copernicus Global Land Cover data) and ancillary environmental datasets, including Digital Elevation Model (DEM) derived slope and aspect, global aridity index, bioclimatic variables, and soil datasets, combined with field-inventory data and vegetation data derived from the Global Biodiversity Information Facility (GBIF). By integrating these data within a modeling and monitoring framework, the study produced scalable, reproducible, and policy-relevant indicators that reflect biodiversity patterns and change in Ghana's forests. The rationale for selecting these EBVs stems from the fact that they are directly aligned with the goals of Ghana's NBSAP and provide cost-effective, spatially explicit alternatives to traditional field-based monitoring methods. The study also addresses key information gaps in species-level monitoring, land cover standardization, and ecosystem change assessment, supporting Ghana's commitment under the CBD, REDD+, and Sustainable Development Goals (SDGs 13 and 15). Ultimately, this research provides a framework that enhances monitoring, reporting, and verification (MRV) of biodiversity and ecosystem changes, guiding conservation planning and ultimately contributing to global efforts to reduce biodiversity loss. A systematic literature review used the Web of Science Core Collection to situate this research within the broader scientific context. The review focused on publications that address the effects of EBVs on ecosystem structure and species populations. Table 2 summarizes the search queries and number of publications identified, while Figures 2 and 3 illustrate the temporal trends of global, Ghanaian, and Tropical Africa-specific publications.

Table 2: Search queries and the number of publications related to EBV classes used to search in Web of Science

EBV Class	Search Code	Focused Area	No. of publications
Ecosystem Structure (Global)	"remote sensing" OR satellite OR "Earth observation" OR lidar OR "synthetic aperture radar" OR SAR And "land cover" OR "forest fragmentation" OR fragmentation OR "aboveground biomass" OR biomass OR AGB And biodivers* OR "ecosystem structure" OR "essential biodiversity variable*" OR EBV*	Land cover, fragmentation, biomass	3391
Ecosystem Structure (Regional, Ghana)	"remote sensing" OR satellite OR "Earth observation" OR lidar OR "synthetic aperture radar" OR SAR And "land cover" OR "forest fragmentation" OR fragmentation OR "aboveground biomass" OR biomass OR AGB And biodivers* OR "ecosystem structure" OR "essential biodiversity variable*" OR EBV* And Ghana OR "West Africa" OR "tropical Africa"	Land cover, fragmentation, biomass	66
Species populations (Global)	"remote sensing" OR satellite OR "Earth observation" OR lidar OR "synthetic aperture radar" OR SAR And "species distribution" OR "species richness" OR "species diversity" OR "species abundance" OR occupancy And biodivers* OR "species population*" OR "essential biodiversity variable*" OR EBV*	Species diversity, species distribution, species abundance	1527
Species populations (Regional, Ghana)	"remote sensing" OR satellite OR "Earth observation" OR lidar OR "synthetic aperture radar" OR SAR And "species distribution" OR "species richness" OR "species diversity" OR "species abundance" OR occupancy And biodivers* OR "species population*" OR "essential biodiversity variable*" OR EBV* And Ghana OR "West Africa" OR "tropical Africa"	Species diversity, species distribution, species abundance	18

Figure 2: Number of publications in the preceding years, between January 2004 and December 2024, focusing on global EBVs related to ecosystem structure and species populations.

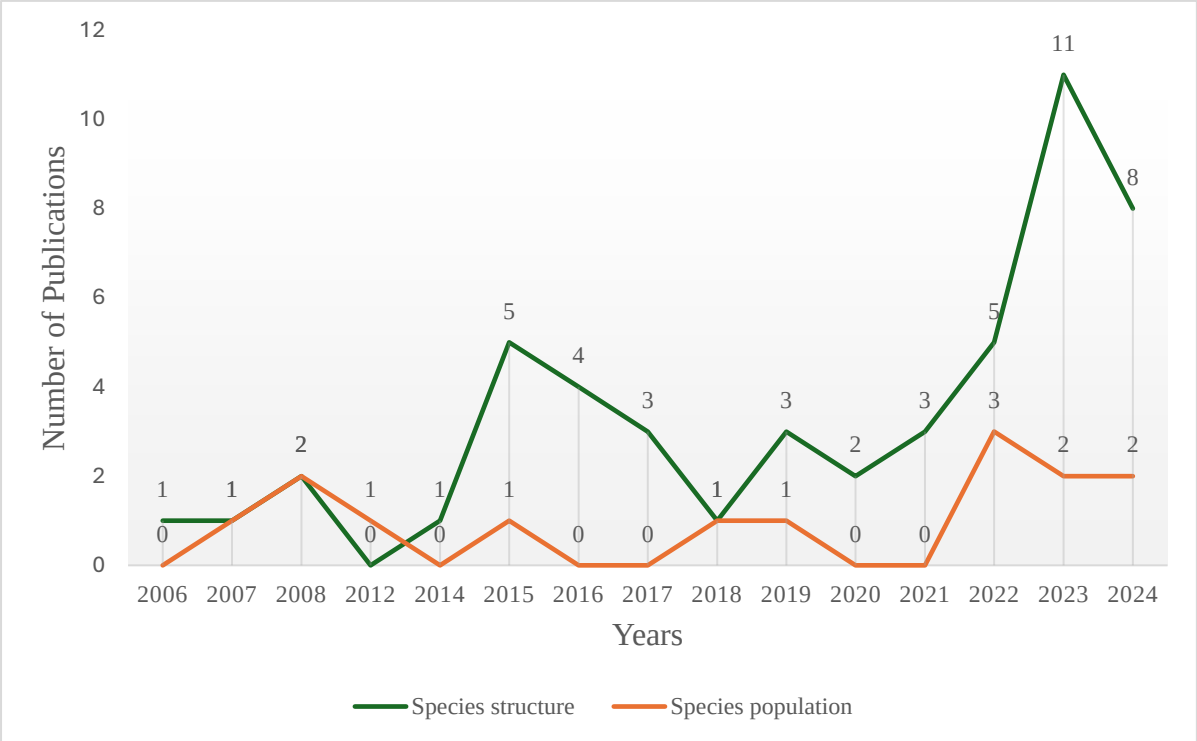

Figure 3: Number of publications in the preceding years, between January 2004 and December 2024, focusing on EBVs related to ecosystem structure and species populations in Africa and Ghana.

The publication trends (Figures 2 and 3) indicate that EBV-related research is comparatively higher globally, especially since 2010. Studies on ecosystem structure EBVs dominate, while studies on species population EBVs have received less attention, although they are steadily increasing in number. For Africa, and, by extension, Ghana, the number of studies on EBVs is significantly lower, particularly in the species population domain, underscoring the limited national-level implementation of the EBVs framework despite its relevance for biodiversity monitoring and policy reporting. These findings highlight the research gap that this study seeks to address.

1.2 Objectives

In line with the aim of operationalizing EBVs for biodiversity monitoring in Ghana, the study pursues the following specific objectives:

i) Estimate forest species diversity in tropical forests using PlaneScope satellite data and field-based diversity indices in Ghana.

ii) Assess the challenges and opportunities for adopting the International Standards Organization (ISO) 1944-2 land cover standards in Ghana for harmonized land cover mapping.

iii) Map the distribution and population abundance of dominant forest tree species in Ghana and evaluate their implications for conservation prioritization.

iv) Assess the effects of climate change (aridification) and forest fragmentation on above-ground biomass (AGB).

1.3 Hypothesis

The following hypothesis guides this thesis:

i) There is a significant relationship between spectral variability derived from PlanetScope imagery and field-measured tree species diversity indices, allowing robust prediction of forest diversity.

ii) An ISO 19144-2-based land cover legend and dataset provides clearly defined land cover classes, enhancing the accuracy, interoperability, and usability of land cover information for forest monitoring.

iii) iv) Species distribution models combined with abundance estimates can identify priority areas for conservation.

iv) a. H1a: Decreasing AI (aridification) reduces AGB directly, with humid zones (higher AI) maintaining higher mean AGB than semi-arid zones.

b. H1b: Decreasing AI (aridification) has an indirect effect on AGB, mediated by forest fragmentation and biodiversity.

c. H2: AGB exhibits a non-linear response to structural attributes of fragmentation (Fragmentation metrics), with varying contributions across different dimensions of fragmentation.

1.4 Thesis Structure

The thesis is organized into chapters addressing key EBVs and biodiversity monitoring components, using RS and field-based approaches. The first chapter presents a comprehensive literature review that provides an overview of the EBV framework and highlights relevant literature on RS applications for biodiversity assessment. This chapter also covers land cover mapping standards and interoperability, forest fragmentation metrics, and approaches for mapping tree species distribution, abundance, and diversity. The second chapter describes the methodology, including information on the study area and the conceptual framework used in the research. It also outlines the methodological approaches for land cover mapping, fragmentation analysis, species diversity modeling, and the statistical and geospatial analysis techniques used for model development, evaluation, and validation.

The third chapter presents the results of this thesis, which are three published and one submitted articles. There is another chapter on the discussion, which includes an overall review of the articles' outcomes, focusing on key findings, knowledge gaps, and methodological limitations. Furthermore, the thesis also comprises sub-chapters on international collaborations and additional achievements during the study. Lastly, the Conclusion and recommendations are included to summarize the overall concept of the thesis, findings, and future scope.

2.0 Literature Review

This chapter is organized as follows. Section 2.1 introduces the Essential Biodiversity Variable (EBV) framework, its six classes, and the policy context that motivates standardized biodiversity indicators. Section 2.2 reviews how RS supports the operationalization of EBVs, outlining optical, Synthetic Aperture Radar (SAR), Light Detection and Ranging (LiDAR), hyperspectral sensors, and multi-source data integration. Section 2.3 focuses on land cover as a core EBV variable under the ecosystem structure EBV: Section 2.3.2 presents international standards and interoperability; Section 2.3.2 summarizes RS advances for land cover mapping and machine-learning methods; and Section 2.3.3 reviews Ghana's land-cover efforts, highlighting the need for the adoption of an ISO-aligned national land cover legend and dataset. Section 2.4 examines forest fragmentation and structural indicators, covering theoretical concepts of fragmentation, widely used landscape metrics, scale effects, and implications for biodiversity and policy. Section 2.5 addresses species populations, tree species distribution, abundance, and diversity, with Section 2.5.1 summarizing optical/SAR/LiDAR contributions, and Section 2.5.2 comparing key modeling approaches. Section 2.5.3 details diversity estimation from RS.

2.1 The Essential Biodiversity Variable (EBV) Framework

The lack of standardized, consistent, scalable indicators across countries and regions has long hindered biodiversity monitoring. Following the establishment of the CBD in 1994, parties were encouraged to strengthen biodiversity protection efforts and to develop NBSAPs. Adopting the Strategic Plan for Biodiversity (2011 – 2020) and its 20 Aichi Biodiversity targets further emphasized the importance of developing robust indicators to assess progress (GOFC-GOLD, 2017). However, national biodiversity monitoring systems often differ widely in their design, suffer from inconsistent data collection, and lack openly shared datasets, creating significant challenges for tracking progress toward the Aichi biodiversity targets (Schmeller et al., 2015).

The GEO BON was established to harmonize global, regional, and national biodiversity observation systems to address these challenges. GEO BON proposed the concept of EBVs as a framework to guide biodiversity monitoring efforts. EBVs are the minimum measurements required to detect and document biodiversity change across spatial and temporal scales (Pereira, Bruford, et al., 2013a). This framework also aims at integrating data from multiple sources, including in situ observations, citizen science, and RS, into indicators that inform science and policy (Haase et al., 2018).

Initially conceptualized in 2013, EBVs are organized into six classes: (i) genetic composition, (ii) species populations, (iii) species traits, (iv) community composition, (v) ecosystem function, and (vi) ecosystem structure. These variables are designed to capture different dimensions of biodiversity, ranging from genes and species to ecosystems (Haase et al., 2018). Like other

Essential variables (EVs), such as the Essential Climate Variables (ECVs) by the climate science community, EBVs are required to meet the criteria of scientific robustness, feasibility, scalability, and policy relevance (Kissling et al., 2018).

RS has been highlighted as a critical enabler of the EBV framework. Pettorelli (2016) argued that satellite EO provides a unique capacity to deliver consistent and repeatable biodiversity metrics at a larger scale, helping to overcome the limitations of field-based approaches. Advances in EO platforms, including the Landsat and Sentinel series, LiDAR missions such as Global Ecosystem Dynamics Investigation (GEDI), and upcoming spaceborne initiatives like ESA's Biomass mission, have expanded the potential for monitoring ecosystem structure (e.g., land cover, fragmentation, and above-ground biomass) and species populations (Cavender-Bares et al., 2020).

Despite these advances, challenges exist in defining and operationalizing a universally accepted set of EBVs. There are disagreements regarding which biodiversity variables can feasibly be monitored remotely, how to integrate them with in situ observations, and how to ensure continuity of observations across time and space (Cavender-Bares et al., 2020). Furthermore, while some countries and institutions have adopted EBV-related indicators, such as South Africa's National Biodiversity Institute, many tropical countries, including Ghana, continue to lack standardized EBV-aligned monitoring frameworks.

Overall, the EBV framework has emerged as a cornerstone for biodiversity monitoring and reporting, linking scientific advances in RS and ecological observations with international policy needs under the CBD and IPBES (Pereira, Bruford, et al., 2013). By emphasizing a limited yet essential set of variables, EBVs offer a practical pathway for harmonizing biodiversity data collection and ensuring that future monitoring efforts are scalable, cost-effective, and policy-relevant.

2.2 Remote sensing for biodiversity monitoring

RS has become a significant source of technology in biodiversity monitoring because it enables repeated, spatially consistent, and large-scale measurements of ecosystems and species habitats (Wang & Gamon, 2019). Compared to field inventories, which are labor-intensive, time-consuming, and spatially restricted, RS provides the opportunity for repeatable observations critical for long-term monitoring (Nagendra, 2001). These advantages make RS particularly relevant for operationalizing EBVs, which requires scalable datasets across spatial and temporal scales.

RS technologies can broadly be categorized into passive, active, and laser scanning/hyperspectral systems. Optical sensors, such as Landsat and Sentinel-2, capture reflected solar radiation in the visible to short-wave infrared bands of the electromagnetic radiation spectrum, allowing vegetation indices and phenological metrics to be derived (Drusch

et al., 2012). However, their performance may be limited in heterogeneous forests due to mixed pixels, cloud coverage, and moderate spatial resolution (Griffiths et al., 2014). SAR sensors, such as Sentinel-1, overcome cloud limitations and provide information on forest structure, biomass, and moisture through their microwave backscatter (Lucas et al., 2010). LiDAR and hyperspectral systems, both airborne and spaceborne, provide fine-scale structural information but are often limited by the high acquisition cost and narrow coverage (Fassnacht et al., 2016).

Numerous studies have demonstrated the application of RS in biodiversity monitoring. For instance, Landsat time series have been used to track forest disturbance and recovery across the Carpathians, providing insights into habitat dynamics over three decades (Griffiths et al., 2014). At a global scale, the Moderate Resolution Imaging Spectroradiometer (MODIS) and Landsat data have supported the development of Essential Climate and Biodiversity Variables related to net primary productivity and land cover change (Pettorelli, 2016). More recently, Sentinel-2 data have been applied for mapping tree species composition in European forests (Immitzer et al., 2016), while Sentinel-1 SAR backscatter has been linked to tropical forest diversity and structure (Hoffmann et al., 2022). In addition, airborne LiDAR campaigns have been used to model forest biomass and canopy complexity as proxies for habitat quality (Asner et al., 2017).

In recent years, integrating multiple optical remote sensing data sources has become a key strategy (Pasetto et al., 2018). Combining optical, SAR, and digital elevation data enhances classification accuracies and allows for better modeling of biodiversity indicators, such as species distribution and biomass (Persson & Lindberg, 2018). The increasing availability of free satellite data through programs like Copernicus and Landsat, combined with advances in cloud computing platforms such as Google Earth Engine (GEE), has also made it possible to process large data volumes for national and regional-scale biodiversity (Azzari & Lobell, 2017).

Despite these advances, high spatial resolution data are still costly and limited in coverage, while differences in forest structure, climate, and availability of reference data present make the acquisition and usage of RS data challenging (Wulder et al., 2004). Nevertheless, integrating RS with in-situ and biodiversity repositories offers one of the most promising pathways to achieve harmonized, repeated, and scalable biodiversity assessments.

2.3 Land Cover Mapping, Standards, and Remote Sensing

Land cover is a fundamental EBV under the class ecosystem structure and is the basis for understanding forest fragmentation, biomass, and habitat distribution (Skidmore et al., 2021). It is also linked to two central Sustainable Development Goals (SDGs), SDG13 (Climate Action) and SDG15 (Life on Land), as well as frameworks such as REDD+ and Land Degradation Neutrality (LDN) (Njomaba, Mushtaq, et al., 2025). Accurate, standardized, and comparable land cover information is critical for monitoring biodiversity and ecosystem change.

2.3.1 Land Cover Standards and Interoperability

The growing demand for a consistent land cover dataset across scales has spurred the development of international standards (F. Mensah et al., 2024). Technical communities such as the Open Geospatial Consortium (OGC) and the ISO provide frameworks to ensure data accuracy, interoperability, and policy relevance (ISO/TC 211, 2022). Specifically, ISO/TC 211 on Geographic Information/Geomatics established the ISO 19144 series, which defines standardized approaches for land cover and land use classification (ISO 19144-2, 2012). A key innovation within this framework is the Land Cover Meta Language (LCML), which provides a flexible, hierarchical system to describe land cover features based on structural and functional attributes (Mushtaq et al., 2024). LCML has been adopted by the Food and Agriculture Organization's (FAO) Land Cover Legend Registry (LCLR), which currently hosts more than 30 sub-national and national legends developed according to ISO standards (Mushtaq et al., 2024). Despite this initiative, many countries still lack standardized national land cover legends, limiting global, regional, and national comparability of land cover datasets, weakening the link between national monitoring and international reporting frameworks (Potapov et al., 2022).

Several classification systems have been developed globally, including the European CORINE Land Cover, the United States Geological Survey (USGS) Anderson Classification, and the EAGLE framework (Njomaba, Mushtaq, et al., 2025). While these systems support regional needs, they are not interoperable with each other, further underscoring the importance of ISO-based harmonization (Seebach et al., 2011).

2.3.2 Remote Sensing Advances in Land Cover Mapping

Land observation missions have historically provided global time-series data since the 1970s, enabling long-term land cover change analysis (Wulder et al., 2022). The sentinel missions under the European Copernicus Program have significantly improved spatial and temporal resolutions, particularly with Sentinel-2's multispectral instrument (10 – 20m) and Sentinel-1 (Drusch et al., 2012).

Machine learning approaches, such as Random Forest (RF), Support Vector Machines (SVM), and deep learning models like Convolutional Neural Networks (CNN), have achieved classification accuracies above 90% in heterogeneous landscapes (Maxwell et al., 2018). These methods and cloud computing platforms, such as Google Earth Engine, enable monitoring of national to regional-scale land cover (Azzari & Lobell, 2017).

However, persistent challenges remain: spectrally similar classes, such as cropland and grassland, are difficult to distinguish, while high-resolution imagery is still costly for operational national monitoring (Herold et al., 2008). In Sub-Saharan Africa, additional challenges include fragmented institutional responsibilities, limited adoption of international standards, and reliance on global datasets that may not reflect national realities (Tsendbazar et al., 2016)

2.3.3 Land Cover Monitoring in Ghana

In Ghana, national land cover mapping efforts began in the early 2000s, with the Center for Remote Sensing and Geographic Information Services (CERSGIS) and the Forestry Commission producing sub-national datasets (e.g., 1990, 2000, 2010, 2012, 2015) under various initiatives, including the Forest Preservation Program (Ghana Forestry Commission, 2018). These maps were often produced at the subnational, municipal, and district levels and rely on existing global data, such as the ESA land cover data (Njomaba, Mushtaq, et al., 2025).

Despite these efforts, Ghana still lacks a standardized national land cover reference system aligned with the ISO 19144-2 land cover standards. Again, most maps use varying classification schemes, definitions of land cover classes, and objectives, limiting their comparability across time and with international datasets (F. Mensah et al., 2024). Consequently, global products such as ESA's Climate Change Initiative Land Cover and Copernicus Global Land Cover maps are often used in national reporting, despite sometimes diverging from locally produced maps (Conchedda & Tubiello, 2021).

Developing a standardized ISO-based national land cover legend and dataset for Ghana would bridge these gaps, improve data interoperability, and strengthen reporting to global conventions. Moreover, it would enhance the integration of land cover as an EBV for biodiversity monitoring, directly supporting Ghana's commitments under the CBD and its NBSAP.

2.4 Forest fragmentation and Structural Indicators

Forest fragmentation, defined as the process by which large, continuous forest areas are divided into smaller, more isolated patches, is critical under the Ecosystem Structure EBV subclass (Pereira, Bruford, et al., 2013b). Fragmentation alters ecosystem integrity, reduces habitat connectivity, and intensifies edge effects, impacting species populations, biodiversity resilience, and ecosystem functioning (GOFC-GOLD, 2017). Both anthropogenic activities (e.g., land conversion, logging, mining, agriculture) and natural processes (e.g., firestorms, climate change) contribute to fragmentation (Haddad et al., 2015).

The IUCN Red List ecosystem criteria include habitat fragmentation and degradation as indicators of declining ecosystems. The framework recognizes that ecosystems with more isolated and fragmented patches are more vulnerable and at a high risk of collapse (Keith et al., 2013). Understanding where and how fragmentation occurs, whether in ecosystem interiors, edges, or peripheries, is crucial, as ecological processes such as productivity, nutrient cycling, and water regulation may not be uniformly distributed (Riitters et al., 2000). A global analysis by Ma et al.(2023) found that increased fragmentation contributed to forest loss between 2000 and 2012, highlighting essential risks for biodiversity conservation and management.

RS has been applied in fragmentation analysis, providing repeatable and synoptic coverage over long periods. Using Landsat and RS data, Toivonen et al. (2023) analyzed forest fragmentation

patterns, combining spectral information with NDVI-based change detection. Similarly, Carranza et al. (2014) analyzed three decades of fragmentation in the dry Chaco using Landsat imagery and applied the Fragmentation Statistics Software-derived (FRAGSTATS) metrics, including percent forest cover, edge density, mean patch size, and patch density. Their results revealed forest loss and structural reconfiguration over time, underscoring the importance of multi-temporal approaches for fragmentation analysis.

Beyond temporal monitoring, methodological considerations also play a crucial role. Fynn & Campbell (2019) explored how the spatial resolution of satellite images (Landsat, Sentinel, NAIP, UAV) influences fragmentation indices. Their study demonstrated that metrics such as patch density, largest patch index, and edge density vary significantly with image resolution, highlighting the importance of image resolution in fragmentation studies. Commonly used metrics are presented in Table 3.

Table 3. Forest fragmentation metrics, equations for computation, and their descriptions. Variables include N = total number of patches, A = total landscape area, eik = total edge length of patch i, aij = area of patch j, m = number of patches, LSI = landscape shape index. All metrics follow landscape ecological equations adopted from Enaruvbe & Atafo (2018) and McGargical et al. (2023).

Fragmentation metrics	Equation	Description
Number of patches (NP)	$NP = N$	Total number of discrete forest patches within the buffer. Higher NP indicates greater fragmentation.
Landscape Shape Index (LSI)	$SI = \frac{0.25 \sum_{k=1}^{m} e_{ik"}}{\sqrt{A}}$	Quantifies shape complexity by standardizing total edge length to landscape area; 0.25 corrects for raster geometry.
Mean Shape Index (MSI)	$MSI = \frac{LSI}{N}$	Average shape irregularity of forest patches; higher values indicate more complex patch form.
Edge density (ED)	$ED = \frac{\sum_{k=1}^{m} e_{ik"}}{A} X\ 1000$	Total length of forest edges (m) per hectare of landscape area (A). indicates the relative amount of edge habitat.
Patch area mean (Area_MN)	$AREA_{MN} = \frac{1}{n}\sum_{j=1}^{n} AREA(patch_j)$	Arithmetic means of forest patch areas. Reflects average patch size and connectivity.

While global fragmentation analysis are informative, national and regional studies are required to support policy. In Ghana, fragmentation is mainly driven by agricultural expansion, illegal mining, logging, and fire (Bonsu & Bonin, 2023). A few regional studies have been conducted, documenting the relationship between forest disturbance, biodiversity, and biomass. For example, Addo-Fordjour et al. (2009) reported declines in woody biomass and species richness with increasing forest disturbance, but without modeling fragmentation metrics. Similarly, Mensah et al. (2017) found from their studies that biodiversity positively influences forest productivity in Ghana; however, these relationships were explored independently of spatial configurations. With the role fragmentation plays in forest ecosystem integrity, assessing its impacts on biodiversity will support effective forest management practices.

2.5 Species Populations: Mapping Tree Species Distribution, Abundance, and Diversity

Tree species composition and distribution are critical biodiversity indicators influencing ecosystem functioning, productivity, and habitat provision (Arekhi et al., 2017). The loss of tree species due to land use change, mainly deforestation and fragmentation, poses serious threats to ecosystem services and biodiversity conservation (Oli & Subedi, 2015; Wang & Gamon, 2019). Monitoring tree species populations is therefore a key indicator for biodiversity assessments, as species population trends are central to EBVs and global monitoring frameworks (Pereira, Bruford, et al., 2013a); however, traditional approaches such as field inventories remain costly, labor-intensive, and spatially restricted.

2.5.1 Remote sensing for Tree Species Distribution

Early work with Landsat data provided insights into forest type classification, but often failed to capture details at the species-level due to mixed pixels and moderate spatial resolution (Griffiths et al., 2014). Medium-resolution sensors, such as Sentinel-2, have recently advanced tree species mapping due to their red-edge and Shortwave Infrared (SWIR) bands, which offer frequent revisit cycles. Immitzer et al. (2016) demonstrated the ability to separate seven deciduous and coniferous species in Bavaria at 10m resolution using supervised classification. Later, Hemmerling et al.(2021) showed that incorporating multitemporal Sentinel-2 data with Sentinel-1 further improved classification accuracy by exploiting phenological differences between species. Similarly, Persson & Lindberg (2018) confirmed the value of Sentinel-2 satellite imagery for identifying species in boreal environments.

Radar and LiDAR sensors complement optical imagery by capturing detailed information about forest structure. Fagua et al. (2021) revealed that Sentinel-1 radar backscatter correlates with species diversity in tropical forests, while Bruggisser et al. (2021) found moderate correlations between radar-based forest structure, such as tree height, cover, and diversity in temperate forests. LiDAR has proven helpful for estimating vertical forest structure, height, crown size,

and stem density, and it is critical for biomass and carbon stock estimation (Bergen et al., 2009; Steinmann et al., 2013).

2.5.2 Methodological Approaches: From MaxEnt to Ensemble Classifiers

Different statistical and machine learning approaches have been applied in the modeling and predicting tree species distribution and diversity using RS and field-based data.

i) Maximum Entropy (MaxEnt): MaxEnt is one of the most popular species distribution models and is primarily helpful for presence-only data. Chiang et al. (2016) applied the MaxEnt approach with Landsat-8 imagery and topographic variables in Mongolia to generate probability maps of tree species distribution. This approach successfully identified species-environment relationships but overestimated species distribution, highlighting the need for additional explanatory variables.

ii) Random Forests (RF): An ensemble machine learning approach that effectively handles high-dimensional spectral data. Liu et al. (2018) combined Landsat-8, Sentinel-2, and Digital Elevation Model (DEM) data in subtropical China to classify four tree species. This achieved an accuracy of 82.8%, with the inclusion of terrain data further improving the results. Alberto et al. (2018) compared RF, SVM, and K-nearest Neighbor (KNN) for Andes Mountain forests modeling and found that the RF approach performs well, particularly when integrating DEM variables with spectral data.

iii) Support Vector Machines (SVM): This approach is effective in high-dimensional spectral spaces, particularly for Sentinel-2 and hyperspectral data. Studies by Immitzer et al. (2016) and Hemmerling et al. (2021) demonstrated that the SVM method captures more minor spectral and phenological differences between species, producing high classification accuracy in heterogeneous forest environments.

iv) K-nearest Neighbor (KNN): This method is a simple classifier, used as a baseline in several studies (Alberto et al., 2018). While capable of classifying forest types, KNN is more sensitive to noisy data and less accurate in complex environments,

2.5.3 Mapping Tree Species and Abundance

Beyond species classification, RS has been applied to estimate tree diversity indices such as the Shannon-Wiener Index (H'), Simpson's Diversity Index (D_2), Species richness (S), and Species evenness (J'). The spectral variation hypothesis, that higher spectral heterogeneity corresponds to higher biodiversity, has underpinned most research in this area (Rocchini et al., 2013). Rampheri et al. (2022) estimated tree diversity in South Africa's Blouberg Nature Reserve using remotely sensed data and bioclimatic variables, linking results to community-based conservation efforts. Reyes-Palomeque et al. (2021) mapped forest age classes in Mexico's Yucatan Peninsula, relating age to structural and compositional attributes of forest species

diversity. Their study confirmed that RS-derived forest age maps can provide valuable insights into successional dynamics, which are critical for biodiversity conservation and effective forest management.

3.0 Materials and methods

This chapter describes the study area, the Essential Biodiversity (EBV) framework employed, the remote sensing datasets used, and the methodological approaches applied to data collection, processing, and analysis. Given the novelty of applying the EBV framework to assess and monitor biodiversity in West Africa, this section emphasizes the procedures developed during the research phase. The methodology was primarily tested across Ghana's ecological zones, spanning from dry savannah to moist evergreen forest and a forest reserve area; however, the framework can be adapted to other tropical landscapes. Therefore, its application in different ecological or climatic regions would require recalibration and streamlining datasets to country-based indicators that reflect local conditions and policy. Based on the outcomes of this study, it is already possible to anticipate which EBV indicators are most critical for explaining biodiversity change and carbon dynamics under varying environmental processes in Ghana. The EBV framework provided the foundation for organizing and harmonizing datasets for the country, focusing on three key EBV variables: Ecosystem structure, community composition (land cover, forest fragmentation, and above-ground biomass), and species populations (species diversity, distribution, and abundance). RS products, such as PlanetScope, Sentinel-1, Sentinel-2, and ESA Biomass datasets, provided spatially explicit inputs that enabled scalable assessments of land cover, fragmentation, and biomass. These were complemented by field-based data and online databases of species occurrence and diversity data to strengthen the robustness of the models and analysis.

3.1 Study area

In line with the thesis objectives, this study was conducted at two spatial scales: the entire country and the Bobiri Forest Reserve (BFR) in the Ashanti Region (Figure 4). Ghana is a country in West Africa bordered by Burkina Faso to the north, the Ivory Coast to the west, Togo to the east, and the Gulf of Guinea to the south (Figure 4). It covers an area of approximately 238,533 square kilometers. The country is ecologically diverse, ranging from the guinea savannah in the north to the wet evergreen forests in the south (Figure 5), making it an ideal setting for monitoring biodiversity and forest dynamics. Ghana experiences a tropical climate with mean annual temperatures between 21 ℃ and 34.3 ℃, and rainfall patterns ranging from 900 mm in the north to over 2000 mm in the south (Abbam et al., 2018). Despite having about 15 % of its land under protection, widespread anthropogenic pressures such as agriculture, logging, and mining continue to fragment forest landscapes and threaten biodiversity (Lawer, 2024).

For assessing forest tree species diversity (Objective I), which required field-based observations and remote sensing optical information, the BFR was the study area where a field data campaign was conducted. However, for all three other objectives: Assessment of land cover standards (objective II), the mapping of dominant tree species distribution and their population abundance (objective III), and the evaluation of the effects of climate change on AGB modulated by forest fragmentation and biodiversity (objective IV), the study covered the entire country. This broad coverage ensures consistency in evaluating ecological and conservation patterns across Ghana's heterogeneous landscapes. The BFR, which is located approximately 25 km northeast of Kumasi in the Ashanti Region of southern Ghana, lies between latitudes 6°40'−6°44' N and longitude 1°15'−1°22' W, covering approximately 30km² (Njomaba et al., 2024). Situated in the semi-deciduous forest zone, the BFR represents the country's broader forest structure. Its canopy is multilayered, averaging 40m with trees up to 60m tall, including a mixture of evergreen and deciduous species such as *Celtis zenkeri, Triplochiton scleroxylon, Sterculia rhinopetala, Negogordonia papaverifera*, among others (Djagbletey, 2014). This reserve experiences a bimodal rainfall pattern, with the major season occurring from April to July and the minor season from September to November, yielding an annual total between 1,200 mm and 1,750 mm. Temperatures remain high year-round, with mean maximum yearly values around 31℃. Topographically, the reserve features a slightly undulating (6-7%) slope with elevations ranging from 180 m to 145m above sea level. The soils vary from sandy to clay and leached sandy-silt types, supporting a diverse range of vegetation. (Djagbletey, 2014; Addo-Fordjour et al., 2009)

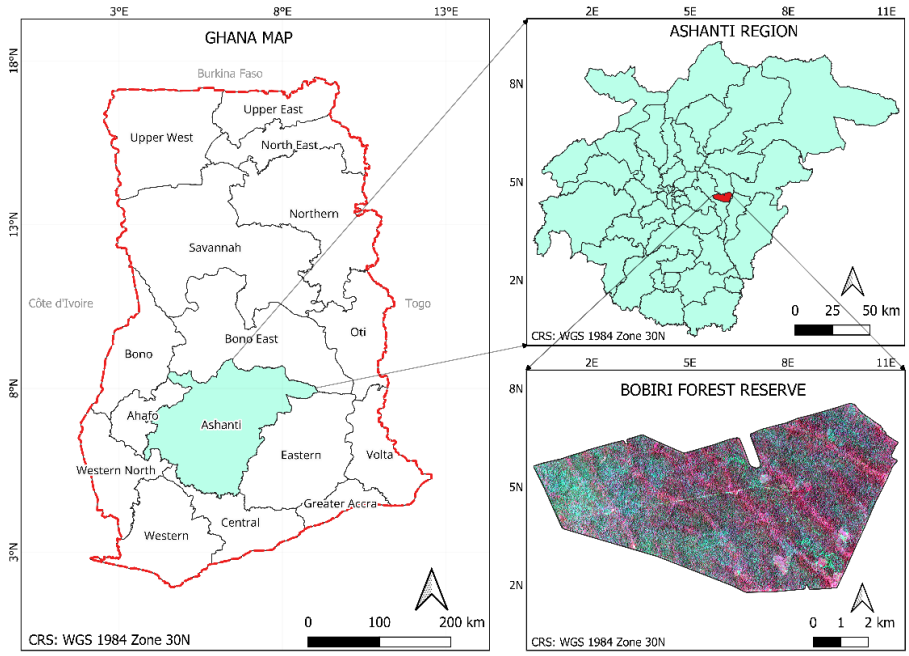

Figure 4: Study area. National map of Ghana with administrative regions and the Ashanti Region highlighted; inset of the Ashanti Region showing districts and the location of BFR (top right); false-color composite of the BFR (bottom right)

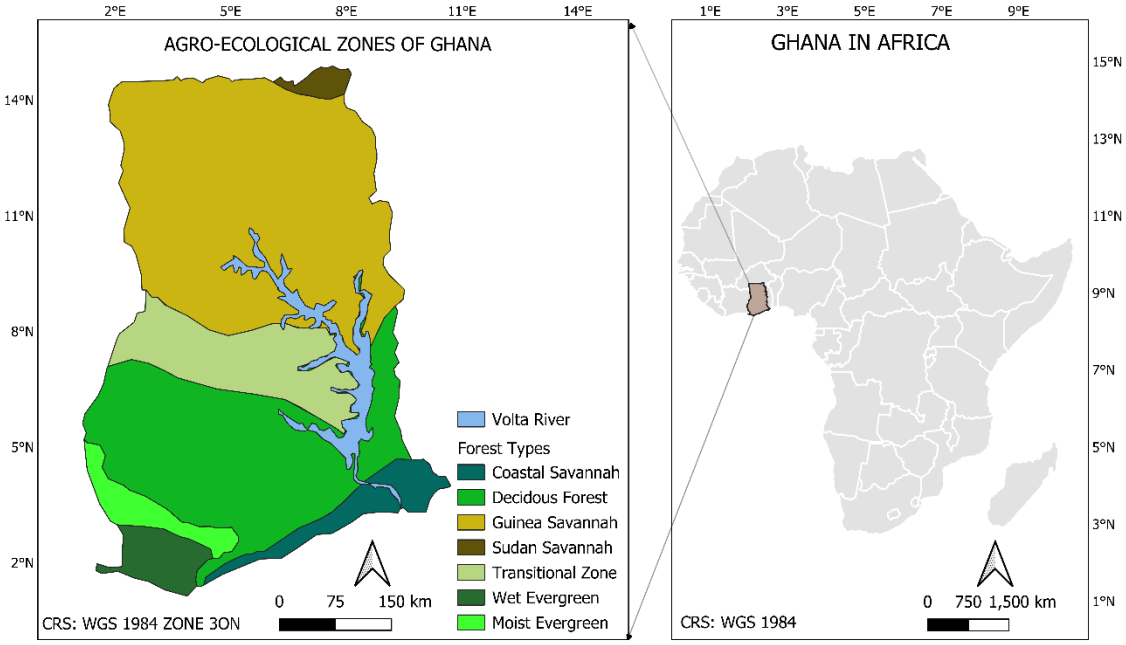

Figure 5: Map of the main ecological zones of Ghana (left) and the country's location within Africa (right).

3.2 Methods

3.3.1 Application of the Essential Biodiversity Variable (EBV) Framework

This study operationalized the EBV framework proposed by the Group on Earth Observation Network (Pereira et al., 2013; Pettorelli, 2016) as an organizing principle for biodiversity monitoring and assessment in Ghana. EBVs provide a globally recognized structure for harmonizing biodiversity measurements across scales, like field observations, RS products, and policy-relevant indicators (Pereira et al., 2013; Pettorelli, 2016). Given Ghana's vast size and ecological heterogeneity, ranging from savannas to semi-deciduous forests and moist evergreen forests, the EBV framework provided a practical means to focus on a limited yet representative and essential set of measurable variables. These variables were selected according to three main criteria:

i. Ecological and conceptual relevance: candidate EBVs were chosen to capture the ecological processes that are most critical to Ghana's forest ecosystem, especially those related to land cover, biomass dynamics, and species diversity. According to Jetz et al. (2019), EBVs are designed to provide a standard set of essential measurements that bridge raw biodiversity observations and policy-relevant indicators. Their framework for species population EBVs, distinguishing between distribution and abundance within a space-time-species cube, re-echoes the importance of capturing both ecosystem structure and species populations as central dimensions of biodiversity monitoring. Applying this rationale, the selected EBVs in this study provide a robust foundation for

assessing forest biodiversity change in Ghana while ensuring alignment with globally recognized ecological priorities and frameworks.

ii. Feasibility of measurements: variables were included only where reliable data sources were available at an appropriate scale. For instance, PlanetScope imagery enables the estimation of species diversity at a high resolution of 3m, and the ESA Climate Change Initiative (CCI) Biomass data provide nationally consistent estimates of AGB at a 100m resolution. The Sentinel-1 and Sentinel-2 datasets provided high spatial resolution imagery for land cover classification. Similar approaches combining field-based inventories with RS products are feasible in the other EBV applications (Kissling et al., 2018; Pettorelli, 2016)

iii. Policy and conservation utility: The selected EBVs were also evaluated in terms of their potential to inform national policy processes and conservation priorities in Ghana. Forests are central to Ghana's commitments under the National Biodiversity Strategy and Action Plan (NBSAP II, 2016-2020); (Ministry of Environment, 2016), the REDD+ Strategy (Forestry Commission, 2015), and reporting obligations under the CBD and the SDGs. EBVs focusing on land cover, ecosystem extent, and species distribution directly address these policy needs by providing standardized and repeatable indicators that can guide conservation prioritization as well as climate adaptation strategies (Geijzendorffer et al., 2016)

Based on these criteria, a set of EBVs was selected to operationalize the four research objectives of this study. Figure 6 presents the conceptual framework for applying the EBV approach in Ghana, which links the study objectives to the selected EBV classes, their data sources, analytical processes, and outputs.

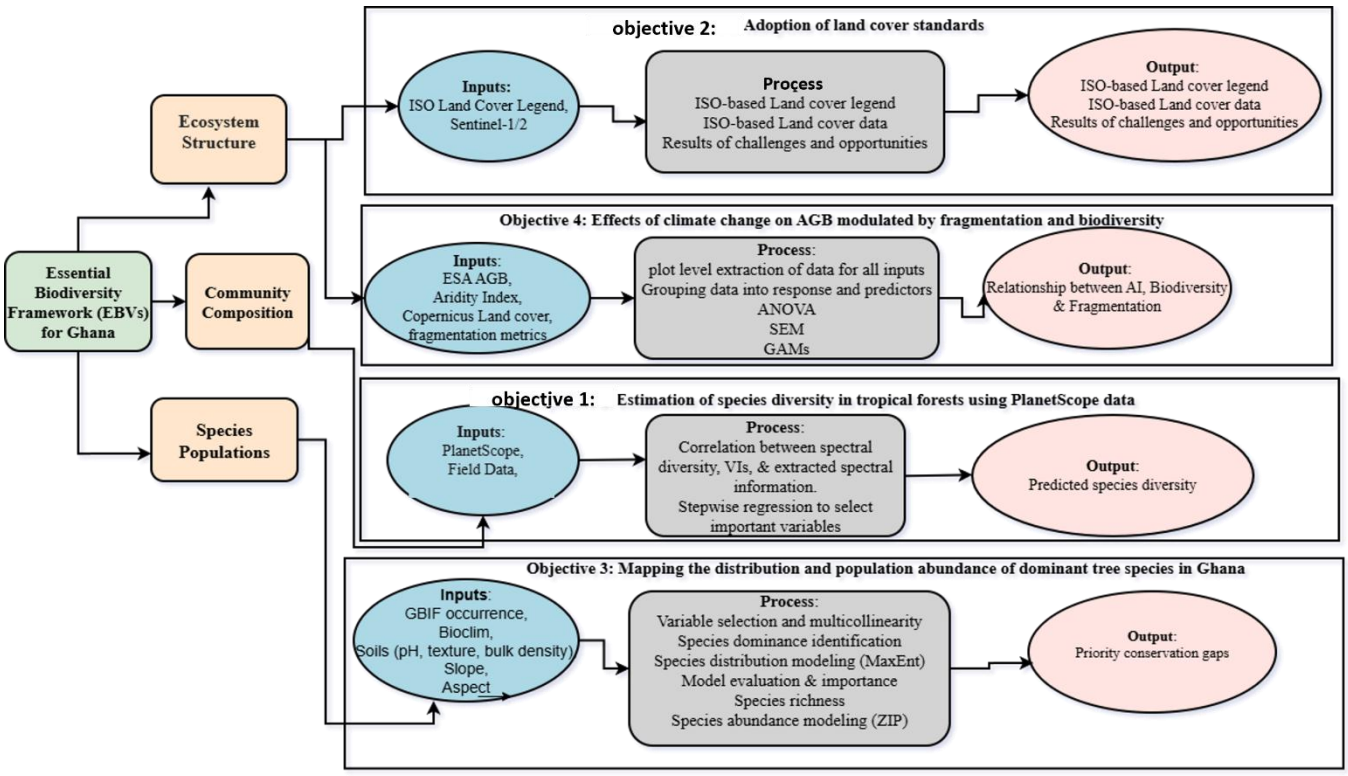

Figure 6: Conceptual framework for applying the Essential Biodiversity Variables (EBVs) approach to biodiversity monitoring in Ghana. The framework links study objectives to EBV classes and outlines processes.

3.3.2 Data Collection and Sources

This study integrated multiple datasets to operationalize the EBV framework, combining RS products, biodiversity vegetation databases, and field-based observations. Data was collected around the selected EBV classes: Ecosystem structure, community composition, and species populations.

3.3.2.1 Field sampling protocol and tree species data collection (Objective 1, Paper I)

Following established protocols for forest inventory, plot sizes ranging from 20 to 200 m² are commonly applied in tall shrub communities, while plot sizes of 200- 25000 m² are recommended for trees in forest ecosystems (Mapfumo et al., 2016; Mutowo & Murwira, 2012). Based on this guidance, a 20 m x 50 m plot size was established for tree species sampling in the BFR. A total of 35 plots was established using a simple random sampling approach with a minimum spacing of 200m between plots to reduce spatial autocorrelation (Oli & Subedi, 2015). Plot locations were also influenced by accessibility, as some areas of the forest were inaccessible. Plot coordinates were recorded using a Global Position System (GPS)- enabled mobile device with a field mapping application. Within each plot, all trees with a diameter at breast height (DBH) ≥ 5cm were measured using a diameter tape, while tree height was recorded using the TruePulse laser rangefinder. Species identification was conducted in the field with the

assistance of a field taxonomist, and their nomenclature was checked against the World Flora online database (WFO, 2021) to ensure taxonomic accuracy. In total, 311 individual trees of the most dominant species were sampled during the June 2023 campaign (Figure 7). The dominant species list was determined through preliminary consultations with forest reserve staff, local experts, and researchers at the Forestry Research Institute of Ghana (FORIG). These species were prioritized because of their ecological importance, prevalence in the reserve, and relevance to biodiversity assessment (Njomaba et al., 2024).

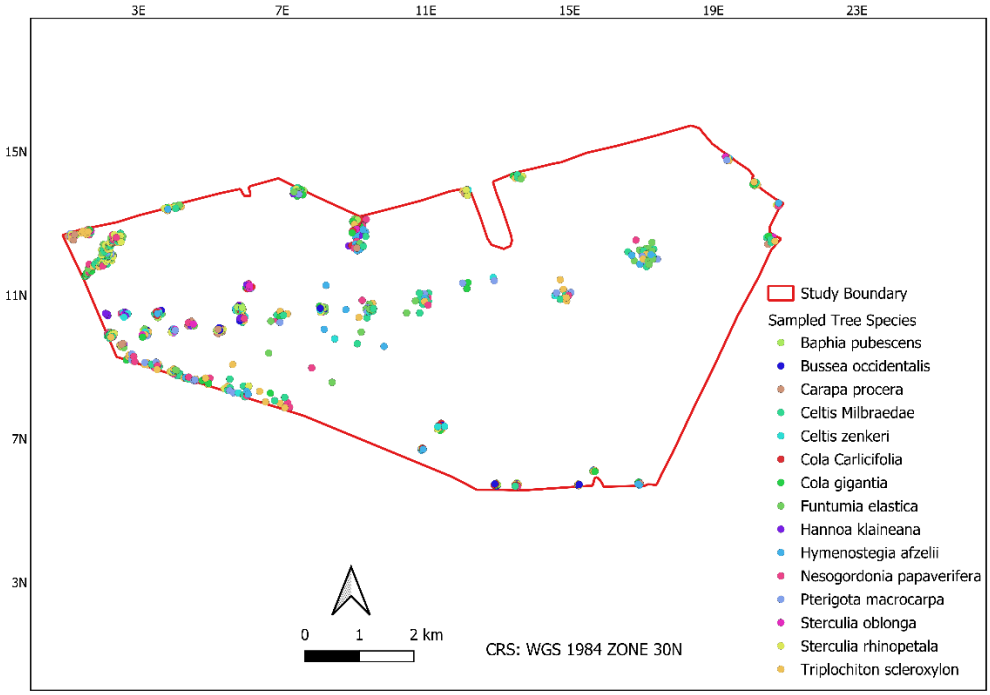

Figure 7: Spatial distribution of sampled tree species within the BFR. The study boundary is in red, with points representing individual trees.

3.3.2.2 Land cover legend and training data collection (Objective 2, Paper II)

To collect training and validation data for preparing a land cover legend, a definition needs to be established from which the land cover classes can be selected and mapped (Njomaba, Mushtaq, et al., 2025). Defining the land cover legend is an essential step in the land cover mapping process, as it provides a method to express the contents of a map (Mushtaq et al., 2022). The legend reflects how the semantic generalization of a specific geographic area has been conceived (De Simone et al., 2022). The categorization process minimizes real-world complexities, where different landscape area types are distributed vertically. Since the definition of classes is an arbitrary process by nature, not establishing a legend for land cover mapping may lead to uncertainties that will affect the accuracy of the final land cover map. It is therefore crucial that the definition of the land cover class meets two minimum requirements: (i) clear and unambiguous class definitions, and (ii) a class boundary that does not overlap with other legend classes (Haub et al., 2015). The West African Land Cover Reference System

(WALCRS) meets these requirements (Gregorio et al., 2022). The WALCRS meets these requirements. The WLCRS is based on three levels, with the schema divided into two broad categories: vegetated and non-vegetated lands. The vegetated category is divided into natural and cultivated, while the non-vegetated category is divided into terrestrial non-vegetated and water (Figure 8). With these broad categories, the various levels are further divided based on their physiognomic or structural characteristics and improved with additional qualitative criteria to classify land features (Mushtaq et al., 2024). In line with recommendations, the WALCRS, which is defined using ISO 19144 LCML (ISO 19144-2, 2012), was used to identify the land cover classes, existing sub-national legends, and datasets for developing an established national legend. National land cover classes were finalized in consultation with national partners, mainly the CERSGIS, the Forestry Commission of Ghana, the Land Use and Spatial Planning Authority (LUSPA), and the Council for Scientific and Industrial Research (CSIR). Workshops were organized using online platforms to identify and agree on the land cover classes, followed by an in-person workshop to validate the land cover classes that had already been defined.

	LEVEL I	LEVEL II	LEVEL III	LEVEL IV	LEVEL V	LEVEL VI	LEVEL VII
Land Cover Legend	Vegetated	Natural and Semi-Natural	Terrestrial	Tree Dominated	Closed	Evergreen	Evergreen
						Dciduous	Dciduous
						Mixed	Mixed
					Open	Evergreen	Evergreen
						Dciduous	Dciduous
						Mixed	Mixed
					Very Open	Evergreen	Evergreen
						Dciduous	Dciduous
						Mixed	Mixed
					Sparse	Sparse	Sparse
				Shrubs Dominated	Closed	Closed	Closed
					Open	Open	Open
					Very Open	Very Open	Very Open
					Sparse	Sparse	Sparse
				Herbs dominated	Closed	Closed	Closed
					Open	Open	Open
			Aquatic or Regulary flooded	Woody dominated areas	Woody Mangroves	Tree Mangrove	Closed Tree Mangrove
							Open Tree Mangrove
						Shrub Mangrove	Closed Shrub Mangrove
							Open Shrub Mangrove
				Herbs dominated areas	Herbs dominated areas	Herbs dominated areas	Herbs dominated areas
		Cultivated/Managed	Cultivated Rainfed	Tree crop plantation	Orchards	Orchards (single crop)	Date Palms
						Orchards (multiple crop)	Orchards (multiple crop)
				Shrub crop	Single layer shrub crop	Qat	Qat
						Cofee	Cofee
					Mixed shrub crop	Mixed shrub crop	Mixed shrub crop
				Herbaceous Crops	Herbaceous Crops	Herbaceous Crops	Herbaceous Crops
			Cultivated Irrigated	Tree crop dominated	Orchards (single crop)	Date Palms	Date Palms
					Orchards (multiple crop)	Orchards (multiple crop)	Orchards (multiple crop)
				Shrub crop dominated	Single layer shrub crop	Qat	Qat
						Cofee	Cofee
					Shadowed shrub crop	Mixed shrub crop	Mixed shrub crop
				Herbaceous Crop dominated	Herbaceous Crop domonated	Herbaceous Crop domonated	Herbaceous Crop domonated
	Non-Vegetated	Terrestrial Non-Vegetated	Natural	Rocks, Coarse Fragments	Bare rocks	Volcanic rocks	Volcanic rocks
						Other Bare Rocks	Other Bare Rocks
					Stony desert	Stony desert	Stony desert
				Soil, Sand deposits	Sandy area	Sandy soil	Loosen and Shifting sand
							Dunes
						Beaches	Beaches
					Bare soil	Bare soil	Bare soil
			Artificial	Buit-up linear & others	Buit-up linear & others	Buit-up linear & others	Buit-up linear & others
				Extraxtion sites – Mine/Quarry	Extraxtion sites – Mine/Quarry	Extraxtion sites – Mine/Quarry	Extraxtion sites – Mine/Quarry
				Built-up Non-Linear	Urban Areas	Urban Areas	Urban Areas
					Rural Villages	Rural Villages	Rural Villages
					Industial and other	Industial and other	Industial and other
					Infrustructure	Airports	Airports
						Other Infrustructure	Other Infrustructure
		Water	Natural	Permanent	Wadi	Wadi	Wadi
					Lagoons	Lagoons	Lagoons
				Seasonal	Wadi	Wadi	Wadi
					Organic deposits	Sebkha	Sebkha
			Artificial	Hydrological Structure	Dams	Dams	Dams
					Fish ponds	Fish ponds	Fish ponds

Figure 8: West African Land Cover Reference System (Gregorio et al., 2022)

Training and validation data collection for land cover classification were done through photo-interpretation techniques using Collect Earth Online (CEO) (CEO, 2018). This allows for integrating files that can be opened in Google Earth Pro with high-resolution imagery. Within the CEO, a project was created using a 10m x 10m plot design, each containing five sample points (Figure 9a). A total of 4,000 samples were randomly allocated across the country, with 10% of these points intentionally repeated as a quality control mechanism. The CEO platform was particularly valuable because of its ability to integrate multi-source satellite data (Sentinel-1 composites, Sentinel-2 composites, Norway's International Climate and Forest Initiative (NICFI) planet mosaics, Mapbox satellite, Google Earth, and OpenStreetMap) and to provide high-performance computing services for large-scale data interpretation. The Google Earth integration further enhanced the workflow by enabling users to export and visualize plots directly in the Google Earth Pro software (Figure 9b). Google Earth Pro also provides a time slider tool allowing users to navigate through imagery from different periods, facilitating temporal comparisons and seasonal assessments. Additionally, the Geo-dash widget within CEO was utilized to analyze NDVI time series, enabling seasonal dynamics to be factored into the interpretation (Figure 10). To address the underrepresentation of some classes and improve classification reliability, an additional 3,577 manually interpreted samples were incorporated, resulting in a total dataset of 7,677 training and validation points (Figure 11). For quality and consistency, the collected samples were reviewed several times and cross-checked with ancillary datasets and existing land cover products. Where differences arose, interpretations were refined. The final dataset was split into 70% training and 30% validation to support classification and accuracy assessment.

(a) (b)

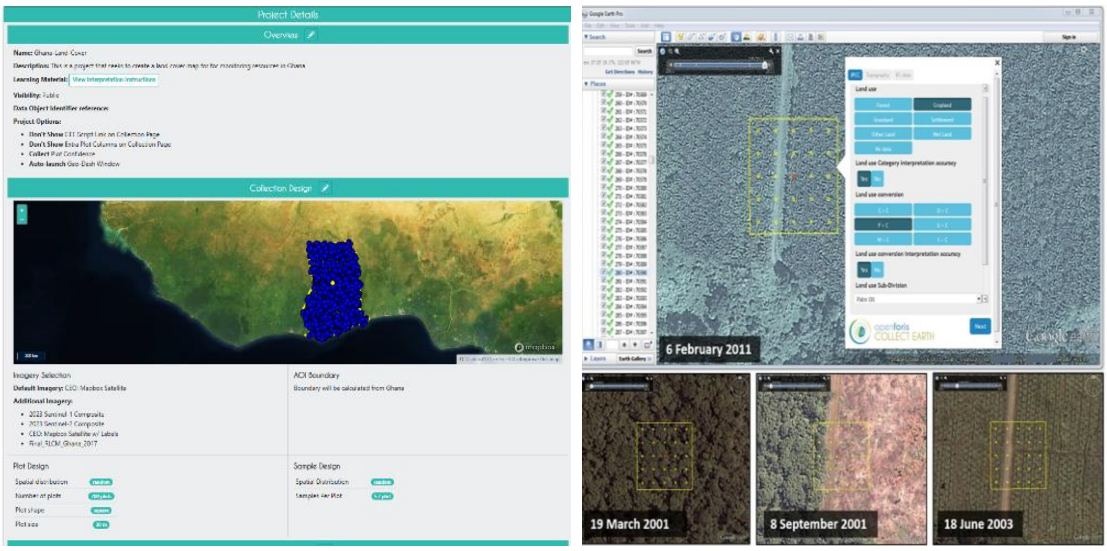

Figure 9: (a) Collect Earth online platform with training data distributed across Ghana, (b) Google Earth Pro visualization of plots with the time slider tool (CEO, 2018)

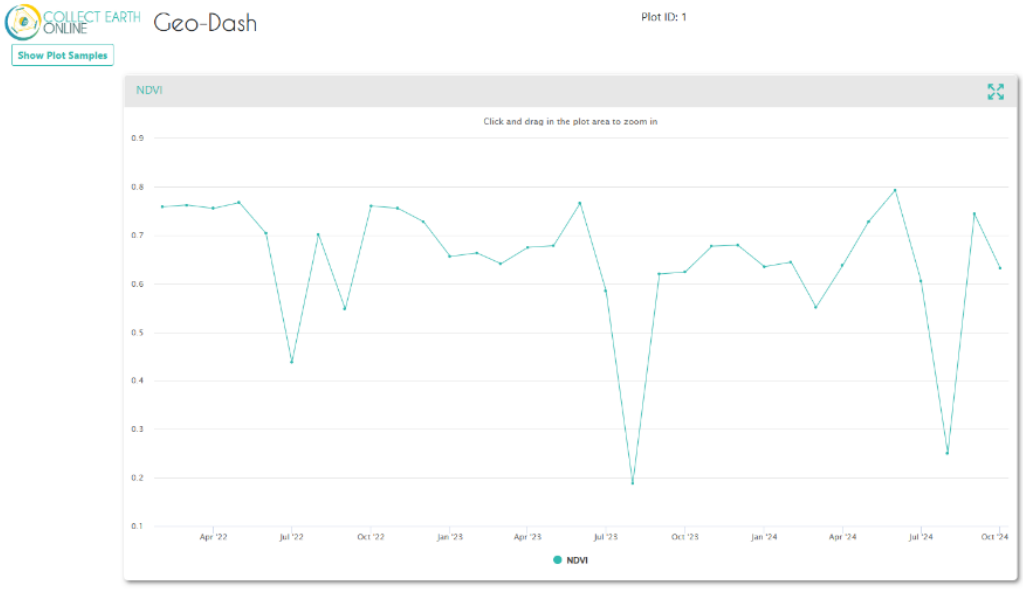

Figure 10: Normalized Difference Vegetation Index (NDVI) time series from the CEO Geo-Dash widget. Temporal profile used during training collection to validate land cover interpretations by capturing seasonal vegetation variability across 2022-2024.

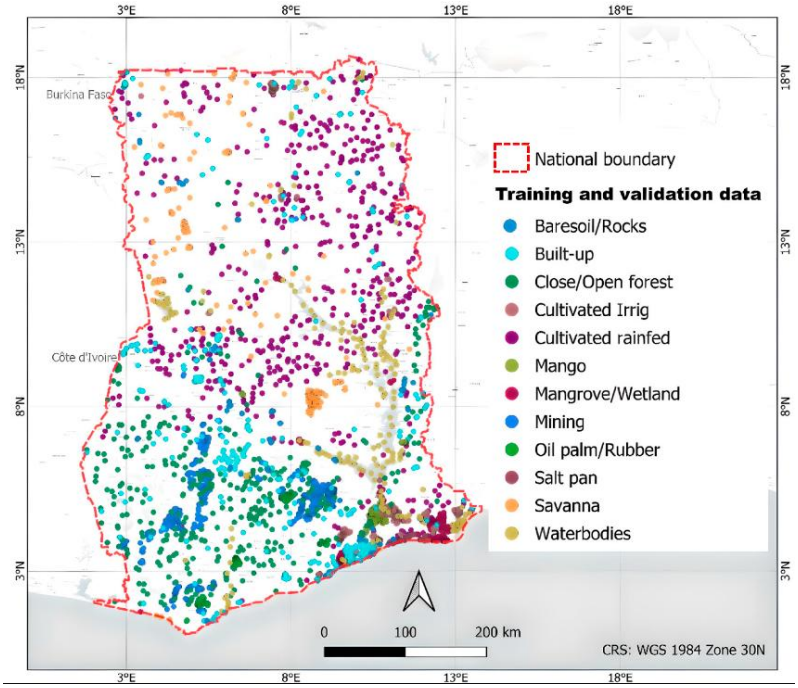

Figure 11: Spatial distribution of training and validation data.

3.3.2.3 Survey data collection (Objective 2, Paper II)

As part of the data collection for objective 1 of this thesis, a structured questionnaire survey was conducted in 2024 to evaluate the challenges and opportunities associated with adopting and implementing land cover standards. The rationale for this survey was to incorporate perspectives of stakeholders actively involved in land cover and land use activities across different geographic scales, thereby ensuring that Ghana's experience could be situated within broader international contexts. The study aimed to gain comparative insights into global

progress and barriers to adopting land cover standards by engaging experts beyond Ghana. The questionnaire was created using Google Forms to ease access and ensure global participation from a vast network of potential respondents, including representatives from government agencies, academia, private institutions, and international organizations. The survey was sent to 800 individuals across 400 organizations. The survey included questions on familiarity and use of LCML standards, adoption of alternative land cover standards, and experiences of non-users of any standards, thereby allowing a comprehensive overview of user contexts and challenges.

3.3.2.4 Vegetation data (GBIF) (Objectives 3 and 4, papers III and IV)

Vegetation data were obtained from the GBIF (https://www.gbif.org/) (Asare, 2021), a biodiversity data infrastructure that provides open access to species records contributed by herbaria, research institutions, and citizen science initiatives. GBIF is particularly valuable in West Africa, where a large amount of vegetation data exists but is often scattered across institutions and underutilized in ecological research. The platform harmonizes records using standardized metadata structures such as Darwin Core, ensuring interoperability and consistency across datasets.

For this study, approximately 30,000 raw records of tree species were initially downloaded for Ghana (Figure 12). The datasets comprised information from multiple sources, including herbarium collections, field notes, and survey data. A comprehensive data cleaning processing workflow was applied to ensure the reliability and consistency of the dataset. Records with missing coordinates, uncertain taxonomy, or locations outside Ghana's national boundaries were excluded. A temporal filter restricted the dataset to records collected between 2000 and 2013, resulting in 9,716 unique records.

All occurrence record points were spatially intersected with the national land cover data prepared by (Njomaba, Mushtaq, et al., 2025) to retain only those within the forest land cover class. This masking step excluded records located in non-forest areas, thereby ensuring only forest-related records were used in subsequent analysis. To reduce spatial bias inherent in GBIF records, a spatial thinning procedure was applied to minimize clustering in heavily sampled regions. Records within certain buffer radii were applied. Records within the radii were merged, retaining a single representative occurrence per grid cell. This process was performed to evaluate the robustness of subsequent analysis and to address residual spatial autocorrelation. Moran's I diagnostics confirmed that the spatial thinning effectively reduced autocorrelation to acceptable levels.

The resulting thinned dataset provided broad coverage across Ghana's major ecological zones and formed the foundation for species richness, fragmentation, AGB, and species distribution analysis. Although GBIF data are inherently limited by sampling bias and inconsistent

taxonomic resolution, the rigorous filtering, spatial standardization, and validation steps undertaken have ensured data quality suitable for robust ecological modeling. GBIF provided a reliable and cost-effective source of vegetation data that complemented RS and field-based datasets used in this thesis.

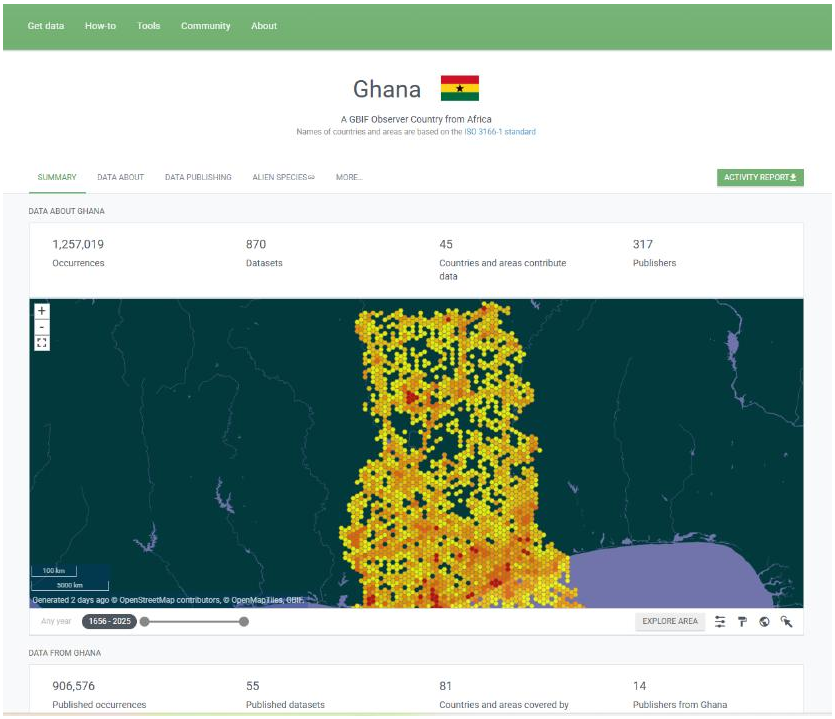

Figure 12: Vegetation occurrence records for Ghana obtained from the GBIF portal (Asare, 2021).

3.4 Remote sensing and environmental datasets (Objectives 1, 2, 3, and 4, papers I, II, III and IV)

Various RS and environmental datasets were assembled to provide information on Ghana's vegetation, biomass, climate, and site conditions. Satellite products included multi-sensor imagery from PlanetScope, Sentinel-2, and Sentinel-1, which offered high and moderate-resolution data for extracting vegetation indices, spectral bands, and textural variable analysis. These datasets were complemented by the ESA CCI Biomass products (Santoro & Cartus, 2024), AGB at 100 m resolution, enabling consistent assessment of forest carbon stocks nationally. Additionally, GEDI footprint data were used to validate AGB estimates, providing an independent benchmark for assessing the accuracy of the satellite-derived biomass layers. Climate information was obtained from the Global Aridity and Potential Evapotranspiration Database (Zomer et al., 2022), which provides long-term estimates of the aridity index derived from precipitation and evapotranspiration balances. This dataset was critical for quantifying the spatial variation in aridification that limits biomass accumulation and species distributions. Additional environmental predictors included the 19 BIOCLIM variables (BIO1-BIO19) from the Worldclim v2.1 database (Booth, 2025), which capture long-term (1970–2000) averages of temperature and precipitation regimes, including seasonality and extremes, and are widely used in ecological and species distribution modeling.

Topographic variables (elevation, slope, and aspect) were derived from the Shuttle Radar Topographic Mission (STRM) DEM at ~1 km resolution. Soil properties (soil pH, organic carbon density, and soil texture, including sand, silt, and clay) were obtained from the SoilGrids database at a 250 m resolution and resampled to 1 km to match the climate layers.

3.4.1 Satellite Image Processing

3.4.1.1 PlanetScope imagery (Objective 1, Paper I)

The PlanetScope surface reflectance products incorporate geometric, radiometric, and atmospheric corrections. Images were selected from May 2023 to coincide with field data collection, ensuring standard quality, absence of cloud cover, and complete coverage of the study area. Four cloud-free image mosaicked scenes were downloaded, and a region of interest (ROI) subset was extracted. Spectral reflectance values of each band were extracted using a 3 x 3 window pixel aggregation, with the mean value applied to approximate plot size conditions (Njomaba et al., 2024).

3.4.1.2 Sentinel-2 and Sentinel-1 (Objective 2, Paper II)

Sentinel-2 surface reflectance imagery covering October 2022 to October 2023 was processed in the GEE platform. Cloud and shadow masking were applied, and spectral indices, including NDVI, NDBI, NDWI, and SAVI, were derived to enhance discrimination between land cover classes, especially similar vegetation types. Median composites were generated, and Gray-level co-occurrence matrix (GLCM) texture features were calculated on NDVI images to capture spatial patterns. Sentinel-1 Ground Range Detected (GRD) data from ascending orbits (VV and VH polarizations) were obtained for the same period. Backscatter metrics, including mean, standard deviation, percentiles, and VV/VH ratios, were extracted. Texture measures were also derived to characterize spatial heterogeneity, which was particularly useful for distinguishing forests from agricultural mosaics. (Njomaba, Mushtaq, et al., 2025).

3.4.1.3 Remote sensing derived information (Objectives 3 and 4, papers III and IV)

For objectives 3 and 4, RS and environmental products datasets were used to quantify AGB, AI conditions, and forest fragmentation conditions at the plot level. Circular buffers were established around each GBIF tree record to harmonize point-based biodiversity records with gridded RS layers. All raster values intersecting these buffers were extracted, and plot-level summaries were generated through aggregation. AGB was derived from the ESA CCI Global Biomass product (v5.0.1, 100m resolution, 2020), calibrated against GEDI footprint data to correct regional bias and improve accuracy. AGB values were aggregated to obtain the mean biomass (Mg ha $^{-1}$), representing the oven-dry mass of trees.

Aridity was extracted from the Global AI dataset (1960 – 2000), while forest fragmentation metrics – number of patches (NP), edge density (ED), mean patch area (AREA_MN), landscape shape (LSI), and mean shape index (MSI) were computed from reclassified forest/non-forest masks of the national land cover dataset of Ghana. The fragmentation metrics were standardized using Principal Component Analysis (PCA) to produce a composite fragmentation index.

For the species distribution and abundance analysis (Objective 3), RS-derived covariates, including the digital elevation model (DEM) - derived variables (elevation, slope, and aspect), climatic layers from WorldClim, forest land cover, vegetation indices, and soil datasets were used as explanatory variables to model the spatial patterns of dominant tree species. A summary of all RS and environmental datasets used in this study, including their spatial and temporal characteristics, variables, and applications, is presented in Table 4.

Table 4: Remote sensing and environmental datasets used in this study

Dataset/Source	Year of acquisition	Spatial resolution	Variables/ Description	Application in the study
PlanetScope (Planet Labs Inc.)	2023	3m	B2, B3, B4, B5, B6, B7, B8, NDVI, EVI, SRI, SAVI, NDRE	Assessing forest species diversity (Objective 1, Paper I)
Sentinel-2 (ESA)	2023	10-20m	(B2, B3, B4, B5, B6, B7, B8, B9, B11, B12, SWIR, NDVI, SAVI, NDWI, NDBI; GLCM texture)	Land cover classification in Ghana (Objective 2, Paper II)
Sentinel-1 (Copernicus)	2023	10m	(VV, VH, VV/VH, SD of VV, SD of VH, 25th percentile, 75th percentile, GLCM)	Land cover classification in Ghana (Objective 2, Paper II)
ESA CCI Biomass	2020	100m	Aboveground biomass estimates (Mg/ha)	(Objective 4, Paper IV) Assessing AGB patterns, linking AGB to AI/diversity
GEDI	2019-2023	25m	Footprint level AGB	(Objective 4, Paper IV) Independent validation of ESA CCI AGB estimates
Global AI	1970-2000 baseline	~1km (30 arc-seconds)	AI derived from precipitation and Evapotranspiration	(Objective 4, Paper III) Assessing AGB patterns, linking AGB to AI/diversity
WorldClim Bioclimatic variables	1970-2000 baseline	~1km (30 are- seconds)	19 bioclimatic variables (e.g., BIO1 – BIO19)	(Objective 3, Paper III) Mapping distribution & Abundance
SoilGrids (ISRIC)	0-30 cm depth	250m (resampled to 1 km)	Soil texture, carbon density, pH, and bulk density	(Objective 4, Paper IV) Mapping distribution & Abundance

STRM (NASA)	Static	~1 km (30 arc-seconds)	Elevation, slope, aspect	(Objective 4, Paper IV) Mapping distribution & Abundance

3.5 Analysis

3.5.1 Estimating tree species diversity from PlanetScope data (Objective 1, Paper I)

Diversity metrics were quantified using the inventory data described in Section 3.3.2.1 and Figure 7, on a per-plot basis, using four indices (*S*, *H'*, D_2, and *J'*) (Table 5). These metrics were then related to PlanetScope spectral bands and vegetation indices through a stepwise linear regression approach. Model choice was guided by R^2, Root Mean Squared Error (RMSE), and Akaike Information Criterion. Information Criterion (AIC); Pearson correlations provided bivariate checks (Njomaba et al., 2024).

Table 5: Diversity indices used in this study and their equations

Species diversity index	Equation	Reference
Species richness (*S*)	$S = N$	(Morris et al., 2014)
Simpson index (D_2)	$D_2 = 1/\sum_{i=1}^{s} p_i^2$	(Morris et al., 2014)(Shannon, 1948)
Shannon index (*H'*)	$H' = -\sum_{i=1}^{s} p_i \ln(p_i)$	(Morris et al., 2014), (Rocchini et al., 2013)
Species Evenness (*J'*)	$J' = -\sum_{i=1}^{s} p_i \ln(P_i) / LN(S)$	(Carlo et al., 1998)

3.5.2 Land cover classification and accuracy assessment (Objective 2, Paper II)

The RF classifier was chosen for land cover mapping due to its non-parametric robustness and strong performance with high-dimensional predictors. RF builds an ensemble of decision trees and products by majority vote. The grid search tuned hyperparameters; the final model used 500 trees, mtry = 6, unlimited depth, and a 70/30 train/validation split (Figure 13). For the input features used in model prediction, the Sentinel-2 reflectance bands and indices, Sentinel-1 backscatter and textures, and GLCM textures on NDVI were computed to enhance class separability. Using the 30% validation data, the overall accuracy, producers' and users' accuracies, and Kappa were computed. Image processing, classification, and validation were done in GEE, and the script is published on the GitHub repository (Njomaba, 2025).

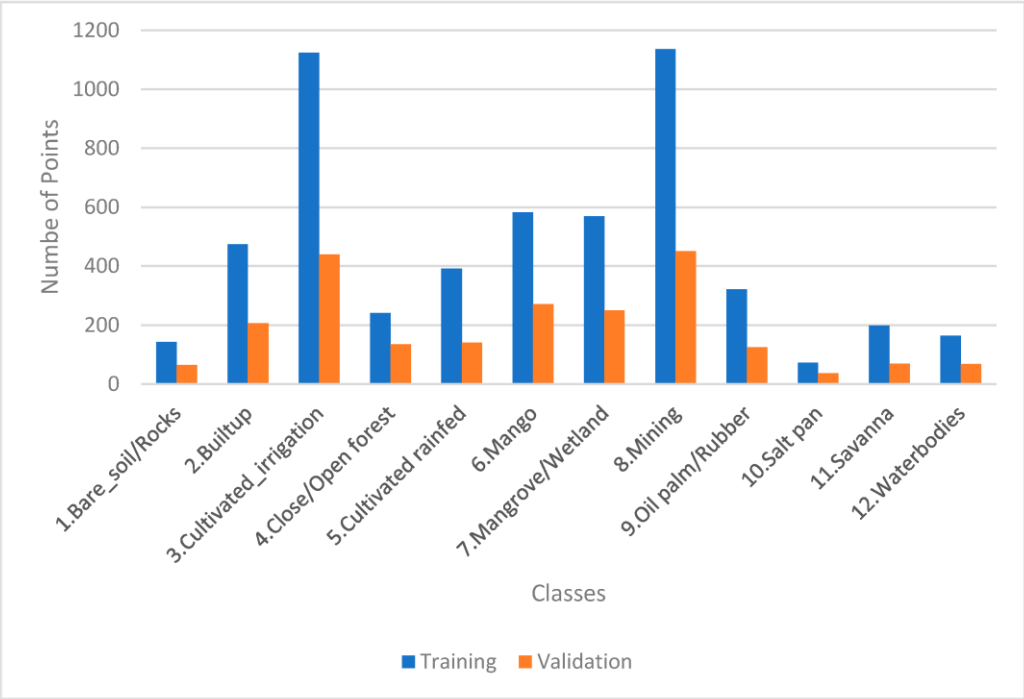

Figure 13: Distribution of training and validation data.

3.5.3 Species distribution, abundance, richness, and conservation gaps. (Objective 2, Paper III)

The Pearson correlation and Variance Inflation Factor VIF were used to perform a feature selection, removing variables with VIF > 10 and highly correlated, as shown in Table 6.

Table 6: Environmental variables used as predictors, selected after conducting a multicollinearity analysis.

Label	Variable	Unit
BIO3	Isothermality (BIO2/BIO7) x 100	%
BIO6	Minimum temperature of the coldest month	^{O}C
BIO13	Precipitation of the wettest month	mm
BIO19	Precipitation of the coldest quarter	mm
Soil pH	The (water)	pH × 10
Soil organic carbon density	Organic carbon content in the soil	T/ha
Soil texture- sand	Sand content in soil	G/kg
Soil-texture-silt	Silt content in soil	G/kg
Forest	Forest cover	N/A
Slope	Slope	m
Aspect	Aspect	Deg

The species occurrence data obtained from the GBIF contained species names, geographic coordinates, and source metadata. To ensure quality, duplicates and records with uncertain geographic coordinates were removed. Given the known issues of spatial clustering in aggregated biodiversity databases, a spatial thinning algorithm was applied at 1 km resolution using the *spThin* package in R (Aiello-Lammens et al., 2015). After cleaning and thinning, a total of 9,716 were retained. To align with forest monitoring standards in West Africa, the data were aggregated into circular plots (Chave et al., 2003). The plot occupancy approach was defined as the number and proportion of plots where a species occurs. This occupancy served as a proxy for relative dominance, providing a spatially interpretable measure of prevalence nationwide. Although presence-only records cannot capture absolute abundance, occupancy-based dominance is widely applied in distributional studies (Elith & Leathwick, 2009). Based on the plot occupancy assessment, the dominant species identified were: *Napoleaoneae leonensis*, *Myrianthus serratus*, and *Penianthus patulinervis*. These species represent ecologically distinct groups and were selected as focal species for modeling habitat suitability and abundance.

Habitat suitability for the three dominant species was modeled using MaxEnt, which estimates a maximum-entropy distribution constrained by environmental covariates as implemented by (Phillips et al., 2006) in the equation:

$$p(x) = \frac{1}{Z} exp\left(\sum_{j} \lambda_j f_j(x)\right) \ldots\ldots\ldots\ldots\ldots\ldots\ldots (1)$$

Where are environmental features, are weights, and Z is a normalizing constant.

Presence-only occurrence was partitioned into five spatial folds using blocking to minimize spatial autocorrelation bias. Background points were sampled within a 30 km buffer around occurrences to ensure ecologically relevant contrasts. Models were fitted with default regularization, and suitability predictions were generated across Ghana. Evaluation metrics of the model were performed, such as:

- Area under the curve (AUC) with spatial cross-validation
- True Skill Statistic (TSS) across thresholds (0.1 – 0.9)
- Omission and commission diagnostics
- Response curves for predictor variables
- Jackknife tests for variable contributions

Species abundance was estimated using the Zero-Inflated Poisson (ZIP) models applied to a 10 x 10 km grid. The ZIP formulation accounts for excess zeros typical in patchy species distributions, with a model adopted from (Lambert, 1992).

$$P(Y = y) = \pi 1_{y=0} + (1 - \pi)\frac{e^{-\lambda}\lambda^{y}}{y!} \ldots\ldots\ldots\ldots (2)$$

Where = probability of excess zeros, λ = Poisson mean, and is an indicator for zero counts. Environmental covariates were included in both the count and zero-inflation components. Models were compared using AIC and Pseudo-R^2. Predictions were bootstrapped (n = 50) to generate uncertainty surfaces, summarized by mean, standard deviation, and coefficient of variation.

Binary habitat suitability maps (applying thresholds per species based on evaluation metrics) were summed to derive species richness maps (Freeman & Moisen, 2008). To prioritize conservation, a composite conservation index was developed by integrating suitability and abundance, following the methods in Oliver et al. (2015):

$$Conservation\ Index\ =\ Suitability\ \times\ Abundance \ldots\ldots\ldots\ldots\ldots (3)$$

Cells in the top decile ($\geq 90^{th}$ percentile) of the composite conservation index distributions were designated priority areas. These were overlaid with Ghana's protected area (PA) data to quantify representation inside and outside PAs, highlighting conservation gaps (Joppa & Pfaff, 2009). (Njomaba, Aikins, et al., 2025)

3.5.4 Assessing the effects of climate change on aboveground biomass mediated by fragmentation and biodiversity.

The global AI (Zomer et al., 2022) was used as a proxy for long-term climate stress and water availability. AI values were subset to Ghana, extracted, and aggregated within a 500m buffer around each GBIF record. Following the UNEP classification scheme, AI values were categorized into four aridity classes (Table 7), serving as a space-for-time substitution (Blois et al., 2013).

Table 7: Classification of Ghana's climate zones based on the Aridity Index (AI) and their land area coverage. The aridity (AI) thresholds follow the United Nations Environmental Program (UNEP) aridity classification scheme. Values indicate the total area (km^2)

Aridity index (AI) values	Climate class (zones)
0.2 ≤AI<0.5	Semi-arid
0.5≤AI<0.65	Dry sub-humid
0.65≤AI<0.8	Sub-humid
0.8≤AI<1.3	Humid

These classes represented Ghana's ecological gradient as an analog for projected climate change impacts. A one-way analysis of variance (ANOVA) was conducted to test for differences in mean AGB across the four aridity zones. This assessed whether biomass declines systematically with increasing aridity. Scheffé's multiple comparison test was applied as a post-hoc procedure, given its robustness to unequal sample sizes and variances. Model formulation adopted from (Fisher, 1935)

$$Y_{ij} = \mu + \tau_i + \epsilon_{ij} \ldots\ldots\ldots\ldots\ldots\ldots (4)$$

Where Y_{ij} is the aboveground biomass of plot *j* in aridity class *i*, is the overall mean, is the effect of the aridity class, and is the error term.

Fragmentation metrics were derived from forest/non-forest rasters using the *landscapemetrics* package in R. Metrics derived are presented in Table 8

Table 8: Forest fragmentation metrics, equations for computation, and their descriptions. Variables include N = total number of patches, A = total landscape area, eik = total edge length of patch i, aij = area of patch j, m = number of patches, LSI = landscape. All metrics follow landscape ecological equations adopted from Enaruvbe & Atafo, 2018, and McGargical et al., 2023

Fragmentation metrics	Equation	Description
Number of patches (NP)	$NP = N$	Total number of patches in the class/landscape.
Landscape Shape Index (LSI)	$SI = \frac{0.25 \sum_{k=1}^{m} e_{ik"}}{\sqrt{A}}$	Overall shape complexity of forest patches
Mean Shape Index (MSI)	$MSI = \frac{LSI}{N}$	Average patch shape complexity
Edge density (ED)	$ED = \frac{\sum_{k=1}^{m} e_{ik"}}{A} X\ 1000$	Amount of edge relative to the landscape area.
Patch area mean (Area_MN)	$AREA_{MN} = \frac{1}{n}\sum_{j=1}^{n} AREA(patch_j)$	Typical patch area, reflecting habitat size

All predictors were standardized using z-scores before analysis. Multicollinearity among the five fragmentation metrics (NP, ED, AREA_MN, MSI, LSI) was evaluated using pairwise correlation and principal component analysis (PCA). Because these metrics were highly intercorrelated (|r| > 0.8 for ED–LSI and ED-AREA_MN), PCA was applied to reduce redundancy and derive an integrated fragmentation gradient. The first principal component (Frag_PC1) explained the majority of total variance and was used as a component fragmentation variable in subsequent models (Figure 14). After dimensionality reduction, Variance Inflation Factor (VIF) diagnostics were performed on the final set of model predictors to ensure that the combined predictors were not strongly collinear. All predictors exhibited VIF < 2 and tolerance > 0.8, confirming negligible multicollinearity and validating their inclusion in SEM and GAM analysis.

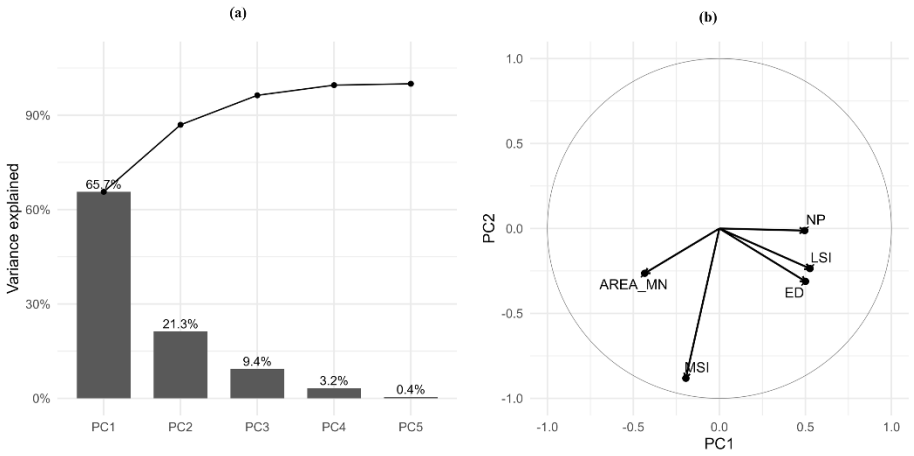

Figure 14: Principal Component Analysis of Fragmentation Metrics.

To assess the direct and indirect pathways through which AI influences AGB, we implemented both linear and nonlinear SEMs. SEMs were used to jointly estimate causal relationships among AI, fragmentation (Frag_PC1), biodiversity (S), and AGB, while accounting for spatial structures. The linear SEM was implemented using the "piecewiseSEM" package in R Studio, with each sub-model fitted as a generalized least squares (GLS) model that included an exponential spatial correlation structure based on plot centroids (x, y). This approach accounts for residual spatial autocorrelation while preserving parameter estimates. All variables were

standardized (z-scores) before modeling to allow comparison of path coefficients (β). The model structure was defined as:

$$\left\{\begin{array}{c} Frag_{PC1} \sim AI \\ Richness \sim AI \\ AGB_{cal} \sim AI + Frag_{PC1} + Richness \end{array}\right\} \quad (5)$$

This structure reflects hypothesized causal pathways where aridity influences forest structure and biodiversity, which in turn affect biomass accumulation. Model fit was evaluated using Fisher's C statistic, Akaike Information Criterion (AIC), and R2 values for each endogenous variable. Standardized path coefficients (β), standard errors, and significance levels were extracted.

To capture potential nonlinear relationships that the linear model could not represent, a complementary nonlinear SEM was developed using the GAM framework. Each sub-model was fitted using thin-plate regression splines with restricted maximum likelihood (REML) optimization in the "mgcv" package. The structure mirrored the linear SEM but specified smooth functions for key predictors:

$$\left\{\begin{array}{c} Frag_{PC1} \sim s(AI) \\ Richness \sim s(AI) \\ AGB_{cal} \sim s(AI) + s(Frag_{PC1}) + s(Richness) + s(x, y) \end{array}\right\} \quad (6)$$

Where s (.) denotes smooth terms and s(x,y) is a bivariate spatial smoother capturing broad-scale spatial autocorrelation. Smoothing bases (k) were selected to balance flexibility and model parsimony, with overfitting constrained by penalization (y = 1.4). Model performance was assessed using AIC, Fisher's C, and variance explained (R2) for each endogenous variable.

Generalized additive models (GAMs):

To explore non-linear relationships between AGB and predictor variables, we used spatial GAMs implemented in the "mgcv" package. The main model took the form.

$$AGB = s(AI, k = 9) + s(Frag\_PC1, k = 9) + s(Richness, k = 9) + s(x, y, k = 80) \quad (7)$$

Where s (.) denotes thin-plate regression splines, k specifies the basis dimension controlling smoothness, and s(x, y) represents a two-dimensional spatial smoother applied to buffer centroids to account for broad-scale autocorrelation. Models were fitted by REML with mild penalization (γ = 1.4) and automatic smooth selection to prevent overfitting. To evaluate the relative influence of individual metrics (NP, AREA_MN, ED, MSI, LSI), we fitted separate spatial GAMs of the form:

$$AGB = s(metric) + s(AI) + s(x, y), \quad (8)$$

with predictors standardized. For each model, we extracted smooth-term statistics (edf, F, p-value) and compared ΔAIC and ΔDev against a baseline model (AGB ~ s(AI) + s(s, y)) to quantify the added explanatory contribution of each metric. Model diagnostics included residual QQ-plots, k-index adequacy tests, and concurvity checks.

4.0 Results

The detailed research results are presented in four scientific articles. In this section, the most significant findings are synthesized, and the research questions posed in the thesis are addressed. The main goal of the thesis was to operationalize EBVs to monitor forest biodiversity change in Ghana by integrating RS and field-based approaches. To achieve this, the study adopted an exploratory framework that combined international land cover standards, optical RS datasets, a data assembly approach using the West African Vegetation Database, structural and climatic variables, and ecological modeling. These components provided an innovative framework for national-level biodiversity monitoring. The methods and framework applied in this research proved very promising for effectively monitoring and assessing changes in forest biodiversity. The framework enabled the focusing of key biodiversity indicators, considering factors such as feasibility, data availability, relevance to Ghana's biodiversity priorities, policy, and applicability to management.

The first objective of this thesis, which assesses forest species diversity in Ghana's tropical forests using PlanetScope data, was addressed in the first published article (Njomaba et al., 2024). The objective, addressed in the second article (Njomaba et al., 2025), focused on the adoption of land cover standards for sustainable development in Ghana, considering both challenges and opportunities. The third article, addressing objective three of the thesis (Njomaba et al., 2025), focuses on mapping the distribution and estimating the population abundance of dominant forest tree species in Ghana, with implications for conservation prioritization. The fourth article, submitted and yet to be published, addresses the fourth objective, which investigates the effects of climate change on aboveground biomass, modulated by forest fragmentation and biodiversity, in Ghana. All these objectives are linked to the three main EBV variables: class of community composition, ecosystem structure, and species population.

4.1 Assessing Forest Species Diversity in Ghana's Tropical Forest Using PlanetScope Data.

Elisha Njomaba[1], James Nana Ofori[2], Reginald Tang Guuroh[3], Ben Emunah Aikins[4], Raymond Kwame Nagbija[5], Peter Surový[1].

[1]Faculty of Forestry and Wood Science, Czech University of Life Sciences (CZU Prague), Kamýcká 129,165 21 Prague, Czech Republic.

[2]Biodiversity Research/Systematic Botany, University of Potsdam, Maulbeerallee 1, 14469 Potsdam, Germany.

[3]CSIR-Forestry Research Institute of Ghana, Kumasi P.O. Box UP 63, Ghana.

[4]School of Public Health, College of Health Sciences, University of Ghana, Accra, P.O. Box LG 13, Ghana.

[5]Faculty of Geoinformation Science & Earth Observation, Department of Natural Resource Management, University of Twente, Drienerlolaan 5, 7522 NB Enschede, The Netherlands

Remote Sens. 2024, 16(3), 463; https://doi.org/10.3390/rs16030463

Author´s contribution: 70 %

Summary of the article

In addition to spectral changes in tropical forests, biodiversity can be assessed through satellite-delivered indicators. This article investigated the potential of PlanetScope multispectral data (3m resolution) to predict forest tree diversity in Ghana's BFR. Tree inventory data collected from 35 plots, where taxonomic identification, DBH, and height measurements were used to compute four diversity indices: H', D_2, S, and J'. Corresponding spectral reflectance and vegetation indices (VIs), Normalized difference vegetation index (NDVI), Enhanced vegetation index (EVI), simple ratio index (SRI), Soil adjusted vegetation index (SAVI), and Normalized difference red edge index (NDRE), were extracted from PlanetScope imagery and statistically analyzed against the field-based diversity measures. The results revealed significant correlations between S and H' with spectral bands, particularly the red (Band 6) and blue (Band 2), while D_2 and J' showed weaker relationships. Stepwise regression models confirmed the predictive capacity of these bands, explaining 47% of the variance in S and 42% in the H'. Predictive diversity maps were generated using these models, showing clear spatial gradients of species richness and Shannon diversity across the reserve. The study demonstrates that PlanetScope data can provide an efficient, scalable approach to mapping forest species diversity in the tropics, complementing traditional field-based surveys.

Full article

remote sensing

MDPI

Article

Assessing Forest Species Diversity in Ghana's Tropical Forest Using PlanetScope Data

Elisha Njomaba [1,*], James Nana Ofori [2], Reginald Tang Guuroh [2,3], Ben Emunah Aikins [4], Raymond Kwame Nagbija [5] and Peter Surový [1]

[1] Faculty of Forestry and Wood Sciences, Czech University of Life Sciences Prague, Kamýcká 129, 165 00 Prague, Czech Republic; surovy@fld.czu.cz
[2] Biodiversity Research/Systematic Botany, University of Potsdam, Maulbeerallee 1, 14469 Potsdam, Germany; james.nana.ofori@uni-potsdam.de (J.N.O.); rtguuroh@csir-forig.org.gh (R.T.G.)
[3] CSIR-Forestry Research Institute of Ghana, Kumasi P.O. Box UP 63, Ghana
[4] School of Public Health, College of Health Sciences, University of Ghana, Accra P.O. Box LG 13, Ghana; benaikins56@gmail.com
[5] Faculty of Geoinformation Science & Earth Observation, Department of Natural Resource Management, University of Twente, Drienerlolaan 5, 7522 NB Enschede, The Netherlands; r.k.nagbija@student.utwente.nl
* Correspondence: njomaba@fld.czu.cz; Tel.: +420-773-101-545

Abstract: This study utilized a remotely sensed dataset with a high spatial resolution of 3 m to predict species diversity in the Bobiri Forest Reserve (BFR), a moist semi-deciduous tropical forest in Ghana. We conducted a field campaign of tree species measurements to achieve this objective for species diversity estimation. Thirty-five field plots of 50 m × 20 m were established, and the most dominant tree species within the forest were identified. Other measurements, such as diameter at breast height (DBH ≥ 5 cm), tree height, and each plot's GPS coordinates, were recorded. The following species diversity indices were estimated from the field measurements: Shannon–Wiener (H'), Simpson diversity index (D_2), species richness (S), and species evenness (J'). The PlanetScope surface reflectance data at 3 m spatial resolution was acquired and preprocessed for species diversity prediction. The spectral/pixel information of all bands, except the coastal band, was extracted for further processing. Vegetation indices (VIs) (NDVI—normalized difference vegetation index, EVI—enhanced vegetation index, SRI—simple ratio index, SAVI—soil adjusted vegetation index, and NDRE—normalized difference red edge index) were also calculated from the spectral bands and their pixel value extracted. A correlation analysis was then performed between the spectral bands and VIs with the species diversity index. The results showed that spectral bands 6 (red) and 2 (blue) significantly correlated with the two main species diversity indices (S and H') due to their influence on vegetation properties, such as canopy biomass and leaf chlorophyll content. Furthermore, we conducted a stepwise regression analysis to investigate the most important spectral bands to consider when estimating species diversity from the PlanetScope satellite data. Like the correlation results, bands 6 (red) and 2 (blue) were the most important bands to be considered for predicting species diversity. The model equations from the stepwise regression were used to predict tree species diversity. Overall, the study's findings emphasize the relevance of remotely sensed data in assessing the ecological condition of protected areas, a tool for decision-making in biodiversity conservation.

Keywords: PlanetScope data; Shannon diversity; species richness; tropical forest; species diversity indices; spectral bands; vegetation indices; ecosystem services; biodiversity conservation; spatial resolution

Citation: Njomaba, E.; Ofori, J.N.; Guuroh, R.T.; Aikins, B.E.; Nagbija, R.K.; Surový, P. Assessing Forest Species Diversity in Ghana's Tropical Forest Using PlanetScope Data. *Remote Sens.* **2024**, *16*, 463. https://doi.org/10.3390/rs16030463

Academic Editor: Michael Sprintsin

Received: 28 November 2023
Revised: 17 January 2024
Accepted: 23 January 2024
Published: 25 January 2024

1. Introduction

Forest biodiversity is essential to terrestrial ecosystems and provides humanity with many crucial ecosystem goods and services [1]. Some vital ecosystem services include the forest nutrient cycle, headwater conservation, and carbon storage [2]. Factors including

climate change, soil erosion, species introduction, and invasion cause changes in forest diversity [3]. Therefore, properly managing forest resources can help conserve biodiversity, water, and soil within forest ecosystems [4].

Tropical forests have a unique reputation for their global role in biodiversity conservation, climate stability, and human well-being [5]. Tropical forests also host the largest biodiversity in terrestrial ecosystems and play a fundamental role in the carbon cycle. Therefore, improvements in forest monitoring, such as understanding species richness and ecological and structural traits [6], are relevant for implementing climate change-related agreements for biodiversity conservation [7]. Long-term biodiversity conservation depends on knowledge of the vegetation structure, species richness, diversity, and ecological characteristics.

Measuring species diversity includes two components: richness and evenness. Richness refers to the total number of species within a given area, while evenness measures how similar species are in abundance [8]. Species richness and evenness are two independent diversity measure criteria that may differ in their response to local habitat factors [8]. Recent studies have shown that the relationship between richness and evenness appears weaker than expected [9]. These two diversity components may vary and could be influenced by different ecological factors. For instance, extreme weather in a highly diversified forest may cause species extinction, reducing species richness but increasing the distribution's evenness. Other studies have also demonstrated that species evenness could impact ecosystem productivity and other functions, as species richness does [10]. It is, therefore, logical that species evenness and richness are both considered to gain a deeper understanding of the effects of different species diversity patterns [11].

Various indices have been proposed to capture information about the species diversity of a plant community [12]. The main objective of a diversity index is to obtain a quantitative estimate of biological variability that can be used to compare biological entities in space or time. Species diversity indices can, therefore, be divided into simple and composite indices [13]. The most common simple index is species richness. However, this index usually under-emphasizes species abundance information [14]. Composite indices combine species richness and evenness into a single value and are widely used in ecology. These indices have the benefits of being simple to calculate and having a long application history. However, most of them prefer to express the information of only one component between richness and evenness and sacrifice the information of another component, such as the Shannon–Wiener (H') and Simpson index (D_2), which are the most used indices for describing species diversity in forest ecosystems [15]. A major additional drawback of a composite index is the ambiguity in its definition [15]. For example, the Shannon–Werner index can be interpreted as a measure of the uncertainty in the identity of an individual randomly selected from a community, where a higher degree of uncertainty implies greater diversity. The Simpson index is a probability that does not have a straightforward, ecologically meaningful interpretation [16]. From this perspective, it is necessary to consider all four diversity indicators: species richness, species evenness, Shannon–Wiener index, and Simpson diversity index to compensate for the weaknesses in each diversity index. This will give a much more detailed understanding of the forest diversity, considering the richness, evenness, abundance, and relative abundance among the other indicators.

Species diversity can be defined as the variability of living organisms in an ecosystem [4]. It may also be considered the diversity between and within species in a particular ecosystem [17]. Species diversity is a significant ecosystem component due to its role in the hydrological cycle and climate regulation [18]. Species diversity has declined globally despite the enactment of global conservation agreements, such as the Convention on Biological Diversity (CBD), in which most biodiversity hotspots are found in the tropics [19]. For instance, after decades of forest destruction, the tropical forests in Ghana have experienced extensive species extinction and diversity loss. Of the more than 2100 plant species found in forest zones of Ghana, 23 are endemic. Seven hundred and thirty economic tree species in the forest zones, most of which have a dimension of 5 cm or more at breast height, are

threatened or extinct [20]. Hence, the effective conservation of tree diversity in the tropical forests of Ghana is a critical priority, requiring the establishment of an effective approach capable of identifying early warning signs of diversity change at multiple scales [21]. This information is crucial for designing and introducing policies and management actions to halt the decline in tree diversity and create more resilient forest areas [22].

Remote sensing technology plays a crucial role in supporting biodiversity monitoring. Remote sensing data can provide information on an area to various extents, with shorter revisit times and lower costs than classical field surveys. Huesca et al. [23] argued that traditional field surveys are mostly costly and involve a lot of time and financial resources with lower spatial extents. The Landsat satellite series has provided valuable data for monitoring and mapping the Earth's surface for over 40 years [2]. The Landsat-8 satellite, launched in 2013, enhanced the imaging capacity of this series, introducing new spectral bands in the blue and short-wave infrared (SWIR) ranges and improving the sensor signal/noise ratio and the image radiometric resolution [3]. The Operational Land Imager (OLI) sensor supplies optical images with 30 m spatial resolution, eight spectral bands, and 16 days of temporal resolution [4]. Sentinel-2, a multispectral sensor of medium spatial resolution produced by the European Space Agency (ESA), was conceived to ensure the continuity of global data on the Earth's surface. This mission was launched in 2015 and presented a wide swath (290 km), a revisit time (five days, with two satellites), a medium spatial resolution (10, 20, and 60 m), and a relatively good number of spectral bands (13).

Landsat and Sentinel data have been used to assess tropical forest diversity. Madonsela et al. [2] identified the best vegetation index (NDVI, EVI, SAVI, and SRI) in estimating species diversity by comparing vegetation indices in Landsat 8 multispectral data with alpha-diversity index (Shannon index, species richness index, and Simpson index), using principal component analysis (PCA). Kumar et al. [4] calculated forest species diversity with information-theory-based indices using Sentinel-2 sensors. While medium-resolution data provide some spatial detail compatible with the size of vegetation units and biomass field observations, obtaining cloud-free, high spatial, temporal, and spectral resolution imagery is usually problematic. Hence, properly assessing tropical forest species diversity might not be feasible. Although there are usually trade-offs in the properties of satellite sensors, such as spatial resolutions and temporal revisit time, studies have shown that obtaining optimal spatial, spectral, and temporal information is vital for better forest structure estimation [21,24,25].

The recent advancement in CubeSat, a small satellite composed of a 1U unit ($10 \times 10 \times 10$ cm^3) with a mass of 1.33 kg [26], provides unique spatial and temporal observations due to large constellations of small satellites. PlanetScope, provided by Planet, comprises one of the largest CubeSat constellations. With more than 130 satellites, the PlanetScope satellites enable daily observations with approximately 3.7 m spatial resolution. Although spectral resolution and radiometric consistency should be considered, the frequent observation and high spatial resolution of the PlaneScope data offer new opportunities for land cover monitoring. Several studies have used PlaneScope data for forest cover and structural mapping [27–30].

The retrieval of biophysical variables based on remote sensing data is derived from a preferred individual spectral wavelength range, such as the red-edge band, which highlights vegetation vigor. Alternatively, a spectral index is employed as a proxy for a vegetation trait [31]; for instance, the NDVI is a popular and frequently used spectral index. According to Peng et al. [32], the most common and best vegetation index in estimating S, H and D_2 index is the EVI, NDVI, SAVI, and SRI because they can minimize atmospheric noise and soil background and improve the estimation of plant species diversity in a dense canopy.

Considering that the PlanetScope data allows almost daily images over an area with a spatial resolution of 3 m and eight spectral bands, and the fact that not enough research has made use of the PlaneScope data in assessing forest species diversity, this research explores the potential for using PlanetScope to assess and predict tropical species diversity.

This research is guided by the following research question: (1) What is the relationship between species diversity and the spectral bands of PlanetScope data? (2) How can species diversity be best predicted based on the PlanetScope data? The findings of this study will help inform biodiversity conservation and the management of BFRs.

2. Materials and Methods

2.1. Study Area

This study was conducted in the BFR in southern Ghana, in the Ashanti Region (Figure 1). The reserve lies between latitude 6° 40′ and 6° 44′North of the Equator and longitudes 1° 15′ and 1° 22′West of the Greenwich. It is approximately 25 km northeast of Kumasi, Ashanti's regional capital. The BFR covers an area of roughly 30 square kilometers. This forest is part of the tropical rainforest biome of West Africa, which exhibits high biodiversity, and it is home to various plant and animal species, including endemic and endangered species [33]. The forest structure is characterized by an upper canopy layer comprising a mixture of deciduous and evergreen species in approximately equal proportions. The average canopy height is approximately 40 m, with emergent trees up to 60 m tall. Common species found in this study area include *Celtis zenkeri*, *Celtis milbraedii*, *Triplochiton scleroxylon*, *Sterculia rhinopetala*, *Funtumia elastica*, *Baphia nitida*, *Cleidion gabonicum*, *Nesogordonia papaverifera*, *Hymnostegia afzeli*, *Turraenthus africanus*, and *Trichilia prieuriana* (*Djagblatey*) [34]. The landscape is undulating with a 6–7% slope and an elevation between 180 m and 245 m above sea level. The soil varies from sandy to clay and passes into gray-leached sandy or silty soil [34]. The study area experiences a tropical climate with distinct wet and dry seasons. The site has a bimodal rainfall regime known as the major and minor seasons, with the major typically starting from April to July, followed by the little dry season in August, and the minor season continues from September to November, followed by the main dry season in December, [35]. Annual rainfall in the forest varies between 1200 and 1750 mm. The mean yearly maximum temperature ranges between 30.9 and 31.6 °C, averaging 31.1 °C.

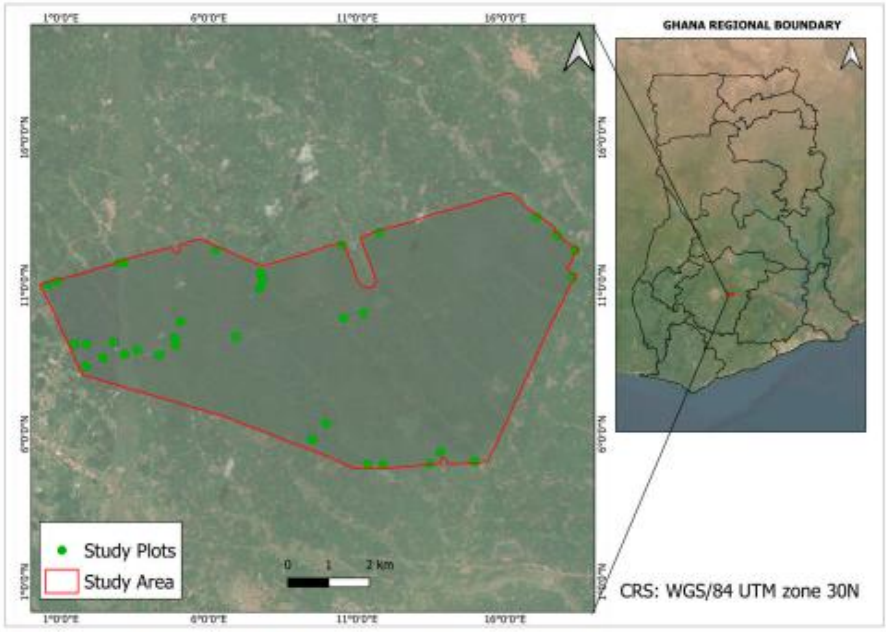

Figure 1. Study location (Bobiri Forest Reserve, Ghana).

2.2. Remote Sensing Data Acquisition and Preprocessing

PlanetScope data with a 3 m spatial resolution from Planet Lab Inc. (Kurfürstendamm, Berlin, Germany) [36] was used in this study. All spectral bands were included (i.e.,

blue, green, green, yellow, red, red edge, and near-infrared (NIR); Table 1), except for the coastal blue band, with nearly daily global coverage. The PlanetScope data, available at https://www.planet.com/ (accessed on 6 September 2023), was accessed through a research and education license.

Table 1. PlanetScope spectral band description.

Dataset	Spatial Resolution (m)	Band Name/Number	Wavelength (nm)	Date of Image Acquisition
PlanetScope	3.0	Blue	465–515	19 April 2023
		GreenI *	513–549	
		Green	547–585	
		Yellow *	600–620	
		Red	600–620	
		RedEdge *	697–713	
		NIR	845–885	

All spectral bands that were used for processing and extraction with their wavelengths and band names. * Only included when ordering 8-band bundles.

We used the PlanetScope surface reflectance product, incorporating geometric, radiometric, and atmospheric corrections [36]. To retain as much good data as possible, the acquisition date was set to the closest period of the data collection, May 2023, that met the following criteria: "standard" quality level, no cloud cover, and images that fell within a subset area. We used the surface reflectance scenes because the surface reflectance data preserves calculated pixel values, no color balancing or adjustments are applied, and with adequate preprocessing, they are suitable for use cases such as forest and crop health monitoring and wildfire assessment, among others [37]. Consequently, four scenes of already mosaiced images for the targeted subset devoid of cloud cover were downloaded. The next step was to perform a subset of the image using an ROI (region of interest) (Figure 2). Furthermore, we used the pixel extraction tool in SNAP with a window size of 3 × 3, which is the closest to the plot size. We selected mean as the aggregation method to extract the spectral reflectance values of each band within the PlanetScope image for all plots.

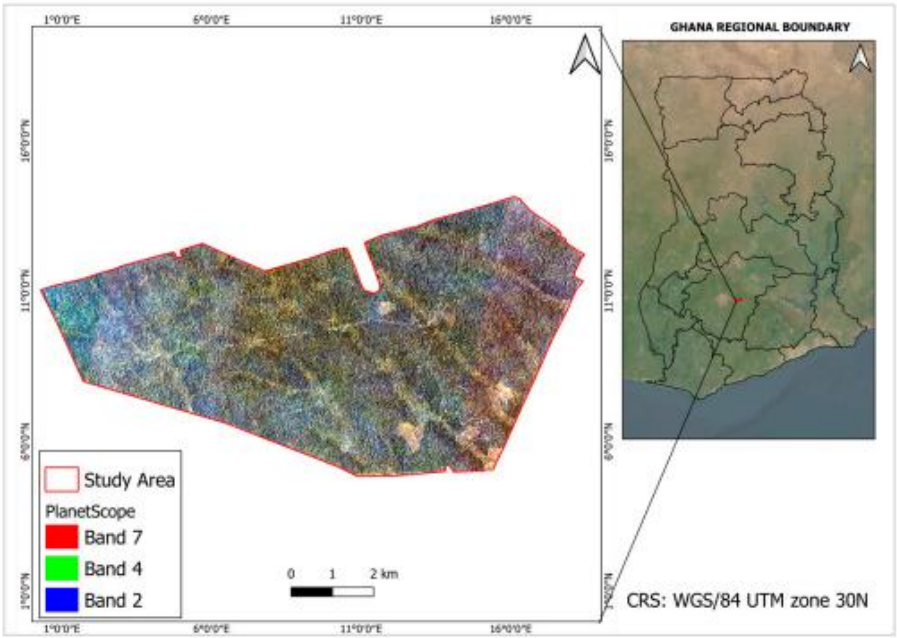

Figure 2. Preprocessed RGB composite of PlanetScope data.

Finally, the forward stepwise regression method was used to check the influence of potential predictors, in this case, the spectral reflectance bands and VIs, on the outcome of the two main species diversity indices (S and H'). At each step, variables were chosen based on their Akaike's information criterion (AIC), which was used to limit the total number of variables included in the final model. According to Pearse et al. [38], the stepwise selection of variables is a useful and effective data analysis tool when the outcome being studied is relatively new, the importance of individual covariates may not be known, and associations with the outcome are not well known, which is the case in this research.

2.3. Tree Species Data

2.3.1. Field Sampling Protocol and Tree Species Data Collection

Mapfumo et al. [39] and Mutowo et al. [40] have proven that sampling of plot sizes widely used ranges between 20 and 200 m^2 in tall shrub communities and 200–25,000 m^2 for tall trees in woods and forests. Their research guided us in selecting the plot size for species sampling. Tree species were sampled from 35 plots with a 20 m × 50 m plot size. A simple random sampling approach was used to define the placement of the plots following the research conducted by Oli et al. [41], with a minimum distance of 200 m apart to avoid overlapping of sampling plots [42]. Although this was the original protocol, we sampled the plots according to the accessible areas because of the inaccessibility of some parts of the forest. A mobile device with a field map application and Global Positioning System functionality was used to record plot coordinates. Three hundred and eleven individual tree species of the 15 most dominant within the forest were sampled, and their diameter at breast height (DBH) ≥5 cm was recorded using a diameter tape. The maximum heights of the trees were recorded using a TruePulse device. Species identification was performed with the help of a plant taxonomist, and the nomenclature was verified using the readily available online repository The World Flora Online [43]. The 15 most dominant tree species in the study area were identified. This was determined through engagement with individuals who worked within the Forest Reserve and the staff at the Forestry Research Institute of Ghana (FORIG). The collection of tree species data was conducted in June 2023.

2.3.2. Estimating the Diversity of Tree Species

The H' and D_2 are the most frequently used indices in ecological literature, according to Mandosola et al. [44] and Peng et al. [32]. Tree species diversity was quantified in each plot using four diversity measures. S, J', H', and D_2 (Table 2). Although H' and D_2 consider both species richness (the number of different species) and abundance (the number of individual trees within species), these aspects of diversity have a bearing on the spectral signal captured by the remote sensing device [45]; hence, they were computed separately to test their relationship with the spectral reflectance of the bands and vegetation indices.

Table 2. Vegetation indices used in this study and their equations.

Vegetation Index	Equation	Reference
Normalized difference vegetation index (*NDVI*)	$NDVI = \frac{NIR - RED}{NIR + RED}$	[46]
Enhanced vegetation index (*EVI*)	$EVI = G \times (NIR - RED)/(NRI + C1 \times RED - C2 \times BLUE + L)$	[47]
Simple ratio index (*SRI*)	$SRI = \frac{NIR}{RED}$	[48]
Soil-adjusted vegetation index (*SAVI*)	$SAVI = \frac{NIR - RED}{(NIR + RED + L)} \times (1 + L)$	[49]
Normalized difference red edge index	$NDRE = \frac{NIR - REDEDGE}{(NIR + REDEDGE)}$	[50]

L is a soil fudge factor that varies from 0 to 1 depending on the soil coefficients adopted in the MODIS-EVI algorithm are $L = 1$, $C1 = 6$, $C2 = 7.5$, and $G = 2.6$.

2.4. Relationship between Tree Species Diversity Indices and Remotely Sensed Data

Using stepwise linear regression analysis, we investigated the relationships between species diversity indices (Table 3) with response variables and spectral band information (Table 1) as predictor variables. The root mean square error (RMSE), coefficient of determination (r^2), and Akaike's information criterion (AIC) of the regression guided the selection of the most appropriate model to show species diversity. The prediction model had the smallest RMSE and AIC, and the highest r^2. According to Peng et al. [32], the RMSE measures how close the model predicts field measurements, r^2 measures the proportion of variance in the dependent variable predicted from the independent variable, and AIC estimates the quality of each model relative to the other models. In addition to the regression, we evaluated the correlation between variables using Pearson's correlation coefficients.

Table 3. Diversity indices used in this study and their equations.

Species Diversity Index	Equation	Reference
Species richness	$S = N$	[12]
Simpson index	$D_2 = 1/\sum_{i=1}^{s} p_i^2$	[12,51]
Shannon index	$H' = -\sum_{i=1}^{s} p_i \ln(p_i)$	[12,52]
Species evenness	$J' = -\sum_{i=1}^{s} p_i \ln(p_i)/LN(S)$	[53]

where N is the total number of tree species in a sample; p_i, the proportional abundance of species I relative to the total abundance of all species S in a plot $\ln(p_i)$ is the natural logarithm of this proportion.

3. Results

The predominant species (top six) identified in the BFR were *Sterculia rhinopetala*, *Tripochiton scleroxylon*, *Celtis milbraedae*, *Cola gigantia*, and *Hymenostegia afzelii* (Table 4). Among the tree species selected for this study, the highest number of individual trees was recorded for *Sterculia oblonga*. In contrast, the lowest number of individual trees was recorded for *Baphia pubescens*.

Table 4. Tree species list and their frequencies within the study area.

Family	Scientific Names	Number of Individual Tree Species
1. *Leguminosae-Papilionoideae*	*Baphia pubescens*	16
2. *Leguminosae-Caesalpinioideae*	*Bussea occidentalis*	18
3. *Ulmaceae*	*Celtis zenkeri*	19
	Celtis mildbraedii	27
4. *Malvaceae*	*Cola caricifolia*	17
	Cola giganti	26
	Nesogordonia papaverifera	18
	Pterygota macrocarpa	20
	Sterculia Oblonga	20
	Sterculia rhinopetala	28
	Triplochiton scleroxylon	27
5. *Meliaceae*	*Carapa Procera*	18
6. *Apocynaceae*	*Funtumia elastica*	18
7. *Simaroubaceae*	*Hannoa klaineana*	14
8. *Leguminosae*	*Hymenostegia afzelii*	25
Total		311

3.1. Correlation between Diversity Indices and Remotely Sensed Data

Using a Pearson correlation matrix, we performed a correlation analysis between the diversity indices, spectral bands, and vegetation indices. S and H' are the diversity variables that correlated significantly with the spectral bands and VIs. D_2 and J' showed no significant correlation with the spectral bands and VIs. Regarding the spectral bands,

our results showed bands 6, 5, 4, 3, and 2 (red, yellow, green, greeni, and blue) correlated with S and H'; however, band 6 had the highest correlation with S, with a correlation coefficient of 0.61 and $p < 0.001$. Similarly, spectral bands 6, 5, 4, 3, and 2 demonstrated a positive correlation with H'; however, band 6 showed the highest correlation with H′, with a coefficient of 0.58 and $p < 0.01$. Almost all VIs (NDVI, NDRE, SAVI, SRI) demonstrated a negative correlation with both S and H'; however, NDRE showed the highest correlation with a coefficient of −0.48 and $p < 0.05$, followed by the NDVI with a correlation coefficient of 0.17 for S and 0.40 for H, and $p < 0.5$ for both S and H' (Figure 3).

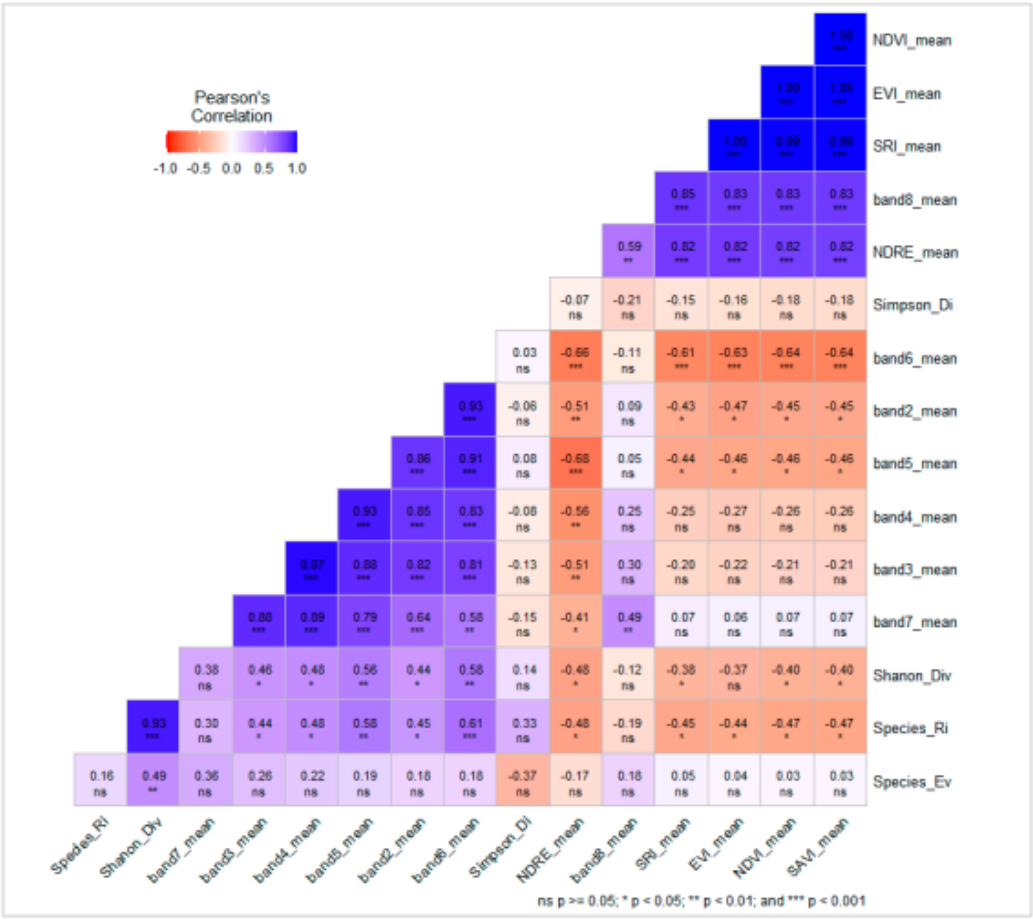

Figure 3. Correlation matrix between diversity indices, spectral bands, and vegetation indices: band2_mean = mean of spectral band 2, band3_mean = mean of spectral band 3, band4_mean = mean of spectral band 4, band5_mean = mean of spectral band 5, band6_mean = mean of spectral band 6, band7_mean = mean of spectral band 7, band8_mean = mean of spectral band 8, NDVI_mean = mean of the NDVI, EVI_mean = mean of the EVI, SAVI_mean = mean of the SAVI, SRI_mean = mean of the SRI, NDRE_mean = mean of the NDRE, Species_Ri = species richness (S), Species_Ev = species evenness (J'), Shanon_Div = Shannon diversity index (H'), and Simpson_Di = Simpson diversity index (D_2).

To predict species diversity within the BFR, a forward stepwise regression model with species richness and Shannon index as predictor variables and the mean spectral bands and VIs of the PlanetScope data as response variables were used to obtain the subset of variables that results in the best model. For species richness prediction, the stepwise model showed that mean spectral band 6 (red) and mean spectral band 2 (blue) were the most important variables that produced a good model with an ($r^2 = 0.47$), (RMSE = 1.00) and (AIC = 85.15).

Similarly, for the prediction of the Shannon diversity index, mean spectral bands 6 and 2 produced a good model with an (r^2 = 0.42), (RMSE = 0.17), and (AIC = −10.74). We did not predict the Simpson diversity index and species evenness because they did not demonstrate a correlation with the spectral bands and VIs. The results show that the best models for estimating tree species diversity (S and H′) using PlanetScope data were derived from spectral bands 6 and 2. The obtained model equations (Table 5) were used to calculate species richness and the Shannon diversity index in a GIS environment using the raster calculator function in QGIS. Figure 4 shows species diversity predicted maps (*S* and *H′*) for the BFR. The diversity map (Figure 4a) shows species richness (*S*) within the BFR. Some areas within the BFR had species richness between 2 and 4, while only smaller areas towards the south-east have a species richness of 5, with the rest showing species richness of 1. In general, species richness was fairly distributed across the study area. Also, the diversity map (Figure 4b) indicates that the Shannon diversity index within the BFR is generally moderately scattered over the entire region. Therefore, the results show some species diversity levels in the BFR.

Table 5. Regression equations for plant diversity prediction based on the best-predicted model with the lowest AIC and RMSE and the highest R^2.

Diversity Index	Regression Equation	R^2	RMSE	AIC
S	Species_Ri~−4.23 + 23.45 × band6_mean − 22.18 × band2_mean	0.47	1.00	85.15
H′	Shanon_Div~0.08 + 3.45 × band6_mean − 3.14 × band2_mean	0.42	0.17	−10.74

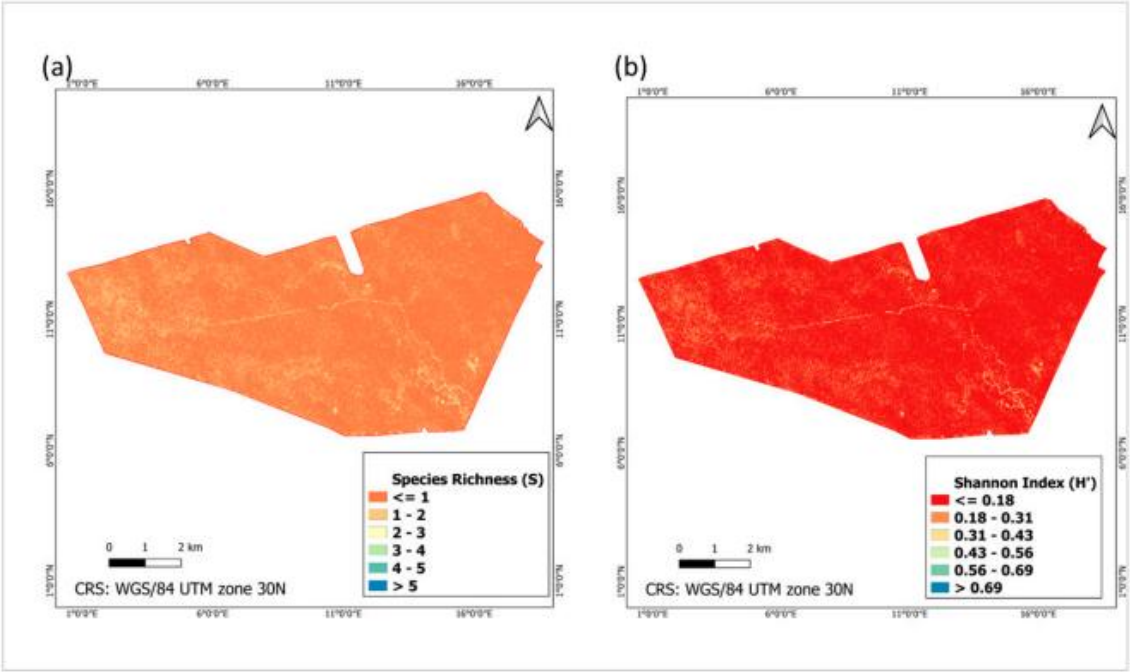

Figure 4. Species diversity thematic maps derived from the stepwise predicted model. (**a**) *S*—species richness (**b**) *H′*—Shannon index.

3.2. Stepwise Linear Regression for Species Diversity Prediction

The equations (Table 5) were employed to estimate S and H' by substituting the corresponding bands in the raster calculator in QGIS. The equations were used to predict S and H' across the study area. The resulting maps provide spatial insights into the distribution of predicted diversity values based on the spectral band information. The intercept (−4.23) represents the estimated S when both the mean spectral of bands 6 and 2 are zero. The coefficient for the spectral mean of band 6 (23.45) indicates the estimated change in S for a one-unit increase in the mean of spectral band 6. The coefficient for the mean of spectral band 2 (−22.18) indicates the estimated change in S for a one-unit increase in the mean of spectral band 2. For the H' prediction, the intercept (0.08) represents the estimated H' when both the spectral mean of bands 6 and 2 are zero. The coefficient of the spectral mean of band 6 (3.45) indicates the estimated change in H' for a one-unit increase in the spectral mean of band 6. The coefficient for the mean of spectral band 2 (−3.14) indicates the estimated change in H' for a one-unit increase in the spectral mean of band 2. The positive coefficient for band 6 in both S and H' predictions suggests that higher values of this band are associated with increased S and H' while the negative coefficients for band 2 suggests that higher values of band 2 are associated with decreased S and H'(Table 5). For S prediction, the model achieved an R^2 value of 1.00, indicating a good fit to the data, while for the prediction of H', the mode achieved an R^2 value of 0.42 indicating that approximately 42% of the variability in the H' is explained by the model.

The models emphasize the importance of both bands in predicting species diversity, with specific bands 6 and 2 having different impacts on S and H'. the high R^2 value for S may indicate a strong relationship between the selected bands and S, while the R^2 value for H' suggests a moderate level of explanatory power.

4. Discussion

The BFR is one of Ghana's most important protected areas, incorporating local communities for biodiversity conservation [35]. The reserve has a wide range of indigenous tree species, approximately 120 bird species, and a butterfly sanctuary with about 340 butterfly species that can potentially contribute to economic growth through tourism [54]. Therefore, monitoring and assessing tree species diversity in the area is essential for sustainable conservation. Thus, understanding tree species diversity in biodiversity conservation is crucial because it provides reserve management with the necessary baseline information regarding the distribution of tree species and their changes within the forest reserve, which is essential in the planning and managing forest reserves. Remote sensing data provides valuable information to achieve such desired results.

The PlaneScope imagery is increasingly used for scientific applications focused on terrestrial ecosystems. A common use case is land cover and land use changes, where the spatial resolution and temporal frequency of the image can provide information related to fine-scale land cover changes that may not be captured by moderate resolution sensors such as Landsat 8 OLI and Sentinel-2 MSI [55,56]. Similarly, using PlanetScope imagery to estimate land surface phenology is a natural use case becoming more common. For example, John et al. [57] used PlanetScope imagery to detect the timing of flowering in alpine wildflowers in Washington State, Chen et al. [58] used PlanetScope imagery in combination with Sentinel-2 to monitor flowering phenology in almond orchards in the Central Valley of California. These studies have consistently demonstrated that PlanetScope imagery provides an effective basis for monitoring phenology from remote sensing. However, each of the studies discussed focuses on individual phenological events within ecosystems, and none has assessed the capabilities or potential of PlanetScope data in predicting species diversity. Our results demonstrate a significant relationship between some spectral bands of PlanetScope imagery and species diversity and the ability to predict species diversity with this spectral information.

The significant relationship between the spectral bands of PlanetScope data (red and blue) and species diversity variables (S and H') suggests that satellite images such

as PlanetScope would help predict biodiversity in tropical forests [3]. According to Badourdine [59], the green and red edge bands are particularly sensitive to photosynthetic pigment content, suggesting their link or relationship between taxonomic information, photosynthetic activity, and spectral information. Tesfaye and Awoke [60] also confirmed in their studies that the red band, which falls within the visible part of the electromagnetic spectrum, influences vegetation properties, such as canopy biomass and leaf chlorophyll content. Also, the red and blue bands are reported to be the chlorophyll absorption regions. Conti et al. [61] found that the blue band, which relates to pigments, including carotene and xanthophylls, tends to correlate with species diversity after performing a principal component analysis of all spectral bands with species diversity. With the area being a tropical, moist, semi-deciduous forest, and the study period rainy, vegetation in the area is assumed to have contained the chlorophyll pigments, carotene, and xanthophylls, culminating in the absorption of such chemicals and, thus, correlation with species diversity. Therefore, it is unsurprising that the red and blue bands had a significant relationship with tree species diversity, as measured by S and H' within the BFR.

Our findings are consistent with those of Gyamfi-Ampadu. [62] and Imran et al. [63] who demonstrated that the red part of the spectrum, that is, the red band, was best for estimating species diversity, hence their correlation with the species diversity (S and H'). It must also be noted that the reserve lies in Ghana's tropical moist, semi-deciduous south-east forest zone and hence receives higher annual rainfall and a short dry season. This situation ensures that the reserve is dominated by healthy vegetation. Although our results showed a correlation between species diversity and the red and blue bands, this correlation was positive, similar to Conti et al. [61]. The positive correlation between the diversity indices (S and H') and spectral reflectance of bands 6 and 2 of the PlanetScope data confirms their sensitivity to the nature and structure of the forest and the vegetation properties (Gyamfi-Ampadu) [62]. According to Kulawardhana. [64], the positive correlation of spectral bands with species diversity is due to species-specific differences in pigment content, leaf structure, and canopy structural components such as leaf area index. Therefore, the importance of the visible bands in plant diversity prediction can be justified by the fact that this portion of the spectrum, especially bands in the red and blue, is the major leaf pigment absorption range, which is sensitive to mainly chlorophyll *a*, and *b* contents, according to the sensitivity analysis reported by Zhao et al. [65].

According to Cabacinha et al. [66], even though some authors like Foody and Cutler [67] have not found any strong correlations between vegetation indices and species diversity, one can expect a relationship between them since it is related to the richness, i.e., the number of species in the community, and the abundance representing the distribution of individuals by species. In the Pearson correlation performed to assess the relationship between H', S, and VIs, H' and S showed a better correlation with the NDVI (−0.47), SAVI (−0.47), and NDRE (−0.48). This may be because the VIs were calculated using the NIR and red edge bands, which have been suggested for discriminating species diversity [32,68]. Additionally, according to Fajji et al. [69], different VIs are computed by combining two or more spectral bands, assuming that multi-band analysis would provide further information. Furthermore, the results of the study could be attributed to the sensitivity of the VIs to variability in vegetation characteristics, i.e., shape and size of the tree, water content, and associated background. The results could also be attributed to environmental factors such as the amount of rainfall and temperature received in the study area.

This finding is consistent with those of Arekhi et al. [68], who found the NDVI having the highest significant correlation with H' calculated from basal area (3 × 3 Shannon index basal area (SIBA) with r = 0.685 in the Gonen Dam watershed in Turkey. Furthermore, the research of Gaitan et al. [70] showed a strong correlation between the NDVI and species richness in steppe ecosystems. According to Madonsela et al. [44], the differences in sensitivity to vegetation characteristics could be explained by the different measurement scales of the VIs. For instance, in the study of Rampheri et al. [71], the VIs that had a better relationship with H' (NDVI and SAVI) have a measurement scale that ranges from −1 to

1. Overall, the type of forest and complexity of forest stands in terms of multi-layers and species composition can affect the outcome of estimations.

Similar to the correlation results, the stepwise regression analysis demonstrated that bands 2 (blue) and 6 (red) were the most important variables explaining species diversity. According to Rejauar et al. [72], the green and red bands are the two main absorption bands of two primary leaf pigments: The chlorophyll pigment (green pigments) and the Xanthophylls. These strong absorption bands induce a peak in the reflectance of the yellow–green bands (550 nm), so chlorophyll is called the green pigment. This accounts for the relationship observed in our results between the blue, green, and red bands with species diversity indices (S and H'), which aligns with Mockel et al. [73].

The results of this study demonstrated variations in species diversity (S and H'). The relatively high S within the study area can be attributed to the protected nature of the forest, with fewer human-induced activities and favorable conditions, such as humid and warm temperatures. For example, Li et al. [74] observed a high diversity of Salicaceae species in warm and wet areas other than regions in China. The increased rainfall in the area can also account for the relatively high species richness. Shoko et al. [75] found that environments with high soil moisture favor the increased production of C3 above-ground biomass (AGB). In addition, solar radiation in the area may cause a high evapotranspiration rate. According to these studies, solar radiation is the primary energy source that regulates terrestrial ecosystems' chemical, physical, and biological processes. Therefore, the evapotranspiration rate defines the species diversity [74,76]. Our results show moderate H' values, with some areas showing high values. In the research of Naidu et al. [77], they reported a Shannon–Wiener index (H') for all six plots varying from 3.59 to 4.05, which falls within the range of 0.67 to 4.86 reported in tropical forests in the Indian sub-continent [78]. These values correspond to the values obtained in our results.

Considering the results of this study, the use of remote sensing data (PlanetScope) to predict tree species diversity plays a vital role in conservation management. These results imply that PlanetScope spectral bands explain species diversity variations better than VIs. This demonstrates how ecological knowledge and satellite-based information can be effectively combined to address a wide range of current natural resource conservation/management challenges strategies.

5. Conclusions

This study provides insight into the usefulness of the spectral bands of PlanetScope data in predicting species diversity in a tropical forest such as the BFR. A correlation test assessed the relationship between spectral bands, VIs, and species diversities (S and H'). Stepwise regression was also used to select the most important variable from all response variables, providing a good model for predicting species diversity. The results showed that the red and blue bands of the visible spectrum range are most important in predicting species diversity.

In conclusion, the BFR in Ghana is a vital protected area with a rich biodiversity, including numerous indigenous tree species and diverse bird and butterfly populations. The sustainable conservation of tree species diversity within this reserve is paramount as it provides baseline information for effective forest management. Even though the results show a prediction of species diversity, we recommend incorporating data from other sensors, such as lidar and radar, and environmental variables to improve such predictions.

Author Contributions: Conceptualization—E.N. and P.S. Methodology—E.N., J.N.O., R.T.G., B.E.A., R.K.N. and P.S. Investigation—E.N., J.N.O. and P.S. Original draft preparation—E.N. and J.N.O. Funding acquisition—E.N. and P.S. All authors have read and agreed to the published version of the manuscript.

Funding: This research was funded by the Faculty of Forestry and Wood Sciences—FFWS, Czech University of Life Sciences Prague, (IGA/FLD/A_11_23 (Internal grant number: 43140/1312/3189).

Data Availability Statement: Data are available upon request.

Acknowledgments: Many thanks to all the individuals and institutions that assisted with data collection of this study. Special k acknowledgement the contributions of the Forestry and Research Institute of Ghana in Kumasi for their effective collaboration and willingness to provide all the needed assistance for the data collection campaign. Special thanks to the Staff of the Bobiri Forest Reserve (Manfred and Bolt) for their support and further assistance in acquiring data throughout the field campaign. We would like to specially acknowledge John Akomatey and Ebenezer Ampofo Nti (taxonomists) for their instrumental roles, assisting in the tree species identification.

Conflicts of Interest: The authors declare no conflict of interest. The funders had no role in the design of the study, in the collection, analyses, or interpretation of data, in the writing of the manuscript, or in the decision to publish the results.

References

1. Gamfeldt, L.; Snäll, T.; Bagchi, R.; Jonsson, M.; Gustafsson, L.; Kjellander, P.; Ruiz-Jaen, M.C.; Fröberg, M.; Stendahl, J.; Philipson, C.D.; et al. Higher levels of multiple ecosystem services are found in forests with more tree species. *Nat. Commun.* **2013**, *4*, 1340. [CrossRef] [PubMed]
2. Qi, W.; Saarela, S.; Armston, J.; Ståhl, G.; Dubayah, R. Remote Sensing of Environment Forest biomass estimation over three distinct forest types using TanDEM-X InSAR data and simulated GEDI lidar data. *Remote Sens. Environ.* **2019**, *232*, 111283. [CrossRef]
3. Madonsela, S.; Azong, M.; Ramoelo, A.; Mutanga, O. Remote sensing of species diversity using Landsat 8 spectral variables. *ISPRS J. Photogramm. Remote Sens.* **2017**, *133*, 116–127. [CrossRef]
4. Kumar, P.; Dobriyal, M.; Kale, A.; Pandey, A.K.; Tomar, R.S.; Thounaojam, E. Calculating forest species diversity with information-theory based indices using sentinel-2A sensor's of Mahavir Swami Wildlife Sanctuary. *PLoS ONE* **2022**, *17*, e0268018. [CrossRef] [PubMed]
5. Tindan, P.D. Savanna primary livelihoods at the edge of land degradation: Linkages and impacts in Ghana. *Int. J. Innov. Appl. Stud.* **2015**, *10*, 119–131.
6. Behera, S.R.; Dash, D.P. The effect of urbanization, energy consumption, and foreign direct investment on the carbon dioxide emission in the SSEA (South and Southeast Asian) region. *Renew. Sustain. Energy Rev.* **2017**, *70*, 96–106. [CrossRef]
7. Vaglio Laurin, G.; Puletti, N.; Hawthorne, W.; Liesenberg, V.; Corona, P.; Papale, D.; Chen, Q.; Valentini, R. Discrimination of tropical forest types, dominant species, and mapping of functional guilds by hyperspectral and simulated multispectral Sentinel-2 data. *Remote Sens. Environ.* **2016**, *176*, 163–176. [CrossRef]
8. Buckland, S.T.; Magurran, A.E.; Green, R.E.; Fewster, R.M. Monitoring change in biodiversity through composite indices. *Philos. Trans. R. Soc. B Biol. Sci.* **2005**, *360*, 243–254. [CrossRef]
9. Soininen, J.; Passy, S.; Hillebrand, H. The relationship between species richness and evenness: A meta-analysis of studies across aquatic ecosystems. *Oecologia* **2012**, *169*, 803–809. [CrossRef]
10. Zhang, Y.; Chen, H.Y.H.; Reich, P.B. Forest productivity increases with evenness, species richness and trait variation: A global meta-analysis. *J. Ecol.* **2012**, *100*, 742–749. [CrossRef]
11. Crowder, D.W.; Northfield, T.D.; Gomulkiewicz, R.; Snyder, W.E. Conserving and promoting evenness: Organic farming and fire-based wildland management as case studies. *Ecology* **2012**, *93*, 2001–2007. [CrossRef]
12. Morris, E.K.; Caruso, T.; Buscot, F.; Fischer, M.; Hancock, C.; Maier, T.S.; Meiners, T.; Müller, C.; Obermaier, E.; Prati, D.; et al. Choosing and using diversity indices: Insights for ecological applications from the German Biodiversity Exploratories. *Ecol. Evol.* **2014**, *4*, 3514–3524. [CrossRef] [PubMed]
13. Chao, A.; Wang, Y.T.; Jost, L. Entropy and the species accumulation curve: A novel entropy estimator via discovery rates of new species. *Methods Ecol. Evol.* **2013**, *4*, 1091–1100. [CrossRef]
14. Wilsey, B.J.; Chalcraft, D.R.; Bowles, C.M.; Willig, M.R. Relationships among indices suggest that richness is an incomplete surrogate for grassland biodiversity. *Ecology* **2005**, *86*, 1178–1184. [CrossRef]
15. Hakkenberg, C.R.; Song, C.; Peet, R.K.; White, P.S. Forest structure as a predictor of tree species diversity in the North Carolina Piedmont. *J. Veg. Sci.* **2016**, *27*, 1151–1163. [CrossRef]
16. Tuomisto, H. A consistent terminology for quantifying species diversity? Yes, it does exist. *Oecologia* **2010**, *164*, 853–860. [CrossRef] [PubMed]
17. Pimentel, D.; Stachow, U.; Takacs, D.A.; Brubaker, H.W.; Amy, R.; Meaney, J.J.; Neil, J.A.S.O.; Onsi, D.E.; Corzilius, D.B.; Dumas, A.R.; et al. Conserving Biological Diversity in Most biological diversity exists in Agricultural/Forestry Systems. *Bioscience* **1992**, *42*, 354–362. [CrossRef]
18. Hector, A.; Bagchi, R. Biodiversity and ecosystem multifunctionality. *Nature* **2007**, *448*, 188–190. [CrossRef]
19. Myers, N.; Mittermeier, R.A.; Mittermeier, C.G.; da Fonseca, G.A.B.; Kent, J. Biodiversity hotspots for conservation priorities. *Nature* **2000**, *403*, 853–858. [CrossRef]
20. Appiah, M. Tree population inventory, diversity and degradation analysis of a tropical dry deciduous forest in Afram Plains, Ghana. *For. Ecol. Manag.* **2013**, *295*, 145–154. [CrossRef]

21. Chrysafis, I.; Korakis, G.; Kyriazopoulos, A.P.; Mallinis, G. Predicting tree species diversity using geodiversity and sentinel-2 multi-seasonal spectral information. *Sustainability* **2020**, *12*, 9250. [CrossRef]
22. Nagendra, H.; Lucas, R.; Honrado, J.P.; Jongman, R.H.G.; Tarantino, C.; Adamo, M.; Mairota, P. Remote sensing for conservation monitoring: Assessing protected areas, habitat extent, habitat condition, species diversity, and threats. *Ecol. Indic.* **2013**, *33*, 45–59. [CrossRef]
23. Huesca, M.; Merino-de-miguel, S.; Eklundh, L.; Litago, J.; Cicuéndez, V.; Rodríguez-rastrero, M.; Ustin, S.L.; Palacios-orueta, A. Ecosystem functional assessment based on the "optical type" concept and self-similarity patterns: An application using MODIS-NDVI time series autocorrelation. *Int. J. Appl. Earth Obs. Geoinf.* **2015**, *43*, 132–148. [CrossRef]
24. Astola, H.; Häme, T.; Sirro, L.; Molinier, M.; Kilpi, J. Comparison of Sentinel-2 and Landsat 8 imagery for forest variable prediction in boreal region. *Remote Sens. Environ.* **2019**, *223*, 257–273. [CrossRef]
25. Fagua, J.C.; Jantz, P.; Rodriguez-buritica, S.; Duncanson, L.; Goetz, S.J. Integrating LiDAR, Multispectral and SAR Data to Estimate and Map Canopy Height in Tropical Forests. *Remote Sens.* **2019**, *11*, 2697. [CrossRef]
26. Mura, M.; Bottalico, F.; Giannetti, F.; Bertani, R.; Mancini, M.; Orlandini, S.; Travaglini, D.; Chirici, G. Exploiting the capabilities of the Sentinel-2 multi spectral instrument for predicting growing stock volume in forest ecosystems. *Int. J. Appl. Earth Obs. Geoinf.* **2018**, *66*, 126–134. [CrossRef]
27. Riihimäki, H.; Luoto, M.; Heiskanen, J. Remote Sensing of Environment Estimating fractional cover of tundra vegetation at multiple scales using unmanned aerial systems and optical satellite data. *Remote Sens. Environ.* **2019**, *224*, 119–132. [CrossRef]
28. Csillik, O.; Kumar, P.; Mascaro, J.; Shea, T.O.; Asner, G.P. Monitoring tropical forest carbon stocks and emissions using Planet satellite data. *Sci. Rep.* **2019**, *9*, 17831. [CrossRef] [PubMed]
29. Baloloy, A.B.; Blanco, A.C.; Candido, C.G.; Argamosa, R.J.L.; Dumalag, J.B.L.C.; Dimapilis, L.L.C.; Paringit, E.C. Estimation of mangrove forest aboveground biomass using multispectral bands, vegetation indices and biophysical variables derived from optical satellite imageries: Rapideye, planetscope and sentinel-2. *ISPRS Ann. Photogramm. Remote Sens. Spat. Inf. Sci.* **2018**, *4*, 29–36. [CrossRef]
30. Mulatu, K.A.; Decuyper, M.; Brede, B.; Kooistra, L.; Reiche, J.; Mora, B.; Herold, M. Linking Terrestrial LiDAR Scanner and Conventional Forest Structure Measurements with Multi-Modal Satellite Data. *Forests* **2019**, *10*, 291. [CrossRef]
31. Viña, A.; Gitelson, A.A.; Nguy-robertson, A.L.; Peng, Y. Remote Sensing of Environment Comparison of different vegetation indices for the remote assessment of green leaf area index of crops. *Remote Sens. Environ.* **2011**, *115*, 3468–3478. [CrossRef]
32. Peng, Y.; Fan, M.; Song, J.; Cui, T.; Li, R. Assessment of plant species diversity based on hyperspectral indices at a fine scale. *Sci. Rep.* **2018**, *8*, 4776. [CrossRef] [PubMed]
33. Baffour-Ata, F.; Antwi-Agyei, P.; Nkiaka, E. Climate variability, land cover changes and livelihoods of communities on the fringes of bobiri forest reserve, Ghana. *Forests* **2021**, *12*, 278. [CrossRef]
34. Djagbletey, G. Impact of Selective Logging on Plant Diversity, Natural Recovery and Vegetation Carbon Stock: The Case of Bobiri Forest Reserve. Ph.D. Thesis, Kwame Nkrumah University of Science and Technology, Kumasi, Ghana, 2014.
35. Addo-Fordjour, P.; Anning, A.K.; Larbi, J.A.; Akyeampong, S. Liana species richness, abundance and relationship with trees in the Bobiri forest reserve, Ghana: Impact of management systems. *For. Ecol. Manag.* **2009**, *257*, 1822–1828. [CrossRef]
36. Planet Labs. Planet Imagery Product Specifications. Web Document. 2019. Available online: https://assets.planet.com/docs/combined-imagery-product-spec-april-2019.pdf (accessed on 6 September 2023).
37. Wang, J.; Yang, D.; Detto, M.; Nelson, B.W.; Chen, M.; Guan, K.; Wu, S.; Yan, Z.; Wu, J. Multi-scale integration of satellite remote sensing improves characterization of dry-season green-up in an Amazon tropical evergreen forest. *Remote Sens. Environ.* **2020**, *246*, 111865. [CrossRef]
38. Pearce, J.; Ferrier, S. An evaluation of alternative algorithms for fitting species distribution models using logistic regression. *Ecol. Model.* **2000**, *128*, 127–147. [CrossRef]
39. Mapfumo, R.B.; Murwira, A.; Masocha, M.; Andriani, R. The relationship between satellite-derived indices and species diversity across African savanna ecosystems. *Int. J. Appl. Earth Obs. Geoinf.* **2016**, *52*, 306–317. [CrossRef]
40. Mutowo, G.; Murwira, A. Relationship between remotely sensed variables and tree species diversity in savanna woodlands of Southern Africa. *Int. J. Remote Sens.* **2012**, *33*, 6378–6402. [CrossRef]
41. Oli, B.N.; Subedi, M.R. Effects of management activities on vegetation diversity, dispersion pattern and stand structure of community-managed forest (*Shorea robusta*) in Nepal. *Int. J. Biodivers. Sci. Ecosyst. Serv. Manag.* **2015**, *11*, 96–105. [CrossRef]
42. Paudel, S.; Sah, J.P. Effects of Different Management Practices on Stand Composition and Species Diversity in Subtropical Forests in Nepal: Implications of Community Participation in Biodiversity Conservation. *J. Sustain. For.* **2015**, *34*, 738–760. [CrossRef]
43. WFO. Wold Flora Online. Published on the Internet. 2021. Available online: https://about.worldfloraonline.org. (accessed on 6 September 2023).
44. Madonsela, S.; Cho, M.A.; Ramoelo, A.; Mutanga, O.; Naidoo, L. Estimating tree species diversity in the savannah using NDVI and woody canopy cover. *Int. J. Appl. Earth Obs. Geoinf.* **2018**, *66*, 106–115. [CrossRef]
45. Oldeland, J.; Wesuls, D.; Rocchini, D.; Schmidt, M.; Jürgens, N. Does using species abundance data improve estimates of species diversity from remotely sensed spectral heterogeneity? *Ecol. Indic.* **2010**, *10*, 390–396. [CrossRef]
46. Rouse, R.W.H.; Haas, J.A.W.; Deering, D.W. *Monitoring Vegetation Systems in the Great Plains with ERTS*; NASA Special Publication: College Station, TX, USA, 1974.
47. Huete, A.R. A soil-adjusted vegetation index (SAVI). *Remote Sens. Environ.* **1988**, *25*, 295–309. [CrossRef]

48. Tucker, C.J. Red and Photographic Infrared Linear Combinations for Monitoring Vegetation. *Remote Sens. Environ.* **1979**, *8*, 127–150. [CrossRef]
49. Huete, A.; Justice, C.; Van Leeuwen, W. Modis Vegetation Index (mod 13). In *Algorithm Theoretical Basis Document Version 3*; NASA: Washington, DC, USA, 1999; pp. 295–309.
50. Modzelewska, A.; Stereńczak, K.; Mierczyk, M.; Maciuk, S.; Bałazy, R.; Zawiła-Niedźwiecki, T. Sensitivity of vegetation indices in relation to parameters of Norway spruce stands. *Folia For. Pol. Ser. A* **2017**, *59*, 85–98. [CrossRef]
51. Simpson, E. Measurment of Diversity. *Nature* **1949**, *163*, 688. [CrossRef]
52. Shannon, C. A Mathematical Theory of Communication By c. E. Shannon Ixtroduction. *Bell Syst. Tech. J.* **1948**, *27*, 519–520. [CrossRef]
53. Carlo, H.R.; Herman, P.; Soetaery, K. Indices of diversity and evenness. *Oceanis* **1998**, *24*, 61–87.
54. Mensah, I.; Ernest, A. Community Participation in Ecotourism: The Case of Bobiri Forest Reserve and Butterfly Sanctuary in Ashanti Region of Ghana. *Am. J. Tour. Manag.* **2013**, *2013*, 34–42.
55. Loranty, M.M.; Davydov, S.P.; Kropp, H.; Alexander, H.D.; Mack, M.C.; Natali, S.M.; Zimov, N.S. Vegetation Indices Do Not Capture Forest Cover Variation in Upland Siberian Larch Forests. *Remote Sens.* **2018**, *10*, 1686. [CrossRef]
56. Pickering, J.; Tyukavina, A.; Khan, A.; Potapov, P.; Adusei, B.; Hansen, M.C. Using Multi-Resolution Satellite Data to Quantify Land Dynamics: Applications of PlanetScope Imagery for Cropland and Tree-Cover Loss Area Estimation. *Remote Sens.* **2021**, *4*, 2191. [CrossRef]
57. John, A.; Ong, J.; Theobald, E.J.; Olden, J.D.; Tan, A.; Hillerislambers, J. Detecting Montane Flowering Phenology with CubeSat Imagery. *Remote Sens.* **2020**, *12*, 2894. [CrossRef]
58. Cheng, Y.; Vrieling, A.; Fava, F.; Meroni, M.; Marshall, M.; Gachoki, S. Remote Sensing of Environment Phenology of short vegetation cycles in a Kenyan rangeland from PlanetScope and Sentinel-2. *Remote Sens. Environ.* **2020**, *248*, 112004. [CrossRef]
59. Badourdine, C. Exploring the link between spectral variance and upper canopy taxonomic diversity in a tropical forest: Influence of spectral processing and feature selection. *Remote Sens. Ecol. Conserv.* **2022**, *9*, 235–250. [CrossRef]
60. Aklilu Tesfaye, A.; Gessesse Awoke, B. Evaluation of the saturation property of vegetation indices derived from sentinel-2 in mixed crop-forest ecosystem. *Spat. Inf. Res.* **2021**, *29*, 109–121. [CrossRef]
61. Conti, L.; Malavasi, M.; Galland, T.; Komárek, J.; Lagner, O.; Carmona, C.P.; de Bello, F.; Rocchini, D.; Šímová, P. The relationship between species and spectral diversity in grassland communities is mediated by their vertical complexity. *Appl. Veg. Sci.* **2021**, *24*, 1–8. [CrossRef]
62. Gyamfi-Ampadu, E.; Gebreslasie, M.; Mendoza-Ponce, A. Evaluating multi-sensors spectral and spatial resolutions for tree species diversity prediction. *Remote Sens.* **2021**, *13*, 1033. [CrossRef]
63. Imran, H.A.; Gianelle, D.; Scotton, M.; Rocchini, D.; Dalponte, M.; Macolino, S.; Sakowska, K.; Pornaro, C.; Vescovo, L. Potential and Limitations of Grasslands α -Diversity Prediction Using Fine-Scale Hyperspectral Imagery. *Remote Sens.* **2021**, *13*, 2649. [CrossRef]
64. Kulawardhana, R.W. Remote sensing of vegetation: Principles, techniques and applications. By Hamlyn G. Jones and Robin a Vaughan. *J. Veg. Sci.* **2011**, *22*, 1151–1153. [CrossRef]
65. Zhao, F.; Guo, Y.; Huang, Y.; Reddy, K.N.; Lee, M.A.; Fletcher, R.S.; Thomson, S.J. Early detection of crop injury from herbicide glyphosate by leaf biochemical parameter inversion. *Int. J. Appl. Earth Obs. Geoinf.* **2014**, *31*, 78–85. [CrossRef]
66. Cabacinha, C.D. Relationships between floristic diversity and vegetation indices, forest structure and landscape metrics of fragments in Brazilian Cerrado. *For. Ecol. Manag.* **2009**, *257*, 2157–2165. [CrossRef]
67. Foody, G.M.; Cutler, M.E.; Mcmorrow, J.; Pelz, D.; Tangki, H.; Boyd, D.S.; Douglas, I.A.N. Mapping the biomass of Bornean tropical rain forest from remotely sensed data. *Glob. Ecol. Biogeogr.* **2001**, *10*, 379–387. [CrossRef]
68. Arekhi, M.; Yılmaz, O.Y.; Yılmaz, H.; Akyüz, Y.F. Can tree species diversity be assessed with Landsat data in a temperate forest? *Environ. Monit. Assess.* **2017**, *189*, 586. [CrossRef]
69. Fajji, N.G.; Palamuleni, L.G.; Mlambo, V. Evaluating derived vegetation indices and cover fraction to estimate rangeland aboveground biomass in semi-arid environments. *S. Afr. J. Geomat.* **2017**, *6*, 333–348. [CrossRef]
70. Gaitán, J.J.; Bran, D.; Oliva, G.; Ciari, G.; Nakamatsu, V.; Salomone, J.; Ferrante, D.; Buono, G.; Massara, V.; Humano, G.; et al. Evaluating the performance of multiple remote sensing indices to predict the spatial variability of ecosystem structure and functioning in Patagonian steppes. *Ecol. Indic.* **2013**, *34*, 181–191. [CrossRef]
71. Rampheri, M.; Dube, T.; Dhau, I. Use of remotely sensed data to estimate tree species diversity as an indicator of biodiversity in Blouberg Nature Reserve, South Africa. *Geocarto Int.* **2022**, *37*, 526–542. [CrossRef]
72. Rejauar, R.; Hassan Abu, H.I. NDVI Derived Sugarcane Area Identification and Crop Condition Assessment. *Plan Plus* **2004**, *1*, 2.
73. Möckel, T.; Dalmayne, J.; Schmid, B.C.; Prentice, H.C.; Hall, K. Airborne hyperspectral data predict fine-scale plant species diversity in grazed dry grasslands. *Remote Sens.* **2016**, *8*, 133. [CrossRef]
74. Li, W.; Shi, M.; Huang, Y.; Chen, K.; Sun, H.; Chen, J. Climatic change can influence species diversity patterns and potential habitats of salicaceae plants in China. *Forests* **2019**, *10*, 220. [CrossRef]
75. Shoko, C.; Mutanga, O.; Dube, T. Remotely sensed C3 and C4 grass species aboveground biomass variability in response to seasonal climate and topography. *Afr. J. Ecol.* **2019**, *57*, 477–489. [CrossRef]
76. Silva, B.; Álava-Núñez, P.; Strobl, S.; Beck, E.; Bendix, J. Area-wide evapotranspiration monitoring at the crown level of a tropical mountain rain forest. *Remote Sens. Environ.* **2017**, *194*, 219–229. [CrossRef]

77. Naidu, M.T.; Premavani, D.; Suthari, S.; Venkaiah, M. Assessment of tree diversity in tropical deciduous forests of Northcentral Eastern Ghats, India. *Geol. Ecol. Landsc.* **2018**, *2*, 216–227.
78. Panda, P.C.; Mahapatra, A.K.; Acharya, P.K.; Debata, A.K. Plant diversity in tropical deciduous forests of Eastern Ghats, India: A landscape level assessment. *Int. J. Biodivers. Conserv.* **2013**, *5*, 625–639.

4.2 Adopting Land Cover Standards for Sustainable Development in Ghana: Challenges and Opportunities.

Elisha Njomaba[1*], Fatima, Mushtaq[2], Raymond Kwame Nagbija[3], Silas Yakalim[4], Ben Emunah Aikins[5], Peter Surovy[1]

[1]Faculty of Forestry and Wood Sciences, Czech University of Life Sciences Prague, Kamýcká 129, 165 00 Prague, Czech Republic.

[2]Food and Agriculture Organization of the United Nations (FAO), Viale delle Terme di Caracalla, 00153 Rome, Italy.

[3]Faculty of Geoinformation Science & Earth Observation, Department of Natural Resource Management, University of Twente, Drienerlolaan 5, 7522 NB Enschede, The Netherlands.

[4]Touton Ghana, Monitoring and Evaluation Department, 20-36 N Airport Road, Accra, Ghana.

[5]School of Public Health, College of Health Sciences, University of Ghana, Accra, P.O. Box LG 13, Ghana

*Author to whom correspondence should be addressed.

Land 2025, 14(3), 550; https://doi.org/10.3390/land14030550
Author´s contribution: 70 %

Summary of the article

This article focused on developing and adopting standardized land cover datasets in Ghana to address inconsistencies in existing classifications and improve interoperability for sustainable development and reporting frameworks. Using a multi-sensor approach (Sentinel-1, Sentinel-2 optical imagery, and ancillary data), a national land cover map was produced in accordance with ISO 19144-2 standards, with a legend derived from the West African Land Cover Reference System. The classification, implemented with the random forest algorithm, achieved an overall accuracy of 90%, confirming the method's robustness in a heterogeneous landscape. Stakeholder engagement at global, regional, and national levels highlighted challenges to adoption, including limited familiarity with standards, lack of documentation, and the perceived complexity and cost of implementation. Nonetheless, the study demonstrated opportunities for harmonization, enhanced accuracy, and improved capacity for monitoring land cover change in support of the SDGs reporting. While the methodology offers a scalable model for integrating international standards into national systems, the limited institutional adoption underscores the need for stronger awareness, training, and localized guidance to ensure sustainable adoption.

Full article

land

MDPI

Article

Adopting Land Cover Standards for Sustainable Development in Ghana: Challenges and Opportunities

Elisha Njomaba [1,*], Fatima Mushtaq [2], Raymond Kwame Nagbija [3], Silas Yakalim [4], Ben Emunah Aikins [5] and Peter Surovy [1]

[1] Faculty of Forestry and Wood Sciences, Czech University of Life Sciences Prague, Kamýcká 129, 165 00 Prague, Czech Republic; surovy@fld.czu.cz
[2] Food and Agriculture Organization of the United Nations (FAO), Viale delle Terme di Caracalla, 00153 Rome, Italy; fatima.mushtaq@fao.org
[3] Faculty of Geoinformation Science & Earth Observation, Department of Natural Resource Management, University of Twente, Drienerlolaan 5, 7522 NB Enschede, The Netherlands; r.k.nagbija@student.utwente.nl
[4] Touton Ghana, Monitoring and Evaluation Department, 20-36 N Airport Road, Accra, Ghana; s.yakalim@touton.com
[5] School of Public Health, College of Health Sciences, University of Ghana, Accra P.O. Box LG 13, Ghana; benaikins56@gmail.com
* Correspondence: njomaba@fld.czu.cz; Tel.: +420-773-101-545

Abstract: The adoption of land cover standards is essential for resolving inconsistencies in global, regional, and national land cover datasets. This study examines the challenges associated with integrating existing datasets, including variations in land cover class definitions, classification methodologies, limited interoperability, and reduced comparability across scales. Focusing on Ghana as a case study, this research aims to develop a land cover legend and land cover map aligned with International Organization for Standardization (ISO) 19144-2 standards, evaluate the effectiveness of improving land cover classification and accuracy of data, and finally, assess the challenges and opportunities for the adoption of land cover standards. This study uses a multi-sensor remote sensing approach, integrating Sentinel-1 and Sentinel-2 optical imagery with ancillary data (elevation, slope, and aspect), to produce a national land cover dataset for 2023. Using the random forest (RF) algorithm, the land cover map was developed based on a land cover legend derived from the West African land cover reference system (WALCRS). The study also collaborates with national and international organizations to ensure the dataset meets global reporting standards for Sustainable Development Goals (SDGs), including those for land degradation neutrality. Using a survey form, stakeholders in the land cover domain were engaged globally (world), regionally (Africa), and nationally (Ghana), to assess the challenges to and opportunities for the adoption of land cover standards. The key findings reveal a diverse range of land cover types across Ghana, with cultivated rainfed areas (28.3%), closed/open forest areas (19.6%), and savanna areas (15.9%) being the most dominant classes. The classification achieved an overall accuracy of 90%, showing the robustness of the RF model for land cover mapping in a heterogeneous landscape such as Ghana. This study identified a limited familiarity with land cover standards, lack of documentation, cost implication, and complexity of standards as challenges to the adoption of land cover standards. Despite the challenges, this study highlights opportunities for adopting land cover standards, including improved data accuracy, support for decision-making, and enhanced capacity for monitoring sustainable land cover changes. The findings highlight the importance of integrating land cover standards to meet international reporting requirements and contribute to effective environmental monitoring and sustainable development initiatives.

Academic Editor: Linda See

Received: 24 January 2025
Revised: 26 February 2025
Accepted: 3 March 2025
Published: 5 March 2025

Citation: Njomaba, E.; Mushtaq, F.; Nagbija, R.K.; Yakalim, S.; Aikins, B.E.; Surovy, P. Adopting Land Cover Standards for Sustainable Development in Ghana: Challenges and Opportunities. *Land* **2025**, *14*, 550. https://doi.org/10.3390/land14030550

Keywords: standards; interoperability; sustainable development goals; geospatial; land cover; legend; Ghana; harmonization

1. Introduction

Innovation, broadly defined as the development or use of new ideas or behaviors [1], drives economic development, and is critical for sustainable development in all sectors. As innovations develop, standards are required to ensure the performance, conformity, sustainability, and safety of new products and processes [2]. Standards are also needed in achieving global agendas such as SDGs by supporting consistency, safety, quality, and interoperability across various data and sectors [3]. The use of spatial information to support the achievement of SDGs, such as through the geographic information systems domain, has continuously been increasing, facilitating the integration of all kinds of geographic information to enable more effective policies and decision-making as well as collaborative geospatial information management across organizations and levels of government [4].

In this context, technical communities like the Open Geospatial Consortium (OGC) and the ISO publish standards that focus on geographic data and information. Such standards are essential for the geospatial domain and related applications for data accuracy, efficient sharing, and supporting innovative solutions. Implementing and contributing to these standards helps organizations maintain interoperability, improve workflows, and achieve the effective governance and management of geographic information. Technical committees, such as the ISO Technical Committee (TC) 211 on Geographic Information/Geomatics, have established a structured set of standards [5]. For example, the ISO/TC 211 Working Group 7 on "Information Communities" focuses on standardization issues related to the conceptual modeling of geographic features, including aspects such as land cover and land use, and the ISO/TC 211 Advisory Group 13 advises ISO/TC 211 on the implementation of land cover and land use standards [6]. Among these standards, the ISO 19144 series serves as a foundation for collaboration and highlights the significance of land cover and land use standards [7]. One of the key components of this framework is the land cover meta language (LCML), introduced in ISO19144-2, which serves as a standardized language for describing land cover classes in a way that ensures global comparability, interoperability, and consistency across datasets. The LCML standard enables users to define land cover features based on structural and functional characteristics [7].

Land cover and land use mapping play an important role in the monitoring and assessment of environmental changes, which helps inform policy directions as well as advance SDGs [8]. Recent developments in remote sensing and machine learning approaches have led to transformation in this field, ensuring the use of high-resolution, dynamic, and scalable data for the analysis of the Earth's surface, which are essential for monitoring the progress and implementation of SDGs [9] However, monitoring this progress using available land cover information faces various constraints, including the use of non-standardized land cover approaches and inconsistent methodologies, particularly in the Sub-Saharan Africa regions where the use of localized methods is limited, resulting in inconsistent information over time between different national entities, regions, and reporting frameworks, including the United Nations Framework Convention on Climate Change (UNFCC) or the United Nations Framework Convention to Combat Desertification (UNCCD) [7]. To solve the inconsistent reporting between different entities, several standardized legends were prepared, such as the European CORINE (Coordination of Information on the Environment) system [10], the US Geological Survey Anderson Legend [11], and the EAGLE group land cover schema [12], among others. However, these legends suit their own needs

and are not interoperable with each other. Also, advances in remote sensing, such as the expansion of multi-sensor satellite systems like Senstine-2, Sentinel-1, and Landsat, have increased access to high-resolution, multi-temporal imagery [13]. Coupled with machine learning algorithms like the random forest algorithm [14] and deep learning algorithms such as convolutional neural networks, these tools now achieve classification accuracies exceeding 90% in complex landscapes [15]. Similarly, cloud-based platforms like Google Earth Engine (GEE) enable the large-scale processing of time-series data, which facilitate large-scale analyses of phenomena such as deforestation and urbanization [16]. Despite the technological advances, some limitations exist. Similar classes in terms of their spectra information, such as croplands and grasslands, remain difficult to distinguish [17]. Furthermore, for monitoring land resources at the local and global levels and specific uses or larger reporting, ensuring the interoperability between legends and systems, as well as reliance on standardized classification systems with such advanced remote sensing and combined machine learning techniques, has the potential to significantly improve the sustainability and accuracy of the land resources information provided from land cover areas. For example, the development of a regional land cover reference system, such as for West Africa [11], helps address the wide diversity of land cover in various countries and links them within a region. This regional land cover reference system focuses on technical aspects of standardization but neglects the integration of ISO standards into national systems in ways that align with local needs, capacities, and reporting priorities. Hence, this research focuses on developing a country-specific ISO 1944-2 legend and land cover data.

While a land cover reference system exists for West Africa, Ghana does not yet possess a national land cover reference and monitoring system. In Ghana, like in many countries, the process for land cover mapping by national entities started in the 2000s, with sub-national and national maps such as those produced by the Centre for Remote Sensing and Geographic Information Services (CERSGIS) and the Resource Management Support Centre (RMSC) of the Forestry Commission [18]. Later, the Forestry Commission developed maps for 1990, 2000, 2010, 2012, and 2015 under the Forest Preservation Program [18]. Even though there have been efforts to produce national land cover products, the focus has been on sub-national, municipal, and district levels, and often rely on existing global data such as the European Space Agency's (ESA) land cover data, among others. Hence, the sustainability and accuracy of these land cover products are often limited by the lack of standardization due to changing objectives, varying methodologies, and classification systems, hindering data utility and comparability.

While various international standards and software developed based on these standards exist to support the interoperable land cover methodological development process, the adoption of the standards remains limited. About 32 sub-national, national, regional, and international legends are available on the land cover legend registry (LCLR) hosted by the United Nations Food and Agricultural Organization (FAO). The LCLR hosts legends developed following the standard ISO 19144-2 [19], reflecting that 164 countries have not developed available national legends following international land cover and land use standards. This results in various interoperability limitations and limited comparability of results between regions, countries, and global and local levels. In addition, this results in the limited use and recognition of national legends in global dataset development, and global datasets are mostly being used to report to international frameworks rather than national datasets, including when national data already exist and are available. This is reflected, for example, when reporting for land degradation neutrality, where most of the countries used global datasets of land cover, and the difference between global datasets and national datasets can be very significant [20]. For example, Conchedda and Tubiello [21]

compared various global land cover and identified differences of up to 67% for cropland, particularly in countries like Brazil. Similarly, Seebach et al. [22] examined multiple global forest cover datasets across different nations and observed notable variations. For instance, in Denmark, the JRC high-resolution forest cover map for the year 2000 recorded 12% forest cover, while the CORINE Land Cover 2000 dataset reported just 3%. Hence, a stronger consideration of national datasets for national and/or global programs has the potential to significantly increase accuracy as well as the adoption of the results and support actions for SDGs.

Thus, the objective of this article is to assess the potential for the adoption of land cover and land use standards by (1) preparing a legend for Ghana as a pilot country in Sub-Saharan Africa following the standards ISO 19144-2, (2) preparing a land cover dataset of Ghana for 2023, and (3) engaging experts in Ghana, Africa and globally to document the challenges and the opportunities of the adoption of standards for land cover to make this process sustainable. By developing a national-specific ISO 19144-2 legend, generating a national land cover dataset by leveraging multi-sensor remote sensing, machine learning (random forest), and LCML, and documenting challenges and opportunities through expert engagement, this study fills the gap by providing a practical and scalable model for integrating international standards into national land cover mapping. This approach not only strengthens data comparability and supports SDG reporting but also reduces the dependency on global datasets that may fail to reflect local realities. This approach has broader implications for land management, climate monitoring, and sustainable development across Sub-Saharan Africa.

2. Materials and Methods

The methodological approach is developed around the three main objectives, i.e., (i) developing a national land cover legend following ISO 19144-2, (ii) developing a national land cover dataset without field data and validation but with online photo interpretation data collection platforms, considering the limited resources available, and (iii) assessing the challenges and opportunities by receiving feedback from international and regional experts (Figure 1).

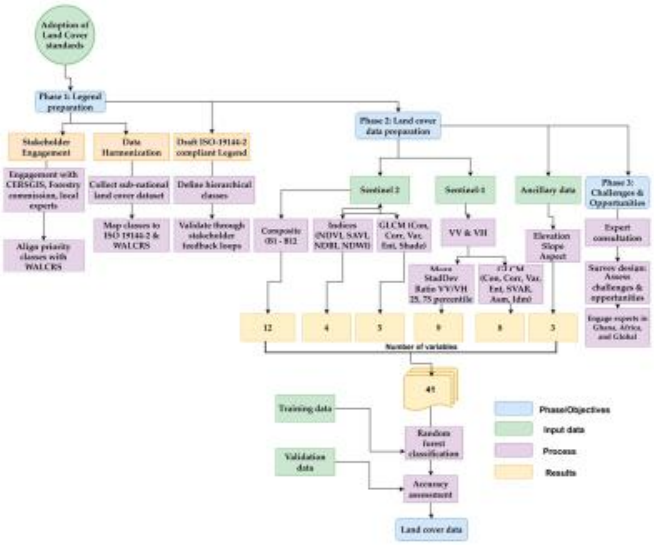

Figure 1. Methodological flow: authors' own construct.

2.1. Area of Interest (AOI)

This area of interest (AOI) considers different spatial levels, starting with the global context and the national context, with Ghana as the case study. Ghana (Figure 2) is located on the west coast of Africa and shares its eastern, western, and northern borders with Togo, Côte d'Ivoire, and Burkina Faso, respectively. Its southern border is the Gulf of Guinea and the Atlantic Ocean. The geographical coordinates of the country are 7.9465° N, 1.0232° W, and the country occupies an area of 238,533 km^2 [23] Ghana is divided into 16 administrative regions, subdivided into a total of 261 districts.

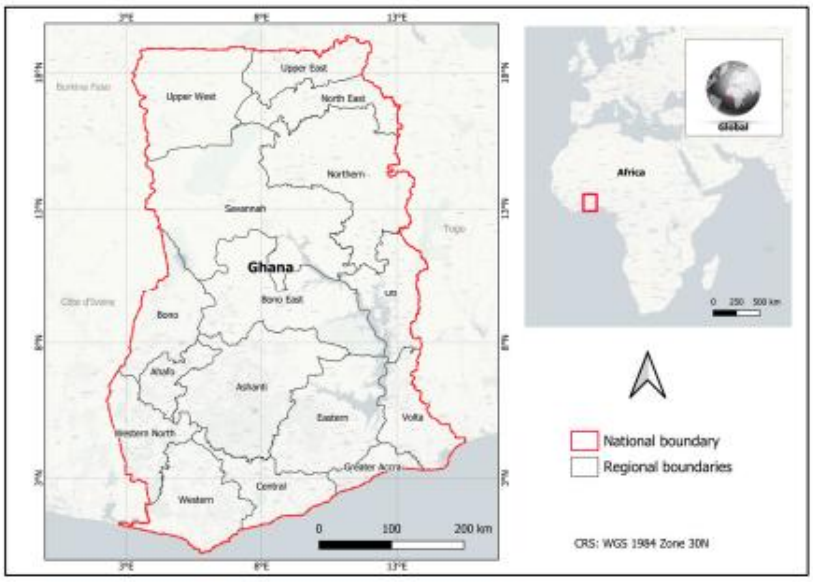

Figure 2. Area of interest: Africa, global view, and Ghana as a case study (source of administrative boundary data: [24]).

2.2. Land Cover Legend

Defining the land cover legend is an important step in a land cover mapping process, as it provides a method to express the content of a map. The legend reflects how the semantic generalization of a specific geographic area has been conceived [25]. The process of categorization is meant to minimize the complexity of the real world, where different area types are distributed on a continuum. Since the definition of classes is an arbitrary process by nature, this may lead to uncertainties that will affect the accuracy of the final land cover map. It is, therefore, important that the definition of the LCL meets two minimum requirements: (i) clear and unambiguous class definitions and (ii) a class boundary that does not overlap with other legend classes [26]. The WALCRS meets these requirements. The WALCRS is, therefore, based on three levels, with the whole schema divided into two major categories: vegetated and non-vegetated. The vegetated category is further divided into natural and cultivated, while the non-vegetated category is divided into terrestrial-non-vegetated and water. With these broadly defined categories, the various levels are further divided based on their physiognomic or structural characteristics and improved with additional qualitative criteria to classify land features., the vegetated area is level 1; level 2 is separated by vegetation artificiality, which takes us to natural or seminatural vegetation and cultivated or managed vegetation at level 3. Semi-natural vegetation is further divided into tree-dominated areas, shrub-dominated areas, and herb-dominated areas based on their growth from dominance at level 4.

In line with such recommendations, the WALCRS [27], which was defined using ISO 19144 LCML (ISO 19144-2, 2012), was used for the identification of the land cover

classes and existing legends and datasets. National land cover classes were finalized in consultation with national partners, mainly CERSGIS, the Environmental Protection Agency (EPA), and the Land Use and Spatial Planning Authority (LUSPA). The description of the land cover classes was translated using the land characterization system software (LCHS) [28], an implementation tool of the ISO standard (ISO 19144-2) LCML [29].

2.3. Land Cover Dataset

2.3.1. Training and Validation Data Collection

First, the land cover classes needed for training data collection were established from the WALCRS, where we identified the available classes in the context of Ghana. The training and validation data collection process involved in this work was performed using photo interpretation techniques and existing land cover data of some areas in Ghana. Data were collected using Collect Earth Online (CEO: [30]) and Google Earth Pro with high-resolution imagery. For CEO, a project for training data collection was designed using a 10 m-by-10 m plot, each containing five sample points. A total of 4000 training samples were randomly allocated, with 10% repeated samples as part of a quality control check. By using the Collect Earth Online platform, we leveraged its capabilities to handle multi-source satellite data (e.g., including Sentinel-1 composite, Sentinel-2 composite, Mapbox satellite, Google Earth, OpenStreetMap, and NICFI Planet satellite data) and offer high-performance computing services. Normalized Difference Vegetation Index (NDVI) time series were also analyzed using the CEO's Geo-dash widget to understand seasonal variations. In addition to the 4000 randomly allocated sample points, an additional 3677 samples were manually included, making a total data sample of 7677. The number of training and validation data used for the classification is shown in Figure 3, while the spatial distribution of training and validation data is shown in Figure 4.

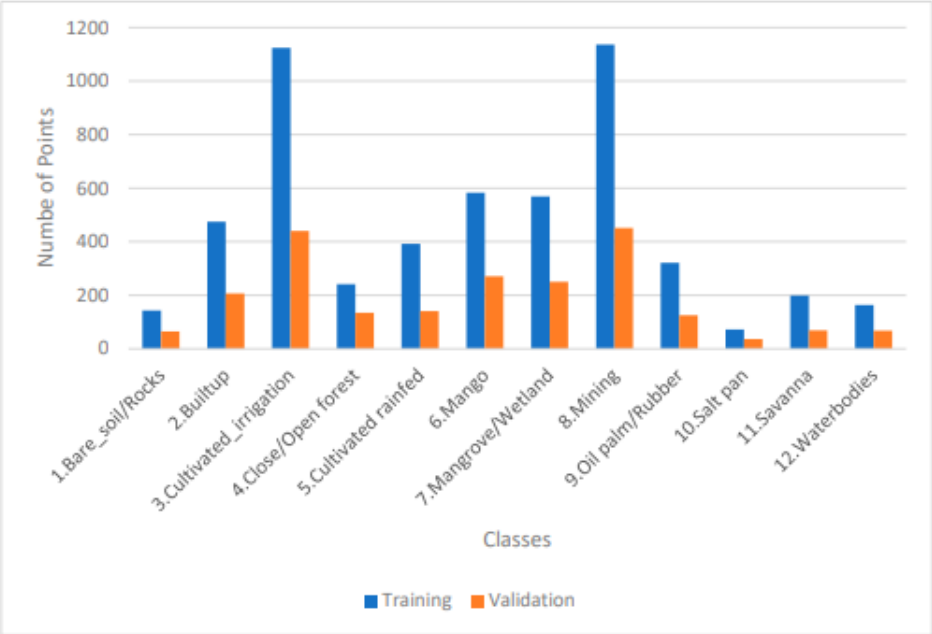

Figure 3. Distribution of training and validation data.

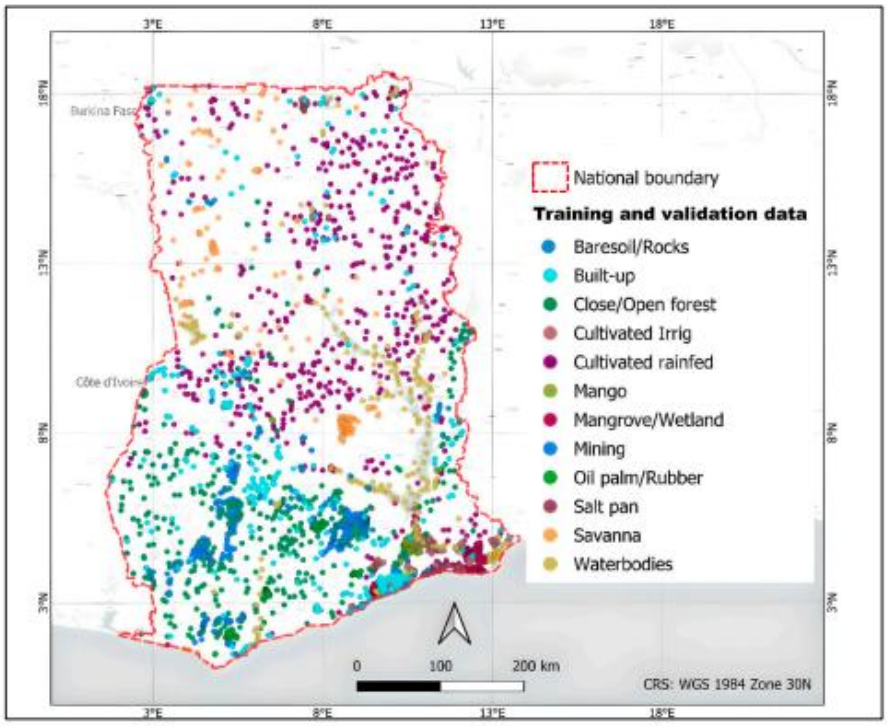

Figure 4. Spatial distribution of training and validation data.

2.3.2. Data Validation Procedure

A validation process involving quality control checks, stakeholder engagements, and comparison with existing land cover data was implemented to ensure the quality and reliability of the collected training and validation data. The initial 4000 randomly generated samples were selected, with 10% being intentionally repeated as part of the quality control mechanism to ensure consistency in land cover labeling. The additional 3677 manually selected sample points were incorporated based on local expertise to enhance data representativeness. The collected samples were verified with existing global land cover maps of Ghana and sub-national land cover maps. Furthermore, stakeholders and local experts were consulted, integrating indigenous knowledge to refine the training and validation data. High-resolution satellite imagery from the CEO and Google Earth Pro was used to visually verify land cover types. Also, the CEO's Geo-dash widget provided NDVI time-series analysis to capture seasonal variations, serving as an additional validation process. To further ensure robustness, the dataset was split into 70% training and 30% validation, with classification accuracy assessed using standard metrics, including overall accuracy, user accuracy, producer accuracy, and the kappa coefficient. These validation measures ensured that the dataset was reliable and representative of actual land cover conditions in Ghana.

2.3.3. Satellite Image Preparation

This study used a multi-sensor approach where three types of remote sensing data, optical data (Sentinel-2), SAR data (Sentinel-1), and other ancillary information, were integrated as predictors for the land cover classification. Sentinel-2 surface reflectance images were accessed for the period from October 2022 to October 2023, covering an entire year. The year 2023 was chosen because this year provided images with less cloud coverage. The one-year time frame is considered adequate for capturing yearly phenology [31]. Also, since one of the objectives of this article is to prepare an up-to-date land cover classification

using recent satellite imagery, the single year allows for consistency in data acquisition and processing. Each scene in the image went through a cloud and shadow masking process using the algorithms implemented in GEE. A set of four spectral indices, including the Normalized Difference Vegetation Index (NDVI), Normalized Difference Built-up Index (NDBI), Normalized Difference Water Index (NDWI), and Soil-Adjusted Vegetation Index (SAVI), were computed and added, resulting in a collection that includes the selected reflectance bands. These indices have been carefully selected for their capacity to differentiate and identify specific classes. For instance, the NDVI is important in quantifying biomass, monitoring deforestation, and analyzing ecosystem dynamics [32]; the NDBI is focused on built-up areas by analyzing the difference between the near-infrared and the shortwave infrared bands, serving as a robust tool for mapping the built-up infrastructure and urban sprawl [33]; the NDWI looks at variations between the green and near-infrared bands, helping to detect waterbodies, wetlands, and moisture contents in landscapes [34]; and the SAVI accounts for soil influences on vegetation indices [35]. The median values from each scene for all Sentinel-2 bands were used to create seasonal image stacks, and finally, GLCM (gray-level co-occurrence matrix) texture variables were applied to the NDVI images. The GLCM is a method used as an image-processing technique to extract information about spatial patterns of the intensity of pixels in an image [36]. Sentinel-1 Ground Range Detected (GRD) data were also obtained for the same date range and resampled to the same resolution as the Sentinel-2 resolution. All Sentinel-1 images are in ascending orbits with vertical transmit and vertical receive (VV) and vertical transmit and horizontal receive (VH) polarization. The descending orbit images were not used because there were no images for this orbit in the study area. The calculated predictors include mean, standard deviation, ratio of VV to VH, 25th and 75th percentile, and texture variables for VH and VV bands. The texture predictors provide information about the spatial arrangements of pixel intensities, capturing the spatial relationships between pixels. This helps to distinguish between different land cover types based on their spatial patterns [37]. Apart from the satellite images, three additional ancillary predictors (elevation, slope, and aspects) were resampled to the resolution of Sentinel-2 data and included. All variables used for the classification are provided in Table 1.

Table 1. Variables used for the classification process.

Name	Feature/Index Formula
Original Sentinel-2 Bands	Blue, Green, Red, rededge1, rededge2, rededge3, Near Infrared (NIR), rededge4, Water vapor, Short Wave Infrared (SWIR1), SWIR2, SWIR3
Spectral Indices	NDVI = (NIR − Red)/(NIR + Red) NDBI = (SWIR1 − NIR)/(SWIR1 + NIR) NDWI = (Green − SWIR1)/(Green + SWIR1) SAVI = ((NIR − Red)/(NIR + Red + 0.5)) × (1 + 0.5)
Sentinel-2 Texture (GLCM)	Contrast, Correlation, Variance, Entropy, Shade
Sentinel-1 Features	VV, HH, VV/HH, VH, SD of VV, SD of VH, 25th percentile, 75th percentile.
Sentinel-1 Texture (GLCM, VV, and VH)	Contrast, Correlation, Variance, Entropy, Inverse Difference Moment (IDM), Angular Second Moment (ASM), Sum Average (SAVG)
Ancillary Data	Elevation, Slope, Aspect

2.3.4. Classification and Accuracy Assessment

The RF classifier is used, which is a widely used supervised machine learning algorithm for land cover classification. The RF technique is a non-parametric technique that

builds a robust model using multiple decision trees to predict outcomes. It handles large datasets with numerous variables effectively without requiring prior knowledge of their interrelationships and is resilient against outliers, ensuring reliable predictions [38]. The hyperparameters, including the number of trees and variables per split, were tuned using a systematic exploration of a set of potential inputs through a grid-search scheme [38]. Based on this tuning, the land cover classifier was run with 500 trees and 6 variables per split, using the default maximum depth of trees, which is unrestricted, and 70% of data for training. The random forest algorithm returns three important measures: the selection rate of each candidate variable, the Gini index, and the permutation of predictor variables as an estimate of importance. The mean decrease accuracy, which is a measure of how much the accuracy decreases when a variable is excluded, was used to generate this variable's importance due to its simplicity [39]. All variables were used for the classification, since almost all variables were important. This is shown in Figure A1. The training data samples were carefully assessed to ensure balanced and representative data for classification. We ensured that all classes were at least 100. However, certain classes were underrepresented; hence, those classes were manually added and validated with high-resolution imagery coupled with expert knowledge.

The accuracy assessment was undertaken with respect to the validation data to assess the classification accuracy (30% of the visually interpreted randomly sampled points described above). The accuracy parameters calculated are overall accuracy, user accuracy, producers' accuracy, and kappa coefficient. All image-processing, classification, and accuracy assessments were conducted using GEE. The GEE scripts and datasets used in this study are publicly available on GitHub [40].

2.4. Challenges and Opportunities

A structured questionnaire survey was conducted in 2024 to assess the challenges and opportunities for the adoption and implementation of land cover standards. The survey targeted a broad spectrum of stakeholders from government agencies, academia, private institutions, and international organizations involved in land cover and land use activities across global, regional, and national geographic scales. Including experts from different regions was essential to capture diverse experiences and comparative insights on adopting land cover standards across various contexts. This helps to situate Ghana's progress against international efforts, identifying global challenges such as interoperability issues. Furthermore, given that land cover standards such as ISO 19144-2 are designed for global application, engaging international stakeholders is essential to assess the variability in adoption, barriers to implementation, and opportunities for adoption across different geographic scales. The questionnaire was designed to collect insights from three main respondent groups: those familiar with and using LCML standards, those using other land cover standards, and those not using any standards at all. The survey was designed using Google Forms for ease of access and distribution, allowing global participation and ensuring efficient data collection from stakeholders.

3. Results

3.1. Final Land Cover Legend of GHANA

The land cover characteristics of Ghana encompass a wide range of classes, including diverse types of vegetation, various crop types and categories, non-vegetated areas, urban landscapes, and water bodies. A total of 37 land cover classes are clearly identified from the WALCRS, as presented in Table 2. The final land cover legend for Ghana, as highlighted and presented in Table 2, serves as a standardized reference for broader classifications. However, not every class included in the legend was utilized in the classification process. Some classes

were modified or merged where they exhibited similarities at a specific classification level, ensuring a streamlined and meaningful categorization. Specific descriptions of land cover classes with corresponding images and their Unified Modeling Language (UML) diagrams are detailed in Appendix A, Figures A2–A28.

Table 2. Selected land cover classes from the West African Reference System. The highlighted classes can be identified in Ghana.

Level 1	Level2	Level 3	Level 4	Level 5	Level 6	Level 7
Vegetated area (V)	Natural-Seminatural (Vns)	Terrestrial (Vnt)	Tree dominated area (A)	Closed tree formation/forest (Ad)	Moist forest (Fh) Dry forest (Fs)	
				Open tree formation/forest (Ac)	Woodland (Open) (Fco) Woodland (very open) (Fct)	
			Shrub dominated area (Ab)	Shrub (Medium, High (Abm/h)	Ticket (FO)	
					Open Shrubland (Aro)	
				Shrubland (low/dwarf) (Arb)	Tiger bush (Bt) Open low shrublands (Arbo)	
			Herb dominated area (H)	Savanna (S)	Tree and shrub savanna (Saa) Grass savanna (Sh)	Tree savanna (Sa) Shrub savanna (Sar)
				Steppe (St)	Tree and shrub steppe (Staa) Herbaceous steppe (Sth)	
		Aquatic/flooded (Vnar)	Woody dominated area (Sb)	woody Mangrove (Ml)	Tree mangrove (Ma)	
					Scrub mangrove (Mar)	
				Flooded woody (Bi)	permanently flooded woody (Bip) seasonally flooded woody (Bis)	
			Herbs dominated area (Adh)	Swamps (Ahm)		
				Salt Marsh (Ahms)		
	Cultivated	Cultivated Rainfed	Tree crop plantation (Carf)	Forest plantation (Cpf)	Forest plantation	Oil palm(Cpfo)
				Annual herb cultivation (Cahn)	evergreen (Cfp)	Cocoa(Cpfc)
				Orchards (V)	Forest plantation	Mango(Cpfm)
					deciduous (Cfc)	Rubber plantation
					Forest plantation	(Cpfr)
			Shrub crop (Cab)	Annual herb cultivation (Canh)	mixed (Cfm)	
			Herbaceous crop (Ch)	Shifting herb cultivation (Cth)	Orchards single crop (Vmp)	
					Orchards multiple crop (Vcp)	

Table 2. *Cont.*

Level 1	Level2	Level 3	Level 4	Level 5	Level 6	Level 7
	Cultivated	Cultivated Rainfed	Tree crop plantation (Carf)	Forest plantation (Cpf) Annual herb cultivation (Cahn) Orchards (V)	Forest plantation evergreen (Cfp) Forest plantation deciduous (Cfc) Forest plantation mixed (Cfm)	Oil palm(Cpfo) Cocoa(Cpfc) Mango(Cpfm) Rubber plantation (Cpfr)
			Shrub crop (Cab) Herbaceous crop (Ch)	Annual herb cultivation (Canh) Shifting herb cultivation (Cth)	Orchards single crop (Vmp) Orchards multiple crop (Vcp)	
		Cultivated Irrigated (Ci)	Tree crop dominated (Cad) Shrub crop dominated (Ciab) Herbaceous crop dominated (Cih)	Orchard (single crop) (Vmi) Orchard (multi crop) (Vci) Single crop (Mohi) Multiple crop (Muhi)		
		Cultivated post flooded (Cd)	Post flooded herbaceous cultivation (Chai) Flooded herbaceous cultivation (Chi)			
Non-vegetated area (Zn)	Terrestrial Non-vegetated (Tn)	Natural surface (Sn)	Rocks coarse fragments (Tr)	Bare rocks (Sr) Bowal lateritic crust (Cl)		
			Soil, sand deposit (Ss)	Stony desert (Dp) Sandy desert (Dsa) Salt deposit (Ds) Bare soil (Sn) Beeches (P)	Erg (dunes) (Er)	Longitudinal (Ei) Barchan (Eb) Parabolic (Ep)
		Artificial surface (Sa)	Built-up non-linear (Bnl)	Urban area (Zu) Rural villages (Vr) Infrastructure (I)	Port (Po) Airport (Ae)	
			Built-up linear and others (Bla) Dump and extraction sites (Sd)			
	Water(E)	Natural waterbodies (En)	Permanent waterbody(Pep)	Rivers(R) Lakes(L)		
		Artificial waterbodies(Ea)	Seasonal waterbody(Pes)	River bank(Rr) Wadies(W) Lakeshores(Ri)		

3.2. Land Cover Dataset of Ghana (2023)

The land cover classification of Ghana, as shown in the national map (Figure 5) and accompanying statistics (Table 3), reveals a diverse range of land cover types over a total area of 24,343,056.4 ha. Spatially, the classified land cover map highlights the dominance of agricultural and forested areas in the southern and central regions, while savanna landscapes dominate the northern areas. Built-up areas are concentrated around major urban centers, and waterbodies are prevalent in the south, particularly around Volta Lake (Figure 5). A breakdown of land cover types shows that cultivated rainfed agriculture is the dominant class, covering 6,896,359 hectares (28.3%) of the total area, followed by closed/open forest areas (4,781,444 hectares, 19.6%, and savanna (3,867,151 hectares, 15.9%)). Other significant classes include cultivated irrigation (2,804,122 hectares, 11.5%) and mango (1,024,109 hectares, 4.2%). Smaller land cover categories such as waterbodies (813,574 hectares, 3.3%), mangroves/wetlands (274,440 hectares, 1.1%), and salt pans (33,011 hectares, 0.1%) occupy a minor portion of the landscape. Additionally, built-up areas (466,540 hectares, 1.9%) and mining sites (2,362,189 hectares, 9.7%) reflect significant human activity. Bare soil/rocks and oil palm/rubber constitute minor fractions of the total area.

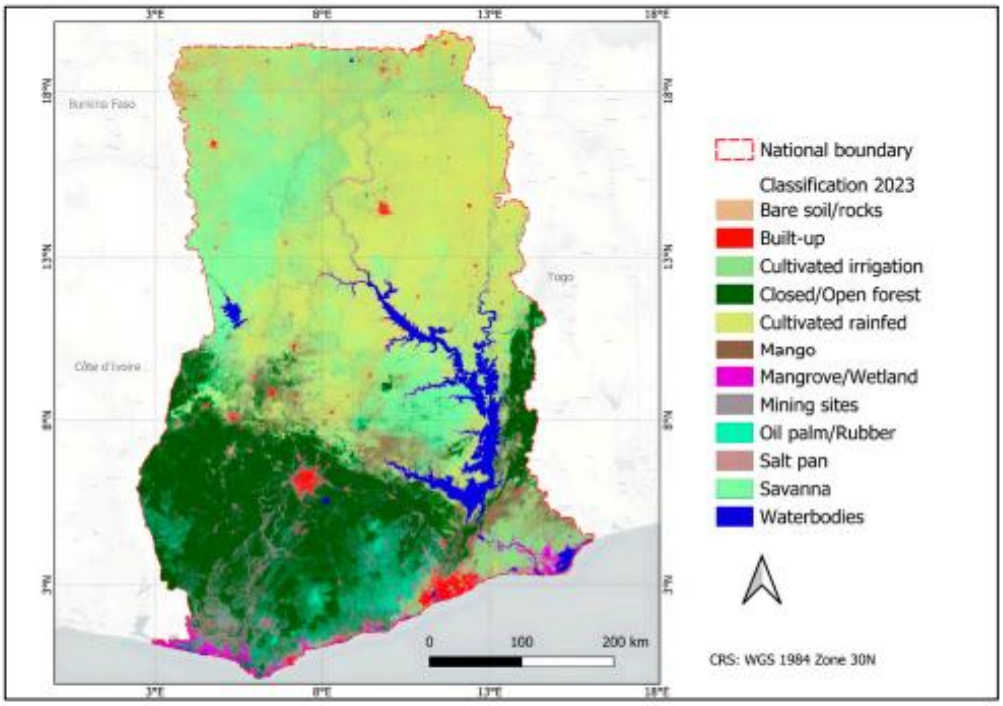

Figure 5. 2023 Land cover map of Ghana 2023.

Table 3. Comparison of land cover area between global data and classification.

Land Cover Class (ESRI)—Global	Area (%)	Land Cover Class (MODIS)—Global	Area (%)	Land Cover Class (National)	Area (%)
Trees	45.2	Grasslands	40.36	Bare soil/rocks	1.7
Flooded vegetation	0.31	Permanent wetlands	0.53	Built-up	1.9
Crops	3.8	Croplands	10.19	Cultivated irrigation	11.5
Built area	3.9	Built-up lands	1.30	Closed/open forest	19.6
Bare ground	0.04	natural vegetation	4.36	Cultivated rainfed	28.3
Clouds	0.01	Barren	0.03	Mango	4.2
Rangeland	46.7	Unclassified	2.75	Mangrove/wetland	1.1
		Evergreen broadleaf forest	3.29	Mining	9.7
		Deciduous needleleaf forest	0.00	Oil palm/rubber	2.5
		Deciduous broadleaf forest	0.07	Salt pan	0.1
		Mixed forest	0.00	Savanna	15.9
		Woody savannas	10.41	Water bodies	3.3
		Savannas	26.73		
Total	100		100		100

A comparison with the global dataset shows significant differences in class representation. For instance, cultivated rainfed agriculture (28.3%) and irrigation (11.5%) in the national land cover data far exceed the land cover statistics reported for ESRI's crop (3.8%) and MODIS's cropland (10.19%) data. Similarly, closed/open forests (19.6%) and savannas (15.9%) in the national data are combined into broad categories like ESRI's rangeland (46.7%) and MODIS's savannas (26.73%). These generalized classes fail to differentiate between Ghana's mosaic of forest–savanna transitions or agroforestry systems, such as mango plantations (4.2%), which are explicitly mapped in the national classification. Again, while the national land cover identified mining (9.7%) and built-up areas (1.9%) as distinct classes, global datasets either omit these categories or misrepresent their scale. MODIS's built-up area (1.3%) underestimates urbanization, while ESRI's built-up area (3.9%) overestimates urbanization by combining scattered settlements with true urban infrastructure. Mangroves/wetlands (1.1%) and salt pans (0.1%) in the national land cover data are either absent or merged into broad classes like MODIS's permanent wetlands (0.53%) or ESRIS's flooded vegetation (0.31%). The results emphasize the value of regionally tailored classifications. While global datasets might claim high accuracy, their broad classes prioritize simplicity over actionable specificity. The land cover map provides insights into Ghana's landscape regarding agricultural expansion, urbanization, deforestation, and mining activities. The high proportion of cultivated land emphasizes the importance of agriculture in the country, while the extent of mining activity signifies the impact of resource extraction on land cover and land use patterns. The presence of water bodies and wetlands shows hydrological features that play a key role in biodiversity conservation as well as water resource management.

Accuracy Assessment

An accuracy assessment was conducted using a confusion matrix to evaluate the classification process (Table 4), which quantifies the agreement between the classification map and the reference data. The overall accuracy of the land cover classification was 90% (Table 5), with individual class accuracies varying across the 12 land cover types, demonstrating a high level of precision in the mapping process. However, accuracy varied across land cover classes. Among the classified land cover types, mining areas achieved the highest producer accuracy (95.80%), indicating that most of the mining sites were correctly identified with less confusion. Similarly, the built-up areas recorded the highest user

accuracy (97.90%), showing that almost all pixels classified as built-up areas were correctly labeled (Table 5), suggesting an indication of the easier identification and distinguishing of anthropogenic land cover types such as mining and urban areas.

Table 4. Land cover map accuracy assessment (confusion matrix).

Class/ Reference	Bare Soil/ Rocks	Built-up land	Cultivated/ Irrigation	Closed/ Open Forest	Cultivated/ Rainfed	Mango	Mangrove/ Wetlands	Mining	Oil Palm/ Rubber Salt Pan	Savanna	Water/ Bodies	Total
Bare soil/ rocks	51	1	5	0	3	0	0	3	0	2	0	0	65
Built-up land	0	185	2	1	0	2	1	12	2	0	0	0	205
Cultivated irrigation.	1	0	397	1	13	6	8	7	1	4	0	2	440
Closed/ Open forest	0	0	0	116	0	2	0	8	5	0	3	1	135
Cultivated rainfed	0	0	17	2	117	1	0	0	1	0	3	0	141
Mango	0	0	9	2	5	245	3	4	3	0	0	0	271
Mangrove/ wetland	0	0	8	1	0	1	226	3	1	2	3	5	250
Mining	0	3	3	4	2	4	1	432	1	0	0	1	451
Oil palm/ rubber	0	0	1	5	0	5	0	9	105	0	0	0	125
Salt pan	0	0	3	0	0	0	0	0	0	33	0	0	36
Savanna	1	0	2	0	11	0	0	0	1	0	54	0	69
Water bodies	1	0	0	0	0	0	1	1	0	1	0	64	68
Total	54	189	447	132	151	266	240	479	120	42	63	73	2025

Table 5. Producer, user, and overall accuracy.

Land Cover Class	Producer Accuracy (%)	User Accuracy (%)
Bare soil/rocks	78.50	94.40
Built-up land	90.20	97.90
Cultivated irrigation	90.20	88.80
Closed/open forest	85.90	87.90
Cultivated rainfed	83.00	77.50
Mango	90.40	92.10
Mangrove/wetland	90.40	94.20
Mining	95.80	90.20
Oil palm/rubber	84.00	87.50
Salt pan	91.70	78.60
Savanna	78.30	85.70
Water bodies	94.10	87.70
Overall Accuracy	90	

However, some land cover types showed lower classification accuracies due to spectral similarities with other classes. For instance, the savanna class recorded producer and user accuracies of (78.30% and 85.70%), respectively, indicating some level of misclassification with cultivated areas. The confusion matrix also shows instances of misclassification, such as bare soil/rocks and salt pans, misclassified with cultivated areas. Despite these challenges, the classification performed well in differentiating major land cover types across Ghana (Table 5).

3.3. Challenges and Opportunities to the Adoption of Land Cover Standards

Out of 148 total survey respondents from around the world, 31 were from Africa (excluding Ghana), 59 were from various other continents, including Europe, North and South America, Asia, and the Middle East, and 54 responses came from Ghana. As expected, most responses came from Ghana since the case study focuses on this country and specifically targets more Ghanaians (Figure 6).

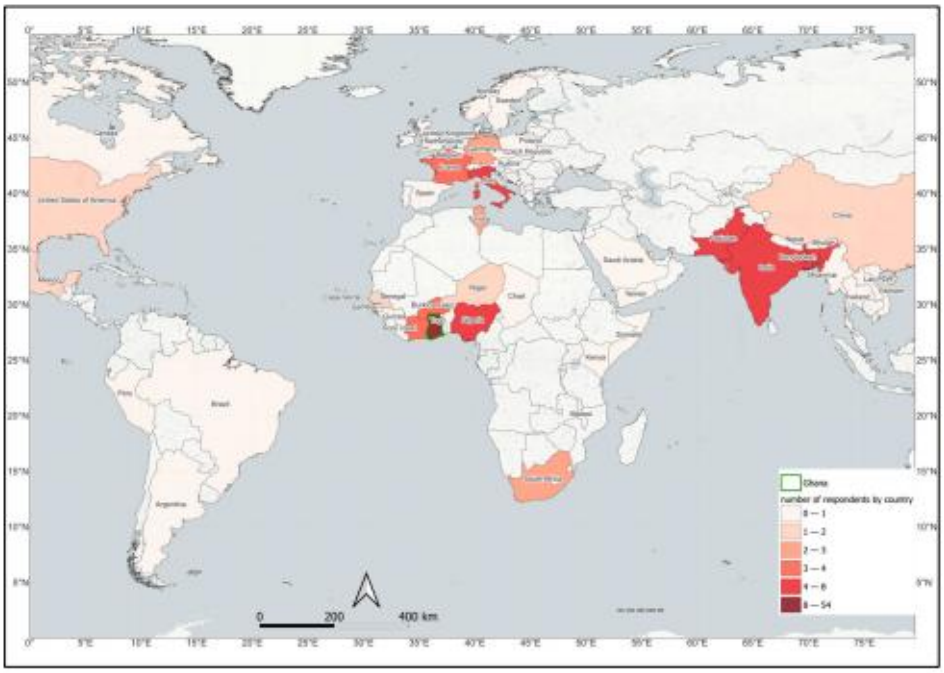

Figure 6. Number of responses received from 48 countries across the world. (Source of responses: [41]; source of administrative boundary: [42]).

To assess the challenges to the adoption of land cover standards, the questionnaire sought to first find whether the respondents were familiar with land cover standards, specifically the land cover meta language, and their use of them. The results (Figure 7) highlight a significant knowledge gap globally, regionally, and nationally. Globally, out of the 148 respondents, 44 (30%) were somewhat familiar, 37 were not very familiar (25), 40 were not familiar at all (27%), and 27 were very familiar (18%). In Sub-Saharan Africa, out of the thirty-one respondents, nine were somewhat familiar (29%), seven were not very familiar (23%), ten were not familiar at all (32%), and five were very familiar (16%). In the case of Ghana, fifteen (28%) out of fifty-four respondents were somewhat familiar, nineteen (35%) were not very familiar, sixteen (30%) were not familiar at all, and four (7%) were very familiar (Figure 7). This lack of familiarity, according to the respondents, stems from LCML's technical complexity, which demands specialized training to navigate its ontology-driven framework, as well as a lack of localized guidance tailored to regions like Ghana. This study further explored whether respondents used LCML or other land cover standards (Figure 8). The findings revealed an inconsistent adoption of standards across the different regions. Globally, out of 148 responses, 48 (32%) use the LCML standards, 58 (39%) use no standards, and 42 (27%) use other standards. In Africa, out of thirty-one respondents, eleven (35%) use LCML standards, eight (26%) do not use any standard, and twelve (39%) use other standards. In Ghana, out of 54 responses, 11 (20%) use LCML standards, 31 (57%) do not use any standard, and 12 (22%) use other standards. This inconsistency reflects institutional and resource barriers: dominant tools like ArcGIS, QGIS,

and Excel offer preconfigured workflows that align with existing user expertise, whereas LCML's adoption is hindered by its lack of integration into widely used platforms, as reported by the respondents.

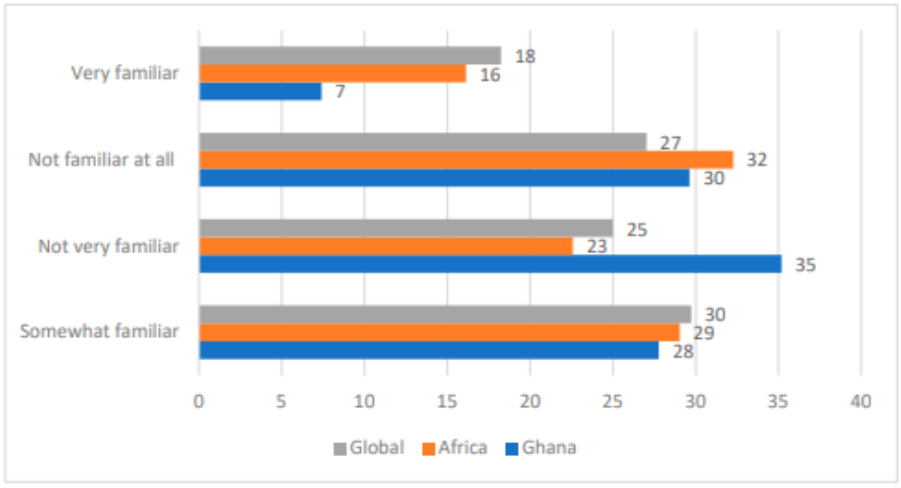

Figure 7. Respondent's familiarity with the land cover meta language: global, African, and Ghanaian context (Source: [41]).

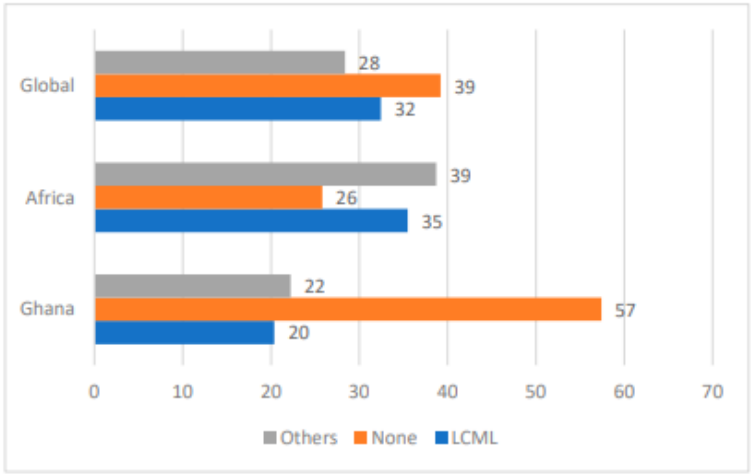

Figure 8. Respondent's use of land cover meta language: global, African, and Ghanaian context (Source: [41]).

This study identified key challenges that hinder the widespread adoption of land cover standards (Figure 9). The results, as reported in Figure 9, show that globally, 46% of respondents identified a lack of guidance materials and documentation as a challenge, while 10% highlighted cost implications, and 44% cited the complexity of the standards. In Africa, 44% of respondents noted a lack of guidance materials, 11% mentioned cost implications, and 44% identified the complexity of the standards. In Ghana, 53% of respondents considered a lack of guidance materials a limitation, 27% pointed to cost implications, and 20% indicated the complexity of the standards. These regional disparities underscore systematic issues. In Ghana, the absence of localized training programs and documentation increases the reliance on non-standardized methods. Meanwhile, the higher emphasis on cost reflects financial constraints, such as software licensing fees for tools like the ArcGIS suite, which compete with investments in LCML training. The reliance on

non-standardized classification systems, particularly in Ghana, constrains interoperability and comparability across datasets.

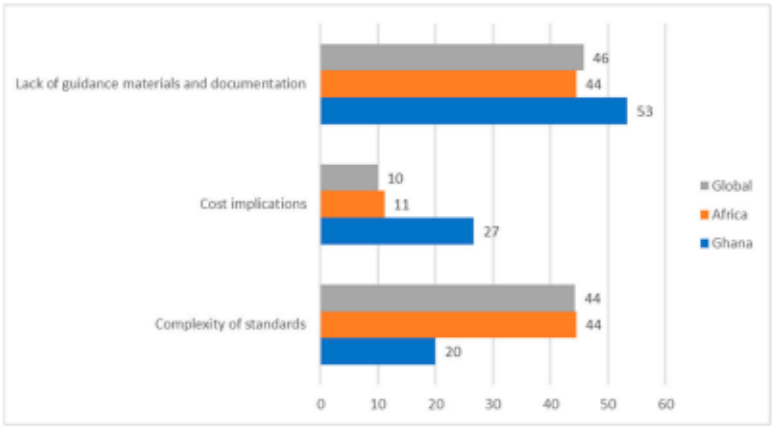

Figure 9. Challenges to the adoption of land cover standards: global, African, and Ghanaian context (Source: [41]).

Despite the challenges, this study also explored the potential benefits and opportunities for the adoption of land cover standards (Figure 10). As reported in Figure 10, the results show that globally, 20% of respondents highlighted data accuracy and reliability as the most significant opportunity, followed by consistency and uniformity (16%), and data integration (15%). In Africa, compliance with national frameworks or guidance was identified by 12% of respondents as the main opportunity, alongside consistency and uniformity (10%), and supporting decision-making and policy development (10%). In Ghana, 25% of respondents emphasized data accuracy and reliability as the most significant opportunity, followed by supporting decision-making and policy development (20%), and data integration (15%). This highlights the strong potential for the increased adoption of land cover standards if governments, institutions, and the international community provide the necessary support.

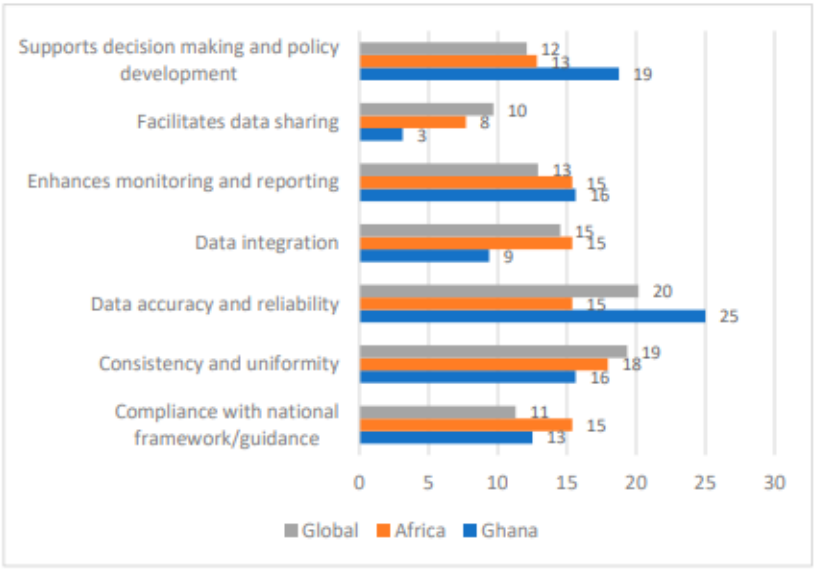

Figure 10. Opportunities for the use and adoption of land cover standards: global, African, and Ghanaian context (Source: [41]).

4. Discussion

The role of land cover legends is to help in the preparation of land cover maps and land cover datasets [43]. For this reason, the land cover legend register (LCLR) has been developed to support the cataloging of legends based on international standards at global, regional, and national levels [44]. The registry database was for land cover legends based on the registry concept that is derived from ISO 19135-1 [4], identified in ISO 19144-1 [45], and makes use of the descriptive meta language described in ISO 19144-2 [29]. By standardizing land cover legends, the LCLR facilitates data exchange, comparison, and integration across different regions and platforms [7]. However, many land cover mapping institutions in West Africa utilize different legends and classification systems, including the WALCRS. The WALCRS is particularly significant for the subregion, offering valuable scientific and developmental applications [46]. The Gambia was the first country to implement this regional land cover reference system, using it to support smallholder agriculture. As highlighted in this study, efforts are underway to expand the implementation of the WALCRS to other parts of the region, including Ghana. The objectives of land cover mapping in West Africa, and for that matter in Ghana, vary. These include agricultural monitoring, ecosystem service assessment, land use planning, land degradation monitoring, greenhouse gas inventories, climate change mitigation and adaptation assessment, and disaster response [46]. These varying objectives have led to inconsistencies in regional land cover maps. The WALCRS helps to simplify the classification of land features and the development of standard land cover legends by using ISO-based LCCS version 3 software developed by FAO to eliminate ambiguities in defining land features and legends, yet their adoption in developing regions such as West Africa remains limited. Comparing Ghana's land cover legend development to similar studies in other African countries, such as The Gambia and Ethiopia, reveals common challenges and unique regional characteristics. The WALCRS has been integrated into national land cover efforts in The Gambia, demonstrating the benefits of standardized classification approaches for agricultural planning [27]. The research conducted in Ethiopia has emphasized the importance of integrating multi-source remote sensing data, including SAR and optical imagery, to improve classification accuracy in diverse landscapes [47]. The methodological approach used in this study has been widely validated in previous studies [48]. However, the application of these methods in Ghana provided insights into the effectiveness of the technique in a West African context, where land cover and land use dynamics are shaped by agricultural expansion, deforestation, and rapid urbanization.

Land cover datasets are equally important as land cover legends, as the latter serves as a fundamental framework for developing and standardizing land cover datasets [43]. Several organizations and countries have developed land cover datasets for different purposes, including national forest resource assessment, estimation of Reducing Emissions from Deforestation and Forest Degradation (REDD+) activity data, biophysical and socioeconomic information integration, and semantic similarity assessment [49]. Several global land cover datasets exist to ensure their wider use and accessibility. Among these are the European Space Agency's European Global Land Analysis and Discovery (ESA GLAD) and ESA's World Cover, among others. Using global land datasets for national land cover representation and analysis presents notable challenges, including inconsistencies in feature estimates, which often result in either overestimation or underestimation. These discrepancies hinder the harmonization and interoperability of land cover datasets across regions and institutions.

A critical issue highlighted in this research is the significant variations between global and national land cover datasets. For example, as shown in Table 3, the built-up area is reported as 3.9% in the ESRI global dataset, 1.3% in the MODIS global dataset, and

1.9% in the national dataset. Similarly, cropland estimates show discrepancies, with 3.8% reported by ESRI, 10.9% by MODIS, and a much higher 46.5% from the national classification. The significant variations observed between Ghana's national dataset and global products reflect a documented challenge in land cover mapping. For instance, in their work, Fritz et al. [50] demonstrated that global datasets like MODIS and ESA GlobCover exhibit discrepancies up to 30% in cropland estimates across Africa due to different class definitions and spatial resolutions. Similarly, Herold et al. [51] reported that built-up areas are often overestimated in coarse-resolution datasets—as was seen in the case of ESRI's estimate and that of Ghana (3.9% vs. 1.9%), because of the spectral confusion between urban infrastructure and bare soil. The inconsistencies align with findings in Southeast Asia, where Tsenbazar et al. [52] reported that MODIS's natural vegetation class conflates ecologically distinct forests and shrublands, depicting Ghana's challenges in differentiating closed forests from savannas. The differences in global datasets often come from generalized class definitions. For instance, ESRI's rangeland merges Ghana's savannas and rainfed agriculture, a situation also observed in Ethiopia, where Wodebo [53] found that global products misclassified agroforest systems as homogeneous grasslands. Such an oversight undermines implementations like REDD+ reporting, where precise forest definitions are critical. Comber et al. [54] attributed these issues to semantic uncertainties, where inconsistent terminology leads to mismatched interpretations across regions.

Ghana's national dataset addresses these challenges by adopting the WALCRS, which provides regionally tailored classes such as mango plantations, mining sites, salt pans, oil palm, and rubber, which are absent in global datasets. This approach aligns with recommendations by Di Gregorio. [27], who argued that localized adaptations of the FAO's LCML improve accuracy in heterogeneous landscapes. For instance, The Gambia's use of the WALCRS reduced cropland estimation errors by 22% compared to MODIS [27], while Kuenzer et al. [55] demonstrated that integrating SAR and optical data, as performed in Ethiopia, enhances the discrimination of spectrally similar classes like irrigated and rainfed agriculture.

A major consequence of the challenges to the adoption of land cover standards, as was seen in this research, is the lack of documentation of the standards. This was seen in the three spatial levels: global, African, and Ghanaian contexts. In instances where efforts are being made to describe land features, class definitions are often incomplete or ambiguous. Additionally, the inconsistent use of terminologies adds to the complexity, where the same terms are applied to different concepts or different terms are used for the same concept [46]. These inconsistencies pose significant challenges in generating standardized and comparable datasets, which are essential for accurate environmental monitoring, national change assessments, and cross-regional analyses. Addressing these challenges requires targeted efforts toward capacity building, developing legend translation protocols for existing datasets, and refining guidelines for future mapping projects to enhance harmonization and compatibility.

In Ghana, national entities such as the Ghana Standards Authority (GSA), in collaboration with stakeholders in the land cover sector, including the Forestry Commission and the Lands Commission, should be encouraged to adopt these standards. The international community can support these efforts through awareness-raising initiatives and technical assistance. By integrating these strategies, land cover standards can be effectively incorporated into mapping activities, leading to the creation of consistent, reliable, and interoperable datasets that are essential for both local and global environmental assessments. Despite the challenges associated with adopting land cover standards, their adoption presents major opportunities. One such opportunity is the ability to support decision-making and policy. Another significant advantage is the enhancement of data accuracy and

reliability, ensuring that the generated datasets are robust and suitable for a wide range of applications. This finding aligns with the International Standards for Land Cover: From Concepts to Practices report [56], which highlights that land cover standards provide a structured framework to ensure data interoperability and consistency in reporting. The report emphasizes that such standards ensure data are consistent, reliable, and comparable across different regions and countries. Additionally, they support a country's objectives of informed decision-making, sustainable land use planning, and effective monitoring of progress toward SDGs. It is important to also state that the adoption of land cover standards would allow for the continuous updating of maps, comparative validation, and comprehensive land resources assessment, e.g., as required for government obligations to report on carbon accounting or as response to environmental treaties [57].

The results of this study have several applications for land use planning, environmental monitoring in line with SDGs, and policy implementation. The high-accuracy and high-resolution land cover classification provides reliable baseline information for land-monitoring programs, including deforestation trading, land degradation, agricultural expansion analysis, and urban growth assessment. Similar approaches have been successfully applied in countries such as Brazil for Amazon forest monitoring [58], landscape degradation in Tunisia [59], and monitoring SDG indicators on land degradation in Nigeria, Bangladesh, Uruguay, and Angola [60].

While this study demonstrates the application of remote sensing and land cover standards as well as classification methods, some limitations must be acknowledged. First, while the usage of image interpretation, knowledge of the area, and expert engagement produces a good classification output, the classification may pose a challenge. Although the classification performed well, incorporating actual ground truth field-based training and validation data could enhance the accuracy, particularly land cover types with similar spectral information, such as forest, savanna, and cultivated irrigated and rainfed classes. Furthermore, the study relied on a single year (2023) of land cover data rather than a time-series analysis, which may limit the ability to capture seasonal variations and long-term changes in land cover. The absence of a multi-year dataset means that land cover changes and trends, as well as deforestation rates and urban expansion, cannot be assessed over a period, which is critical for the environmental planning and sustainable management of land cover.

5. Conclusions

This study underscores the critical importance of adopting land cover standards for sustainable development in Ghana, Africa, and globally. By developing a national land cover legend based on ISO 19144-2 standards and creating a land cover dataset for 2023, the research addresses key challenges related to data inconsistency and interoperability. The findings reveal a diverse range of land cover types across Ghana, with cultivated rainfed areas, savannas, and closed/open forests being the most dominant. The study also demonstrates the effectiveness of integrating multi-sensor remote sensing data, including Sentinel-1 and Sentinel-2, with ancillary information such as elevation and slope. Using the random forest classification algorithm, the research achieved an overall accuracy of 90%, highlighting its robustness for land cover classification in Ghana's heterogeneous landscape. A key contribution to this research is the establishment of a national land cover legend and dataset for Ghana, which provides a foundation for future land cover mapping efforts. Unlike some research that relies heavily on global land cover datasets, this research has demonstrated that, in some instances, there are discrepancies in land cover estimates compared to national products. This study introduces a localized land cover dataset tailored to Ghana's environmental conditions. The study also identified the

challenges and opportunities for the adoption of land cover standards. Challenges such as limited familiarity with land cover standards, inconsistent definitions, and resource constraints remain significant barriers to the widespread adoption of these standards. Despite these obstacles, this study highlights the opportunities offered by standardized land cover approaches, including improved data accuracy, enhanced reliability, and their critical role in supporting informed policy-making and sustainable land use planning. To address the challenges and maximize the opportunities, targeted efforts are needed to build capacity, refine guidelines, and foster international collaboration. Such initiatives will improve the adoption of land cover standards and ensure effective environmental monitoring and sustainable resource management. Further research should explore cross-regional comparisons, applying similar methodologies in other West African countries to establish a regionally harmonized land cover dataset. By advancing knowledge in this field, these efforts will support the development of more effective land management, sustainable resource management, and climate resilience planning at the local, regional, and global scales.

Author Contributions: Conceptualization, E.N. methodology, E.N., F.M., and B.E.A.; software, E.N.; validation, E.N., F.M., and B.E.A.; formal analysis, E.N.; investigation, E.N., F.M., and B.E.A.; resources, E.N., F.M., B.E.A., R.K.N., S.Y., and P.S.; data curation, E.N., R.K.N., and S.Y.; writing—original draft preparation, E.N.; writing—review and editing, F.M., B.E.A., R.K.N., S.Y., and P.S.; visualization, E.N. and F.M.; supervision, P.S.; project administration, E.N.; funding acquisition, P.S. and E.N. All authors have read and agreed to the published version of the manuscript.

Funding: This research was funded by the Faculty of Forestry and Wood Sciences—FFWS, Czech University of Life Sciences Prague, (IGA/FLD/A_11_23 (Internal grant number: 43140/1312/3189)).

Data Availability Statement: The GEE scripts and datasets used for this research are publicly accessible through the GitHub repository [40].

Acknowledgments: The authors would like to thank the Geospatial Unit of the FAO and co-authors for their input.

Conflicts of Interest: Author Silas Yakalim was employed by Touton Ghana. The remaining authors declare that the research was conducted in the absence of any commercial or financial relationships that could be construed as a potential conflict of interest.

Abbreviations

The following abbreviations are used in this manuscript:

AOI	Area of Interest
CEO	Collect Earth Online
CERSGIS	Centre for Remote Sensing and Geographic Information Services
ESA	European Space Agency
FAO	Food and Agriculture Organization of the United Nations
GEE	Google Earth Engine
GSA	Ghana Standards Authority
ISO	International Organization for Standardization
LCML	Land Cover Meta Language
LCLR	Land Cover Legend Registry
MODIS	Moderate Resolution Imaging Spectroradiometer
NDWI	Normalized Difference Water Index
NDBI	Normalized Difference Built-up Index
NDVI	Normalized Difference Vegetation Index
REDD+	Reducing Emissions from Deforestation and Forest Degradation

RF	Random Forest
RMSC	Resource Management Support Centre
SAR	Synthetic Aperture Radar
SAVI	Soil-Adjusted Vegetation Index
SDGs	Sustainable Development Goals
UML	Unified Modeling Language
UNCCD	United Nations Framework Convention to Combat Desertification
UNFCC	United Nations Framework Convention on Climate Change
UN-GGIM	United Nations Committee of Experts on Global Geospatial Information Management
VH	Vertical Transmit and Horizontal Receive
VV	Vertical Transmit and Vertical Receive
WALCRS	West African Land Cover Reference System

Appendix A

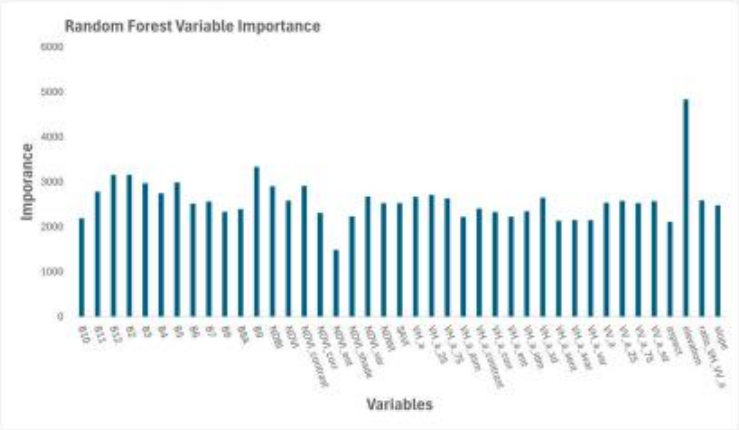

Figure A1. Variable importance.

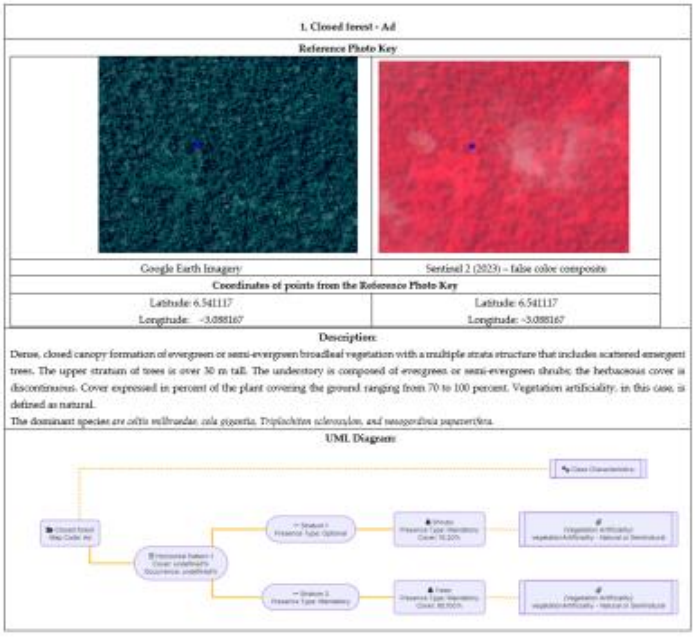

Figure A2. Closed forest land cover class description, photo key interpretation, and UML diagram.

2. Open forest - Ac

Reference Photo Key

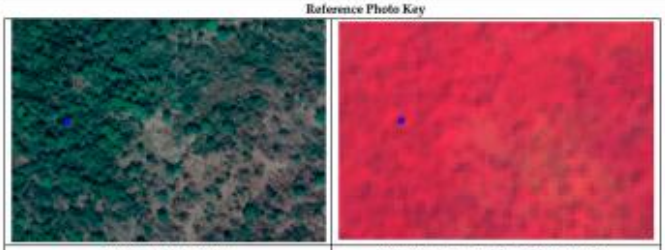

Google earth imagery	Sentinel 2 (2023) – false color composite
Coordinates of points from the Reference Photo Key	
Latitude: 7.270479 Longitude: −1.073958	Latitude: 7.270479 Longitude: −1.073958

Description:

This class is very basic and generic, constituted by one mandatory stratum defining the overall class aspect. The strata are constituted by one basic element tree. The element tree has two attributes: Cover expressed in the percentage of the plants covering the ground ranging from 20 to 70 percent. Vegetation artificiality, in this case, is defined as natural.

UML Diagram:

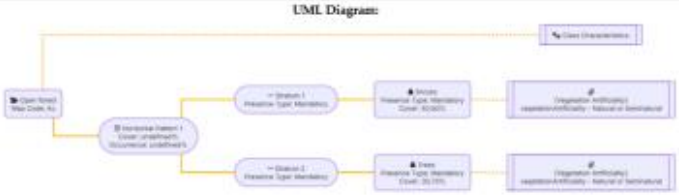

Figure A3. Open forest land cover class description, photo key interpretation, and UML diagram.

3. Thicket - FO

Reference Photo Key

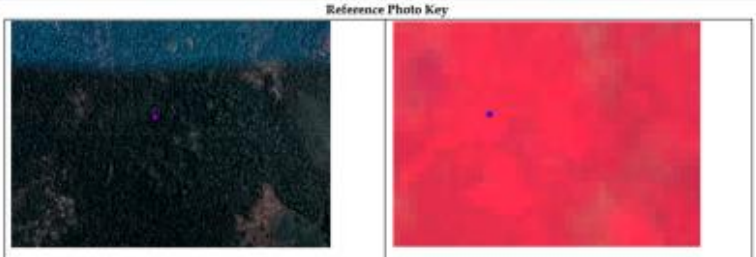

Google earth imagery	Sentinel 2 (2023) – false color composite
Coordinates of points from the Reference Photo Key	
Latitude: 5.247048 Longitude: −0.876357	Latitude: 5.247048 Longitude: −0.876357

Description:

Dense stand of shrubs, often thorny, forming generally impenetrable cover, with minimal or no herbaceous ground cover.

UML Diagram:

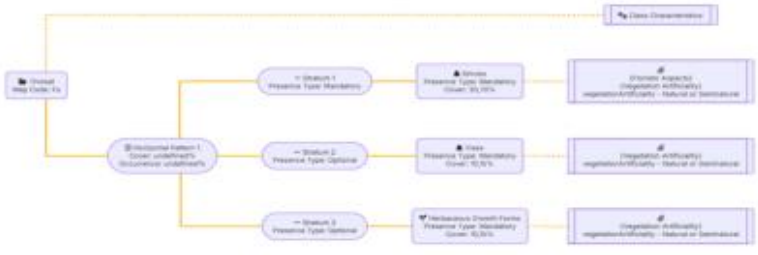

Figure A4. Thicket land cover class description, photo key interpretation, and UML diagram.

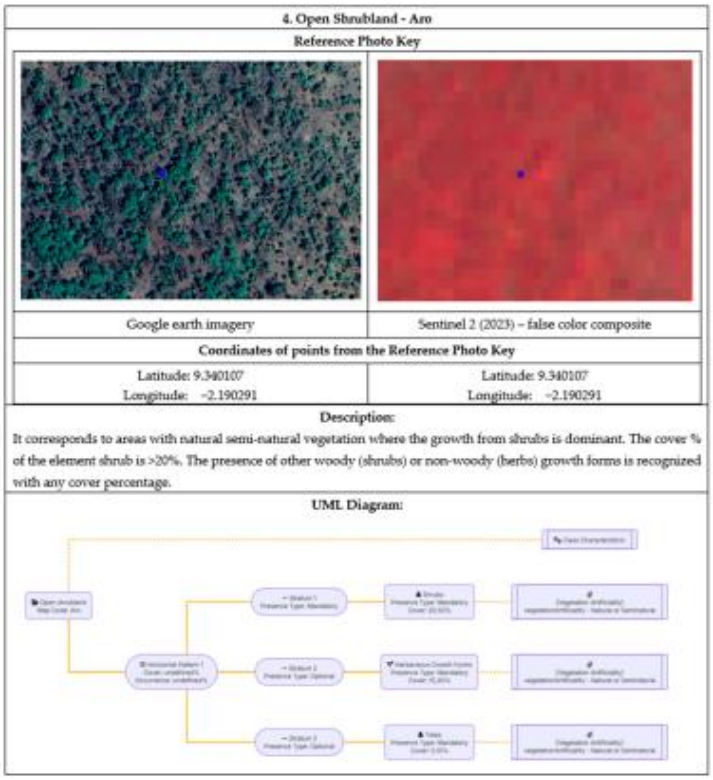

Figure A5. Open shrubland land cover class description, photo key interpretation, and UML diagram.

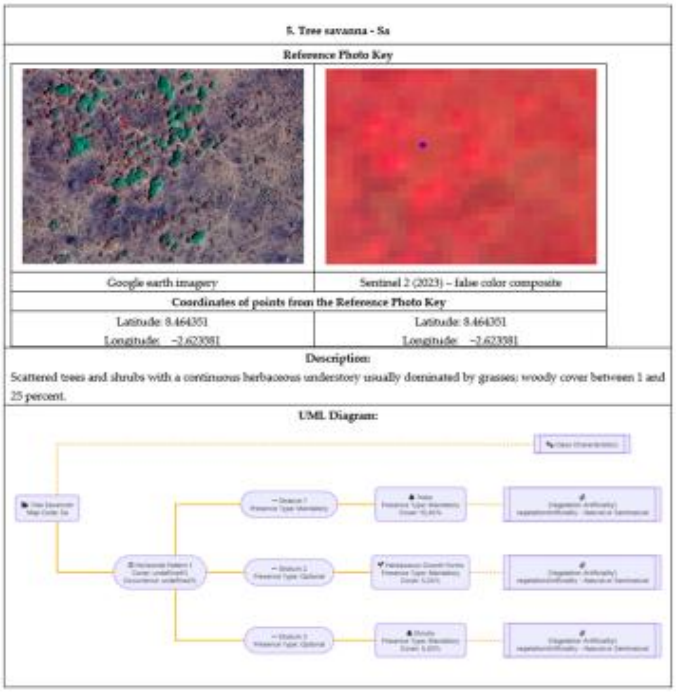

Figure A6. Tree savanna land cover class description, photo key interpretation, and UML diagram.

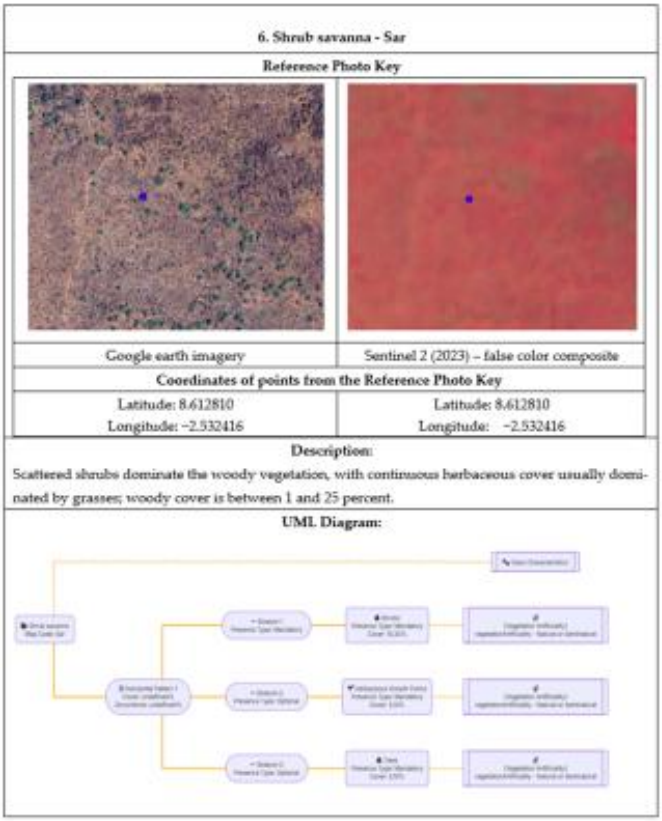

Figure A7. Shrub savanna land cover class description, photo key interpretation, and UML diagram.

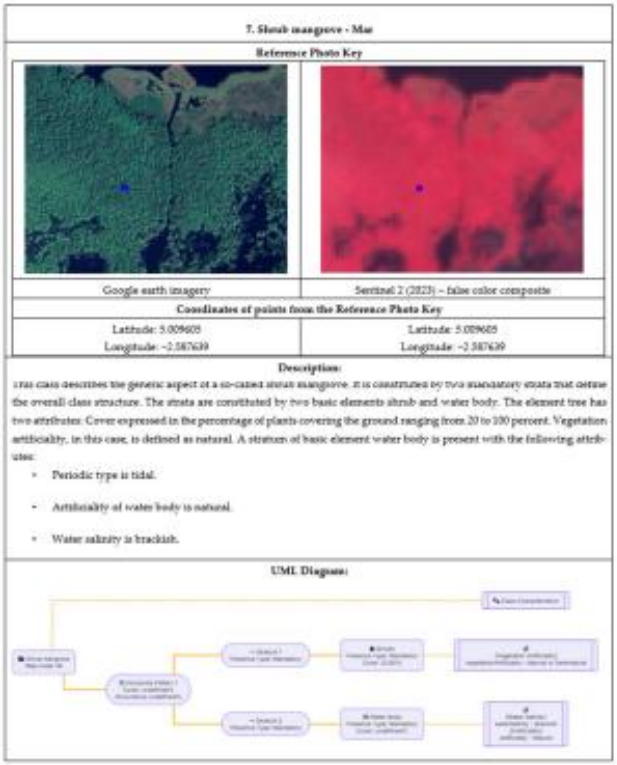

Figure A8. Shrub mangrove land cover class description, photo key interpretation, and UML diagram.

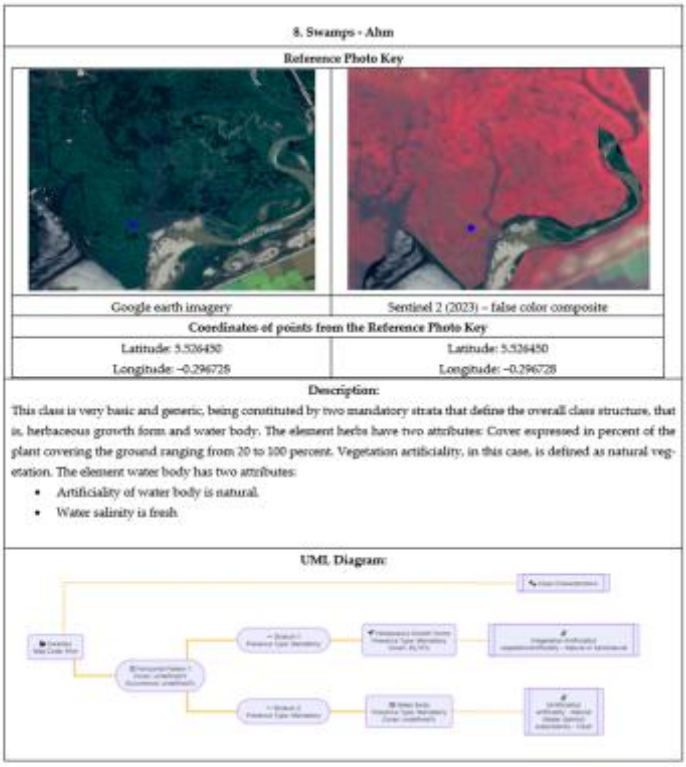

Figure A9. Swamp land cover class description, photo key interpretation, and UML diagram.

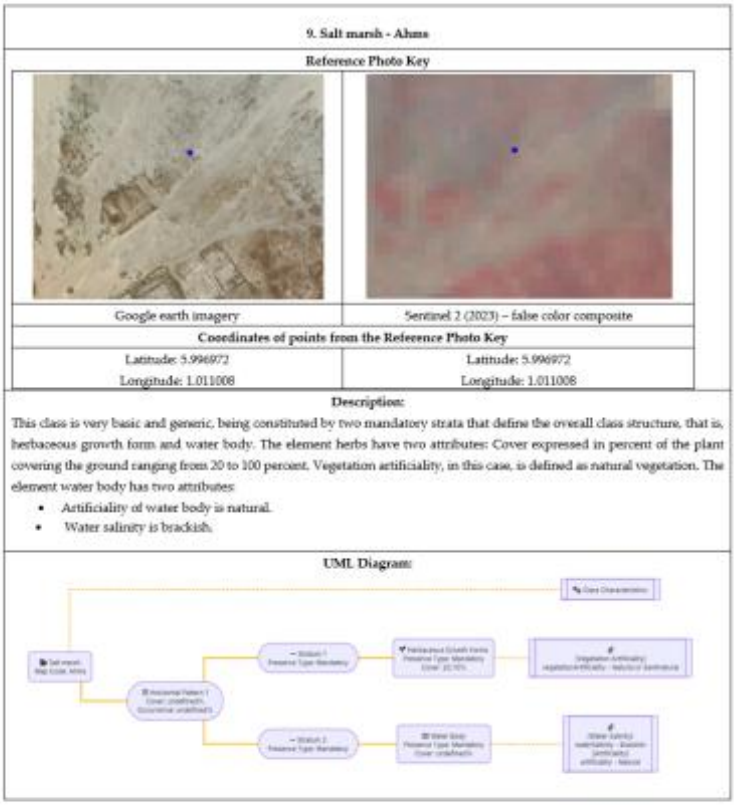

Figure A10. The salt marsh land cover class description, photo key interpretation, and UML diagram.

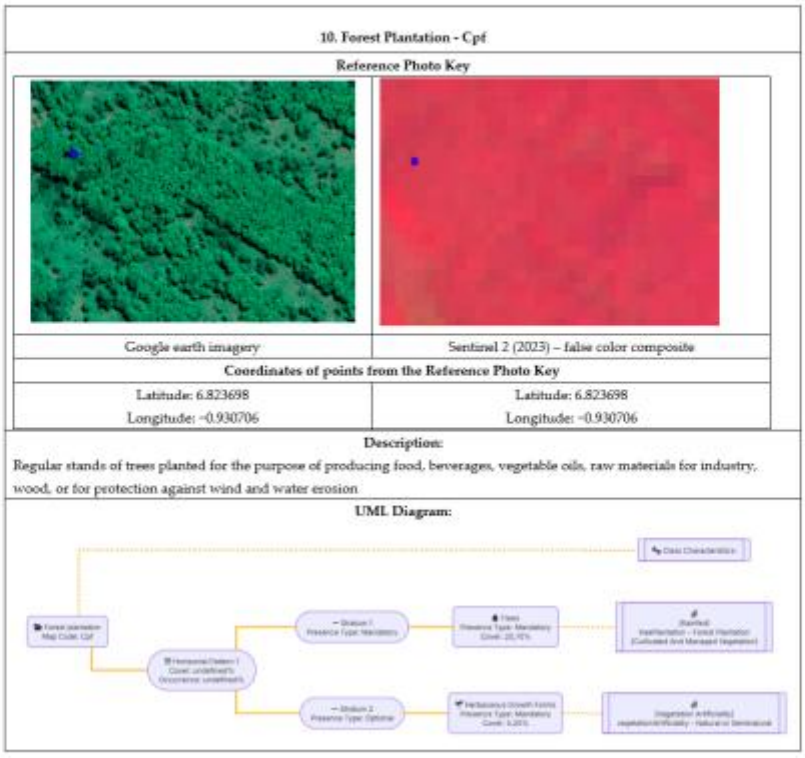

Figure A11. Forest plantation land cover class description, photo key interpretation, and UML diagram.

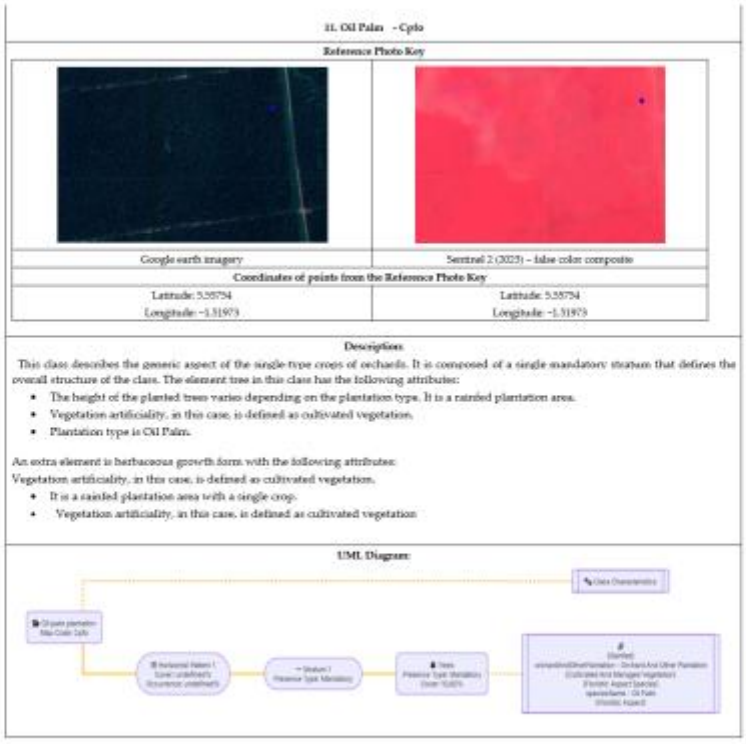

Figure A12. Oil palm plantation land cover class description, photo key interpretation, and UML diagram.

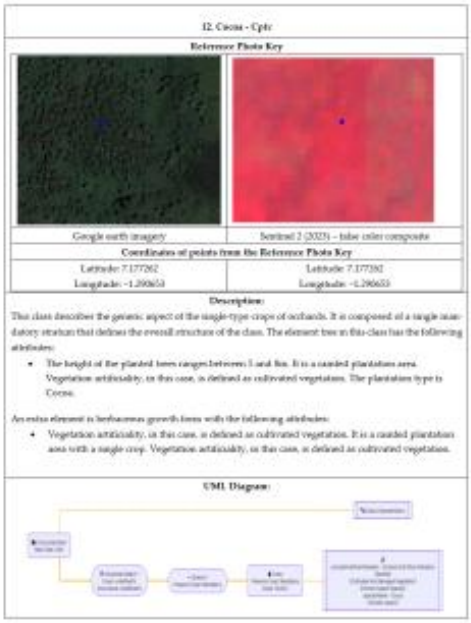

Figure A13. Cocoa plantation land cover class description, photo key interpretation, and UML diagram.

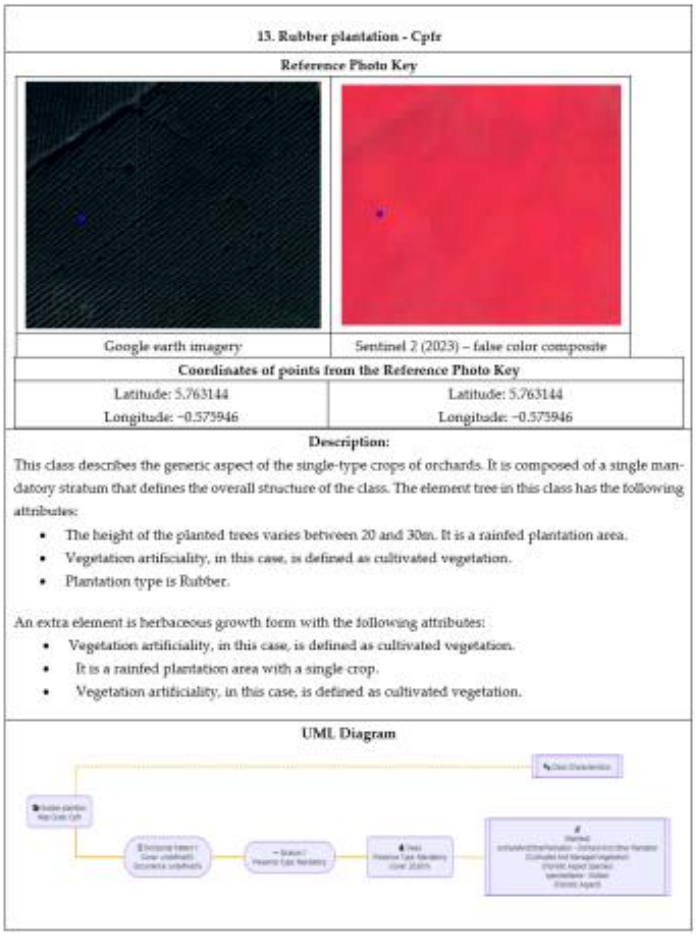

Figure A14. Rubber plantation land cover class description, photo key interpretation, and UML diagram.

14. Mango plantation - Cpfm

Reference Photo Key

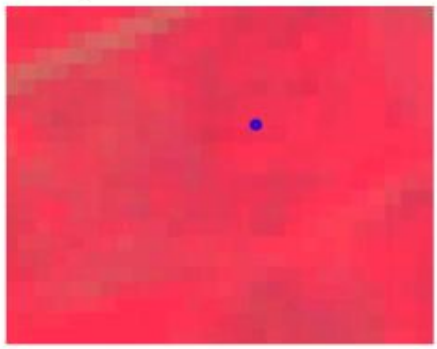

Google earth imagery	Sentinel 2 (2023) – false color composite
Coordinates of points from the Reference Photo Key	
Latitude: 6.018207 Longitude: 0.003395	Latitude: 6.018207 Longitude: 0.003395

Description:

This class describes the generic aspect of the single-type crops of orchards. It is composed of a single mandatory stratum that defines the overall structure of the class. The element tree in this class has the following attributes:

- The height of the planted trees varies between 2 and 5m. It is a rainfed plantation area.
- Vegetation artificiality, in this case, is defined as cultivated vegetation.
- Plantation type is Mango.

An extra element is herbaceous growth form with the following attributes:

- Vegetation artificiality, in this case, is defined as cultivated vegetation.
- It is a rainfed plantation area with a single crop.
- Vegetation artificiality, in this case, is defined as cultivated vegetation.

UML Diagram

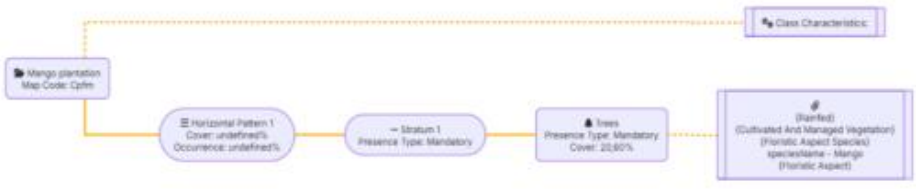

Figure A15. Mango plantation land cover class description, photo key interpretation, and UML diagram.

15. Pineapple– Cih

Reference Photo Key

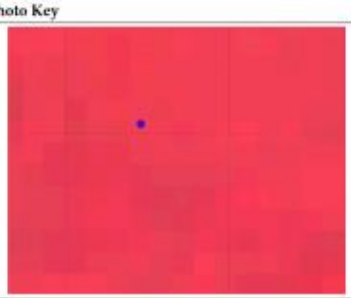

Google earth imagery	Sentinel 2 (2023) – false color composite
Coordinates of points from the Reference Photo Key	
Latitude: 5.776591 Longitude: −0.558617	Latitude: 5.776591 Longitude: −0.558617

Description:

It corresponds to areas with cultivated irrigated agriculture where the growth-form herb is dominant. A common crop is pineapple. Two derived classes are foreseen classified as single crop and multiple crops, sub-divided according to the different cropping intensities that characterize the dominant element plantation.

UML Diagram:

Figure A16. Pineapple land cover class description, photo key interpretation, and UML diagram.

16. Paddy Rice - Chi

Reference Photo Key

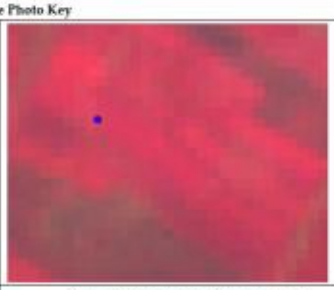

Google earth imagery	Sentinel 2 (2023) – false color composite
Coordinates of points from the Reference Photo Key	
Latitude 5.793496 Longitude 0.053134	Latitude: 5.793496 Longitude 0.053134

Description:

It corresponds to cultivated agriculture with the flooded areas where the growth-form herb is dominant. The element herb has the following attributes:

- Herbaceous crops are permanently flooded.
- Floristic aspect species: Rice.
- Vegetation artificiality, in this case, is defined as cultivated vegetation.

A basic element of water has the following attributes:

- Monthly periodic variation
- The artificiality of the water body is natural.
- Water salinity is fresh.

UML Diagram:

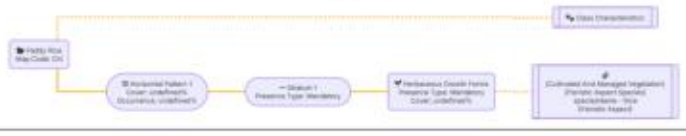

Figure A17. Paddy rice land cover class description, photo key interpretation, and UML diagram.

17. Beaches - P

Reference Photo Key

Google earth imagery	Sentinel 2 (2023) – false color composite
Coordinates of points from the Reference Photo Key	
Latitude 5.506940 Longitude: – -0.329044	Latitude 5.506940 Longitude: –0.329044

Description:

This class is very basic and generic, being constituted by one mandatory stratum that defines the overall class structure. The strata are constituted by one basic element lose and shifting sand.

UML Diagram:

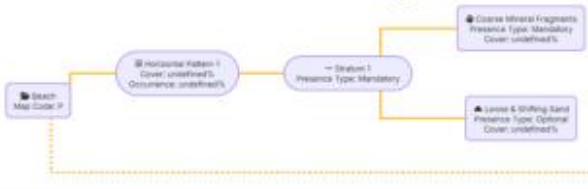

Figure A18. Beach land cover class description, photo key interpretation, and UML diagram.

18. Bare Soil - Sn

Reference Photo Key

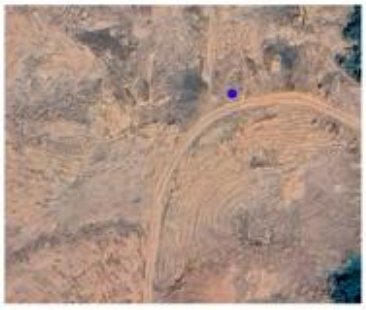

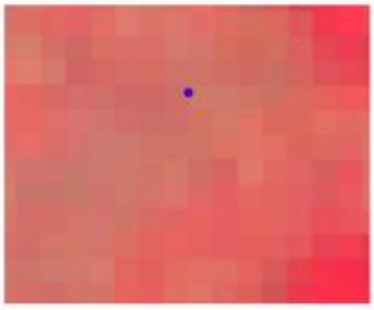

Google earth imagery	Sentinel 2 (2023) – false color composite
Coordinates of points from the Reference Photo Key	
Latitude 6.130785 Longitude: –0.349517	Latitude 6.130785 Longitude: –0.349517

Description:

This class is very basic and generic, being constituted by one mandatory stratum that defines the overall class structure. The strata are constituted by one basic element: bare soil.

UML Diagram:

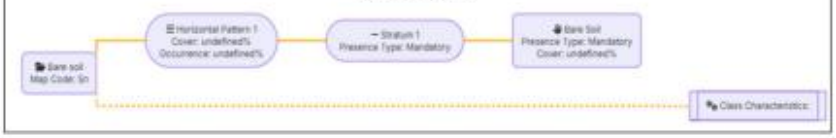

Figure A19. Bare soil land cover class description, photo key interpretation, and UML diagram.

19. Rocks - Sr

Reference Photo Key

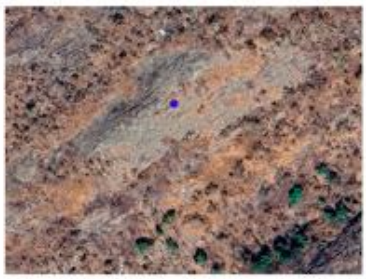

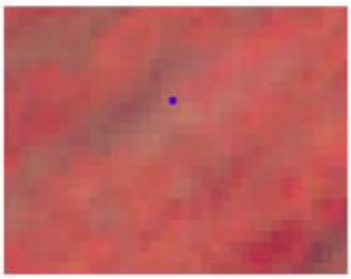

Google earth imagery	Sentinel 2 (2023) – false color composite
Coordinates of points from the Reference Photo Key	
Latitude 9.751418 Longitude: −2.129097	Latitude 9.751418 Longitude: −2.129097

Description:

This class is very basic and generic, being constituted by one mandatory stratum that defines the overall class structure. The strata are constituted by one basic element: rocks.

UML Diagram:

Figure A20. Rocks land cover class description, photo key interpretation, and UML diagram.

20. Urban areas (Built-up) - Zu

Reference Photo Key

Google Earth imagery	Sentinel 2 (2023) – false color composite
Coordinates of points from the Reference Photo Key	
Latitude 6.696653 Longitude: −1.608574	Latitude 6.696653 Longitude: −1.608574

Description:

It corresponds to the artificial and impervious surfaces paved with hard materials and built-up non-linear. The presence of sub-surfaces is recognized by the types of artificial surfaces.

UML Diagram:

Figure A21. Urban areas land cover class description, photo key interpretation, and UML diagram.

21. Port- Po	
Reference Photo Key	
	
Google earth imagery	Sentinel 2 (2023) – false color composite
Coordinates of points from the Reference Photo Key	
Latitude 5.632393 Longitude: 0.009817	Latitude 5.632393 Longitude: 0.009817
Description: Artificial surfaces with rural area geographical aspects, including buildings and other artificial surfaces	
UML Diagram: 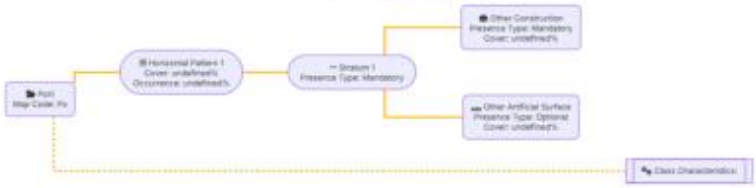	

Figure A22. Port land cover class description, photo key interpretation, and UML diagram.

22. Airport- Bni	
Reference Photo Key	
	
Google earth imagery	Sentinel 2 (2023) – false color composite
Coordinates of points from the Reference Photo Key	
Latitude 5.605532 Longitude: -0.169699	Latitude 5.605532 Longitude: -0.169699
Description: Built-up areas with facilities for flights to take off and land	
UML Diagram: 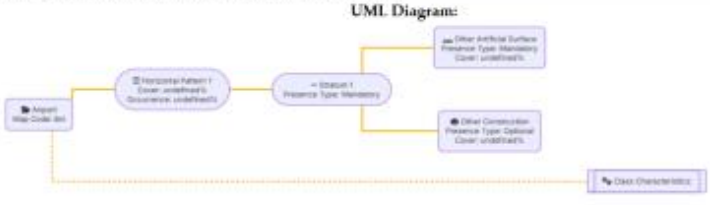	

Figure A23. Airport land cover class description, photo key interpretation, and UML diagram.

23. Dump and extraction sites - Sd

Reference Photo Key

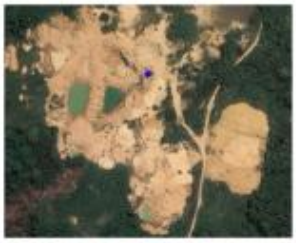

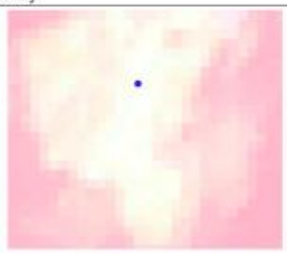

Google earth imagery	Sentinel 2 (2023) – false color composite
Coordinates of points from the Reference Photo Key	
Latitude 5.281636 Longitude: −1.594401	Latitude 5.281636 Longitude: −1.594401

Description:

Land used for disposal of waste materials is known as dump sites. Extraction sites are defined by the absence of the original land cover, which is removed by human activity or machinery for the extraction of sand, stone, mineral, or coal.

UML Diagram:

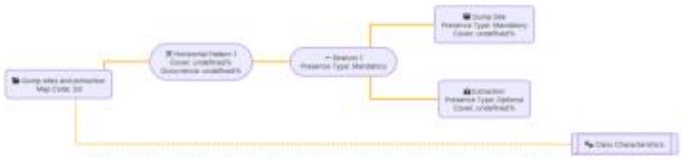

Figure A24. Dump sites and extraction land cover class description, photo key interpretation, and UML diagram.

24. Rivers - R

Reference Photo Key

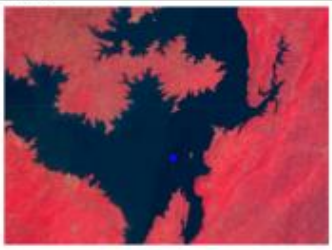

Google earth imagery	Sentinel 2 (2023) – false color composite
Coordinates of points from the Reference Photo Key	
Latitude 6.551704 Longitude: 0.07143	Latitude 6.551704 Longitude: 0.07143

Description:

The rivers are natural water courses that serve as water drainage channels. A basic element of a water body has the following attributes:

- Water dynamics is flowing.
- The artificiality of the water body is natural.
- Water salinity is fresh.

UML Diagram:

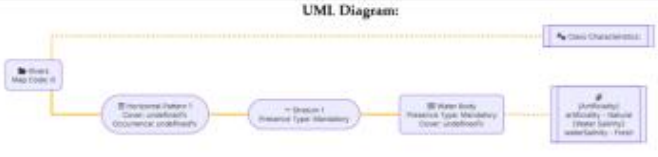

Figure A25. Rivers land cover class description, photo key interpretation, and UML diagram.

25. Lakes - L

Reference Photo Key

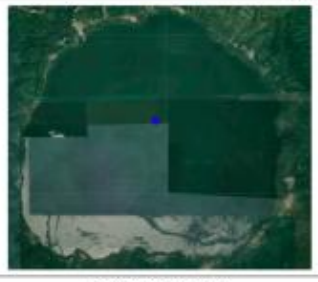

Google earth imagery

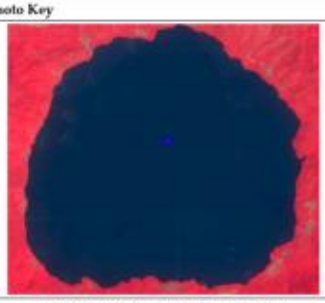

Sentinel 2 (2023) – false color composite

Coordinates of points from the Reference Photo Key

Latitude 6.50117 Longitude: -1.40649	Latitude 6.50117 Longitude: -1.40649

Description:

A natural standing water reservoir that is bigger than a pond and has an irregular shape. This class consists of one mandatory stratum. A basic element of a water body has the following attributes:

- Monthly periodic variation.
- Water dynamics is standing.

UML Diagram:

Figure A26. Lakes land cover class description, photo key interpretation, and UML diagram.

26. Lagoon - La

Reference Photo Key

Google earth imagery

Sentinel 2 (2023) – false color composite

Coordinates of points from the Reference Photo Key

Latitude 5.896496 Longitude: 0.936793	Latitude 5.896496 Longitude: 0.936793

Description:

A natural standing water reservoir that is bigger than a pond and has an irregular shape. This class consists of one mandatory stratum. A basic element of a water body has the following attributes:

- Monthly periodic variation.
- Water dynamics is standing.

UML Diagram:

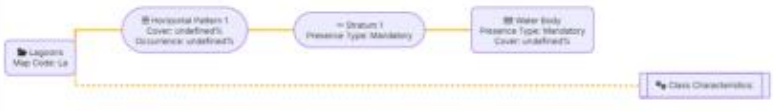

Figure A27. Lagoons land cover class description, photo key interpretation, and UML diagram.

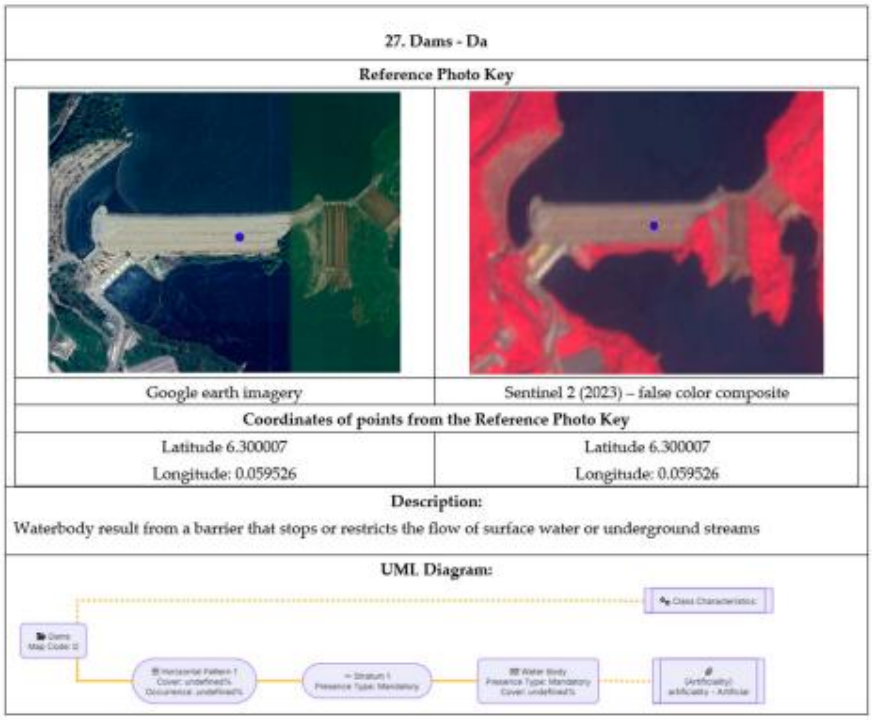

Figure A28. Dams land cover class description, photo key interpretation, and UML diagram.

References

1. Taylor, S.P. What Is Innovation? A Study of the Definitions, Academic Models and Applicability of Innovation to an Example of Social Housing in England. *Open J. Sci.* **2017**, *5*, 128–146. [CrossRef]
2. Allen, R.H.; Sriram, R.D. The Role of Standards in Innovation. *Technol. Forecast. Soc. Change* **2000**, *64*, 171–181. [CrossRef]
3. ISO. *Standards and Public Policy: A Toolkit for National Standards Bodies*; The International Organization for Standardization: Geneva, Switzerland, 2023. Available online: https://www.iso.org/publication/PUB100476.html (accessed on 7 August 2024).
4. ISO. *A Guide to the Role of Standards in Geospatial Information Management*, 3rd ed.; The International Organization for Standardization: Geneva, Switzerland, 2021. Available online: http://standards.unggim.ogc.org/unggim_guide.html#_introduction (accessed on 7 August 2024).
5. *ISO/TC 211 SO/TC 211*; Geographic Information/Geomatics. The International Organization for Standardization: Geneva, Switzerland, 1994. Available online: https://www.iso.org/committee/54904.html (accessed on 7 August 2024).
6. UN-GGIM. The Global Fundamental Geospatial Data Themes for Africa. Available online: https://ggim.un.org/meetings/2018-Addis_Ababa/ (accessed on 29 November 2024).
7. Mushtaq, F.; Brien, C.D.O.; Parslow, P.; Åhlin, M.; Gregorio, A.D.; Latham, J.S.; Henry, M. Land Cover and Land Use Ontology—Evolution of International Standards, Challenges, and Opportunities. *Land* **2024**, *13*, 1202. [CrossRef]
8. Shumili, L.; Kolotii, A.; Lavereniuk, M.; Yailymov, B. Use of Land Cover Maps as Indicators for Achieving Sustainable Development Goals. In Proceedings of the IGARSS 2018—2018 IEEE International Geoscience and Remote Sensing Symposium, Valencia, Spain, 22–27 July 2018. [CrossRef]
9. Zaka, M.M.; Samat, A. Advances in Remote Sensing and Machine Learning Methods for Invasive Plants Study: A Comprehensive Review. *Remote Sens.* **2024**, *16*, 3781. [CrossRef]
10. Bossard, M.; Feranec, J.; Otahel, J. *CORINE Land Cover Technical Guide: Addendum 2000*; European Environment Agency: Copenhagen, Denmark, 2000. Available online: https://www.eea.europa.eu/publications/tech40add/at_download/file (accessed on 7 August 2024).
11. Anderson, J.; Hardy, E.; Roach, J.; Witmer, R. *A Land Use and Land Cover Classification System for Use with Remote Sensor Data*; USGS Publications Warehouse: Washington, DC, USA, 2001; Volume 2001. [CrossRef]
12. Ahlqvist, O.; Varanka, D.; Fritz, S.; Janowicz, K. *Land Use Cover and Land Cover Semantics: Principles, Best Practices, and Prospects*; CRC Press: Boca Raton, FL, USA, 2015. [CrossRef]
13. Phiri, D.; Simwanda, M.; Salekin, S.; Ryirenda, V.R.; Murayama, Y.; Ranagalage, M.; Oktaviani, N.; Kusuma, H.A.; Zhang, T.; Su, J.; et al. Remote Sensing Sentinel-2 Data for Land Cover/Use Mapping: A Review. *Remote Sens.* **2020**, *12*, 2291. [CrossRef]

14. Belgiu, M.; Drăgu, L. Random Forest in Remote Sensing: A Review of Applications and Future Directions. *ISPRS J. Photogramm. Remote Sens.* **2016**, *114*, 24–31. [CrossRef]
15. Zhu, X.; Chen, J.; Gao, F.; Chen, X.; Masek, J.G. An Enhanced Spatial and Temporal Adaptive Reflectance Fusion Model for Complex Heterogeneous Regions. *Remote Sens. Environ.* **2010**, *114*, 2610–2623. [CrossRef]
16. Gorelick, N.; Hancher, M.; Dixon, M.; Ilyushchenko, S.; Thau, D.; Moore, R. Google Earth Engine: Planetary-Scale Geospatial Analysis for Everyone. *Remote Sens. Environ.* **2017**, *202*, 18–27. [CrossRef]
17. Klouček, T.; Moravec, D.; Komárek, J.; Lagner, O.; Štych, P. Selecting Appropriate Variables for Detecting Grassland to Cropland Changes Using High Resolution Satellite Data. *PeerJ* **2018**, *6*, e5487. [CrossRef]
18. Ghana Forestry Commission. *Framework for National Forest Monitoring System*; Ghana Forestry Commission: Accra, Ghana, 2018. Available online: https://redd.unfccc.int/files/nfms_framework_doc_ghana.pdf (accessed on 7 August 2024).
19. FAO. Land Cover Legend Registry. Available online: https://data.apps.fao.org/lclr-tool/en/ (accessed on 29 November 2024).
20. Minelli, S.; Connor, B.O.; Teich, I. *The Land Story Brand Guide*; Land Leader: Melbourne, Australia, 2022; ISBN 9789295118911.
21. Conchedda, G.; Tubiello, F.N. *Land Cover Statistics Global, Regional and Country Trends*; FAO: Rome, Italy, 2021. Available online: https://openknowledge.fao.org/bitstreams/9c99a5bc-a0f8-4c4a-a64d-1523c93afde1/download (accessed on 7 August 2024).
22. Seebach, L.M.; Strobl, P.; San Miguel-Ayanz, J.; Gallego, J.; Bastrup-Birk, A. Comparative Analysis of Harmonized Forest Area Estimates for European Countries. *Forestry* **2011**, *84*, 285–299. [CrossRef]
23. CILSS. *Landscapes of West Africa—A Window on a Changing World*; CILSS: Ouagadougou, Burkina Faso, 2016. [CrossRef]
24. HDX. Ghana—Subnational Administrative Boundaries. Available online: https://data.humdata.org/dataset/cod-ab-gha (accessed on 24 January 2025).
25. De Simone, L.; Ouellette, W.; Gennari, P. Operational Use of EO Data for National Land Cover Official Statistics in Operational Use of EO Data for National Land Cover Official Statistics in Lesotho. *Remote Sens.* **2022**, *14*, 3294. [CrossRef]
26. Haub, C.; Kleinewillinghöfer, L.; Garcia, V.; Eftas, M.; Di, A.; Fao, G.; Gallego, J.; Leo, O.; Jrc, E.C.; Vito, Q.D. *Protocol for Land Cover Validation*; SIGMA–Stimulating Innovation for Global Monitoring of Agriculture: Panevėžys, Lithuania, 2015. Available online: https://www.eftas.de/upload/15356999-SIGMA-D33-2-Protocol-for-land-cover-validation-v2.0-2015-06-22vprint.pdf (accessed on 7 August 2024).
27. Di Gregorio, A.; Mushtaq, F.; Aw, M.; Henry, M.; Mamane, B.; Mahamane, M.; Assoumana, B.T.; Mimouni, M.; Aubee, E.; Enaruvbe, G.O.; et al. *West African Land Cover Reference System*; FAO: Rome, Italy, 2022. [CrossRef]
28. FAO. Land Characterization System Software. Available online: https://www.fao.org/geospatial/resources/tools/land-characterization-system-software/en/ (accessed on 28 November 2024).
29. *ISO 19144-2:2023*; Geographic Information—Classification Systems—Part 2: Land Cover Meta Language (LCML). The International Organization for Standardization: Geneva, Switzerland, 2023. Available online: https://www.iso.org/standard/81259.html (accessed on 7 August 2024).
30. CEO. Collect Earth Online. Available online: https://collect.earth/ (accessed on 23 January 2025).
31. Forests National Corporation (FNC). *Republic of Sudan National Land Cover Map*; Forests National Corporation: Khartoum, Sudan, 2021. Available online: https://www.fao.org/fileadmin/user_upload/faoweb/Themes__pages/Forests/REDD-NFM/Sudan_MRV/Sudan_Land_cover_report.pdf (accessed on 7 August 2024).
32. Rouse, J.W.; Haas, R.H.; Schell, J.A.; Deering, D.W.; Harlan, J.C. *Monitoring the Vernal Advancements and Retrogradation of Natural Vegetation*; Final Report; NASA/GSFC: Greenbelt, MD, USA, 1974; pp. 1–137. Available online: https://ntrs.nasa.gov/api/citations/19750020419/downloads/19750020419.pdf (accessed on 7 August 2024).
33. Zha, Y.; Gao, J.; Ni, S. Use of Normalized Difference Built-up Index in Automatically Mapping Urban Areas from TM Imagery. *Int. J. Remote Sens.* **2003**, *24*, 583–594. [CrossRef]
34. Gao, B. NDWI—A Normalized Difference Water Index for Remote Sensing of Vegetation Liquid Water from Space. *Remote Sens. Environ.* **1996**, *58*, 257–266. [CrossRef]
35. Huete, A.R. A Soil-Adjusted Vegetation Index (SAVI). *Remote Sens. Environ.* **1988**, *25*, 295–309. [CrossRef]
36. Tassi, A.; Vizzari, M. Object-Oriented Lulc Classification in Google Earth Engine Combining Snic, Glcm, and Machine Learning Algorithms. *Remote Sens.* **2020**, *12*, 3776. [CrossRef]
37. Maskell, G.; Chemura, A.; Nguyen, H.; Gornott, C.; Mondal, P. Remote Sensing of Environment Integration of Sentinel Optical and Radar Data for Mapping Smallholder Coffee Production Systems in Vietnam. *Remote Sens. Environ.* **2021**, *266*, 112709. [CrossRef]
38. Krstajic, D.; Buturovic, L.J.; Leahy, D.E.; Thomas, S. Cross-Validation Pitfalls When Selecting and Assessing Regression and Classification Models. *J. Cheminform.* **2014**, *6*, 10. [CrossRef]
39. Elisha, N.; Ofori, J.N.; Aikins, B.E.; Adzraku, G. Mapping Perennial Crops in Africa: A Case Study of Oil Palm in Ghana. *J. Geogr. Environ. Earth Sci. Int.* **2021**, *25*, 1–20. [CrossRef]
40. Njomaba, E. Ghana Land Cover Classification with Google Earth Engine. Available online: https://github.com/Elisha-Njomaba/Ghana_LandCover_GEE (accessed on 14 February 2025).

41. *ISO TC211/AG13*; Geographic Information/Geomatics. The International Organization for Standardization: Geneva, Switzerland, 2022. Available online: https://www.fao.org/geospatial/events/detail/en/c/1506665/ (accessed on 7 August 2024).
42. Sambus Geospatial Limited World Boundaries Shapefiles WFL1. Available online: https://opendata.sambusgeospatial.com/content/2f62b676933340b2a5e34a76634beb4c/about (accessed on 24 January 2025).
43. Mosca, N.; Di Gregorio, A.; Henry, M.; Jalal, R.; Blonda, P. Object-Based Similarity Assessment Using Land Cover Meta-Language (LCML): Concept, Challenges, and Implementation. *IEEE J. Sel. Top. Appl. Earth Obs. Remote Sens.* **2020**, *13*, 3790–3805. [CrossRef]
44. Mushtaq, F.; Henry, M.; O'Brien, C.D.; Di Gregorio, A.; Jalal, R.; Latham, J.; Muchoney, D.; Hill, C.T.; Mosca, N.; Tefera, M.G.; et al. An International Library for Land Cover Legends: The Land Cover Legend Registry. *Land* **2022**, *11*, 1083. [CrossRef]
45. *ISO 19144-1:2009*; Geographic Information—Classification Systems—Part 1: Classification System Structure. The International Organization for Standardization: Geneva, Switzerland, 2009. Available online: https://www.iso.org/standard/32562.html (accessed on 7 August 2024).
46. Mensah, F.; Mushtaq, F.; Bartel, P.; Abramowitz, J.; Cherrington, E.; Mahamane, M.; Mamane, B.; Dieye, A.M.; Sanou, P.; Enaruvbe, G. Land Cover Mapping in West Africa: A Collaborative Process. *Land* **2024**, *13*, 1712. [CrossRef]
47. Kebede, E.; Bekeko, Z. Expounding the Production and Importance of Cowpea (*Vigna unguiculata* (L.) Walp.) in Ethiopia. *Cogent Food Agric.* **2020**, *6*, 1769805. [CrossRef]
48. Rodriguez-Galiano, V.F.; Ghimire, B.; Rogan, J.; Chica-Olmo, M.; Rigol-Sanchez, J.P. An Assessment of the Effectiveness of a Random Forest Classifier for Land-Cover Classification. *ISPRS J. Photogramm. Remote Sens.* **2012**, *67*, 93–104. [CrossRef]
49. Cover, L.; Jalal, R.; Iqbal, Z.; Henry, M.; Franceschini, G.; Islam, M.S.; Akhter, M.; Khan, Z.T.; Hadi, M.A.; Hossain, M.A.; et al. Toward Efficient Land Cover Mapping: An Overview of the National Land Representation System And. *IEEE J. Sel. Top. Appl. Earth Obs. Remote Sens.* **2019**, *12*, 3852–3861. [CrossRef]
50. Fritz, S.; See, L.; McCallum, I.; Schill, C.; Obersteiner, M.; Van Der Velde, M.; Boettcher, H.; Havlík, P.; Achard, F. Highlighting Continued Uncertainty in Global Land Cover Maps for the User Community. *Environ. Res. Lett.* **2011**, *6*, 044005. [CrossRef]
51. Herold, M.; Mayaux, P.; Woodcock, C.E.; Baccini, A.; Schmullius, C. Some Challenges in Global Land Cover Mapping: An Assessment of Agreement and Accuracy in Existing 1 km Datasets. *Remote Sens. Environ.* **2008**, *112*, 2538–2556. [CrossRef]
52. Tsendbazar, N.E.; de Bruin, S.; Mora, B.; Schouten, L.; Herold, M. Comparative Assessment of Thematic Accuracy of GLC Maps for Specific Applications Using Existing Reference Data. *Int. J. Appl. Earth Obs. Geoinf.* **2016**, *44*, 124–135. [CrossRef]
53. Wola, A.W. Land Use or Land Cover Change and Its Driving Forces in Mago National Park, Southern Ethiopia. *J. Biomed. Res. Environ. Sci.* **2023**, *4*, 693–705. [CrossRef]
54. Comber, A.; Fisher, P.; Wadsworth, R. What Is Land Cover? *Environ. Plan. B Plan. Des.* **2005**, *32*, 199–209. [CrossRef]
55. Kuenzer, C.; van Beijma, S.; Gessner, U.; Dech, S. Land Surface Dynamics and Environmental Challenges of the Niger Delta, Africa: Remote Sensing-Based Analyses Spanning Three Decades (1986–2013). *Appl. Geogr.* **2014**, *53*, 354–368. [CrossRef]
56. FAO. *International Standards for Land Cover: From Concepts to Practices*; FAO: Rome, Italy, 2023. [CrossRef]
57. Herold, M.; Latham, J.S.; Di Gregorio, A.; Schmullius, C.C. Evolving Standards in Land Cover Characterization. *J. Land Use Sci.* **2006**, *1*, 157–168. [CrossRef]
58. Silva Junior, C.H.L.; Pessôa, A.C.M.; Carvalho, N.S.; Reis, J.B.C.; Anderson, L.O.; Aragão, L.E.O.C. The Brazilian Amazon Deforestation Rate in 2020 Is the Greatest of the Decade. *Nat. Ecol. Evol.* **2021**, *5*, 144–145. [CrossRef] [PubMed]
59. Shiri, Z.; Frija, A.; Rejeb, H.; Ouerghemmi, H.; Le, Q.B. Data on the Land Cover Transition, Subsequent Landscape Degradation, and Improvement in Semi-Arid Rainfed Agricultural Land in North–West Tunisia. *Data* **2024**, *9*, 96. [CrossRef]
60. Ghosh, A.; Rambaud, P.; Finegold, Y.; Jonckheere, I.; Martin-ortega, P.; Jalal, R.; Adebayo, A.D.; Alvarez, A.; Borretti, M.; Caela, J.; et al. Monitoring Sustainable Development Goal Indicator 15.3.1 on Land Degradation Using SEPAL: Examples, Challenges and Prospects. *Land* **2024**, *13*, 1027. [CrossRef]

4.3. Mapping species distribution and estimating population abundance of dominant forest tree species in Ghana: implications for conservation prioritization.

Elisha Njomaba[a], Ben Emunah Aikins[b], Peter Surový[a]

[a] Faculty of Forestry and Wood Science, Czech University of Life Sciences (CZU Prague), Kamýcká 129,165 21 Prague, Czech Republic.

[b] School of Public Health, College of Health Sciences, University of Ghana, Accra, Box LG 13, Ghana.

Author´s contribution: 80 %

Summary of the article

Ghana's forests are under severe pressure from deforestation and degradation, making the mapping of species distribution and abundance essential for effective conservation. This study used GBIF tree records and climatic, soil topographic, and land cover variables to model the distributions of three dominant tree species*: Napoleonaea leonensis, Myrianthus serratus, and Penianthus patulinervis*. Habitat suitability was predicted using MaxEnt, while Zero-inflated Poisson models estimated abundance, and the combined results were used to assess richness and identify conservation gaps. Suitability peaked in the southern forest zones, but abundance patterns revealed gaps across the PA network. Model performance was high (AUC 0.93-0.66; TSS up to 0.85), with *Penianthus patulinervis* showing the strongest abundance model (pseudo-R2 = 0.63). A composite index of suitability and abundance identified 23.5 million ha of conservation hotspots, but only 30% fell inside PAs. These findings highlight significant protected gaps and provide an evidence-based framework for prioritizing the conservation of Ghana's dominant forest species.

Full article

Trees, Forests and People 22 (2025) 101019

Contents lists available at ScienceDirect

Trees, Forests and People

journal homepage: www.sciencedirect.com/journal/trees-forests-and-people

Mapping species distribution and estimating population abundance of dominant forest tree species in Ghana: implications for conservation prioritization

Elisha Njomaba [a,*], Ben Emunah Aikins [b], Peter Surovy [a]

[a] Faculty of Forestry and Wood Sciences, Czech University of Life Sciences Prague, Kamýcká 129, 165 00 Prague, Czech Republic
[b] School of Public Health, College of Health Sciences, University of Ghana, Accra, Box LG 13, Ghana

ARTICLE INFO

Keywords:
Species distribution models
Habitat suitability
Abundance estimation
Tropical forest trees
Conservation planning
Ghana
Protected areas
MaxEnt model

ABSTRACT

Understanding the spatial distribution and abundance of tree species is critical for the conservation of biodiversity in Ghana's rapidly declining forests. This study applied Species Distribution Models (SDMs) to assess habitat suitability, abundance patterns, species richness, and conservation gaps of three dominant tree species, *Napoleonaea leonensis*, *Myrianthus serratus*, and *Penianthus patulinervis*, within the semi-deciduous and evergreen humid forest zones of Ghana. Tree occurrence records were compiled from the Global Biodiversity Information Facility (GBIF) database and used as input data for the modeling. Environmental variables, including bioclimatic variables, land cover, topography, and soil properties, were obtained from various online platforms. Habitat suitability was modeled for all three dominant species using the MaxEnt algorithm after correlation and Variable Inflation Factor (VIF) filtering to minimize collinearity. Zero-inflated Poisson (ZIP) models were used to estimate the abundance, while species richness was derived from stack suitability and abundance predictions. MaxEnt suitability models performed strongly across species. Area under Curve (AUC) ranged 0.93–0.96 for *Myrianthus serratus* and *Napoleonaea leonensis*. Threshold-based metrics were also high (Kappa: *Napoleonaea leonensis* 0.72, *Myrianthus serratus* 0.74, *Penianthus patulinervis* 0.82; True Skill Statistics (TSS): *Napoleonaea leonensis* 0.76, *Myrianthus serratus* 0.85, *Penianthus patulinervis* 0.85). Abundance models showed good explanatory power (Pseudo-R^2: *Napoleonaea leonensis* 0.283, *Myrianthus serratus* 0.475, *Penianthus patulinervis* 0.632; Akaike Information Criterion (AIC) 484.14, 335.73, and 185.87, respectively). Species richness indicated stronger values inside Protected Area (PAs) than outside (mean richness 0.102 inside vs. 0.019 outside). The composite conservation index delineated 23,536,682 ha of hotspot areas with 6,984,6670 ha (30 %) within PAs, highlighting protection gaps in unprotected forest areas. By integrating suitability, abundance, and richness, this study provides an evidence-based framework to guide prioritization and strengthen forest management activities in Ghana.

1. Introduction

Tropical forests are among the most species-rich ecosystems on Earth and play a vital role in maintaining biodiversity, regulating climate, and supporting human livelihoods (Poorter et al., 2015; Vancutsem et al., 2021). Although they cover <10 % of the planet's land surface, they harbor more than two-thirds of terrestrial biodiversity and provide ecosystem services that extend beyond their geographic boundaries (Giam, 2017). Their carbon storage capacity makes them essential for global climate regulation, while their cultural and economic importance is reflected in people's reliance on forest products for subsistence and trade (Lewis et al., 2015). This ecosystem faces accelerating pressures from agricultural expansion, logging, mining, and climate change, driving deforestation, degradation, and fragmentation at alarming rates (FAO, 2020). In the face of these global challenges, localized studies in tropical forests, such as those in Ghana, have become critical for developing targeted conservation strategies. Ghana's experience of rapid deforestation and ecosystem degradation mirrors global patterns, making it an ideal case for understanding and addressing the broader challenges facing tropical forests worldwide.

Once covered by a vast, evergreen, semi-deciduous forest that forms part of the Upper Guinean biodiversity hotspot, Ghana has undergone

* Corresponding author.
E-mail addresses: njomaba@fld.czu.cz (E. Njomaba), benaikins56@gmail.com (B.E. Aikins), surovy@fld.czu.cz (P. Surovy).

https://doi.org/10.1016/j.tfp.2025.101019

Available online 19 September 2025

severe forest loss and degradation over recent decades. Between 2000 and 2019, the country recorded one of the highest rates of primary forest loss in the tropics (Vancutsem et al. 2021). Agricultural expansion, particularly cocoa farming, along with logging and mining, has reduced forest extents, altered species composition, and disrupted ecological processes critical to long-term forest resilience (Foley et al., 2005; Acheampong et al., 2019). Linking these local patterns to the global biodiversity crisis underscores the urgency of developing and applying a comprehensive species distribution modeling (SDM) approach for tree species in Ghana, which will contribute to local conservation efforts and introduce a methodology that can be adapted for global tropical forest conservation, addressing both biodiversity and climate change challenges.

Despite the recognized importance of tropical forests, research in West Africa has paid limited attention to modeling tree species distributions, particularly those that are ecologically dominant and central to ecosystem functioning (Cuni-Sanchez et al., 2021). SDMs are computational tools that predict species distribution across geographic areas based on environmental and climatic variables (Zizka et al., 2021). By statistically linking species occurrence records to environmental variables, SDMs can identify areas of suitable habitat, predict distributional shifts under climatic and environmental changes, and inform spatial conservation prioritization (Elith and Leathwick, 2009). In tropical regions, approaches, such as MaxEnt, are particularly valuable given the scarcity of absence data and the challenges of exhaustive sampling (Merow et al., 2013). However, despite their demonstrated potential, most applications of SDMs in tropical regions have concentrated on modeling the distribution of animal species, particularly mammals and birds (Geldmann et al., 2013; Freeman et al., 2019). This taxonomic imbalance risks skewing conservation priorities towards fauna while neglecting the plant communities that underpin ecosystem function (Chazdon, 2008). Additionally, existing SDMs, particularly in West Africa, have given limited attention to spatial abundance patterns and multi-species richness, which are critical for effective conservation planning. Recent studies on tropical forest conservation, such as those by Marshall et al. (2021) and Qazi et al. (2022), have called for more comprehensive approaches that integrate habitat suitability, abundance, and richness into conservation frameworks. Therefore, this study seeks to respond to these calls.

Although few tree-focused SDMs have been attempted, they face some challenges. For instance, plot data for trees are often spatially biased towards accessible locations, limiting model representativeness (Beck et al., 2014). In addition, environmental drivers, such as soil properties, disturbance regimes, and microclimatic variability, are difficult to capture at broad scales, and habitat suitability predictions do not necessarily translate into abundance or demographic viability (Valladares et al., 2014). These limitations highlight the need for approaches that go beyond binary presence and absence outputs to models that integrate abundance, richness, and conservation coverage, thus generating outputs directly applicable to forest management and policies.

To address these gaps, this study focused on modeling three well-documented, functionally important tree species of Ghana's moist forests: *Napoleonaea leonensis, Myrianthus serratus,* and *Penianthus patulinervis*, selected because their ecology and regional distributions are comprehensively treated in West African floras and Ghana forest ecology, and because their uses underscore management relevance (Hawthorn and Jongkind, 2006; Addo-Fordjour et al., 2022). For instance, *Myrianthus serratus* supports primates and large herbivores through its fruit production (Oates et al., 2000), whereas *Napoleanaea leonensis* contributes to understory diversity and regeneration dynamics (Hall and Swaine, 1981). *Penianthus patulinervis*, a widespread liana, influences forest architecture and competition dynamics (Campbell, 2005). Beyond their ecological significance, these species are widely distributed in the high forest zones of Ghana, including the evergreen and semi-deciduous moist belts, representing the main forest ecosystems of the country, according to the vegetation data explored from the GBIF database (Asare, 2021). The strategic focus on these species allows this study to address these critical gaps in SDMs while generating insights directly applicable to conservation and forest management in Ghana and beyond.

Based on this rationale, this study aimed to model the current suitability of the three dominant species using presence records and the MaxEnt algorithm with predictors such as climatic, land cover, topographic, and edaphic conditions, providing a nationwide suitability map. The study also sought to estimate spatial abundance patterns by integrating plot occupancy and abundance data with suitability predictions, advancing the SDM methodology by moving beyond presence-only suitability outputs to more ecologically realistic measures of species dominance and viability. Additionally, we sought to map species richness and assess conservation representation by overlaying predicted distributions with Ghana's protected area network, directly informing conservation planning by identifying where tree diversity is safeguarded and where critical gaps remain. Finally, we identified composite priority areas for preservation by integrating suitability, abundance, and richness into a single framework.

By integrating habitat suitability, abundance estimation, species richness mapping, and conservation gap analysis into a single framework, this study makes novel contributions to tropical forest research and practice. The study represents a nationwide contribution of tree-focused SDMs for ecologically dominant species, addressing long-standing taxonomic biases in West African conservation, and demonstrates methodological advancements that link habitat suitability to abundance and multiple species richness.

2. Materials and methods

2.1. Study area

The study was conducted in Ghana, a West African country bordered by Burkina Faso to the north, Côte d'Ivoire to the west, Togo to the east, and the Gulf of Guinea to the south (Fig. 1), featuring a coastline of approximately 555 km (Kusi, 2025). Geographically, Ghana lies between 7.9465° N and 1.0232° W and covers a total land area of 238,539 km^2 (Armah et al., 2011). The terrain has a mean elevation of 190 m, ranging from sea level on the Atlantic coast to 885 m on Mount Afadjato, the highest peak in the country. Administratively, Ghana is divided into 16 regions and has a population of approximately 30.8 million, growing at an annual rate of 2.2 % (Ghana Statistical Services, 2021). The country has a tropical climate, with high temperatures and alternating wet and dry seasons. The mean annual temperature ranges from 26.1 °C to 28.9 °C. Rainfall is highest in the southwestern town of Axim (2159 mm/year), gradually declining northward to 1016–1270 mm and dropping further to 762–1016 mm in the northeast part of the country. Ecologically, the country comprises two main vegetation zones: tropical forests and savannah zones (Wagner and Cobbinah, 1993). The forest zone covers approximately 44 % of the land area and includes Wet Evergreen, Moist Evergreen, Upland Evergreen, Moist Semi-Deciduous, and Dry Semi-Deciduous forests. The savannah zone covers about 56 % and consists of the Transition zone, the Guinea savannah, the Sudan savannah, and the Coastal savannah types.

The High Forest Zone is dominated by agroforestry systems with economically important tree crops, such as cocoa, oil palm, rubber, kola, and coffee. Guinea savannah is characterized by farmland that contains species such as *Vitellaria paradoxa* (shea tree) and *Parkia biglobosa* (African locust bean tree). Common native tree species across these ecosystems include *Celtis zenkeri, Celtis milbraedii, Triplochiton scleroxylon, Sterculia rhinopetala, Funtumia elastica, Baphia nitida, Cleidion gabonicum, Nesogordonia papaverifera, Hymnostegia afzelii, Turraenthus africanus, Trichilia prieuriana, Myrianthus serratus, Napoleonaea leonensis, and Penianthus patulinervis*.

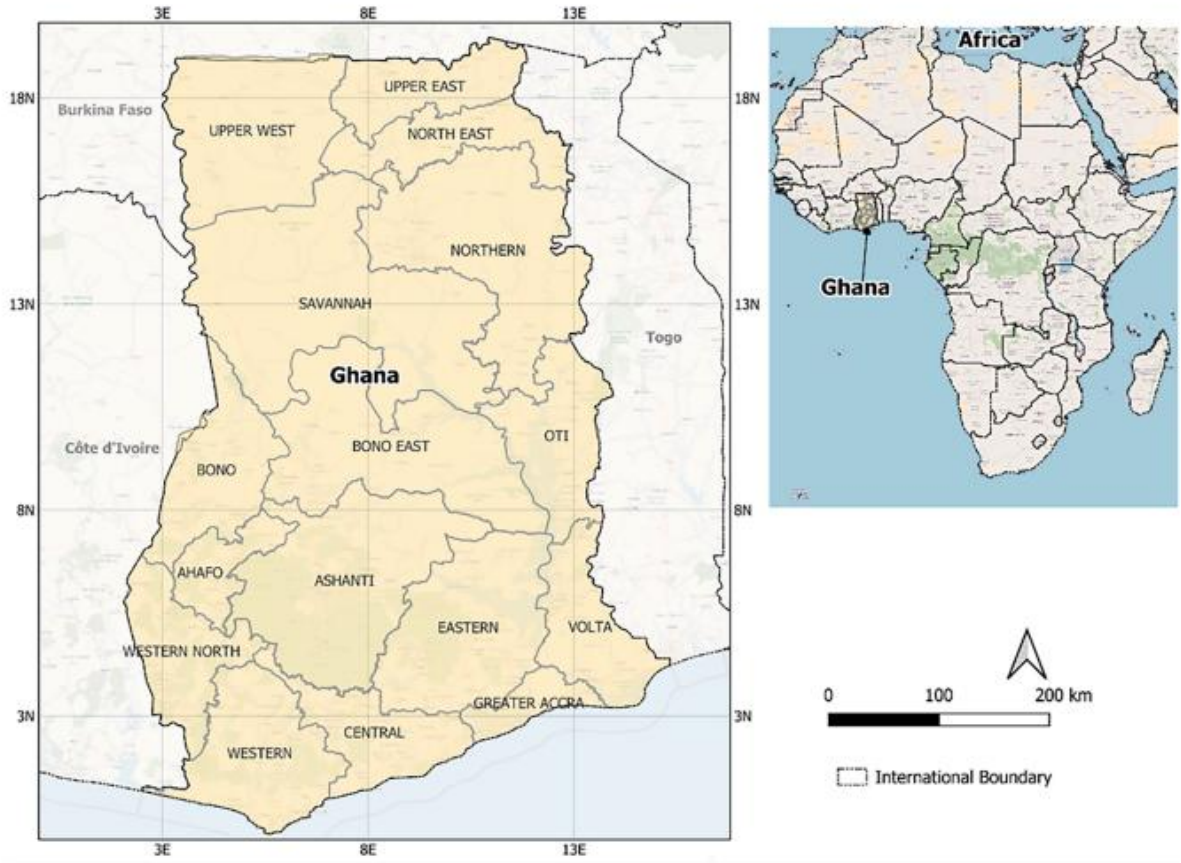

Fig. 1. Map of Ghana showing administrative regions (left) and the location of Ghana within Africa (right). The map (left) highlights international boundaries and the main regional divisions.

2.2. Vegetation occurrence data processing and dominant species identification

Vegetation occurrence data for all trees in Ghana were obtained from the Global Biodiversity Information Facility (GBIF; www.gbif.org) and accessed on March 8, 2025. The downloaded records included the species name, geographic coordinates, and source metadata. All duplicates and entries with questionable geographic coordinates were removed to ensure data quality. To address spatial clustering and sampling bias commonly associated with aggregated biodiversity records, especially from open databases such as GBIF, we applied a spatial thinning algorithm at 1 km resolution using the **spThin** package in R Studio software (Aiello-Lammens et al., 2015). This process resulted in 9716 tree occurrence records in Ghana. To ensure standardization of spatial resolution and align with landscape-scale conservation analysis, circular plots with a radius of 28.2 m corresponding to an area of 0.25 hectares were created, resulting in around 282 plots across the study area. This plot size aligns with the common forest monitoring standards in West Africa and balances the need for ecological resolution with computational scalability (Chave et al., 2003).

The plot occupancy approach was adopted, which is defined as the number and proportion of 0.25 ha plots where the species is present. This was used as a proxy for relative abundance and distributional dominance. Although presence-only data do not capture true abundance, the plot-based occupancy metric offers a spatially interpretable measure of the prevalence of a species at the national scale. This approach is widely used in species distribution modeling (Elith and Leathwick, 2009). Based on the plot occupancy framework, the top three spatially distributed species across 0.25 ha plots were *Napoleonaea leonensis*, *Myrianthus serratus*, and *Penianthus patulinervis*. These species span diverse ecological niches and functional groups within Ghana's forest ecosystems.

2.3. Environmental variables and preprocessing

Environmental variables were selected as predictors to represent the ecological constraints influencing species distribution across Ghana. These variables capture key climatic, topographic, edaphic, and land cover characteristics relevant to the environmental niches of the modeled tree species (Phillips et al., 2006). All environmental layers were processed and harmonized to ensure spatial projection, resolution, and extent consistency. Nineteen bioclimatic variables (BIO1-BIO19) were obtained from the WorldClim v2.1 database (https://www.worldclim.org/data/bioclim.html) at 30 arc-seconds (~1 km) resolution. These bioclimatic variables (Table 1) represent long-term (1970–2000) averages of temperature and precipitation patterns, including measures of seasonality and extreme climatic conditions known to influence plant physiology and distribution (Fick and Hijmans, 2017; Hijmans et al., 2005).

Topographic variables were derived from the Shuttle Radar Topography Mission (SRTM) Digital Elevation Model (DEM) at 30 arcseconds (~1 km), accessed through the geodata package in R Studio. Additional variables, including slope and aspect, were calculated from this elevation dataset. These variables capture local variations in terrain and

Table 1
Description of environmental variables preliminarily selected as predictors.

Label	Variable	Unit
BIO1	Annual mean temperature	◦C
BIO2	Mean diurnal range [mean of monthly (max-temp – min-temp)]	◦C
BIO3	Isothermality (BIO2/BIO7) x 100	%
BIO4	Temperature seasonality (standard deviation) x 100	%
BIO5	Maximum temperature of the warmest month	◦C
BIO6	Minimum temperature of the coldest month	◦C
BIO7	Annual temperature range (BIO5 – BIO6)	◦C
BIO8	Mean temperature of the wettest quarter	◦C
BIO9	Mean temperature of the driest quarter	◦C
BIO10	Mean temperature of the warmest quarter	◦C
BIO11	Mean temperature of the coldest quarter	°◦C
BIO12	Annual precipitation	mm
BIO13	Precipitation of the wettest month	mm
BIO14	Precipitation of the driest month	mm
BIO15	Precipitation seasonality (coefficient of variation)	mm
BIO16	Precipitation of the wettest quarter	mm
BIO17	Precipitation of the driest quarter	mm
BIO18	Precipitation of the warmest quarter	mm
BIO19	Precipitation of the coldest quarter	mm
Elevation	Elevation	m
Slope	Slope	m
Aspect	Aspect	Deg
SoilpH	SoilpH	pH × 10
Soil organic carbon density	Soil organic carbon density	t/ha
Soil texture (sand, silt, clay)	Soil texture	G/kg
Forest cover	Forest cover	N/A

microclimate relevant to forest structure and the spatial distribution of species.

Soil variables were sourced from the SoilGrids database (https://soilgrids.org/) at an original resolution of 250 m, including soil pH, soil organic carbon density, and soil texture fractions (clay, silt, and sand content). These layers were projected and resampled to align with the 1 km resolution of the climate layers using bilinear interpolation to preserve continuous variation. A binary forest cover raster (forest and non-forest) was also resampled to match all layers and included, derived from the national land cover data from Njomaba et al. (2025), to account for vegetation structure and land cover. This variable served as a proxy for habitat type and anthropogenic disturbance. All environmental variables were re-projected to WGS 84/UTM Zone 30 N, masked to the national boundary of Ghana, and stacked into a unified raster brick for model fitting.

2.4. Variable selection and multicollinearity

We conducted a multicollinearity assessment and feature selection before modeling to improve model interpretability and reduce overfitting. A Pearson correlation matrix was computed among the continuous environmental predictors to visualize pairwise relationships and identify highly correlated variables. In addition, we applied the Variance Inflation Factor (VIF) method to detect multicollinearity. Variables with a VIF greater than 10 were considered to exhibit strong collinearity and were excluded from the modeling process, following common ecological modeling practice (Guisan et al., 2017; Dormann et al., 2013).

After the multicollinearity test, variables greater than 10 were removed because of their strong correlation with other variables. These include 11 continuous variables: BIO1, BIO2, BIO4, BIO5, BIO7, BIO8, BIO9, BIO10, BIO11, BIO12, and Elevation. Hence, the model was run with 10 less correlated and more important variables: temperature (BIO3 and BIO6), precipitation (BIO13 and BIO19), edaphic (soil organic carbon density, soil texture-sand, and soil texture-silt), vegetation cover (forest), and topography (slope and aspect) (Table 2). These variables were more relevant in characterizing the environmental conditions related to species distribution. This approach is essential for reducing the potential bias and variance inflation caused by collinear variables, which has been widely adopted in ecological niche modeling frameworks to improve model performance (Phillips et al., 2006).

2.4.1. Species distribution modeling using MaxEnt

A species distribution model was developed using the MaxEnt algorithm, which is suitable for presence-only data and is widely recognized for its robust habitat suitability predictions. MaxEnt was chosen over alternative regression or machine-learning approaches (e.g., GLMs, GAMs, Random Forest, etc.) because it requires relatively small sample sizes and has consistently demonstrated high predictive accuracy. It is also less prone to overfitting compared to other machine-learning approaches when appropriate regularization is applied, and it provides interpretable response curves and variable contributions (Phillips et al., 2006; Elith and Leathwick, 2009). These strengths make the MaxEnt particularly suitable for our dataset, which consists primarily of occurrence records without reliable absence data. In this study, the three most dominant tree species were identified through occurrence frequency analysis: *Myrianthus serratus*, *Napoleonaea leonensis*, and *Penianthus*

Table 2
Environmental variables used as predictors: selected after multicollinearity analysis.

Label	Variable	Unit	Description
BIO3	Isothermality (BIO2/BIO7) x 100	%	Evaluates how large the day-to-night temperature oscillates relative to the annual temperature range.
BIO6	Minimum temperature of the coldest month	°C	Determines the coldest temperature a species experiences annually, influencing survival limits and range boundaries.
BIO13	Precipitation of the wettest month	mm	Indicates water availability during the peak rainy period, critical for species dependent on seasonal moisture.
BIO19	Precipitation of the coldest quarter	mm	Helps to characterize how the amount of precipitation during the coldest quarter may affect the distribution of the species.
Soil pH	The (water)	pH × 10	Influences nutrient availability and soil chemistry, affecting species' growth and distribution based on soil acidity preferences.
Soil organic carbon density	Organic carbon content in the soil	T/ha	Represents soil fertility and organic matter, affecting species establishment and productivity.
Soil texture-sand	Sand content in soil	G/kg	Impacts soil drainage and aeration, which influences species' root development and water availability.
Soil-texture-silt	Silt content in soil	G/kg	Affects soil moisture retention and nutrient holding capacity, shaping species' habitat suitability.
Forest	Forest cover	N/A	Defines habitat presence or absence, directly influencing species occurrence by providing the necessary structural environment.
Slope	Slope	m	Affects soil erosion, water runoff, and microclimate, which can restrict or favor species adapted to certain terrain steepness.
Aspect	Aspect	Deg	Determines sun exposure and microclimate variability, influencing species distributions sensitive to temperature and moisture gradients.

patulinervis. Species occurrence points were spatially transformed to align with environmental raster stack projections. Given the reliance on presence-only data, a spatial blocking approach was employed to partition the data into five spatial folds, improving the model evaluation by accounting for spatial autocorrelation and providing robust cross-validation (Roberts et al., 2017). Background points were generated randomly within a 30 km buffer surrounding all known occurrences for each species, ensuring environmentally relevant pseudo-absence data for contrast in model training. Each dataset combined presence (coded as 1) and background points (coded as 0) with extracted environmental values from the filtered covariate set.

MaxEnt models were fitted using the Maxent package in R, employing default regularization parameters to balance model complexity and avoid overfitting. Five-fold spatial cross-validation was implemented for each species based on spatially defined folds, ensuring that the training and testing datasets were spatially independent. Habitat suitability predictions were then generated for each tree species by applying the fitted MaxEnt models across the country with environmental raster layers. This resulted in continuous suitability maps representing the relative likelihood of suitable habitat conditions at the grid cell level, allowing for comparisons.

2.4.2. Model evaluation and variable importance

The predictive performance of MaxEnt models was assessed using the Area Under the Receiver Operating Characteristic Curve (AUC), a widely accepted metric for evaluating species distribution (Pearson et al., 2004; Guisan and Zimmermann, 2000). To provide an unbiased assessment, independent test datasets representing 25 % of the total occurrence points were used for model evaluation, following protocols from Elith and Leathwick (2009). The AUC metric quantifies the ability of the model to discriminate between the presence and background points across all possible threshold values. It measures the probability that a randomly chosen presence site is assigned a higher predicted suitability than a randomly selected background location. An AUC of 1 indicates perfect discrimination, whereas 0.5 corresponds to random performance (Phillips et al., 2006). In presence-only modeling frameworks, such as MaxEnt, the absence data are replaced by randomly sampled background points. Therefore, the specificity and related Receiver Operating Characteristic (ROC) interpretations differ from those of traditional presence-absence models. Here, the false-positive rate (1-specificity) corresponds to the fractional predicted area of the study region rather than the true commission error, and the maximum achievable AUC is often less than one (Jorge et al., 2007). Despite this, the AUC remains a robust indicator of model discrimination ability. Sensitivity (true positive rate) and specificity (true negative rate) were computed over thresholds to understand the model behavior across the prediction cutoffs. Omission and commission errors were also examined to identify the thresholds that effectively balance the prediction errors.

We generated response curves for each environmental predictor to further assess the variable importance and model response, holding other covariates at their mean values. This helped to visualize the relationship between individual predictors and predicted habitat suitability, facilitating the ecological interpretation of the models. Jackknife tests of variable importance were conducted to evaluate the contribution of each predictor to model gain and overall performance. These tests involved sequentially removing variables to examine their impact on model accuracy. Model evaluation metrics were calculated within a spatial blocking cross-validation framework to account for spatial autocorrelation and improve generalizability (Roberts et al., 2017). We computed the mean AUC and True Skill Statistic (TSS) across folds, with TSS providing a threshold-dependent measure of model accuracy that balances sensitivity and specificity (Allouche et al., 2006). The optimal TSS was determined by testing the thresholds from 0.1 to 0.9 and selecting the value maximizing TSS. Summary statistics of the model performance were compiled for the three dominant tree species.

2.5. Species richness mapping and protected area analysis

Continuous habitat suitability maps generated with MaxEnt for the three dominant species were converted into binary presence-absence maps to assess spatial patterns of species richness. Specific thresholds were applied based on model evaluation metrics to optimally differentiate suitable from unsuitable habitats (Liu et al., 2016). These binary maps were combined and summed to create a species richness raster representing the number of species predicted to co-occur in each spatial unit (Freeman and Moisen, 2008). The raster of species richness was visualized to identify biodiversity hotspots across Ghana. To assess conservation coverage, a richness map was overlaid with protected area boundaries from the Protected Planet database (https://www.protectedplanet.net/en), which provides the most current and comprehensive global protected area data. Summary statistics, including the mean and maximum species richness inside and outside protected areas, were computed to evaluate the representativeness of the protected area network for the target species (Joppa and Pfaff, 2009). Hotspots were defined as grid cells where all three species overlapped (richness = 3), highlighting priority conservation areas, and the proportion of hotspots falling within protected areas was calculated to estimate conservation effectiveness (Myers et al., 2000).

2.6. Species abundance estimation and uncertainty mapping

To estimate the spatial patterns of population abundance for Ghana's dominant forest tree species, we employed Zero-Inflated Poisson (ZIP) models. This approach is suitable for ecological count data exhibiting excess zeros, which is a common feature in plot-based species surveys with patchy distributions (Zuur et al., 2009). ZIP models combine a binomial process (modeling presence vs. absence) with a Poisson process (modeling counts conditional on presence), offering improved flexibility for sparse datasets. We aggregated species occurrence data at a 10 km × 10 km grid, computing abundance as the count of individuals per species per grid cell. Environmental variables were extracted from the raster layers, including bioclimatic variables, edaphic factors, and forest cover. All variables were resampled to a consistent resolution before model fitting. For each top species, we fit the ZIP models with both the count and zero-inflation components using all available covariates. Model performance was evaluated using the Akaike Information Criterion (AIC) and pseudo-R^2.

We implemented bootstrap resampling (n= 50 iterations) for uncertainty quantification for each species. In each iteration, a ZIP model was refit on a bootstrapped dataset and used to predict abundance across the landscape. The resulting predictions were summarized by computing the mean, standard deviation, and coefficient of variation across all iterations to provide spatially explicit estimates of the model uncertainty. These uncertainty maps were used to assess the spatial robustness of the predictions, highlighting both high-confidence regions and areas requiring caution owing to prediction instability. This approach aligns with best practices in ecological modeling, where quantifying uncertainty is critical for informing conservation decisions (Oliver et al., 2015; Dormann et al., 2008).

2.7. Priority conservation areas and protection gaps

High-priority areas for dominant forest tree species were identified by developing a composite index that integrates habitat suitability and predicted abundance through a multiplicative approach, supporting spatial conservation planning. This approach combines the suitability models from the SDM and the abundance from the ZIP model to reflect habitat values comprehensively (Oliver et al., 2015). Raster layers of predicted suitability and abundance were multiplied for each species after aligning their spatial resolution. The resulting composite index raster reflects the grid level where both suitable environmental conditions and high expected abundance coincide. To identify spatial

hotspots, we calculated the 90th percentile threshold of the composite index across the landscape and designated all values above this threshold as priority areas. This top 10 % subset corresponds to the most valuable ecological zones of the species.

3. Results

3.1. Dominant forest tree species across Ghana

A total of 282 unique 0.25-hectare circular plots were used to calculate the number of plots where each species occurred. Out of the 1756 recorded tree species, we identified the five most dominant species occurring across Ghana. *Napoleonaea leonensis* was the most widely occurring species in 51 plots (18.1 %) of all records. *Myrianthus serratus* was followed by 39 plots (13.8 %), and *Penianthus patulinervis* appeared in 18 plots (6.4 %). Two species, *Rinorea welwitschia* and *Peperomia fernandopoiana*, occurred in four plots (1.4 %) and three plots (1.1 %), respectively (Fig. 2). These results indicate a relative prevalence, identifying the most distributed forest tree species in Ghana.

3.2. Modeled habitat suitability for the three most dominant tree species

Habitat suitability models were generated for the three most dominant species identified across the country: *Myrianthus serratus, Napoleonaea leonensis*, and *Penianthus patulinervis*. The predictions represent the spatial distribution of suitable habitats derived from environmental variables using the MaxEnt algorithm. *Myrianthus serratus* (Fig. 3A) showed high habitat suitability, primarily in the southern forest zone, particularly in Ghana's southwestern and southeastern regions. These regions exhibit dense forest cover and high annual rainfall, aligning with the species' ecological preferences. *Napoleonaea leonensis* (Fig. 3B) showed broader habitat suitability, covering the central and western parts of the country. This suggests a wider environmental niche under varying climatic and edaphic conditions. *Penianthus patulinervis* (Fig. 3C) generally exhibited low suitability patterns, with high suitability areas concentrated in the southernmost parts of the country. These spatial predictions provide insights into the ecological distribution of key forest species and offer a spatial framework for the conservation and monitoring of forest ecosystems across Ghana.

3.2.1. Model performance and evaluation

An evaluation and performance of the modeling for all three species was performed, where the distribution models for *Myrianthus serratus, Penianthus patulinervis*, and *Napoleonaea leonensis* performed well across all three evaluation metrics, such as the AUC, Kappa, and TSS (Fig. 4). AUC values were consistently high, ranging from 0.93 (*Napoleonaea leonensis*) to 0.96 (Myrianthus serratus), indicating good discrimination between suitable and unsuitable areas. Kappa values, which seek to quantify the agreement between predicted and observed presence–absence beyond chance, ranged from 0.72 (*Napoleonaea leonensis*) to 0.82 (*Penianthus patulinervis*), with (*Myrianthus serratus*) at 0.74. TSS values followed a similar pattern, ranging from 0.76 (*Napoleonaea leonensis*) to 0.85 (*Myrianthus serratus* and *Penianthus patulinervis*), confirming good predictive accuracy and balance between sensitivity and specificity. Error bars indicate some variability across cross-validation runs, but the relatively narrow range for AUC compared to Kappa and TSS suggests that the discrimination ability was more stable than the threshold-dependent metrics. Overall, *Myrianthus serratus* achieved the highest AUC, *Penianthus patulinervis* achieved the highest Kappa, and *Myrianthus serratus* and *Penianthus patulinervis* shared the highest TSS.

3.2.2. Variable importance

The jackknife test of variable importance (Fig. 5) revealed differences in the contributions of the environmental predictors to the habitat suitability models of the three studied species. For *Napoleonaea leonensis* (Fig. 5-A), the most influential variables were soil texture (silt and sand), slope, and bio 19 (precipitation of coldest quarter), with substantial contributions from forest cover and soil organic carbon density. In *Myrianthus serratus* (Fig. 5-B), soil texture (sand), slope, forest cover, and temperature-related variables (bio 6: minimum temperature of the coldest month and bio 19) were the dominant predictors. For *Penianthus patulinervis* (Fig. 5-C), slope, soil texture (sand), forest cover, and bio 6 were the most significant variables. Overall, soil texture, slope, forest cover, precipitation, and some temperature-related bioclimatic variables consistently influenced model performance across species, although the magnitude of their influence varied.

3.2.3. Response curves

The response curves (Fig. 6) illustrate how the probability of a

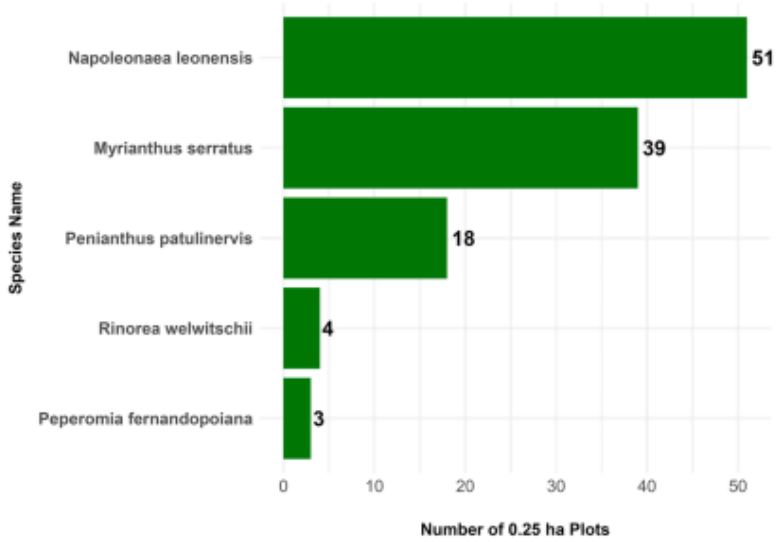

Fig. 2. Plot occupancy of the five most dominant forest tree species across Ghana. The bar chart shows the number of 0.25-hectare plots (out of 182 total) in which each species was recorded.

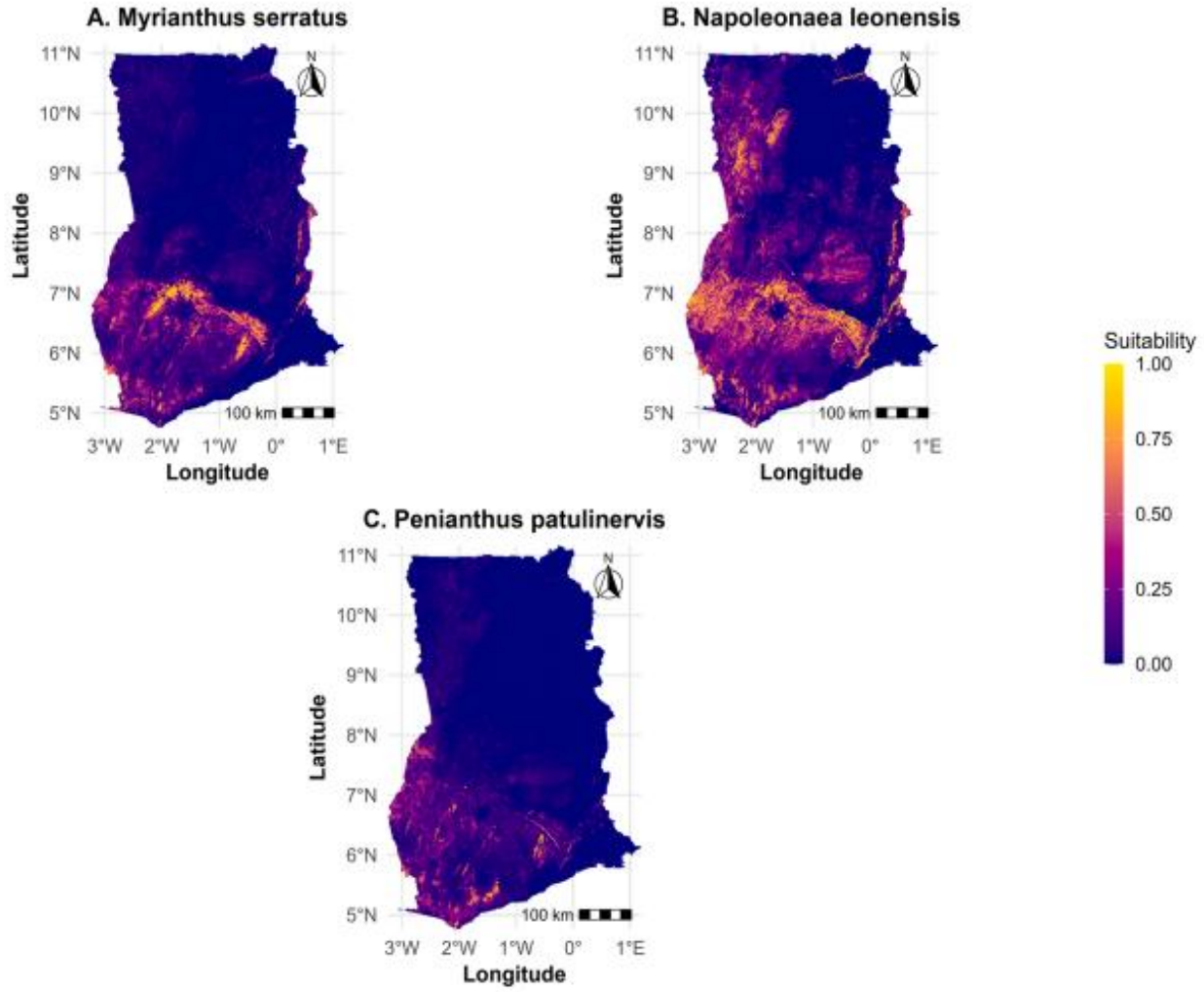

Fig. 3. Spatial habitat suitability predictions: (A), (B), and (C) illustrate the model outputs for the three focal species across Ghana. The color intensity reflects the predicted suitability (low= dark blue, high= yellow).

suitable habitat changes along the gradients of the top four environmental variables for each species, as identified by the jackknife test of variable importance (Fig. 5). For *Myrianthus serratus*, habitat suitability increased steadily with greater forest cover, whereas suitability declined with increasing values of BIO19 and Soil texture (silt). Suitability also increased moderately with slope, reaching maximum values at mid-range slope gradients. Suitability *for Napoleonaea leonensis* was highest at intermediate values of BIO3 and BIO6, with forest cover positively associated with habitat suitability. In contrast, BIO19 exhibited a negative relationship with suitability, with higher precipitation during the coldest quarter linked to reduced habitat suitability. For *Penianthus patulinervis*, suitability declined with increasing BIO6 and BIO19 values. In contrast, forest cover and slope showed positive associations with suitability, with the highest probabilities observed in dense forest areas and moderate-to-steep slopes. Overall, the response curves reflected the variable importance patterns identified in the jackknife test, highlighting the combined influence of climatic variables (temperature and precipitation), habitat structure (forest cover), and topographic features (slope) in shaping species-specific habitat suitability.

3.3. Abundance estimation

3.3.1. Predicted abundance maps and model performance

The ZIP abundance models predicted the spatial patterns of tree abundance across Ghana for the three focal species (Fig. 7). *Penianthus patulinervis* exhibited the highest predicted abundances, with high-density areas concentrated in the country's southwestern and central forest zones. *Myrianthus serratus* showed moderate abundance patterns, with hotspots appearing in fragmented forest landscapes and transitional forest zones. In contrast, *Napoleonaea leonensis* displayed more patchy abundance distributions, with fewer areas of high predicted density.

Model evaluation statistics (Table 3) revealed differences in predictive performance among species. *Penianthus patulinervis* achieved the best fit, with the lowest AIC (185.87) and the highest pseudo-R^2 (0.632), indicating strong explanatory power and reliable spatial predictions. *Myrianthus serratus* followed, with a pseudo-R^2 of 0.475 and an AIC of 335.73, suggesting a moderate predictive strength. *Napoleonaea leonensis* had the weakest model performance (pseudo-R^2= 0.273, AIC= 484.14), reflecting greater unexplained variation in its abundance estimates. Overall, these results indicate that abundance prediction accuracy was highest for species with broader and distinct environmental

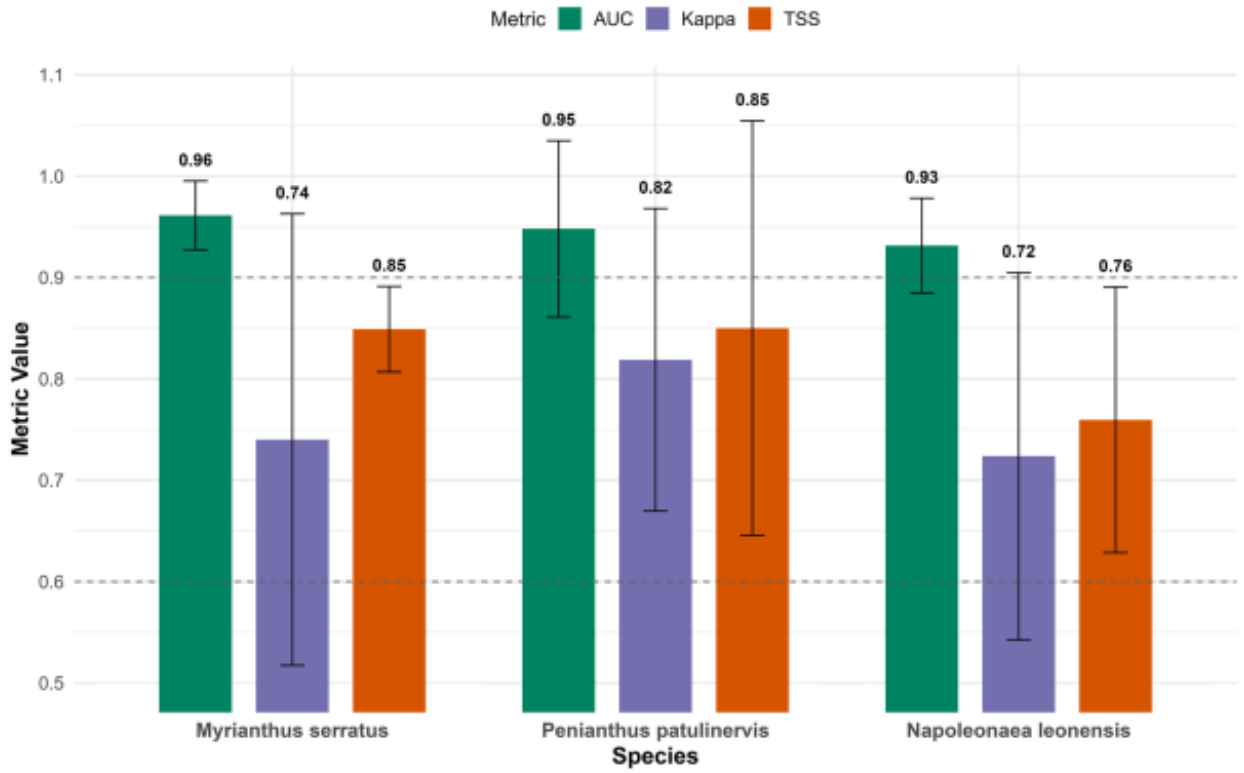

Fig. 4. Model performance metrics (AUC, Kappa, and TSS) for *Myrianthus serratus*, *Penianthus patulinervis*, and *Napoleonaea leonensis*. Error bars represent the standard deviation across replicates.

niches and lowest for species with narrower or more fragmented habitat distributions.

3.3.2. Abundance model uncertainty

To assess the reliability of the predicted abundance patterns, coefficient of variation (CV) maps were generated for each species (Figure B1, A-C). These maps indicate the relative uncertainty across the predictions of the ZIP abundance models. Uncertainty was generally low across most of the high abundance areas for *Myrianthus serratus*, more spatially variable for *Napoleonaea leonensis*, with moderate to high CV values throughout predicted suitable areas, reflecting greater model sensitivity to environmental conditions for this species, and minimal uncertainty for *Penianthus patulinervis* in the central-southern regions of high predicted abundance, but increased towards the northern and far eastern areas, consistent with lower occurrence densities in these regions.

3.4. Species richness and conservation hotspots

The spatial pattern of species richness (Fig. 8) revealed that areas of highest predicted co-occurrence of the three priority species were concentrated in the southwestern forest zone of Ghana, particularly along the moist evergreen region and the transition belt. The maximum richness reached three species per grid cell, although most of the country had zero or one species. With protected area (PA) data overlaid, richness hotspots were found inside and outside PAs, although a greater proportion of richness occurred in PA boundaries. The mean predicted richness inside PAs (0.102) was more than five times higher than that outside PAs (0.019), and the maximum observed richness inside PAs (three species) exceeded that outside PAs (two species) (Table 4). At the individual PA level, the Atewa Range Forest Reserve had the highest mean richness (2.125) and the maximum possible richness of three species, followed by Neung South (mean 1.286, max 3), Jama Asemkrom (mean 1.5, max 2), and Cape Three Points (mean 1.25, max 2). Several other PAs, such as the Boin River, Bobiri, and Abisu, also supported high local richness ($\geq$ 2 species max) (Table A1), despite relatively small areas. In addition, most PAs, particularly those in the northern savannas, had predicted richness values of zero.

3.5. Priority areas based on suitability and abundance

The composite index, derived from the predicted habitat suitability and estimated abundance, identified priority conservation areas concentrated primarily within Ghana's southwestern and south-central parts, with smaller patches occurring along the eastern portion of the country (Fig. 9). These high-index areas generally correspond to regions of high species co-occurrence and abundance aligned with known forested landscapes and biodiversity-rich zones. The total extent of hotspot areas (defined as pixels within the upper range of the composite index) was 23,536,682 ha, of which 6,984,670 ha fell within existing protected areas. This represented 30 % of the identified hotspot areas under protection (Table 5). The remaining 70.3 % of hotspots were located outside the protected area, indicating gaps in conservation coverage.

4. Discussion

This section provides an integrated spatial assessment of habitat suitability, abundance, and richness patterns for key forest tree species in Ghana, combining vegetation data obtained from a database and environmental predictors to identify priority conservation areas. The approach, which integrated MaxEnt habitat suitability models, plot occupancy-based abundance estimation, and species richness mapping, revealed patterns in Ghana's forest biodiversity distribution and the

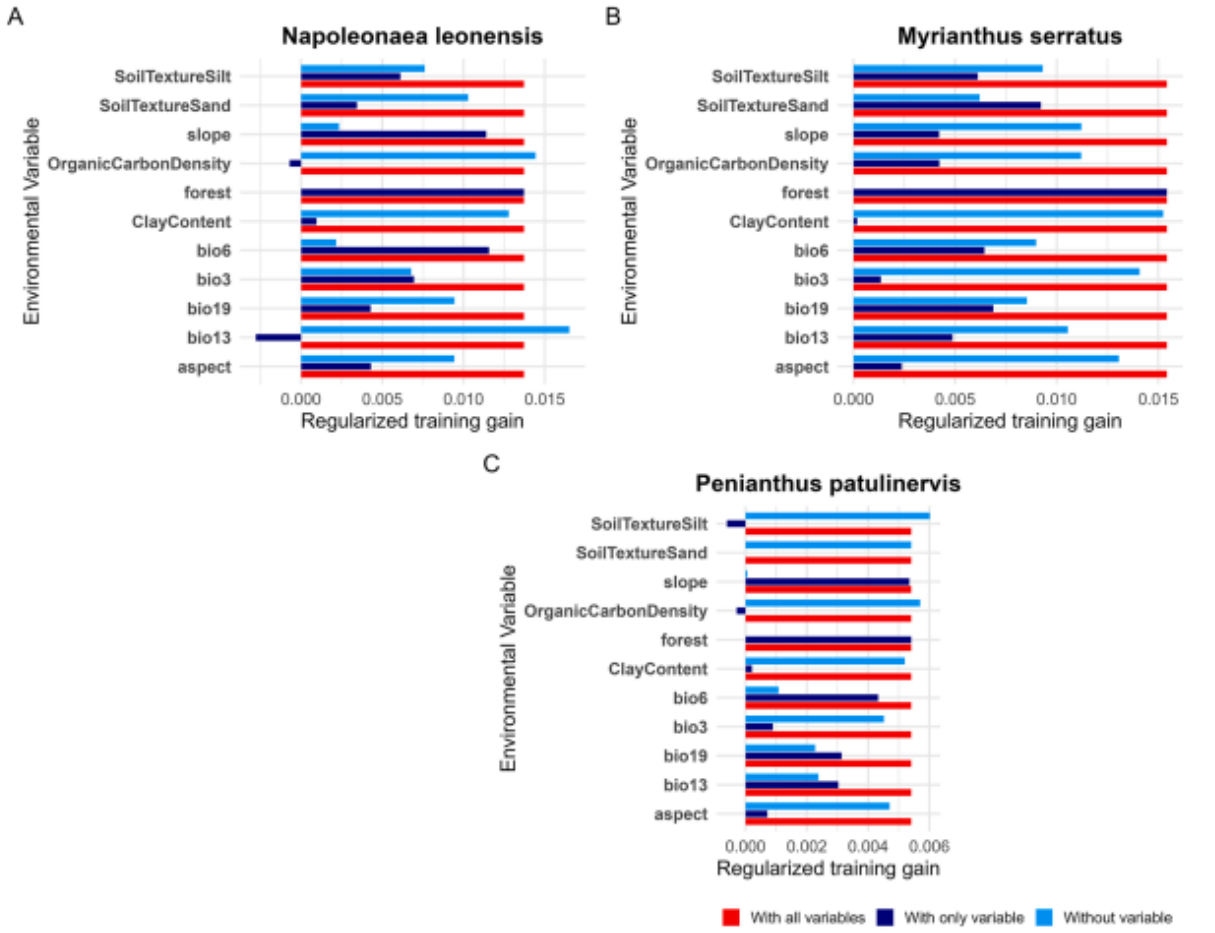

Fig. 5. Jackknife test of variable importance for Napoleonaea leonensis (A), Myrianthus serratus (B), and Penianthus patulinervis (C). Bars show the model gain with all variables (red), with only the tested variable (blue), and without the tested variable (light blue).

degree to which these areas are represented in current protected areas.

4.1. Dominance and distribution of key forest species

Out of the 1756 forest tree species recorded, *Napoleonaea leonensis*, *Myrianthus serratus*, and *Penianthus patulinervis* were the most dominant, occurring in 18.19 %, 13.8 %, and 6.45 % of plots, respectively. Dominance in this context reflects a high frequency of occurrence and broad spatial distribution, which are often used as indicators of ecological resilience, competitive advantage, or adaptation to a wide range of environmental conditions (Grime, 1998; Magurran and McGill, 2011). The presence of *Napoleonaea leonensis and Myrianthus serratus* supports earlier findings from West African floristic surveys, where these species are reported among the common species of moist evergreen and semi-deciduous forest assemblages (Hawthorn and Jongkind, 2006). Their prevalence may be attributed to their tolerance to different soil types, effective seed dispersal mechanisms, and adaptability to primary and secondary forest conditions (Schupp et al., 2010). The broader distribution of *Napoleonaea leonensis* across wet evergreen and moist semi-deciduous forests in Ghana suggests broad ecological coverage, a pattern also observed in Guinea and Liberia, which could make it less vulnerable to localized habitat changes (Hutchinson and Dalziel, 1928).

In contrast, *Penianthus patulinervis* showed a more geographically restricted distribution in the southernmost forested areas. Such restrictions on their distribution may result in narrower habitat requirements, potential sensitivity to environmental change, or dependence on specific microhabitats. Species with limited ranges are often at a higher risk of habitat loss and fragmentation (Schupp et al., 2010), making it a potential conservation concern despite not being rare where it occurs. Overall, the dominance patterns observed suggest that while widespread species may be more resilient to environmental change, range-restricted dominant species could act as early indicators of ecological stress, necessitating closer monitoring.

4.2. Habitat suitability and environmental drivers

The MaxEnt models showed strong discrimination across the three species modeled and broadly consistent inference about the role of climate, habitat structure, topography, and soils. For instance, the importance of temperature and precipitation in our models, particularly variables related to the minimum temperature of the coldest month (BIO6), isothermality (BIO3), and precipitation of the coldest quarter (BIO19), is consistent with similar research in the context of Ghana, showing that tree distributions are strongly associated with rainfall seasonality, isothermality, and temperature seasonality (Amissah et al., 2014). Similar bioclimatic variables (BIO6 and BIO19) have been among the top predictors in other species distribution modeling across some African countries, underscoring their ecological significance for tropical

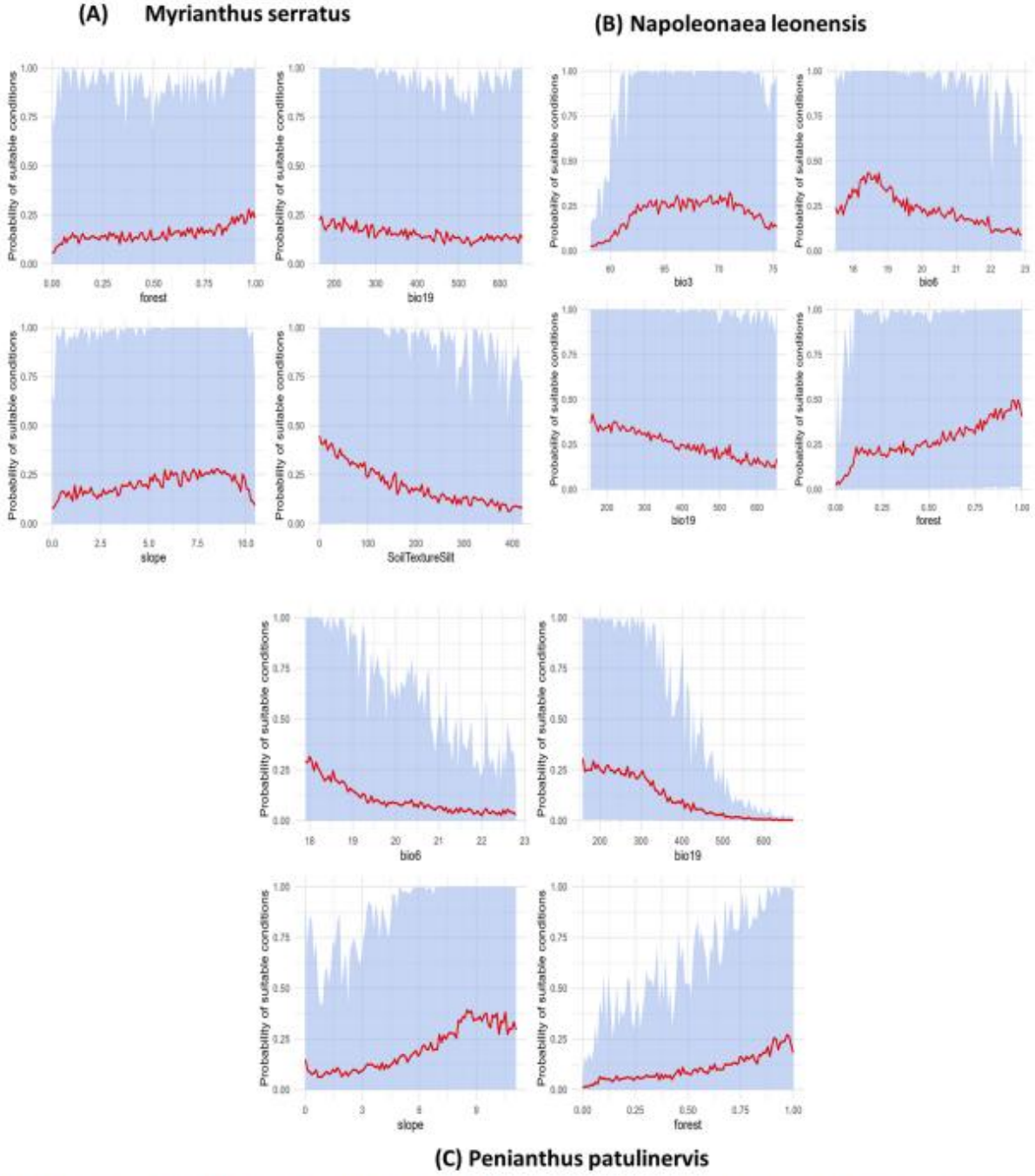

Fig. 6. Response curves showing the relationship between habitat suitability and the top four environmental variables for each species as determined by the jackknife test of variable importance. The red line represents the predicted probability of suitable conditions, and the shaded area indicates the variability across the prediction range.

taxa (Zhao et al., 2024; Mkala et al., 2023, and Abuhay et al., 2025). In addition to the importance of these key bioclimatic variables, habitat structure in the form of forest cover is necessary for species distribution modeling. The positive association observed with forest cover aligns with the general pattern that land cover and vegetation structure are strong and significant predictors in MaxEnt habitat models (Wilson et al., 2013). In Ghana, recent works have emphasized how changes in forest cover shape biodiversity patterns and should be integrated into distribution modeling analysis (Marshall et al., 2021). The emergence of forest cover for model predictions of all three species underscores the role that forest structure plays in regulating microclimates and buffering species from microclimatic variability. Ewers and Banks-Leite (2013)

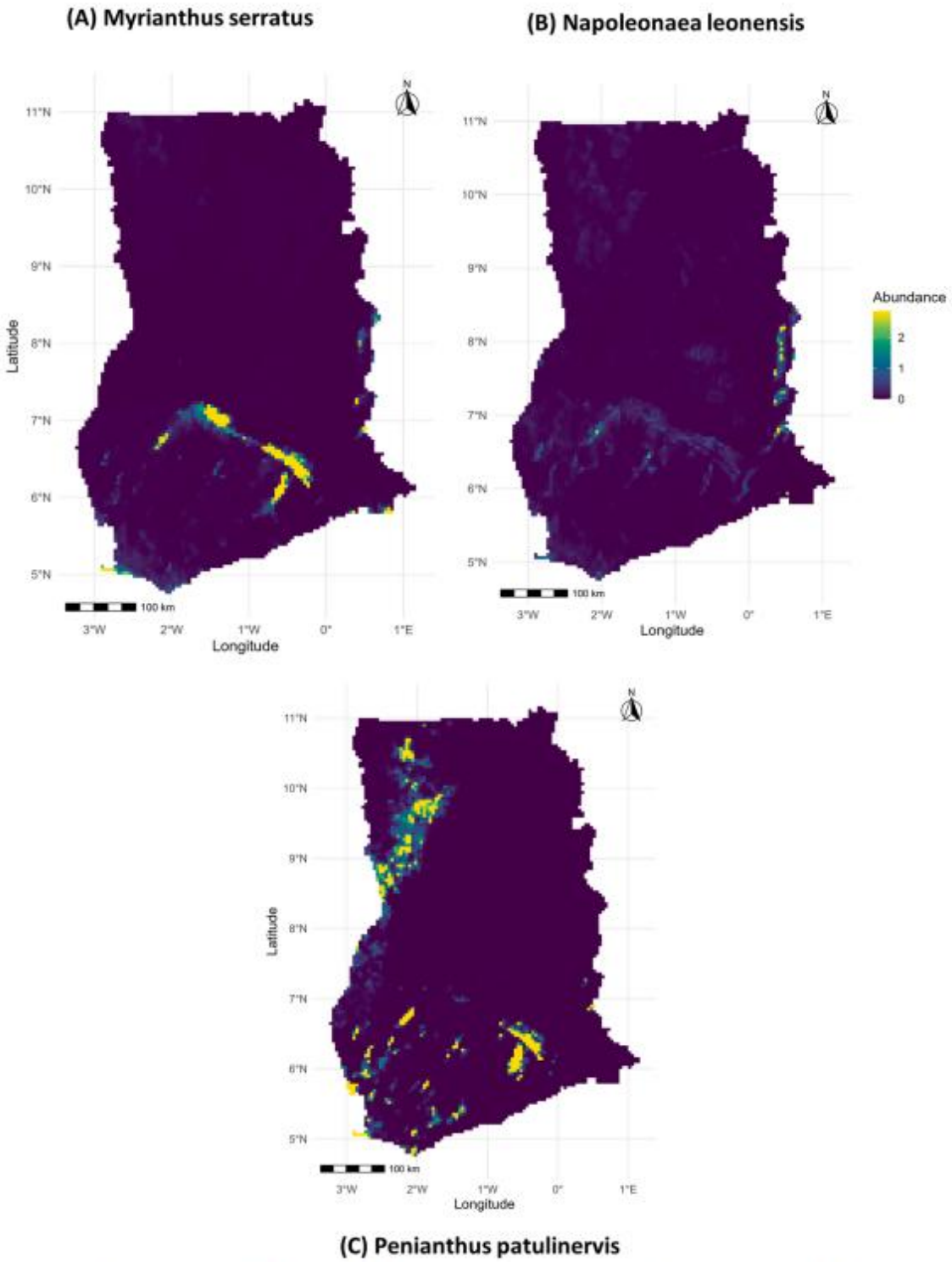

Fig. 7. Predicted abundance maps from zero-inflated Poisson (ZIP) models for Myrianthus serratus (top left), *Napoleonaea leonensis* (top right), and *Penianthus patulinervis* (bottom). Warmer colors indicate a higher predicted abundance.

Table 3
Performance metrics for ZIP abundance models showing Akaike Information Criterion (AIC) and pseudo-R^2 values for each species.

Species	AIC	Pseudo-R^2
Napoleonaea leonensis	484.14	0.273
Myrianthus serratus	335.73	0.475
Penianthus patulinervis	185.87	0.632

showed that forest fragmentation disrupts this buffering effect, increasing temperature extremes at the edges. Similarly, Ismaeel et al. (2024) demonstrated that understory temperatures are significantly cooler and more stable when buffered by the canopy and temperature.

The spatial configuration of habitats is further shaped by topography, which modifies climatic influences and habitat structures at finer scales. Topography, measured as slope, was informative for *Myrianthus serratus* and *Penianthus patulinervis*. Similar to findings from West and Central Africa, this reflects how topographic heterogeneity structures species composition by influencing drainage patterns, soil depth, and microclimatic stability, while also providing sheltered areas that protect species from environmental disturbances (Addo-Fordjour et al., 2022). In Ghana, slope interacts with forest-use and logging history to shape community composition, further explaining its predictive value (Duah-Gyamfi et al., 2014). These topographic gradients are linked to edaphic variations, which also account for why soil properties, particularly soil texture, have emerged as significant predictors of species distribution. They regulate rooting conditions, water retention, and nutrient availability, directly constraining species' realized niches (Fayolle et al., 2012). The importance of soil texture across species corroborates the findings of Eiserhardt et al. (2011), who showed that integrating geological and soil data into SDMs improves model realism, particularly in heterogeneous tropical landscapes.

4.3. Abundance patterns and model uncertainty

Spatial abundance predictions highlighted a pronounced concentration of high-abundance areas in the southern forest zone, particularly in protected forest reserves and moist evergreen belts. This pattern is consistent with the role of intact canopy cover and reduced anthropogenic disturbance in sustaining mature forest tree populations (Laurance

Table 4
Summary of mean and maximum species richness inside and outside Ghana's protected areas.

Metric	Value
Mean richness in protected areas	0.102
Mean richness outside protected areas	0.019
Maximum richness in protected areas	3.000
Maximum richness outside protected areas	2.000

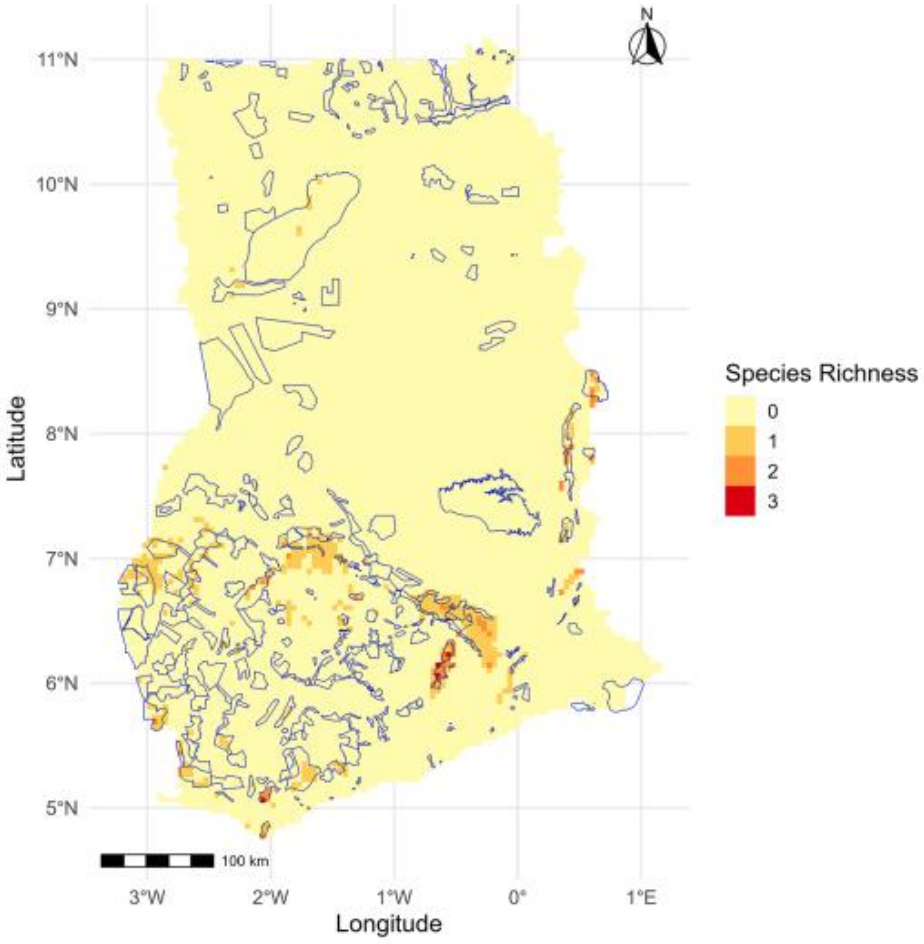

Fig. 8. Predicted species richness with PA boundaries.

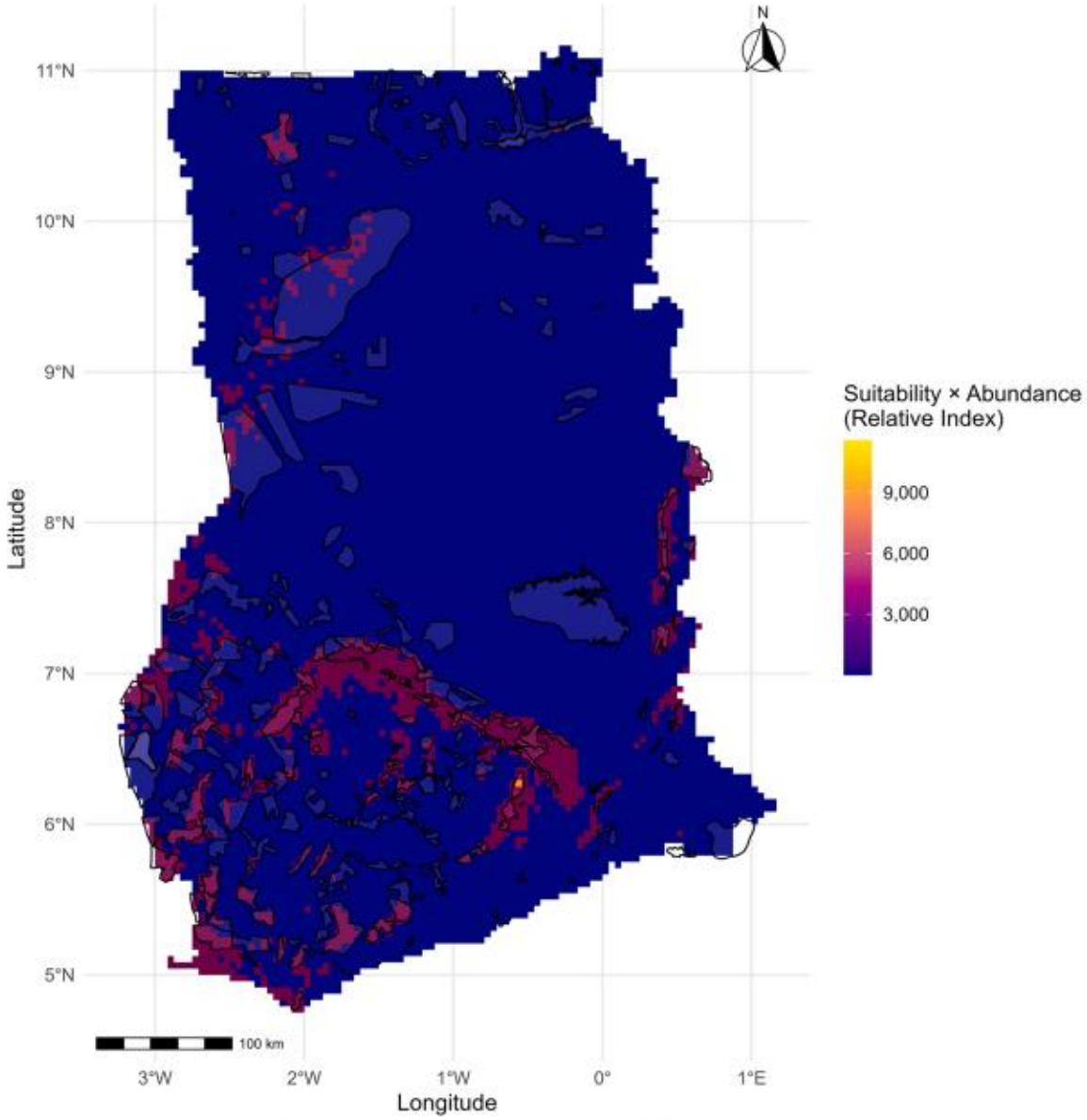

Fig. 9. Composite priority areas in Ghana based on predicted habitat suitability and estimated abundance of target species. Warmer colors indicate higher priority scores, and black outlines represent existing protected areas.

Table 5
Summary of hotspot area coverage within Ghana, showing the total extent, area within protected areas, and percentage protected.

Metric	Value
Total hotspot area (ha)	23,536,682
Hotspot area in protected areas (ha)	6,984,6670
Percentage of protected areas (%)	30

et al., 2011). In contrast, the predicted abundance was lower in fragmented or transitional forest zones, likely due to increased logging activities, agricultural conversion, and microclimatic stress (Lewis et al., 2015). In assessing the performance of abundance prediction, uncertainty analysis based on the coefficient of variation from cross-validation predictions revealed spatially structured model uncertainty. Low uncertainty values occurred in areas with dense sampling and stronger environmental predictors, whereas higher uncertainty was concentrated in regions with sparse plot coverage. This spatial pattern is typical for species abundance estimates, where extrapolating poorly sampled environmental space increases predictive variability (Wenger and Olden, 2012). From a conservation perspective, there is a need to prioritize plot surveys or sample data in high-uncertainty zones to refine abundance models, particularly where these areas overlap with potential biodiversity hotspots. For example, areas around the northern parts of the predicted suitable habitat for *Myrianthus serratus* and *Napoleonaea leonensis* fall within highly uncertain areas, meaning that management decisions there would benefit from targeted ecological verification.

4.4. Species richness and representation in protected areas

Species richness patterns showed a south-to-north decline, with the richest sites concentrated in the moist evergreen and semi-deciduous forest zones of southern Ghana. Peak richness occurred in the Atewa

Range, Neung South, and Boin River forest reserves, which are recognized as biodiversity hotspots due to their unique geology, intact canopy, and high floristic coverage (Pooter et al., 2015). Other reserves such as the Asukoko River, Bobiri, Togo Plateau, Jama Asemkrom, and Cape Three Points supported two of the three species, often in association with heterogeneous terrain and riparian habitats that sustain microclimatic stability. Analysis of richness in Ghana's protected area network showed that protected areas had significantly higher richness than unprotected areas. This is consistent with global evidence that PAs, particularly forest reserves, act as refugia for biodiversity by maintaining canopy cover, limiting disturbance, and protecting key ecological gradients (Geldmann et al., 2013).

While the richest zones, such as the Atewa Range, Neung South, Boin River, and Bobiri, are formally protected, several moderately rich areas lie outside the PA zones, including transitional forest zones and unprotected riparian corridors. Such regions could provide critical connectivity for species movement under climate change, a gap also observed globally in tropical PA networks (Watson et al., 2014).

4.5. Implication for forest biodiversity management

The integration of habitat suitability, abundance, and richness, as well as conservation priority analysis (composite index), provides a clear basis for strategic biodiversity management in Ghana's forests. Priority should be given to protecting areas where intact canopies, favorable topography, and optimal climatic conditions overlap, as these locations are likely to serve as strongholds for multiple forest species under current and future climates. Expanding protection to unreserved high-richness hotspots and improving connectivity between fragmented habitats are critical for maintaining ecological processes and species persistence. Management should also incorporate adaptive monitoring, focusing field verification on abundance hotspots with high uncertainty, and ensuring that robust, spatially explicit data guides conservation investments. Approaches such as community-managed forests, restoration of degraded corridors, and integration of biodiversity priorities into land-use planning can help bridge the existing protection gaps. In doing so, conservation strategies will be better positioned to safeguard forest biodiversity against ongoing anthropogenic pressures and climate-driven range shifts.

5. Conclusions

This study demonstrates the importance of applying SDMs to ecologically dominant tree species in Ghana's tropical forests, where tree species-focused modeling studies have been primarily limited. By integrating habitat suitability, abundance estimation, and multi-species richness into a unified framework, we provide nationwide maps for three representative species: *Napoleonaea leonensis*, *Myrianthus serratus*, and *Penianthus patulinervis*. These findings underscore three key contributions. First, they address the longstanding taxonomic imbalance in West African conservation planning by shifting the focus from fauna to flora, thereby emphasizing the foundational role of tree communities in sustaining ecosystem functions. Second, they advanced SDM methodology by combining presence-only suitability predictions with abundance and richness analysis, generating more ecologically realistic and management-relevant insights. Finally, by overlaying modeled distributions with protected area boundaries, this study provides an evidence-based assessment of Ghana's conservation effectiveness, identifying landscapes where biodiversity is at the most significant risk of under-representation. Beyond Ghana, the methodological framework presented offers a transferable approach that can be adapted to other tropical regions facing similar challenges of biodiversity loss, data scarcity, and conservation trade-offs. This contributes to local forest management and global debates on biodiversity conservation and climate change mitigation.

While this study advances tree-focused SDM applications, some limitations remain. Data availability for rare or less-studied species continues to constrain model accuracy, whereas the challenge of capturing fine-scale ecological processes and disturbances reduces the predictive precision. Additionally, this study relied primarily on occurrence records from the GBIF, which, although valuable, reflect data collected over varying periods and spatial intensities. Future work should prioritize conducting current field sampling of presence data and complementing it with remote-sensing products and long-term ecological data monitoring to improve model robustness and environmental realism.

Ultimately, this study highlights the urgency and opportunity to incorporate tree species into biodiversity assessments. Strengthening such approaches is essential if tropical forests are to maintain resilient ecosystems that sustain biodiversity, mitigate climate change, and support human well-being in the future.

Funding sources

This research was funded by the Faculty of Forestry and Wood Sciences—FFWS, Czech University of Life Sciences Prague, (IGA/FLD/A_11_23 (grant number: 43140/1312/3189 and grant FORESTin3D) and supported by project TH74010001, funded by the Technological Agency of the Czech Republic through the program Chist-era.

Declaration of generative AI and AI-assisted technologies in the writing process

During the preparation of this work, the authors used GPT-5 to improve the style and grammar of several paragraphs in the text. After using this tool, the authors reviewed and edited the content as needed and take full responsibility for the content of the publication.

CRediT authorship contribution statement

Elisha Njomaba: Writing – review & editing, Writing – original draft, Visualization, Validation, Software, Resources, Project administration, Methodology, Investigation, Formal analysis, Data curation, Conceptualization. **Ben Emunah Aikins:** Investigation, Methodology, Software, Writing – original draft, Writing – review & editing. **Peter Surovy:** Writing – review & editing, Supervision, Resources, Funding acquisition, Conceptualization.

Declaration of competing interest

The authors declare that they have no known competing financial interests or personal relationships that could have appeared to influence the work reported in this paper.

Acknowledgments

Many thanks to the co-authors and supervisor for their insights and contributions to the production of this research.

Supplementary materials

Supplementary material associated with this article can be found, in the online version, at doi:10.1016/j.tfp.2025.101019.

Data availability

Data will be made available on request.

References

Abuhay, Z.T., Ali, A.M., Atickem, A., Zinner, D., 2025. Modeling of past, current and future distribution of suitable habitat for Menelik's bushbuck (Tragelaphus

sylvaticus meneliki Neumann, 1902) in the Ethiopian highlands. BMC Ecol. Evol. 25. https://doi.org/10.1186/s12862-025-02367-x.
Acheampong, E.O., Macgregor, C.J., Sloan, S., Sayer, J., 2019. Deforestation is driven by agricultural expansion in Ghana's forest reserves. Sci. African 5. https://doi.org/10.1016/j.sciaf.2019.e00146.
Addo-Fordjour, P., Afram, I.S., Oppong, J., 2022. Selective and clear-cut logging have varied imprints on tree community structure in a moist semi-deciduous forest in Ghana. Heliyon 8, e11393. https://doi.org/10.1016/j.heliyon.2022.e11393.
Aiello-Lammens, M.E., Boria, R.A., Radosavljevic, A., Vilela, B., Anderson, R.P., 2015. spThin: an R package for spatial thinning of species occurrence records for use in ecological niche models. Ecography (Cop.) 38, 541–545. https://doi.org/10.1111/ecog.01132.
Allouche, O., Tsoar, A., Kadmon, R., 2006. Assessing the accuracy of species distribution models: prevalence, kappa and the true skill statistic (TSS). J. Appl. Ecol. 43, 1223–1232. https://doi.org/10.1111/j.1365-2664.2006.01214.x.
Amissah, L., Godefridus, M.J.M., Frans, B., William, D.H., Lourens, P., 2014. Rainfall and temperature affect tree species distribution in Ghana. J. Trop. Ecol. 30.
Armah, F.A., Odoi, J.O., Yengoh, G.T., Obiri, S., Yawson, D.O., Afrifa, E.K.A., 2011. Food security and climate change in drought-sensitive savanna zones of Ghana. Mitig. Adapt. Strateg. Glob. Chang. 16, 291–306. https://doi.org/10.1007/s11027-010-9263-9.
Asare, 2021. Plants of Ghana. Version 1.1 [WWW Document]. Ghana Herb. Occur. https://doi.org/10.15468/e8rhqm dataset. URL.
Beck, J., Böller, M., Erhardt, A., Schwanghart, W., 2014. Spatial bias in the GBIF database and its effect on modeling species' geographic distributions. Ecol. Inform. 19, 10–15. https://doi.org/10.1016/j.ecoinf.2013.11.002.
Campbell, M.O.N., 2005. Sacred groves for forest conservation in Ghana's coastal savannas: assessing ecological and social dimensions. Singap. J. Trop. Geogr. 26, 151–169. https://doi.org/10.1111/j.0129-7619.2005.00211.x.
Chave, J., Condit, R., Lao, S., Caspersen, J.P., Foster, R.B., Hubbell, S.P., 2003. Spatial and temporal variation of biomass in a tropical forest: results from a large census plot in Panama. J. Ecol. 91, 240–252. https://doi.org/10.1046/j.1365-2745.2003.00757.x.
Chazdon, R.L., 2008. Beyond deforestation: restoring forests and ecosystem services on degraded lands. Science (80-.) 320, 1458–1460. https://doi.org/10.1126/science.1155365.
Cuni-sanchez, A., Hubau, W., Abiem, I., Adhikari, H., Albrecht, T., Altman, J., 2021. High aboveground carbon stock of African tropical montane forests. Nature 596.
Dormann, C., Oliver, P., Jaime, M., Sven, L., Boris, S., 2008. Components of uncertainty in species distribution analysis: a case study of the Great Grey Shrike. Ecology 89.
Dormann, C.F., Elith, J., Bacher, S., Buchmann, C., Carl, G., Carré, G., Marquéz, J.R.G., Gruber, B., Lafourcade, B., Leitão, P.J., Münkemüller, T., Mcclean, C., Osborne, P.E., Reineking, B., Schröder, B., Skidmore, A.K., Zurell, D., Lautenbach, S., 2013. Collinearity: a review of methods to deal with it and a simulation study evaluating their performance. Ecography (Cop.) 36, 27–46. https://doi.org/10.1111/j.1600-0587.2012.07348.x.
Duah-Gyamfi, A., Kyereh, B., Adam, K.A., Agyeman, V.K., Swaine, M.D., 2014. Natural regeneration dynamics of tree seedlings on skid trails and tree gaps following selective logging in a tropical moist semi-deciduous forest in Ghana. Open J. For. 04, 49–57. https://doi.org/10.4236/ojf.2014.41009.
Eiserhardt, W.L., Jens-Christian, S., Kissling, D., Henrik, B., 2011. Geographical ecology of the palms (Arecaceae): determinants of diversity and distributions across spatial scale. Ann. Bot. 108.
Elith, J., Leathwick, J.R., 2009. Species distribution models: ecological explanation and prediction across space and time. Annu. Rev. Ecol. Evol. Syst. 40, 677–697. https://doi.org/10.1146/annurev.ecolsys.110308.120159.
Ewers, R.M., Banks-Leite, C., 2013. Fragmentation impairs the microclimate buffering effect of tropical forests. PLoS One 8. https://doi.org/10.1371/journal.pone.0058093.
FAO, 2020. Global Forest Resources Assessment 2020: main report [WWW Document]. Food Agric. Organ. United Nations. https://doi.org/10.4060/ca9825en. URL (accessed 8.16.25).
Fayolle, A., Engelbrecht, B., Freycon, V., Mortier, F., Swaine, M., Réjou-Méchain, M., Doucet, J.L., Fauvet, N., Cornu, G., Gourlet-Fleury, S., 2012. Geological substrates shape tree species and trait distributions in African moist forests. PLoS One 7, 12–14. https://doi.org/10.1371/journal.pone.0042381.
Fick, S.E., Hijmans, R.J., 2017. WorldClim 2: new 1-km spatial resolution climate surfaces for global land areas. Int. J. Climatol. 37, 4302–4315. https://doi.org/10.1002/joc.5086.
Foley, J.A., DeFries, R., Asner, G.P., Barford, C., Bonan, G., Carpenter, S.R., Chapin, F.S., Coe, M.T., Daily, G.C., Gibbs, H.K., Helkowski, J.H., Holloway, T., Howard, E.A., Kucharik, C.J., Monfreda, C., Patz, J.A., Prentice, I.C., Ramankutty, N., Snyder, P.K., 2005. Global consequences of land use. Science (80-.) 309, 570–574. https://doi.org/10.1126/science.1111772.
Freeman, B., Sunnarborg, J., Peterson, A.T., 2019. Effects of climate change on the distributional potential of three range-restricted West African bird species. Condor 121, 1–10. https://doi.org/10.1093/condor/duz012.
Freeman, E.A., Moisen, G.G., 2008. A comparison of the performance of threshold criteria for binary classification in terms of predicted prevalence and kappa. Ecol. Modell. 217, 48–58. https://doi.org/10.1016/j.ecolmodel.2008.05.015.
Geldmann, J., Barnes, M., Coad, L., Craigie, I.D., Hockings, M., Burgess, N.D., 2013. Effectiveness of terrestrial protected areas in reducing habitat loss and population declines. Biol. Conserv. 161, 230–238. https://doi.org/10.1016/j.biocon.2013.02.018.
Ghana Statistical Services, 2021. Ghana—Population and Housing Census 2021. Summary of final report [WWW Document]. Ghana Stat. Serv. URL https://census2021.statsghana.gov.gh/.
Giam, X., 2017. Global biodiversity loss from tropical deforestation. Proc. Natl. Acad. Sci. U.S.A. 114, 5775–5777. https://doi.org/10.1073/pnas.1706264114.
Grime, J., 1998. Benefits of plant diversity to ecosystems: immediate, filter and founder effects. J. Ecol. 86, 902–910.
Guisan, A., Wilfried, T., Niklaus, Z., 2017. Habitat Suitability and Distribution Models. Cambridge University Press.
Guisan, A., Zimmermann, N.E., 2000. Predictive habitat distribution models in ecology. Ecol. Modell. 135, 147–186. https://doi.org/10.1016/S0304-3800(00)00354-9.
Hall, J., Swaine, M., 1981. Distribution and Ecology of Vascular Plants in a Tropical Rain Forest. Springer, Dordrecht. https://doi.org/10.1007/978-94-009-8650-3.
Hawthorn, W., Jongkind, C.C., 2006. Woody plants of the Western African forest A guide to the forest trees, shrubs and lianes from Senegal to Ghana. Biosystematics.
Hijmans, R.J., Cameron, S.E., Parra, J.L., Jones, P.G., Jarvis, A., 2005. Very high resolution interpolated climate surfaces for global land areas. Int. J. Climatol. 25, 1965–1978. https://doi.org/10.1002/joc.1276.
Hutchinson, D., 1928. International Plant Names Index [WWW Document]. Flora West Trop. Africa. URL https://www.ipni.org/n/urn:lsid:ipni.org:names:469472-1.
Ismaeel, A., Tai, A.P.K., Santos, E.G., Maraia, H., Aalto, I., Altman, J., Doležal, J., Lembrechts, J.J., Camargo, J.L., Aalto, J., Sam, K., Avelino do Nascimento, L.C., Kopecký, M., Svátek, M., Nunes, M.H., Matula, R., Plichta, R., Abera, T., Maeda, E.E., 2024. Patterns of tropical forest understory temperatures. Nat. Commun. 15, 1–10. https://doi.org/10.1038/s41467-024-44734-0.
Joppa, L.N., Pfaff, A., 2009. High and far: biases in the location of protected areas. PLoS One 4, 1–6. https://doi.org/10.1371/journal.pone.0008273.
Jorge, L., Alberto, J.-V., Raimundo, R., 2007. AUC: a misleading measure of the performance of predictive distribution models. Glob. Ecol. Biogeogr. 17, 145–151.
Kusi, K.K., 2025. Trees outside forests in Ghana: current state, spatial distribution, and future projection. Front. For. Glob. Chang. 8, 1–15. https://doi.org/10.3389/ffgc.2025.1540910.
Laurance, W.F., Camargo, J.L.C., Luizão, R.C.C., Laurance, S.G., Pimm, S.L., Bruna, E.M., Stouffer, P.C., Bruce Williamson, G., Benítez-Malvido, J., Vasconcelos, H.L., Van Houtan, K.S., Zartman, C.E., Boyle, S.A., Didham, R.K., Andrade, A., Lovejoy, T.E., 2011. The fate of Amazonian forest fragments: a 32-year investigation. Biol. Conserv. 144, 56–67. https://doi.org/10.1016/j.biocon.2010.09.021.
Lewis, S.L., Edwards, D.P., Galbraith, D., 2015. Increasing human dominance of tropical forests. Science (80-.) 349, 827–832. https://doi.org/10.1126/science.aaa9932.
Liu, C., Newell, G., White, M., 2016. Selection thresholds for predicting species occurrence with presence-only data. J. Biogeogr. 43, 778–789. https://doi.org/10.1002/ece3.1878.
Magurran, A., McGill, B., 2011. Biological Diversity: Frontiers in Measurement and Assessment. Oxford University Press, Oxford.
Marshall, C.A.M., Wieringa, J.J., Hawthorne, W.D., 2021. An interpolated biogeographical framework for tropical Africa using plant species distributions and the physical environment. J. Biogeogr. 48, 23–36. https://doi.org/10.1111/jbi.13976.
Merow, C., Smith, M.J., Silander, J.A., 2013. A practical guide to MaxEnt for modeling species' distributions: what it does, and why inputs and settings matter. Ecography (Cop.) 36, 1058–1069. https://doi.org/10.1111/j.1600-0587.2013.07872.x.
Mkala, E.M., Mwanzia, V., Nzei, J., Oluoch, W.A., Ngarega, B.K., Wanga, V.O., Oulo, M. A., Munyao, F., Kilingo, F.M., Rono, P., Waswa, E.N., Mutinda, E.S., Ochieng, C.O., Mwachala, G., Hu, G.W., Wang, Q.F., Katunge, J.K., Victoire, C.I., 2023. Predicting the potential impacts of climate change on the endangered endemic annonaceae species in east africa. Heliyon 9, e17405. https://doi.org/10.1016/j.heliyon.2023.e17405.
Myers, N., Mittermeier, R.A., Mittermeier, C.G., da Fonseca, G.A.B., Kent, J., 2000. Biodiversity hotspots for conservation priorities. Nature 403, 853–858. https://doi.org/10.1038/35002501.
Njomaba, E., Mushtaq, F., Nagbija, R.K., Yakalim, S., Aikins, B.E., Surovy, P., 2025. Adopting land cover standards for sustainable development in Ghana: challenges and opportunities. Land 14, 550. https://doi.org/10.3390/land14030550.
Oates, J.F., Abedi-Lartey, M., McGraw, W.S., Struhsaker, T.T., Whitesides, G.H., 2000. Extinction of a West African red colobus monkey. Conserv. Biol. 14, 1526–1532. https://doi.org/10.1046/j.1523-1739.2000.99230.x.
Oliver, T.H., Heard, M.S., Isaac, N.J.B., Roy, D.B., Procter, D., Eigenbrod, F., Freckleton, R., Hector, A., Orme, C.D.L., Petchey, O.L., Proença, V., Raffaelli, D., Suttle, K.B., Mace, G.M., Martín-López, B., Woodcock, B.A., Bullock, J.M., 2015. Biodiversity and resilience of ecosystem functions. Trends Ecol. Evol. 30, 673–684. https://doi.org/10.1016/j.tree.2015.08.009.
Pearson, R., Dawson, T., Liu, C., 2004. Modeling species distributions in Britain: a hierarchical integration of climate and land-cover data. Ecography (Cop.) 287, 285–298.
Phillips, S.B., Aneja, V.P., Kang, D., Arya, S.P., 2006. Maximum entropy modeling of species geographic distributions. Ecol. Modell. 190, 231–259. https://doi.org/10.1016/j.ecolmodel.2005.03.026.
Poorter, L., van der Sande, M.T., Thompson, J., Arets, E.J.M.M., Alarcón, A., Álvarez-Sánchez, J., Ascarrunz, N., Balvanera, P., Barajas-Guzmán, G., Boit, A., Bongers, F., Carvalho, F.A., Casanoves, F., Cornejo-Tenorio, G., Costa, F.R.C., de Castilho, C.V., Duivenvoorden, J.F., Dutrieux, L.P., Enquist, B.J., Fernández-Méndez, F., Finegan, B., Gormley, L.H.L., Healey, J.R., Hoosbeek, M.R., Ibarra-Manríquez, G., Junqueira, A.B., Levis, C., Licona, J.C., Lisboa, L.S., Magnusson, W.E., Martínez-Ramos, M., Martínez-Yrizar, A., Martorano, L.G., Maskell, L.C., Mazzei, L., Meave, J. A., Mora, F., Muñoz, R., Nytch, C., Pansonato, M.P., Parr, T.W., Paz, H., Pérez-García, E.A., Rentería, L.Y., Rodríguez-Velazquez, J., Rozendaal, D.M.A., Ruschel, A.

R., Sakschewski, B., Salgado-Negret, B., Schietti, J., Simões, M., Sinclair, F.L., Souza, P.F., Souza, F.C., Stropp, J., ter Steege, H., Swenson, N.G., Thonicke, K., Toledo, M., Uriarte, M., van der Hout, P., Walker, P., Zamora, N., Peña-Claros, M., 2015. Diversity enhances carbon storage in tropical forests. Glob. Ecol. Biogeogr. 24, 1314–1328. https://doi.org/10.1111/geb.12364.

Pooter, L., Sande, V., Thompso, E., Alarcon, A., Alvarez-Sanchez, J., Ascarrunz, N., Balvanera, P., Baraja-Guzman, G., Bongers, F., Carvalho, F.…., 2015. Diversity enhances carbon storage in tropical forests. Glob. Ecol. Biogeogr. 24.

Qazi, A.W., Saqib, Z., Zaman-ul-Haq, M., 2022. Trends in species distribution modeling in context of rare and endemic plants: a systematic review. Ecol. Process. 11. https://doi.org/10.1186/s13717-022-00384-y.

Roberts, D.R., Bahn, V., Ciuti, S., Boyce, M.S., Elith, J., Guillera-Arroita, G., Hauenstein, S., Lahoz-Monfort, J.J., Schröder, B., Thuiller, W., Warton, D.I., Wintle, B.A., Hartig, F., Dormann, C.F., 2017. Cross-validation strategies for data with temporal, spatial, hierarchical, or phylogenetic structure. Ecography (Cop.) 40, 913–929. https://doi.org/10.1111/ecog.02881.

Schupp, E.W., Jordano, P., Gómez, J.M., 2010. Seed dispersal effectiveness revisited: a conceptual review. New Phytol. 188, 333–353. https://doi.org/10.1111/j.1469-8137.2010.03402.x.

Valladares, F., Matesanz, S., Guilhaumon, F., Araújo, M.B., Balaguer, L., Benito-Garzón, M., Cornwell, W., Gianoli, E., van Kleunen, M., Naya, D.E., Nicotra, A.B., Poorter, H., Zavala, M.A., 2014. The effects of phenotypic plasticity and local adaptation on forecasts of species range shifts under climate change. Ecol. Lett. 17, 1351–1364. https://doi.org/10.1111/ele.12348.

Vancutsem, C., Achard, F., Pekel, J.F., Vieilledent, G., Carboni, S., Simonetti, D., Gallego, J., Aragão, L.E.O.C., Nasi, R., 2021. Long-term (1990–2019) monitoring of forest cover changes in the humid tropics. Sci. Adv. 7, 1–21. https://doi.org/10.1126/sciadv.abe1603.

Wagner, M.R., Cobbinah, J.R., 1993. Deforestation and sustainability in Ghana: the role of tropical forests. 91, 35–39.

Watson, J., Dudley, N., Segan, D., Hockings, M., 2014. The performance and potential of protected areas. Nature 515, 67–73.

Wenger, S.J., Olden, J.D., 2012. Assessing transferability of ecological models: an underappreciated aspect of statistical validation. Methods Ecol. Evol. 3, 260–267. https://doi.org/10.1111/j.2041-210X.2011.00170.x.

Wilson, J.W., Sexton, J.O., Todd Jobe, R., Haddad, N.M., 2013. The relative contribution of terrain, land cover, and vegetation structure indices to species distribution models. Biol. Conserv. 164, 170–176. https://doi.org/10.1016/j.biocon.2013.04.021.

Zhao, Q., Li, H., Chen, C., Fan, S., Wei, J., Cai, B., Zhang, H., 2024. Climate change conditions. Using MaxEnt. Insects 15, 1–16.

Zizka, A., Silvestro, D., Vitt, P., Knight, T.M., 2021. Automated conservation assessment of the orchid family with deep learning. Conserv. Biol. 35, 897–908. https://doi.org/10.1111/cobi.13616.

Zuur, A.F., Ieno, E.N., Walker, N.J., Saveliev, A.A., Smith, G.M., 2009. Reviewer: aaron Christ Alaska Department of Fish and Game Mixed Effects models and extensions in ecology with R. JSS J. Stat. Softw. 32, 2–4.

4.4. Effects of climate change on above-ground biomass modulated by forest fragmentation and biodiversity in Ghana.

Elisha Njomaba[1], Ben Emunah Aikins[2], Peter Surový[1]

[1]Faculty of Forestry and Wood Science, Czech University of Life Sciences (CZU Prague), Kamýcká 129,165 21 Prague, Czech Republic.

[2]School of Public Health, College of Health Sciences, University of Ghana, Accra, P.O. Box LG 13, Ghana.

Corresponding Author

njomaba@fld.czu.cz

Author´s contribution: 80 %

Summary of the article

This article examines the interactive effects of climate change (AI), AGB, with forest fragmentation and biodiversity as mediating factors, across Ghana's ecological zones. Using GBIF's tree occurrence records, satellite-derived biomass data, and fragmentation metrics, the study applied SEMs to explore the direct and indirect effects of AI on AGB mediated through fragmentation and biodiversity, and GAMs to explore the functional form of fragmentation and biodiversity effects on AGB. Results showed that the aridity index (AI) had a strong direct effect on AGB, and an indirect effect mediated by increasing fragmentation. SEMs showed that decreasing AI (drier conditions) was associated with greater fragmentation and reduced biomass. Biodiversity (as measured by species richness) had no significant influence on AGB. Among fragmentation metrics, mean patch area (AREA_MN) had the largest influence on AGB, followed by edge density (ED), and landscape shape index (LSI); mean shape index (MSI) and number of patches (NP) were the weakest predictors. Nonlinear SEMs and GAMs further revealed threshold and unimodal responses. Biomass peaked at intermediate patch sizes but declined in highly fragmented landscapes with excessive patch density. These effects highlight the existence of ecological thresholds beyond which fragmentation strongly accelerates biomass loss. Overall, the results demonstrate that aridity, fragmentation, and limited biodiversity affect carbon storage, with dry and transitional forests emerging as the most vulnerable to climate stress and fragmentation.

Full article

Effect of Climate Change on Above-Ground Biomass, Modulated by Forest Fragmentation and Biodiversity in Ghana.

Elisha Njomaba[1]*, Ben Emunah Aikins[2], Peter Surovy[1]

[1*]Faculty of Forestry and Wood Sciences, Czech University of Life Sciences Prague, Kamýcká 129, 165 00 Prague, Czech Republic; njomaba@fld.czu.cz, (ORCID ID: 0000-0002-2165-9272)

[2]School of Public Health, College of Health Sciences, University of Ghana, Accra, Ghana, Box LG 13, Ghana, benaikins56@gmail.com.

Corresponding author: Elisha Njomaba

0. Abstract

Forests play a vital role in the global carbon cycle but face growing anthropogenic pressures, with climate change and forest fragmentation among the most critical. In West Africa, particularly in Ghana, the interaction between increasing aridity and forest fragmentation remains underexplored, despite its significance for forest biomass dynamics and carbon storage processes. This study examined the effect of climate-driven aridification on above-ground biomass (AGB) in Ghana's ecological zones, both directly and indirectly through forest fragmentation and biodiversity, using structural equation modeling (SEM) and generalized additive models (GAMs). Results from this study show that AGB declines along the aridity gradient, with humid zones supporting the highest biomass and semi-arid zones the lowest. The SEM analysis revealed that areas with a lower aridity index (drier conditions) had significantly lower AGB, indicating that aridification reduces forest biomass. Fragmentation indirectly mediated this effect, while biodiversity (as measured by species richness) showed no significant influence. GAMs highlighted nonlinear fragmentation effects: mean patch area (AREA_MN) was the strongest predictor, showing a unimodal relationship with biomass, whereas number of patches (NP), edge density (ED), and landscape shape index (LSI) reduced AGB. Overall, these findings demonstrate that aridity and spatial configuration jointly control biomass, with fragmentation acting as a key mediator of this relationship. Dry and transitional forests emerge as particularly vulnerable, emphasizing the need for management strategies that maintain large, connected forest patches and integrate restoration into climate adaptation policies.

Keywords: Above-ground biomass; Forest fragmentation; Tropical forest; Remote sensing; Climate change; Aridity index.

1. Introduction

Tropical forest ecosystems play a crucial role in regulating the global climate system, acting as significant carbon sinks while supporting biodiversity and maintaining ecosystem functions [1-2]. Among their many ecological contributions, the capacity to store carbon in AGB is critical to mitigating climate change and maintaining ecosystem functions [3]. However, these forests are increasingly threatened by two global drivers: land-use change and climatic variability, which lead to significant changes in biomass dynamics globally [4-5]. In Ghana, these pressures have led to forest degradation, deforestation, and increased fragmentation of forest landscapes [6-7], with a profound impact on woody biomass. Forest fragmentation, a key driver of woody biomass changes, refers to the division of forest landscapes into smaller, isolated patches, decreasing the natural habitat in the landscape [8]. Forest fragmentation results in reduced patch size, increased edge effects, and the isolation of forest fragments, altering microclimatic conditions and disrupting ecological processes, such as species dispersal, gene flow, and nutrient cycling [9-10]. These changes can reduce species richness, alter forest structure, and ultimately diminish. Biodiversity plays a critical role in supporting biomass production, as communities of diverse species can enhance resource-use efficiency, stabilize productivity, and increase resilience to environmental stressors [11]. Thus, biodiversity loss resulting from fragmentation may compound the decline in AGB. Quantifying fragmentation is essential for understanding how landscape structure influences carbon storage dynamics and processes [12]. Most of the fragmentation metrics are strongly correlated, making them redundant if all are chosen for a particular analysis. Selecting a relevant subset from the numerous available metrics can be a challenging task. According to Turner [13], fragmentation metrics must be selected to achieve specific objectives, minimize redundancy, explain pattern variability across the landscape, and encompass a substantial portion of their potential value range. According to Flowers et al. [14], when using fragmentation metrics to quantify landscape structure in forest ecosystems, it is recommended to select metrics that capture the characteristics of the landscape area, edge effects, and shape complexity. Alongside fragmentation, climate change, particularly the decrease in aridity (aridification) and variability in rainfall, has emerged as a critical driver of tropical forest dynamics [15]. Conversion of forests, coupled with climate stress, intensifies fragmentation, reduces biodiversity, and ultimately lowers AGB.

Despite extensive studies on the drivers of AGB in tropical forests in West Africa and Ghana, some critical gaps still remain in literature. Most studies have investigated the direct effects of climate change or forest fragmentation on AGB in isolation, often without considering the interactive effects of these two drivers [16-17]. For example, assessing climate change impacts typically focuses on temperature or precipitation anomalies and their effects on tree growth and mortality [18-19] while those assessing fragmentation tend to concentrate on landscape structural attributes quantified by spatial configuration metrics, such as patch size, edge effects, and landscape connectivity, without considering climatic gradients [10]. This singular approach limits our understanding of how combined environmental conditions jointly influence forest carbon dynamics. In Ghana, existing studies have focused primarily on carbon stock estimation and deforestation monitoring [7-15], with a limited focus on how climate stress, such as humidification or aridification, interacts with fragmentation and biodiversity to influence AGB. Several regional studies, primarily conducted in Ghana, have documented relationships between disturbance, biodiversity, and biomass. For example, Oduro et al. [20] and Addo-Fordjour et al. [21] documented declines in woody biomass and species richness with increasing forest disturbance, but without modeling fragmentation metrics or climatic gradients. Similarly, Mensah et al. [22] reported that biodiversity has a positive influence on forest productivity in Ghanaian and Ivorian forest reserves; These relationships were explored independently of spatial configurations or aridity. Only a few studies, such as those by Brinck et al. [23] and Chidumayo and Gumbo [24], have suggested that fragmentation mediates climate-biomass relationships in African drylands; however, extensive quantification and modeling remain scarce. Given Ghana's climatic gradient from the humid forest zone in the south to the semi-arid savanna zone in the north, it is essential to integrate both climatic and landscape factors when assessing biomass variation. Although climatic stress (e.g., drought and increased temperature) can directly affect biomass, recent findings suggest that its full impact may be amplified or moderated by the degree of forest fragmentation [25]. Thus, the effects of climate change on woody biomass are likely mediated by landscape structure. Yet, these mediating interactions have rarely been explored. Addressing this gap is critical for informing adaptive forest management and carbon conservation strategies. To address these gaps, this study sought to answer the following research questions:

(1) What are the direct and indirect effects of climate change – Aridity Index (AI) on AGB? We hypothesized that decreasing AI (aridification) directly reduces AGB, with wetter zones (higher AI) maintaining higher mean AGB than drier zones. We further hypothesize that decreasing AI (aridification) indirectly influences AGB through its effects on fragmentation and biodiversity.

(2) How do landscape structural attributes, quantified through fragmentation metrics such as number of patches (NP), edge density (ED), mean patch area (AREA_MN), landscape shape index (LSI), and mean shape index (MSI), influence AGB, and what are their relative contributions? We hypothesized that AGB exhibits nonlinear responses to these structural attributes, with varying contributions across different dimensions of fragmentation. Collectively, these questions aim to elucidate the direct and indirect pathways through which climatic aridity, as represented by AI, and landscape structure shape AGB variation across Ghana's ecological zones.

2. Materials and Methods

2.1. Study Area and Datasets

Ghana is a West African country, bordering Burkina Faso to the north, Togo to the east, Côte d'Ivoire to the west, and the Gulf of Guinea to the south (Figure 1). The geographical coordinates of the country are 7.9465° N and 1.0232° W, and it occupies an area of approximately 238,533 km². Ghana is divided into 16 administrative regions and 261 districts [26]. It has diverse terrain and landscapes, including forests, savannas, mangroves, wetlands, and mountains. Several anthropogenic activities, including agriculture, mining, and logging, have contributed to the degradation of the natural vegetation cover [27]. Almost 15% of its land is protected for conserved species, distinct ecosystems, and ecological processes [28]. The country has a tropical climate, with an average minimum and maximum temperatures of 21 °C and 34.3 °C, respectively [29], and precipitation ranging from 900 to 2000 mm per year, with the highest amounts occurring from April to June in the south and from April to November in the north [30]. This study combined environmental and vegetation variables to assess the relationships between forest fragmentation, biodiversity, and aridity.

2.2 Vegetation data extraction

This study employed a data assembly approach in which tree-level occurrence data were obtained from the Global Biodiversity Information Facility (GBIF) website (https://www.gbif.org/) [31]. GBIF is the world's largest global biodiversity information facility, providing open access to data on all life forms. The network aggregates data from various sources using data standards, including Darwin Core, which forms the bulk of GBIF's species and tree occurrence records. The data also included field notes and supplementary literature. A targeted search for tree occurrences within Ghana on March 8, 2025, retrieved a total of 38,399 records. The data were subjected to stages of quality control procedures. First, records lacking valid geographic coordinates, scientific names, collection years, duplicates, and points falling outside Ghana's geographic boundaries were removed. To eliminate outdated datasets, only occurrences recorded between 2000 and 2011 were retained, resulting in 9,716 valid records. Because GBIF data

are known to exhibit strong spatial clustering around well-surveyed areas and regions of higher accessibility [32], a spatial thinning procedure was applied to reduce sampling bias and residual spatial autocorrelation [33]. All occurrences were projected to UTM Zone 30N (EPSG: 32630), and two thinning radii were implemented to generate datasets ready for analysis at different spatial units: a 500m buffer radius, representing fine-scale vegetation distribution patterns, and a 1.5km buffer radius, representing broader landscape-scale heterogeneity. Within each buffer, duplicate coordinates and multiple occurrences of the same species were merged, and a buffer centroid was retained as the representative point. After thinning, the 500m datasets contained 3,388 records, while the 1.5km dataset contained 2,979 records. To ensure that all tree occurrences represented actual forest tree species, the thinned datasets were subsequently masked using the landcover classification dataset produced by Njomaba et al. [26]. All occurrences falling within landcover classes identified as non-forest were excluded, leaving only points intersecting forest pixels. The final filtered datasets contained 1,211 points for the 500m buffer and 1,067 points for the 1.5km buffers, representing verified forest tree occurrences across Ghana. These were used in subsequent analysis at two spatial levels, representing small and landscape-scale vegetation patterns.

2.2.1 Spatial autocorrelation diagnostics

To evaluate residual spatial structure following the spatial thinning procedure, we conducted empirical variograms and Moran's I correlograms for the GBIF occurrence centroids at 500m and 1.5km spatial data (Figure S1-S2; Table S1). The 500m dataset exhibited a variogram still at ≈ 2.9km and Moran's I = 0.537 ($p = 1.6 \times 10^{-195}$), while the 1.5km dataset leveled at ≈ 3.6km with Moran's I = 0.337 ($p = 2.97 \times 10^{-138}$). Independence ($I \leq 0.05$) was not reached within ≤ 6km and ≤ 10km, respectively, indicating moderate residual autocorrelation but sufficient reduction for modeling. These diagnostics validated the choice of thinning radii for the fine- and landscape-level analyses and guided the inclusion of spatial correlation structures in subsequent models.

2.2.2 Biodiversity metric: species richness

In this study, biodiversity was represented using species richness (*S*), a simple yet widely used computational metric that quantifies the number of unique tree species recorded within a spatial unit. Species richness helps in capturing variations in community composition and is particularly suitable for large-scale biodiversity assessments using occurrence-based data [34]. Tree occurrence records from the cleaned GBIF dataset were first harmonized using the GBIF Backbone Taxonomy through the R package '*taxize*' [35], ensuring that synonyms and spelling variants were consolidated under accepted species names. Non-tree taxa, duplicates, and occurrences with incomplete taxonomic

information were excluded. After cleaning, richness was computed as the number of distinct tree species within each 500m and 1.5km buffer zones, corresponding to the analytical units described in section 2.2. Although biodiversity encompasses both computational and structural components, namely species richness and evenness, the computation of evenness metrics, such as Pielou's *J'*, requires species abundance that is unavailable in GBIF's presence-only data. As noted by Meyer et al. [36] and Beck [32], occurrence databases are biased toward collection frequency and survey effort, making abundance metrics unreliable. Therefore, in this study, species richness was used as a robust proxy for local tree diversity, consistent with large-scale studies that rely on presence-only occurrence data [37-38]. While species richness does not fully capture community evenness, it provides an ecologically meaningful and spatially consistent measure of taxonomic diversity across Ghana's forested landscapes.

2.3. Above-ground biomass (AGB) dataset and extraction

The AGB data were derived from the European Space Agency (ESA) Climate Change Initiative (CCI) global AGB product (version 5.0.1; [39]). This dataset provides annual estimates of woody AGB (Mg ha^{-1}) at 100m resolution for multiple years (2010 – 2020), representing oven-dry woody mass of all living trees (stems, branches, twigs, and bark), excluding roots and stumps.

Raster layers from 2017 and 2020 were subset to Ghana's national boundary and resampled to match the analytical grids defined by the 500m and 1.5km GBIF buffer centroids. (section 2.2). Mean AGB and within-buffer standard deviations (SD) were extracted for each circular buffer, ensuring alignment with spatial predictors (aridity, fragmentation, and biodiversity).

To evaluate the temporal consistency and reliability of the ESA AGB layers, the 2017 and 2020 AGB layers were compared across both spatial resolutions. There is an excellent agreement ($r = 0.988$) for both scales, with low bias (-0.66 Mg ha^{-1} at 500m; -0.70 Mg ha^{-1} at 1.5 km), and small errors (RMSE ≈ 10 Mg ha^{-1}, MAE ≈ 6 Mg ha^{-1}). The mean SD values were 55.4–56 Mg ha^{-1} across years, confirming stable spatial variability. Based on these diagnostics, the 2020 AGB layer was retained for all analysis as it provides the most recent and spatially complete estimates (Table S2; Figure S3).

2.3.1 Validation of Above-ground biomass with GEDI biomass footprints

The 2020 ESA CCI AGB layer was validated against the Global Ecosystem Dynamic Investigation (GEDI) Level 2B footprint biomass estimates to assess its accuracy [40]. GEDI provides LiDAR-based estimates of AGB density, derived from waveform structure, representing ~ 25m footprints that directly measure forest vertical structure. GEDI

footprints falling within forested areas as defined by the land cover mask described in section 2.2 were extracted and aggregated to 500m circular buffers to match the AGB spatial scale. The validated employed both unweighted and uncertainty-weighted metrics, as well as Deming regression ($\lambda = 1$) to account for measurement errors in both datasets. The unweighted validation yielded a moderate correlation (r = 0.418; R^2 = 0.175), with an RMSE of 69.0 Mg ha^{-1}, MAE = 25.9 Mg ha^{-1}, and bias = -0.93 Mg ha^{-1}. Weighted validation improved accuracy (r = 0.200; RMSE = 151.1 Mg ha^{-1}, MAE = 6.48 Mg ha^{-1} bias = –6.47 Mg ha^{-1}). The Deming regression yielded a slope of (0.40 ± 0.09) and an intercept of (15.25 ± 3.17 Mg ha^{-1}), indicating a slight underestimation of higher AGB values but overall strong consistency (Figure S4). This demonstrates that large-scale spatial gradients in AGB, particularly along aridity and fragmentation axes, reflect genuine ecological variation rather than artifacts of map bias, supporting the use of ESA-CCI AGB for regional modeling. Similar validation approaches using GEDI footprints have demonstrated the robustness of ESA and other satellite-based biomass products across diverse tropical forest contexts [41-42]. The extracted AGB values were assigned to each GBIF buffer centroid. The 500m datasets were used for fine-scale analysis, such as Analysis of Variance (ANOVA) and Principal Component Analysis (PCA). In contrast, the 1.5km dataset was used for the landscape-level analysis (SEMs and GAMs), where reduced spatial dependence among variables is required.

2.4. Climate data (aridity index)

The Global Aridity Index (Global AI) [43] dataset was applied to model the influence of climatic conditions on AGB distribution in Ghana. The dataset provides moderate-resolution (30 arcseconds, ~1 km^2) global raster data, characterizing aridity conditions based on the ratio of precipitation to reference evapotranspiration over the period 1970-2000. The data were derived from implementing the Food and Agriculture Organization (FAO)-56 Penman–Monteith Reference Evapotranspiration equation, making it a robust measure of rainfall deficit relative to the atmospheric water demand for vegetation regrowth. The following equation defines the Aridity Index (AI):

$$AI = \frac{MA\_Prec}{MA\_ET_0} \quad (1)$$

Where AI = Aridity Index, MA_Prec = Mean Annual Precipitation, and MA_ET0 = Mean Annual Reference Evapotranspiration. Higher AI values indicate more humid conditions, while lower values correspond to drier conditions [44]. In the Global-AI dataset, AI values were scaled by a factor of 10,000 and stored as integers for data

management purposes. Therefore, each raster cell value was multiplied by 0.0001 to retrieve actual AI values. The AI raster was reprojected to UTM Zone 30N (ESPG: 32630) and overlaid with the 500m and 1.5km plot buffers described in section 2.2. Mean AI values were extracted for each buffer. Following the United Nations Environmental Program (UNEP) aridity classification scheme, mean AI values were grouped into four climatic zones (Table 1).

These categorical values were used in further analysis to evaluate differences in AGB across climatic gradients. Because Global-AI datasets represent a multidecadal average rather than a single-year climate product, they provide a stable reference for linking long-term aridity conditions to current patterns of biomass, biodiversity, and landscape fragmentation.

2.5. Forest fragmentation metrics

Forest structural fragmentation was quantified using the land cover dataset from Njomaba et al. [26], a national land cover map explicitly developed for Ghana. This land cover dataset offers a consistent representation of forest cover and other land cover classes. From this land cover raster, all forest-related land cover classes were reclassified as forest, and all other classes were assigned non-forest. This reclassification produced a binary raster (forest = 1, non-forest = 0), which was used as the base forest mask for fragmentation assessment. To characterize the structure, the binary forest raster was clipped to each of the 500m and 1.5km circular buffers defined in Section 2.2, representing fine and landscape-scale forest patterns, respectively. Within each buffer, five complementary fragmentation metrics were computed using fragmentation statistics (FRAGSTATS) algorithms implemented in the "*landscapemetrics*" package [45]. The metrics were selected to represent three principal dimensions of forest spatial structure, such as area, edge, and shape complexity, while minimizing redundancy among highly correlated indices

Patches are those continuous forest pixels within the buffer; edges are measured on the clipped geometry (i.e., patch boundaries cut by the buffer are included, consistent with the default landscape metrics). Metrics were computed separately for the 500m and 1.5km datasets to reflect scale-dependent structure. Summary statistics for all metrics (means and standard deviations at each grain) are reported in Table S3, which are the values used in all analyses.

2.6. Temporal consistency and dataset alignment

Although the input datasets used in this study span different reference periods (Global AI: 1790 – 2000; GBIF tree occurrences: 2000 – 2013; ESA CCI AGB: 2017 – 2020; land cover, 2023), they were aligned conceptually to represent

stable, long-term ecological baselines that reflect persistent climatic, structural, and compositional conditions across Ghana's forest-savanna transition. The AI represents a long-term climatological average capturing multi-decadal moisture regimes that regulate forest productivity and structure, rather than short-term interannual variability. The ESA CCI AGB dataset provides a recent, yet climatically equilibrated, estimate of woody biomass that integrates vegetation responses to long-term moisture and disturbance gradients. Validation against GEDI footprint biomass confirmed that the ESA CCI AGB products are robust for Ghana (section 2.2; Figure S4), supporting their use as a baseline for large-scale carbon mapping. The fragmentation layer, derived from the landcover map of Njomaba et al. [26] for the year 2023. This reflects mid-decade forest structure, consistent with the 2010–2020 period of AGB mapping. Independent assessments by Hansen et al. [47] and Acheampong et al. [48] indicate that national-scale forest loss during this period was gradual and spatially heterogeneous, making the 2023 forest mask representative of prevailing structural conditions. The GBIF biodiversity dataset (2000–2013) aligns temporally with this window and captures distribution patterns shaped by the same underlying climatic and structural drivers. Together, these datasets represent an ecologically coherent time frame suitable for integrating climate, structure, and diversity within a space-for-time substitution (SFTS) framework [49]. This approach assumes that spatial gradients in aridity and fragmentation substitute for long-term temporal changes, enabling inference on how biodiversity and structure jointly influence carbon storage. All datasets were resampled and aggregated to a common analytical support defined by 500m and 1.5km circular buffers. This ensured that AI, fragmentation, and compositional biodiversity variables were compared over consistent spatial extents. While the original datasets differ in native resolution, the buffer-based extraction effectively harmonized them to a shared spatial support, minimizing the modifiable areal unit problem and scale-dependent variance. To assess robustness, a sensitivity analysis was performed comparing results between 500m and 1.5km datasets for all major analyses, showing a consistent direction and significance of key effects. These consistency checks confirm that the cross-scale patterns reported are not artifacts of resolution or temporal misalignment but reflect stable ecological relationships.

2.7. Statistical analysis

2.7.1 Effects of aridity index on above-ground biomass

To assess the effect of climate change on AGB, we employed an SFTS approach, where spatial variation in aridity, expressed through AI, served as a proxy for temporal climatic change, as described by Blois [49]. Ghana's four ecological zones (humid, sub-humid, dry sub-humid, and arid) were used to represent increasing levels of aridification,

with transitions along this gradient interpreted as analogs of projected climate change impacts. A one-way ANOVA was conducted to test differences in mean AGB among the four aridity classes. To ensure model robustness, assumptions of normality, homoscedasticity, and independence were evaluated through residual diagnostics. Potential heteroscedasticity was further addressed by applying heteroscedasticity-consistent (HC3) standard errors, implemented through the 'sandwich' and '*lmtest*' packages in R Studio [50]. Post hoc comparisons were performed using the Scheffé multiple comparison test, which is robust to unequal variances and sample sizes [51]. This method was selected based on the approach used in a similar study by Bastias [11], which employed ANOVA to examine vegetation patterns along environmental gradients. Mean and standard deviations of AGB were summarized for each aridity class to describe biomass variation along the climatic gradient.

2.7.2. Multicollinearity and dimensionality diagnostics

All predictors were standardized using z-scores before analysis. Multicollinearity among the five fragmentation metrics (NP, ED, AREA_MN, MSI, LSI) was evaluated using pairwise correlation and principal component analysis (PCA). Because these metrics were highly intercorrelated ($|r| > 0.8$ for ED–LSI and ED-AREA_MN), PCA was applied to reduce redundancy and derive an integrated fragmentation gradient. The first principal component (Frag_PC1) explained the majority of total variance and was used as a component fragmentation variable in subsequent models (Figure S5). After dimensionality reduction, Variance Inflation Factor (VIF) diagnostics were performed on the final set of model predictors to ensure that the combined predictors were not strongly collinear. This two-step approach follows recommended practices for hierarchical ecological modeling [52], where internal collinearity is removed within metric groups with a PCA, and remaining inter-variable collinearity is verified among the final predictors using the variance inflation factor (VIF). All predictors exhibited VIF < 2 and tolerance > 0.8 (Table S4), confirming negligible multicollinearity and validating their inclusion in SEM and GAM analysis.

2.7.3. Structural equation modeling (SEM)

To assess the direct and indirect pathways through which AI influences AGB, we implemented both linear and nonlinear SEMs. SEMs were used to jointly estimate causal relationships among AI, fragmentation (Frag_PC1), biodiversity (*S*), and AGB, while accounting for spatial structures. The linear SEM was implemented using the "*piecewiseSEM*" package in R Studio, with each sub-model fitted as a generalized least squares (GLS) model that included an exponential spatial correlation structure based on plot centroids (x, y). This approach accounts for residual

spatial autocorrelation while preserving parameter estimates. All variables were standardized (z-scores) before modeling to allow comparison of path coefficients (β). The model structure was defined as:

$$\left\{\begin{array}{c} Frag_{PC1} \sim AI \\ Richness \sim AI \\ AGB_{cal} \sim AI + Frag_{PC1} + Richness \end{array}\right\} \quad (2)$$

This structure reflects hypothesized causal pathways where aridity influences forest structure and biodiversity, which in turn affect biomass accumulation. Model fit was evaluated using Fisher's C statistic, Akaike Information Criterion (AIC), and R^2 values for each endogenous variable. Standardized path coefficients (β), standard errors, and significance levels were extracted (Table S9).

To capture potential nonlinear relationships that the linear model could not represent, a complementary nonlinear SEM was developed using the GAM framework. Each sub-model was fitted using thin-plate regression splines with restricted maximum likelihood (REML) optimization in the "*mgcv*" package. The structure mirrored the linear SEM but specified smooth functions for key predictors:

$$\left\{\begin{array}{c} Frag_{PC1} \sim s(AI) \\ Richness \sim s(AI) \\ AGB_{cal} \sim s(AI) + s(Frag_{PC1}) + s(Richness) + s(x, y) \end{array}\right\} \quad (3)$$

Where s (.) denotes smooth terms and s(x,y) is a bivariate spatial smoother capturing broad-scale spatial autocorrelation. Smoothing bases (k) were selected to balance flexibility and model parsimony, with overfitting constrained by penalization (γ = 1.4). Model performance was assessed using AIC, Fisher's C, and variance explained (R^2) for each endogenous variable.

2.7.4. Generalized additive models (GAMs)

To explore non-linear relationships between AGB and predictor variables, we used spatial GAMs implemented in the "*mgcv*" package [53]. The main model took the form.

$$AGB = s(AI, k = 9) + s(Frag\_PC1, k = 9) + s(Richness, k = 9) + s(x, y, k = 80) \quad (4)$$

Where s (.) denotes thin-plate regression splines, k specifies the basis dimension controlling smoothness, and s(x, y) represents a two-dimensional spatial smoother applied to buffer centroids to account for broad-scale autocorrelation.

Models were fitted by REML with mild penalization ($\gamma = 1.4$) and automatic smooth selection to prevent overfitting. To evaluate the relative influence of individual metrics (NP, AREA_MN, ED, MSI, LSI), we fitted separate spatial GAMs of the form:

$$AGB = s(metric) + s(AI) + s(x, y), \quad (5)$$

with predictors standardized. For each model, we extracted smooth-term statistics (edf, F, p-value) and compared ΔAIC and ΔDev against a baseline model (AGB ~ s(AI) + s(s, y)) to quantify the added explanatory contribution of each metric. Model diagnostics included residual QQ-plots, k-index adequacy tests, and concurvity checks.

3. Results

3.1. Effects of aridity on above-ground biomass

Mean AGB declined along the aridity gradient, from the humid to the semi-arid zone (Table 3; Figure 2). A one-way ANOVA showed a highly significant effect of aridity class on AGB (Type–II test: $F(3,1201) = 466.64$, $p < 2.2 \times 10^{-16}$). Effect sizes were large ($\eta^2 = 0.34$, 95% CI 0.31 – 1.00; $\omega^2 = 0.34$), indicating that approximately one-third of the total variation in biomass was explained by aridity (Table S5). Robust HC3 standard errors confirmed substantially lower AGB in all drier zones relative to humid zones ($p < 0.001$; Table S6). Scheffé post-hoc comparisons indicated clear differences among aridity zones (Humid > Sub-humid > {Dry sub-humid, Semi-arid}), with the two driest classes not differing statistically (Table S7). The comparison between raw and calibrated AGB showed similar effect sizes ($\eta^2 = 0.34$ vs 0.32), confirming that calibration did not alter the strength of the climatic signal (Table S5). However, mean AGB values were consistently higher in the calibrated dataset (Table S7), which was used in all subsequent analysis.

3.2. Structural Pathways: Linear and Nonlinear SEMs

The linear SEM (GLS-based; n = 1066) captured the main causal pathways linking aridity (AI), fragmentation (Frag_PC1), biodiversity (richness), and above-ground biomass (AGB_cal) (Table 4; Figure 3a). The overall model showed a good fit (*Fisher's* C = 3.04, df = 2, $p = 0.219$), indicating no significant missing paths. The model explained 61.9% of the variance in AGB_cal, 30.4% in fragmentation (Frag_PC1), and 0.4% in richness (Table S8). Aridity (AI) had a strong positive effect on AGB_cal ($\beta = +0.792$, $p < 0.001$), implying that more humid conditions promote higher

biomass. In contrast, AI had a negative effect on fragmentation ($\beta = -0.671$, $p < 0.001$), suggesting that drier zones are associated with more fragmented forest structures. Fragmentation, in turn, had a negative effect on AGB ($\beta = -0.223$, $p < 0.001$), indicating that increased fragmentation reduces biomass (Figure 3a, Table S8). The effect of AI on species richness was weak but positive ($\beta = +0.064$, $p < 0.05$), while the path from richness to AGB was non-significant ($\beta = -0.007$, $p < 0.572$).

The nonlinear SEM (GAM-based) revealed consistent structural relationships but captured flexible nonlinear effects among predictors (Figure 3b). Smooth terms indicated significant nonlinear dependencies between AI and fragmentation (edf = 5.94, $F = 23.92$, $p < 0.001$), AI and richness (edf = 3.27, $F = 5.63$, $p < 0.001$), and AI and AGB_cal (edf = 3.77, $F = 21.03$, $p < 0.001$), and fragmentation and AGB_cal (edf = 4.23, $F = 38.61$, $p < 0.001$). In contrast, the richness-AGB path was non-significant ($p = 0.26$).

Model evaluation showed that nonlinear SEM achieved higher explanatory power for AGB_cal ($R^2 = 0.83$) but a weaker fit overall (Fisher's C = 226.34, $p < 0.001$; AIC = 8130.84) compared with the linear SEM (AIC = 4178.46). This tradeoff reflects the improved local flexibility but reduced global parsimony of nonlinear smoothers. Collectively, both models highlight that aridity drives biomass directly and indirectly through fragmentation, with biodiversity contributing marginally to AGB variation (Table 4; Tables S8-S9).

3.3. Functional forms of fragmentation effects

Spatial GAMs, including individual metrics, confirmed significant nonlinear effects of all five metrics on AGB (edf ≈ 3-7; Table 5). AREA_MN showed the strongest contribution (ΔAIC = 386, ΔDev = 0.043), followed by ED (ΔAIC = 268.51, ΔDev = 0.031), LSI (ΔAIC = 256.44, ΔDev= 0.030), MSI (ΔAIC = 156.77, ΔDev = 0.020), and NP (ΔAIC = 71.21, ΔDev = 0.009). In contrast, biodiversity predictors were not significant (Richness: $p = 0.052$). Partial effects for the five individual metrics are provided in Figure 4.

343 # 4. Discussion

344 ## 4.1. Aridity as dominant driver of above-ground biomass decline

345 Our study shows that drier areas support less AGB, with AGB declining systematically from humid to semi-arid zones.
346 Relative to the humid forest, AGB was reduced by ~68% in the sub-humid zone, ~91% in the dry sub-humid zone, and
347 ~97% in the semi-arid zone (Figure 2; Table 3). This supports our hypothesis that decreasing AI (aridification) reduces
348 AGB, which is consistent with the theory and evidence that water availability, shaped by both precipitation and
349 evaporative demand, is a key driver of forest productivity and biomass accumulation [54-19, 55]. In arid and semi-arid
350 zones, intermittent water availability restricts photosynthesis and plant growth, leading to reduced biomass
351 accumulation [56]. Conversely, humid and sub-humid forests in Ghana benefit from high rainfall and moisture
352 availability, which support high photosynthetic rates, dense forest structures, and elevated carbon storage [57]. Scheffé
353 post hoc tests confirmed that these biomass differences among aridity zones were statistically significant, underscoring
354 that the relationship between aridity and AGB is both systematic and ecologically distinct across moisture regimes.
355 Similar patterns of aridity-driven biomass decline have been observed across tropical regions, including the Amazon
356 Basin, Central Africa, and Northern Australia, where increasing dryness and drought have frequently weakened forest
357 carbon sinks [58-59, 60]. These findings reinforce the assertion that the mechanisms driving AGB reduction in Ghana,
358 such as limited water availability and structural degradation, reflect fundamental ecological processes operating
359 throughout the tropics. With climate projections forecasting increased aridification in tropical regions [61], these
360 results have significant implications for forest carbon dynamics.

361 ## 4.2. Fragmentation as mediator of aridity impacts on above-ground biomass

362 Our SEM results demonstrated the effect of aridification on biomass not only directly but also indirectly through its
363 influence on fragmentation. Specifically, higher aridity (lower AI) was associated with greater fragmentation, which
364 in turn decreased AGB. Fragmentation (Frag_PC1) captured landscapes dominated by small, irregularly shaped
365 patches with high edge density and shape complexity (NP, ED, LSI positive loadings; AREA_MN and MSI negative
366 loadings). This indicates that drier zones are not only less productive but also structurally more degraded. The
367 mediating role of fragmentation adds an essential layer to understanding carbon dynamics in Ghana's forest. Numerous
368 studies have demonstrated that fragmentation exacerbates biomass loss beyond that attributable to deforestation alone.
369 By increasing edge exposure, fragmentation accelerates desiccation, tree mortality, and microclimatic stress [62-63].
370 Patch isolation further disrupts seed dispersal, regeneration, and species persistence, undermining long-term forest

stability. In tropical Africa, fragmentation has been linked to reduced carbon storage in both humid forest and savanna-forest mosaics [64-65], consistent with our findings that fragmentation compounds aridity-driven biomass decline.

In Ghana, the dual pressures of climate stress and structural degradation are especially acute in the forest-savanna transition belt, where agricultural expansion (notably cocoa and food crops) has intensified patch proliferation and edge effects [48]. More recently, artisanal mining, known as "galamsey," and industrial gold mining have emerged as additional drivers of forest fragmentation, converting contiguous forests into small, irregular patches with high edge density, even within protected areas [66-67]. Together, these land-use pressures compound the climatic stress captured in our SEM pathways, reinforcing that fragmentation mediates climate impacts by making forests less resilient to aridification. This interpretation is consistent with evidence showing that fragmented tropical forests are disproportionately vulnerable to climate extremes, such as drought [23], and that structural disturbances, such as selective logging, can lead to long-term carbon losses that further weaken forest resilience [68].

4.3. Limited role of biodiversity in mediating aridity–biomass relationships

Species richness and evenness did not significantly mediate the effects of aridity on AGB in either SEMs or GAMs. This suggests that computational diversity plays a minor role under strong climatic stress. Instead, abiotic drivers (aridification) and structural factors (fragmentation) appeared to dominate biomass dynamics. This outcome is consistent with evidence that biodiversity-biomass relationships are strongly context-dependent, varying in strength and direction depending on climate, resource availability, and structural conditions [69-70, 71]. In tropical forests, species richness often enhances biomass through mechanisms such as complementarity and facilitation [70]. However, in dry or transitional ecosystems, biodiversity effects are usually weak or absent because water limitations or structural constraints restrict growth, regardless of species richness [72].

Another possible explanation lies in the biodiversity dataset used. Our species richness measures were derived from occurrence-based GBIF records, which capture species presence rather than abundance. As a result, we could not capture species evenness but only relied on species richness, which is not a great measure of biodiversity. In contrast, above-ground biomass is often disproportionately driven by a few large individuals or dominant species, sometimes referred to as the "big tree effect" [73]. This demographic skew means that biomass and diversity relationships are typically stronger when abundance-weighted diversity metrics, such as basal-area-weighted Shannon or Simpson indices, are available [74-75]. This mismatch between presence-only diversity metrics and abundance-driven biomass likely weakened statistical links in SEM and GAM analysis. Future research could address this limitation by integrating

abundance-based forest inventory with remote-sensing products, which could allow more rigorous testing of biodiversity-biomass pathways.

4.4. Functional responses of biomass to fragmentation metrics

Spatial GAMs provided functional insights into how individual fragmentation metrics influenced AGB across Ghana's landscape. Among the five metrics, AREA_MN exhibited the most substantial contributions with a unimodal response peaking at intermediate patch sizes. This suggests that moderately sized patches may maximize carbon storage by balancing interior habitat and edge effects, whereas extensive patches reduce AGB. Similar unimodal or hum-shaped relationships between patch size and ecosystem function have been observed in other tropical regions, where moderate fragmentation temporarily enhances heterogeneity before degradation dominates [76-77].

In contrast, the NP showed a negative effect on AGB, particularly at high patch densities. This suggests that excessive patch subdivision reduces the availability of the core forest interior, replacing forest with small, isolated patches that are more exposed to edges. The loss of interior habitat minimizes the capacity of forests to maintain large, biomass-rich trees and heightens vulnerability to disturbances. These findings are consistent with studies from the Amazon and Southeast Asia, where increasing patch number accelerated biomass decline by amplifying fragmentation-driven processes such as edge mortality, drought sensitivity, and fire susceptibility [78-79, 80]. For ED, a weak unimodal response was observed. At low to moderate levels of edge creation, biomass appears to increase slightly, which may reflect the role of forest edges in enhancing light penetration and nutrient turnover, thereby stimulating the growth of fast-growing pioneer species [78]. These findings are consistent with studies from the Amazon and Southeast Asia, where increasing patch number accelerates biomass decline by amplifying fragmentation-driven processes, such as edge mortality, drought sensitivity, and fire susceptibility [79-80]. The LSI exhibited a negative relationship with AGB in our models. More regularly shaped patches have larger perimeter-to-area ratios, which expose proportionally greater portions of the forest to edge influences. This reduces the effective area of the forest core, thereby reducing overall biomass [76]. Similar patterns have been documented in both tropical and temperate systems, where complex patch shapes are associated with heightened edge effects, altered species composition, and reduced carbon storage [81-82]. Finally, the mean shape index (MSI) showed the weakest and inconsistent effect from the GAM models for this study. This suggests that shape connectivity alone may not exert strong control over biomass unless coupled with patch size or edge extent. In other words, irregular shapes may only matter for AGB when patches are fragmented enough that edge effects dominate [83]. Previous studies have shown that patch shape complexity is often a secondary driver of

ecological processes compared to patch areas and connectivity [84-85]. Our findings, therefore, highlight MSI as a less robust predictor of biomass compared to AREA_MN, NP, or LSI.

4.5. Anthropogenic land-use pressures and forest fragmentation

The observed patterns of AGB loss and fragmentation are not only climate-driven but also shaped by long-standing anthropogenic activities. In humid and sub-humid zones, cocoa expansion, oil palm cultivation, and subsistence agriculture remain dominant drivers in Ghana [86]. Cocoa farming has been linked to extensive forest encroachment in Ghana and Côte d'Ivoire, accounting for more than 13% of total forest loss in the region [7]. In drier zones, fuelwood harvesting, charcoal production, and shifting cultivation drive fragmentation and hinder regeneration [24]. Illegal artisanal mining ("galamsey") has emerged as an additional driver of deforestation and landscape degradation in Ghana, particularly within forest reserves and riparian zones [66-67]. These activities not only remove forest cover but also degrade soil and water resources, compounding fragmentation effects. Weak governance, insecure land tenure systems, and reliance on wood energy (with over 70% of rural households relying on fuelwood and charcoal) [87] further exacerbate patch proliferation and biomass decline. These socio-ecological dynamics compound climatic stress and help explain pronounced AGB reductions observed along Ghana's aridity gradient.

4.6. Management and policy implications under climate change

Our findings carry important implications for forest management and climate policy. Transitional and dry forests, which exhibited the steepest biomass declines, should be prioritized for ecological monitoring and adaptive interventions. While humid forests remain Ghana's most carbon-rich ecosystems, they are increasingly threatened by fragmentation, induced through climate and anthropogenic activities, requiring policies that maintain large, connected forest patches and minimize edge proliferation. In semi-arid regions, where biomass is inherently low, restoration strategies should emphasize multifunctional land use, such as agroforestry, rather than unrealistic expectations of large carbon sink potential [88].

At the national level, these insights align with the priorities of Ghana's Forest Plantation Strategy (2018-2021) [89] and the Green Ghana Initiative, both of which emphasize forest restoration and connectivity. However, their effectiveness is increasingly challenged by the activities of illegal artisanal mining, which has become one of the leading drivers of forest degradation and watershed destruction in Ghana [90]. These activities undermine ecosystem recovery and reduce the success of reforestation efforts. Addressing this threat requires integrated strategies that go beyond tree planting, including strict enforcement of mining regulations, community-based monitoring, and the

provision of alternative livelihoods [90]. Embedding these measures into national frameworks such as REDD+ and the Green Ghana Initiative will be critical to ensure that gains in forest restoration are not hampered by continuous mining-related degradation. Regionally, Ghana's experience aligns with the African Forest Restoration Initiative (AFR100), a pan-African effort to restore 100 million hectares of degraded land by 2030. Ghana has pledged to restore 2 million hectares under AFR100 [91], but challenges such as artisanal mining, agricultural expansion, weak governance, and climatic stresses leading to forest fragmentation continue to impede restoration efforts. These findings also align with the goals of the United Nations Decade on Ecosystem Restoration (2021-2030), highlighting that tropical transitional and dry forests are particularly vulnerable to climate change and land-use pressures [92]. These global perspectives underscore the urgency of protecting forest ecosystems and maintaining landscape connectivity across the tropics.

4.7. Limitations and future direction

A limitation of this study is the partial temporal mismatch among datasets: the aridity index reflects long-term averages from 1970 to 2000, whereas biomass and vegetation records correspond to 2010, fragmentation (2023), and biodiversity (2000–2013). While the space-for-time substitution framework provides a proxy for assessing climate-biomass relationships, future research should incorporate time-explicit datasets to track ecological and climatic changes directly. Another limitation is the presence of high curvature among smooth terms in the GAMs. Although addressed through PCA-based dimensionality reduction and the inclusion of spatial smoothers, this issue underscores the complexity of disentangling interacting structural variables. Moreover, biodiversity metrics derived from occurrence-based GBIF data may underestimate functional diversity, limiting their exploratory power relative to biomass outcomes. Despite these limitations, SEM and GAM models explained a substantial amount of variance in AGB, demonstrating the combined importance of climatic gradients and landscape structure. Future studies should extend this work by using dynamic modeling approaches that integrate temporal climatic variability, land-use change, and biodiversity composition. Such approaches will strengthen predictions of carbon storage resilience in the face of accelerating aridity and fragmentation pressures.

5. Conclusions

This study demonstrates that aridification (i.e., decreasing AI) is the dominant driver of aboveground biomass variation across Ghana's ecological zones, with biomass declining sharply from humid to semi-arid forests. The 95% reduction in AGB between these extremes underscores the dominant influence of climatic water availability on controlling forest carbon storage. Aridity effects were compounded by forest fragmentation, which mediated additional biomass losses

through reduction in patch size and increase in edge exposure. Spatial GAMs revealed that fragmentation effects were nonlinear: AREA_MN emerged as the strongest predictor, with NP, ED, and LSI contributing secondarily, exhibiting consistently negative effects. MSI was the weakest predictor, suggesting that patch shape complexity alone has little influence without interactions with size or edges.

From a management perspective, these findings emphasize the importance of forest management and conservation. These findings underscore that effective forest management must extend beyond tree cover targets to encompass landscape structural integrity. Conservation and restoration efforts should prioritize dry and transitional forests, maintain large, connected forests, and integrate multifunctional land uses, such as climate-resilient agroforestry, in semi-arid areas. Embedding such strategies into national frameworks, regional efforts, and global agendas will be essential to sustain forest carbon stocks. Our study highlights that protecting moisture-sensitive carbon pools and reducing fragmentation are crucial steps in maintaining the role of tropical forests as a global carbon sink in the face of intensifying climate change.

Data Availability Statement: Data are available upon reasonable request from the authors.

Acknowledgments: The authors extend their profound appreciation to Mr. James Nana Ofori for his pivotal role in ensuring the success of this work.

CRediT authorship contribution statement

Elisha Njomaba: Conceptualization, Data curation, Formal analysis, Investigation, Methodology, Project administration, Resources, Software, Validation, Visualization, Writing – original draft, Writing – review and editing. **Ben Emuna Aikins**: Investigation, Methodology, Software, Writing – original draft, Writing – review and editing. **Peter Surovy**: Conceptualization, Resources, Funding acquisition, Supervision, Writing – review and editing.

Funding sources: This research was funded by the Faculty of Forestry and Wood Sciences—FFWS, Czech University of Life Sciences Prague, (IGA/FLD/A_11_23 (Internal grant number: 43140/1312/3189).

Conflicts of Interest: The authors declare no conflicts of interest. The funders had no role in the study design, collection, analysis, or interpretation of data; writing of the manuscript; or the decision to publish the results.

Declaration of generative AI and AI-assisted technologies in the writing process

During the preparation of this work, the authors used GPT-5 to improve the style and grammar of several paragraphs in the text. After using this tool, the authors reviewed and edited the content as needed and take full responsibility for the content of the publication.

Declaration of competing interests

The authors declare that they have no known competing financial interests or personal relationships that could have appeared to influence the work reported in this paper.

516

517 **References**

518 1. Zhang X, Huang X (2019) Human disturbance caused stronger influences on global
519 vegetation change than climate change. PeerJ 2019:1–15.
520 https://doi.org/10.7717/peerj.7763

521 2. Pan Y, Birdsey R, Fang J, et al (2011) A Large and Persistent Carbon Sink in the World's
522 Forests. Science (80-) 333:988–993. https://doi.org/DOI: 10.1126/science.1201609

523 3. Saatchi SS, Harris NL, Brown S, et al (2011) Benchmark map of forest carbon stocks in
524 tropical regions across three continents. Proc Natl Acad Sci U S A 108:9899–9904.
525 https://doi.org/10.1073/pnas.1019576108

526 4. Tilman D, Lehman C (2001) Human-caused environmental change: Impacts on plant
527 diversity and evolution. Proc Natl Acad Sci U S A 98:5433–5440.
528 https://doi.org/10.1073/pnas.091093198

529 5. Bodart C, Brink AB, Donnay F, et al (2013) Continental estimates of forest cover and
530 forest cover changes in the dry ecosystems of Africa between 1990 and 2000. J Biogeogr
531 40:1036–1047. https://doi.org/10.1111/jbi.12084

532 6. Asubonteng K, Pfeffer K, Ros-Tonen M, et al (2018) Effects of Tree-crop Farming on
533 Land-cover Transitions in a Mosaic Landscape in the Eastern Region of Ghana. Environ
534 Manage 62:529–547. https://doi.org/10.1007/s00267-018-1060-3

535 7. Asare R, Afari-Sefa V, Osei-Owusu Y, Pabi O (2014) Cocoa agroforestry for increasing
536 forest connectivity in a fragmented landscape in Ghana. Agrofor Syst 88:1143–1156.
537 https://doi.org/10.1007/s10457-014-9688-3

538 8. Pyngrope OR, Kumar M, Pebam R, et al (2021) Investigating forest fragmentation through
539 earth observation datasets and metric analysis in the tropical rainforest area. SN Appl Sci
540 3:. https://doi.org/10.1007/s42452-021-04683-5

541 9. García-Gigorro S, Saura S (2005) Forest fragmentation estimated from remotely sensed
542 data: Is comparison across scales possible? For Sci 51:51–63.
543 https://doi.org/10.1093/forestscience/51.1.51

544 10. Haddad NM, Brudvig LA, Clobert J, et al (2015) Habitat fragmentation and its lasting
545 impact on Earth's ecosystems. Sci Adv 1:1–9. https://doi.org/10.1126/sciadv.1500052

546 11. Bastias CC, Rodríguez Castilla G, Salazar Zarzosa P, et al (2025) Differential aridity-
547 induced variations in ecosystem multifunctionality between Iberian Pinus and Quercus
548 Mediterranean forests. Ecol Indic 173:. https://doi.org/10.1016/j.ecolind.2025.113411

549 12. Bonsu K, Bonin O (2023) Assessing landscape fragmentation and its implications for
550 biodiversity conservation in the Greater Accra Metropolitan Area (GAMA) of Ghana.
551 Discov Environ 1:. https://doi.org/10.1007/s44274-023-00023-z

552 13. Turner Monica (1996) Landscape Ecology Theory and Practice. 72–82

553 14. Flowers B, Huang KT, Aldana GO (2020) Analysis of the habitat fragmentation of

554 ecosystems in belize using landscape metrics. Sustain 12:.
555 https://doi.org/10.3390/su12073024

556 15. Aabeyir R, Adu-Bredu S, Agyare WA, Weir MJC (2020) Allometric models for estimating
557 aboveground biomass in the tropical woodlands of Ghana, West Africa. For Ecosyst 7:.
558 https://doi.org/10.1186/s40663-020-00250-3

559 16. Laurance WF, Lovejoy TE, Vasconcelos HL, et al (2002) Ecosystem decay of Amazonian
560 forest fragments: A 22-year investigation. Conserv Biol 16:605–618.
561 https://doi.org/10.1046/j.1523-1739.2002.01025.x

562 17. Malhi Y, Roberts JT, Betts RA, et al (2008) Climate change, deforestation, and the fate of
563 the Amazon. Science (80-) 319:169–172. https://doi.org/10.1126/science.1146961

564 18. Phillips OL, Aragão LEOC, Lewis SL, et al (2009) Drought Sensitivity of the Amazon
565 Rainforest. Science (80-) 323:1344–1347

566 19. Clark DA, Piper SC, Keeling CD, Clark DB (2003) Tropical rain forest tree growth and
567 atmospheric carbon dynamics linked to interannual temperature variation during 1984-
568 2000. Proc Natl Acad Sci U S A 100:5852–5857. https://doi.org/10.1073/pnas.0935903100

569 20. Oduro KA, Mohren GMJ, Peña-Claros M, et al (2015) Tracing forest resource
570 development in Ghana through forest transition pathways. Land use policy 48:63–72.
571 https://doi.org/10.1016/j.landusepol.2015.05.020

572 21. Addo-Fordjour P, Obeng S, Anning A, Addo M (2009) Floristic composition, structure
573 and natural regeneration in a moist semi-deciduous forest following anthropogenic
574 disturbances and plant invasion. Int J Biodivers Conserv 1:21–37

575 22. Mensah S, Veldtman R, Assogbadjo AE, et al (2017) Ecosystem service importance and
576 use vary with socio-environmental factors: A study from household-surveys in local
577 communities of South Africa. Ecosyst Serv 23:1–8.
578 https://doi.org/10.1016/j.ecoser.2016.10.018

579 23. Brinck K, Fischer R, Groeneveld J, et al (2017) High resolution analysis of tropical forest
580 fragmentation and its impact on the global carbon cycle. Nat Commun 8:14855.
581 https://doi.org/10.1038/ncomms14855

582 24. Chidumayo E, Gumbo DJ (2010) The dry forests and woodlands of Africa: managing for
583 products and services. Earthscan Libr

584 25. Chaplin-Kramer R, Ramler I, Sharp R, et al (2015) Degradation in carbon stocks near
585 tropical forest edges. Nat Commun 6:10158. https://doi.org/10.1038/ncomms10158

586 26. Njomaba E, Mushtaq F, Nagbija RK, et al (2025) Adopting Land Cover Standards for
587 Sustainable Development in Ghana: Challenges and Opportunities. Land 14:550.
588 https://doi.org/10.3390/land14030550

589 27. Ampim PAY, Ogbe M, Obeng E, et al (2021) Land cover changes in ghana over the past
590 24 years. Sustain 13:. https://doi.org/10.3390/su13094951

591 28. Lawer EA (2024) Predicting the impact of climate change on the potential distribution of a
592 critically endangered avian scavenger, Hooded Vulture Necrosyrtes monachus, in Ghana.

Glob Ecol Conserv 49:e02804. https://doi.org/10.1016/j.gecco.2024.e02804

29. Ofori SA, Asante F, Boatemaa Boateng TA, Dahdouh-Guebas F (2023) The composition, distribution, and socio-economic dimensions of Ghana's mangrove ecosystems. J Environ Manage 345:118622. https://doi.org/10.1016/j.jenvman.2023.118622

30. Abbam T, Johnson FA, Dash J, Padmadas SS (2018) Spatiotemporal Variations in Rainfall and Temperature in Ghana Over the Twentieth Century, 1900–2014. Earth Sp Sci 5:120–132. https://doi.org/10.1002/2017EA000327

31. Asare (2021) Plants of Ghana. Version 1.1. In: Ghana Herb. Occur. dataset. https://doi.org/10.15468/e8rhqm

32. Beck J, Böller M, Erhardt A, Schwanghart W (2014) Spatial bias in the GBIF database and its effect on modeling species' geographic distributions. Ecol Inform 19:10–15. https://doi.org/10.1016/j.ecoinf.2013.11.002

33. Aiello-Lammens ME, Boria RA, Radosavljevic A, et al (2015) spThin: An R package for spatial thinning of species occurrence records for use in ecological niche models. Ecography (Cop) 38:541–545. https://doi.org/10.1111/ecog.01132

34. Hillebrand H, Bennett MD, Cadotte WM (2008) Consequences of dominance: A review of evenness effects and local and regional ecosystem processes. Ecology 89:1510–1520

35. Chamberlain SA, Szöcs E (2013) taxize: Taxonomic search and retrieval in R. F1000Research 2:. https://doi.org/10.12688/f1000research.2-191.v1

36. Meyer C, Weigelt P, Kreft H (2016) Multidimensional biases, gaps and uncertainties in global plant occurrence information. Ecol Lett 19:992–1006. https://doi.org/10.1111/ele.12624

37. Ficetola GF, Mazel F, Thuiller W (2017) Global determinants of zoogeographical boundaries. Nat Ecol Evol 1:89. https://doi.org/10.1038/s41559-017-0089

38. Sandom C, Faurby S, Sandel B, Svenning J-C (2014) Global late Quaternary megafauna extinctions linked to humans, not climate change. Proceedings Biol Sci 281:. https://doi.org/10.1098/rspb.2013.3254

39. Santoro M, Cartus O (2024) ESA Biomass Climate Change Initiative (Biomass_cci): Global datasets of forest above-ground biomass for the years 2010, 2015, 2016, 2017, 2018, 2019, 2020 and 2021, v5.01. In: NERC EDS Cent. Environ. Data Anal. https://gee-community-catalog.org/projects/cci_agb/#dataset-preprocessing-for-gee. Accessed 5 Apr 2024

40. Dubayah R, Tang H, Armston J, et al (2021) GEDI L2B Canopy Cover and Vertical Profile Metrics Data Global Footprint Level V002 [Data set]. In: NASA L. Process. Distrib. Act. Arch. Cent. https://doi.org/10.5067/GEDI/GEDI02_B.002. Accessed 20 Sep 2025

41. Hu T, Su Y, Xue B, et al (2016) Mapping global forest aboveground biomass with spaceborne LiDAR, optical imagery, and forest inventory data. Remote Sens 8:. https://doi.org/10.3390/rs8070565

632 42. Thapa N, Narine LL, Wilson AE (2025) Forest Aboveground Biomass Estimation Using
633 Airborne LiDAR: A Systematic Review and Meta-Analysis. J For 123:389–412.
634 https://doi.org/10.1007/s44392-025-00029-w

635 43. Zomer RJ, Xu J, Trabucco A (2022) Version 3 of the Global Aridity Index and Potential
636 Evapotranspiration Database. Sci Data 9:1–15. https://doi.org/10.1038/s41597-022-01493-
637 1

638 44. Middleton N, Thomas DS. (1997) World atlas of desertification. In: United Nations
639 Environ. Program. https://opac.library.strathmore.edu/bib/33981. Accessed 5 Apr 2024

640 45. McGargical K, Cushman S, Ene E (2012) Spatial Pattern Analysis Program for Categorical
641 Maps. https://www.fragstats.org

642 46. Enaruvbe GO, Atafo OP (2018) A Long-Term Assessment of Habitat Fragmentation in
643 Coastal Wetlands, Niger Delta, Nigeria. Ife Soc Sci Rev 26:36–47

644 47. Hansen MC, Potapov P V, Moore R, et al (2013) High-Resolution Global Maps of 21st-
645 century forst cover change. Science (80-) 342:850–853

646 48. Acheampong EO, Macgregor CJ, Sloan S, Sayer J (2019) Deforestation is driven by
647 agricultural expansion in Ghana's forest reserves. Sci African 5:.
648 https://doi.org/10.1016/j.sciaf.2019.e00146

649 49. Blois JL, Williams JW, Fitzpatrick MC, et al (2013) Space can substitute for time in
650 predicting climate-change effects on biodiversity. Proc Natl Acad Sci U S A 110:9374–
651 9379. https://doi.org/10.1073/pnas.1220228110

652 50. RCoreTeam (2024) A Language and Environment for Statistical Computing. R version
653 4.3.3. https://www.r-project.org/

654 51. Allen M (2017) The SAGE encyclopedia of communication research methods. SAGE
655 publications.

656 52. Dormann CF, Elith J, Bacher S, et al (2013) Collinearity: A review of methods to deal with
657 it and a simulation study evaluating their performance. Ecography (Cop) 36:27–46.
658 https://doi.org/10.1111/j.1600-0587.2012.07348.x

659 53. Wood S. (2017) Generalized Additive Models: An Introduction with R, Second Edition
660 (2nd ed.). Chapman and Hall/CRC

661 54. Malhi Y, Baker Oliver Philips TR, Almeida S, et al (2004) The above-ground coarse wood
662 productivity of 104 Neotropical forest plots. Glob Chang Biol 10:563–591.
663 https://doi.org/10.1111/j.1529-8817.2003.00778.x

664 55. Phillips SJ, Dudík M (2008) Modeling of species distributions with Maxent: New
665 extensions and a comprehensive evaluation. Ecography (Cop) 31:161–175.
666 https://doi.org/10.1111/j.0906-7590.2008.5203.x

667 56. Choat B, Jansen S, Brodribb TJ, et al (2012) Global convergence in the vulnerability of
668 forests to drought. Nature 491:752–755. https://doi.org/10.1038/nature11688

669 57. Chave J, Andalo C, Brown S, et al (2005) Tree allometry and improved estimation of

carbon stocks and balance in tropical forests. Oecologia 145:87–99. https://doi.org/10.1007/s00442-005-0100-x

58. Lewis SL, Lopez-Gonzalez G, Sonké B, et al (2009) Increasing carbon storage in intact African tropical forests. Nature 457:1003–1006. https://doi.org/10.1038/nature07771

59. Murphy BP, Bowman DMJS (2012) What controls the distribution of tropical forest and savanna? Ecol Lett 15:748–758. https://doi.org/10.1111/j.1461-0248.2012.01771.x

60. Brienen RJW, Phillips OL, Feldpausch TR, et al (2015) Long-term decline of the Amazon carbon sink. Nature 519:344–348. https://doi.org/10.1038/nature14283

61. IPCC (2021) Climate Change 2021 – The Physical Science Basis: Working Group I Contribution to the Sixth Assessment Report of the Intergovernmental Panel on Climate Change. Cambridge University Press, Cambridge

62. Laurance WF, Carolina Useche D, Rendeiro J, et al (2012) Averting biodiversity collapse in tropical forest protected areas. Nature 489:290–294. https://doi.org/10.1038/nature11318

63. Broadbent EN, Asner GP, Keller M, et al (2008) Forest fragmentation and edge effects from deforestation and selective logging in the Brazilian Amazon. Biol Conserv 141:1745–1757. https://doi.org/https://doi.org/10.1016/j.biocon.2008.04.024

64. Taubert F, Fischer R, Groeneveld J, et al (2018) Global patterns of tropical forest fragmentation. Nature 554:519–522. https://doi.org/10.1038/nature25508

65. Aleman JC, Staver AC (2018) Spatial patterns in the global distributions of savanna and forest. Glob Ecol Biogeogr 27:792–803. https://doi.org/10.1111/geb.12739

66. Abugre S, Asigbaase M, Kumi S, et al (2025) Forest landscape degradation, carbon loss and ecological consequences of illegal gold mining in Ghana. Discov For 1:1–19. https://doi.org/10.1007/s44415-025-00020-5

67. Obeng EA, Oduro KA, Obiri BD, et al (2019) Impact of illegal mining activities on forest ecosystem services: local communities' attitudes and willingness to participate in restoration activities in Ghana. Heliyon 5:e02617. https://doi.org/10.1016/j.heliyon.2019.e02617

68. Qie L, Lewis SL, Sullivan MJP, et al (2017) Long-term carbon sink in Borneo's forests halted by drought and vulnerable to edge effects. Nat Commun 8:. https://doi.org/10.1038/s41467-017-01997-0

69. Cardinale BJ, Duffy JE, Gonzalez A, et al (2012) Biodiversity loss and its impact on humanity. Nature 486:59–67. https://doi.org/10.1038/nature11148

70. Jucker T, Avăcăritei D, Bărnoaiea I, et al (2016) Climate modulates the effects of tree diversity on forest productivity. J Ecol 104:388–398. https://doi.org/10.1111/1365-2745.12522

71. Ratcliffe S, Wirth C, Jucker T, et al (2017) Biodiversity and ecosystem functioning relations in European forests depend on environmental context. Ecol Lett 20:1414–1426. https://doi.org/10.1111/ele.12849

709 72. Lammerant R, Rita A, Borghetti M, Muscarella R (2023) Water-limited environments
710 affect the association between functional diversity and forest productivity. Ecol Evol
711 13:e10406. https://doi.org/10.1002/ece3.10406

712 73. Sheil D, Bongers F (2020) Interpreting forest diversity-productivity relationships: volume
713 values, disturbance histories and alternative inferences. For Ecosyst 7:.
714 https://doi.org/10.1186/s40663-020-0215-x

715 74. Chisholm RA, Muller-Landau HC, Abdul Rahman K, et al (2013) Scale-dependent
716 relationships between tree species richness and ecosystem function in forests. J Ecol
717 101:1214–1224. https://doi.org/10.1111/1365-2745.12132

718 75. Sullivan MJP, Talbot J, Lewis SL, et al (2017) Diversity and carbon storage across the
719 tropical forest biome. Sci Rep 7:1–12. https://doi.org/10.1038/srep39102

720 76. Arroyo-Rodríguez V, Fahrig L (2014) Why is a landscape perspective important in studies
721 of primates? Am J Primatol 76:901–909. https://doi.org/10.1002/ajp.22282

722 77. Ewers RM, Banks-Leite C (2013) Fragmentation Impairs the Microclimate Buffering
723 Effect of Tropical Forests. PLoS One 8:. https://doi.org/10.1371/journal.pone.0058093

724 78. Laurance WF, Camargo JLC, Luizão RCC, et al (2011) The fate of Amazonian forest
725 fragments: A 32-year investigation. Biol Conserv 144:56–67.
726 https://doi.org/10.1016/j.biocon.2010.09.021

727 79. Brinck K, Fischer R, Groeneveld J, et al (2017) High resolution analysis of tropical forest
728 fragmentation and its impact on the global carbon cycle. Nat Commun 8:.
729 https://doi.org/10.1038/ncomms14855

730 80. Shen C, Shi N, Fu S, et al (2021) Decline in aboveground biomass due to fragmentation in
731 subtropical forests of China. Forests 12:1–12. https://doi.org/10.3390/f12050617

732 81. Silva Junior CHL, Aragão LEOC, Anderson LO, et al (2020) Persistent collapse of
733 biomass in Amazonian forest edges following deforestation leads to unaccounted carbon
734 losses. Sci Adv 6:. https://doi.org/10.1126/sciadv.aaz8360

735 82. Harper K, Macdonal SE, Burton P, et al (2005) Edge Influence on Forest Structure and
736 Composition in Fragmented Landscapes. Conserv Biol 19:768–782.
737 https://doi.org/https://doi.org/10.1111/j.1523-1739.2005.00045.x

738 83. Fahrig L (2003) Effects of Habitat Fragmentation on Biodiversity. Annu Rev Ecol Evol
739 Syst 34:487–515. https://doi.org/10.1146/annurev.ecolsys.34.011802.132419

740 84. Smith AC, Fahrig L, Francis CM (2011) Landscape size affects the relative importance of
741 habitat amount, habitat fragmentation, and matrix quality on forest birds. Ecography (Cop)
742 34:103–113. https://doi.org/https://doi.org/10.1111/j.1600-0587.2010.06201.x

743 85. Villard MA, Metzger JP (2014) Beyond the fragmentation debate: A conceptual model to
744 predict when habitat configuration really matters. J Appl Ecol 51:309–318.
745 https://doi.org/10.1111/1365-2664.12190

746 86. Acheampong EN, Ozor N, Sekyi-annan E (2014) Development of small dams and their
747 impact on livelihoods: Cases from northern Ghana. African J Agric Res 9:1867–1877.

https://doi.org/10.5897/AJAR2014.8610

87. Dam J, Eijck J, Schure J, Zuzhang X (2017) The charcoal transition: greening the charcoal value chain to mitigate climate change and improve local livelihoods

88. Jose S (2009) Agroforestry for ecosystem services and environmental benefits: An overview. Agrofor Syst 76:1–10. https://doi.org/10.1007/s10457-009-9229-7

89. MESTI (2018) Ministry of Environment, Science, Technology and Innovation (Mesti) Sector Medium-Term Development Plan. Accra, Ghana

90. Hilson G (2017) Shootings and burning excavators: Some rapid reflections on the Government of Ghana's handling of the informal Galamsey mining 'menace.' Resour Policy 54:109–116. https://doi.org/10.1016/j.resourpol.2017.09.009

91. AFR100 (2015) Peopl Restoring Africa's Landscapes. https://afr100.org/

92. Siyum ZG (2020) Tropical dry forest dynamics in the context of climate change: syntheses of drivers, gaps, and management perspectives. Ecol Process 9:. https://doi.org/10.1186/s13717-020-00229-6

5. Discussion

5.1 Summary of addressed knowledge gaps and objectives

Forests are among the most critical terrestrial ecosystems, supporting biodiversity, storing carbon, regulating the climate, and sustaining human livelihoods. However, they face threats from deforestation, fragmentation, and climate change. Despite Ghana's commitment to national and international biodiversity targets, effective monitoring remains constrained by several gaps: biodiversity programs are often fragmented and inconsistent; data accessibility and sharing remain limited; traditional field-based inventories, though invaluable, are labor-intensive, costly, and spatially restricted; and standardized biodiversity indicators for tracking progress toward the global framework are lacking. Together, these challenges have created a gap in scaling biodiversity monitoring to the national level while maintaining accuracy, ecological relevance, and policy alignment. This thesis addressed these gaps through the EBV framework, focusing on ecosystem structure, community composition, and species distribution. By integrating RS, field-based observations centered on the EBV framework, the thesis demonstrates how EBVs can be operationalized for biodiversity monitoring in Ghana. The key features and objectives of the thesis are explained as follows:

a) Objective 1 is addressed in Paper I, which focused on estimating tree species diversity using PlanetScope imagery in combination with field-based diversity indices. Falling under the EBV habitat structure and species composition classes, the study demonstrated strong relationships between spectral signals and field-measured diversity indices. This addressed the gap between localized biodiversity and spatially continuous monitoring.
b) Objective 2 is addressed in Paper II, which developed a proposed ISO 19144-2-based national land cover legend and dataset for Ghana. It also assesses the challenges and opportunities for its adoption within the EBV ecosystem structure class. This was done through a structured expert survey of stakeholders from Ghana and the international community, complemented by land cover classification using the random forest approach on Sentinel-2 and Sentinel-1 data. The study highlights how harmonized land cover frameworks can improve interoperability, accuracy, and adoption of standards in tropical forest monitoring.
c) Objective 3 is addressed in Paper III, an approach for mapping the distribution and abundance of dominant tree species in Ghana and evaluating their implications for conservation prioritization under the EBV species distribution class. Presence-only

occurrence data from GBIF were combined with climatic, topographic, edaphic, and land cover predictors in species distribution models (SDMs) using MaxEnt.

d) Objective 4 is addressed in Paper IV by examining the effects of climate change and forest fragmentation on aboveground biomass under the EBV ecosystem structure class. A space-for-time substitution approach was used, applying the AI as a proxy for climatic stress across ecological zones. AGB estimates from ESA-CCI biomass products were integrated with fragmentation metrics and biodiversity indicators, and both linear and nonlinear approaches were tested.

The objectives and thesis are structured on the hypothesis, which is answered as follows:

a) **Hypothesis**: There is a significant relationship between PlanetScope spectral variability and field-measured tree species diversity indices.

   Answer: Supported in Paper I. Regression and correlation analysis showed that spectral indices, especially those derived from red-edge and near-infrared (NIR) bands, were strong predictors of H', D_2, S, and H' indices, confirming the capacity of PlanetScope imagery to predict tree species diversity.

b) **Hypothesis**: An ISO 19144-2-based land cover legend and dataset improve classification accuracy, interoperability, and usability of land cover information.

   Answer: Both experts engaged through the survey conducted, and the application of land cover standards in generating a land cover legend and dataset demonstrated the added value of standardized land cover data for improving accuracy and enhancing interoperability.

c) **Hypothesis:** Species distribution models combined with abundance estimates can identify priority areas for conservation.

   Answer: while highlighting gaps in protected area coverage, SDMs and abundance analysis produced reliable suitability and species richness maps, identifying hotspots and priority conservation areas.

d) **Hypothesis (H1a)**: Decreasing AI (aridification) reduces AGB, with humid zones (higher AI) maintaining higher mean AGB than semi-arid zones.

   Answer: Confirmed in Paper IV, the ANOVA analysis performed demonstrated significant differences in AGB across the different AI zones.

   Hypothesis (H1b): Decreasing AI (aridification) has an indirect effect on AGB, mediated by forest fragmentation and biodiversity.

   Answer: Through SEM, the hypothesis was confirmed that AI has an indirect effect on AGB, with this effect being mediated by forest fragmentation. However, biodiversity did not emerge as a significant mediating factor in the relationship between AI and AGB.

Hypothesis (H2): AGB exhibits a nonlinear response to structural attributes of fragmentation (Fragmentation metrics) with varying contributions across different dimensions of fragmentation.

Answer: Through the GAM analysis again in Paper IV, results revealed threshold and unimodal responses between fragmentation metrics and AGB. GAMs highlighted nonlinear fragmentation effects.

5.2 Summary of used methodological approaches.

Before the application of the methodological approach in this thesis, a systematic literature review was conducted using Web of Science and Scopus to synthesize the current state of biodiversity monitoring at national and global levels, with a focus on the integration of RS, and the Essential Biodiversity Framework and its application in some specific countries, such as Finland. The Preferred Reporting Items for Systematic Reviews and Meta-Analysis (PRISMA) approach was employed, utilizing selected keywords to identify the most relevant studies, thereby enabling the thesis to situate the methodological framework within ongoing research efforts.

Field data collection was conducted at the BFR to obtain plot-level biodiversity information. Field plots were established, whereby information on tree species was recorded and identified. Species diversity indices, including H', D_2, S, and J', were computed and linked with remotely sensed metrics derived from PlanetScope imagery. Regression models and correlation analysis were used to establish relationships between spectral indices (optical bands, NDVI, EVI, SAVI, NDRE) and field-derived diversity measures (H', D_2, S, and J'), bridging the gap between plot-level observations and spatially continuous monitoring.

A structured questionnaire survey was developed and distributed to stakeholders in Ghana and internationally, targeting experts in land cover mapping, biodiversity monitoring, and geospatial standards. The survey examined the opportunities and challenges associated with adopting ISO 19144-2 land cover standards, offering insights into interoperability, data sharing, and institutional capacities. A national land cover legend was developed following the West African Land Cover Reference System (WLCRS) and aligned with ISO 19144-2 standards to complement the survey. The process involved selecting land cover classes relevant to Ghana's ecosystems through consultation with national stakeholders, ensuring that the legend reflected ecological reality and policy needs. Training data for each class were collected through visual interpretation of high-resolution imagery and expert knowledge with the Collect Earth online (CEO) platform. Using this harmonized legend and training dataset, Sentinel-1 (VV/VH, as well as ratios of these polarizations, and texture variables) and Sentinel-2 (spectral bands, vegetation indices, and textural variables) imagery were used to perform a classification with the Random Forest algorithm in Google Earth Engine. Hyperparameters were tuned using a

grid search optimization to maximize classifier performance. Classification accuracy was evaluated with respect to independent validation samples (30%), and accuracy parameters, including overall accuracy, user's and producer's accuracy, and kappa coefficient.

Species distribution and abundance monitoring were conducted for three dominant tree species using presence data from GBIF together with environmental predictors from bioclimatic variables, soils, topography, and land cover layers. SDMs were fitted using the MaxEnt algorithm with spatial blocking cross-validation to minimize autocorrelation, resulting in continuous habitat suitability maps. Species abundance was estimated using ZIP models, which handle excess zeros in ecological data. Bootstrap resampling was applied to quantify prediction uncertainty. Species richness was mapped by summarizing binary presence-absence predictions from the SDMs, with cells showing overlap of all tree species identified as hotspots. A composite index was created to prioritize conservation by combining habitat suitability and abundance predictions, with the top 10% of values designated as high-priority areas. These results were overlaid with the data on Ghana's protected area networks (PAs) to evaluate coverage and identify biodiversity hotspots outside the PA network.

Together, these approaches combined RS, field surveys, expert knowledge, and advanced ecological modeling to operationalize EBVs for biodiversity monitoring in Ghana, ensuring methodological rigor and policy relevance, ensuring that a standard set of EBV variables exists for biodiversity monitoring in Ghana, and making progress toward achieving the Aichi Targets and all biodiversity-related targets.

Multiple datasets were integrated at the plot level to investigate the effects of climate change on AGB mediated by fragmentation and biodiversity. Tree species occurrence data were first obtained from the GBIF database. For each occurrence point, climatic conditions were characterized by extracting values from AI, which provides long-term estimates of aridity. AGB estimates were obtained at the exact locations from the ESA-CCS global biomass datasets (100 m resolution, reference year 2020), ensuring consistency in spatial alignment with the climatic dataset. Forest fragmentation metrics were derived from the National Land Cover Map (reference year 2023). The database was reclassified into two categories: binary forest and non-forest. Using the forest binary raster, fragmentation indices were computed with the landscapemetrics package in R. The metrics included NP, ED, AREA_MN, LSI, and MSI, capturing both path-level and landscape-level fragmentation patterns. To examine the effects of climatic influences on biomass, the global aridity index dataset was used and grouped into four aridity classes based on the UNEP aridity classification scheme: humid, sub-humid, dry-sub-humid, and semi-arid aridity zones. A space-for-time substitution approach was employed, where variation across aridity zones served as a proxy for projected temporal changes in climate. Statistical differences in mean AGB among aridity zones were tested using ANOVA

and Scheffé's multiple comparison test to identify significant pairwise differences. The SEM approach examined the pathways through which aridity (AI) influences aboveground biomass (AGB). The SEM results assessed both the direct effects of AI on AGB and the indirect effects mediated through fragmentation and biodiversity. Both linear SEMs and nonlinear SEMs were tested to capture flexible, potentially threshold-based relationships. Model fit was assessed using Fisher's AIC and directed separation test. As a complementary approach, spatial GAMs were fitted to explore the functional forms of fragmentation and biodiversity effects on AGB while controlling for aridity.

5.2.1 Limitations of the methodological approaches

The methodological approach for the literature review was only focused on the review of articles and did not consider conference proceedings, technical reports, or institutional documents. As a result, some emerging practices and methods may have been ignored. Some data-fusion modalities relevant to national-scale biodiversity monitoring were only partially captured, including an extensive review on the multitemporal fusion of RS data, co-registration adjustment practices with SAR datasets, and species occurrence (GBIF) data bias, among others. The review of RS preprocessing steps emphasized general principles without exhaustively assessing those consequential in tropical environments.

In Paper I, the estimation of tree species diversity relied mainly on optical RS from PlanetScope in combination with field-derived indices (H', D_2, S, and J'). While the approach demonstrated strong relationships between spectral variability and species diversity, the methodology had a limited scope. Other sensor types, such as LiDAR or radar, were not included, and they could capture complementary structural and non-optical vegetation properties. Similarly, the environmental predictor set was restricted, meaning potentially important ecological gradients were not fully incorporated. Another limitation was the relatively small sample size, since field data collection was constrained by accessibility in the forest reserve. As such, model robustness could be affected, and results may vary if larger datasets were available.

In Paper II, one of the key components of the EBV framework implementation and ISO 19144-2-based national land cover standards is the need for broad collaboration and stakeholder engagement with as many institutions and users of land cover data as possible, especially those reporting to international frameworks. Although this study engaged stakeholders through collaboration efforts with FAO, time and resource limitations meant that consultations were predominantly online and restricted to a few institutions. Feedback from the survey also highlighted the need for capacity development and training in applying the land cover legends and standards, beyond the availability of manuals. The FAO has since initiated follow-up engagements through the Soil Information and Resilience project (SoilFER). As part of this process, I led a team in Ghana to initiate stakeholder engagement and collect training data for

validating the land cover dataset. Nonetheless, continuous stakeholder consultations are necessary for gathering feedback and ensuring long-term adoption. Furthermore, although the photo interpretation approach with the CEO platform proved useful in generating training data, the process relies extensively on local knowledge, which may not always be available. Further applications in other countries should invest in systematic nationwide field data collection and broader stakeholder consultations.

In paper III, species distribution and abundance models were developed to map dominant species using occurrence-based tree species records from GBIF and environmental predictors. A key limitation lies in the spatial autocorrelation of GBIF data, which are concentrated in accessible areas, leaving large regions under sampled. This bias reduces the representativeness of the models and introduces uncertainty in less-sampled zones. Moreover, the models inherently assume that presence data reflect the true ecological niches of species, while fine-scale processes such as disturbance regimes and interactions are not accounted for. Abundance estimation using ZIP models captured general patterns but showed variable predictive performance, particularly in areas with sparse occurrence data.

Paper IV analyzed the effects of climate change and forest fragmentation on AGB using global datasets: ESA-CCI biomass and validated with GEDI footprints, the Global AI, and Copernicus land cover products. A limitation of this methodology is the partial temporal mismatch across datasets: the AI is based on long-term climatic averages from 1970 to 2000, while the biomass data reflect conditions around 2017 to 2020. This mismatch could introduce uncertainty, although the datasets remain ecologically relevant. Additionally, fragmentation metrics were derived from binary forest/non-forest classifications, which simplified complex land cover characteristics and may overlook subtle yet ecologically important land use transitions. The biodiversity component relied on limited field-based indices, which constrained the ability to fully capture species-biomass interactions.

While these findings are informative, they must be interpreted cautiously, given data limitations, and should be strengthened with expanded field surveys and long-term monitoring.

5.3 Key findings

Implementing the EBV framework in Ghana provided an opportunity to address key biodiversity monitoring challenges through expert consultation, RS, field surveys, and advanced modeling. Results from the four research articles collectively demonstrate how EBVs, ranging from ecosystem structure to community composition and species population, can be operationalized to improve monitoring, reporting, and conservation planning in tropical systems.

The most important results from the paper I are the established relationship between species diversity and spectral information of the PlanetScope satellite data. Linking field-based indices to PlanetScope showed that *S* and *H'* were the diversity dimensions most consistently captured by spectral signals. Bands 6 (red) exhibited the strongest relationship (*S*: r = 0.61, $p < 0.001$; *H'*: r = 0.58, $p < 0.01$), complemented by Band 2 (blue), while most vegetation indices (NDVI, NDRE, SAVI, SRI), were negatively related to *S* and *H'*, with NDRE strongest (r = −0.48, $p < 0.05$). Forward stepwise regression retained Bands 6 and 2 for both S ($R^2 = 0.47$; RMSE = 1.00; AIC = 85.15) and *H'* ($R^2 = 0.42$; RMSE = 0.17; AIC = −10.74), yielding spatial predictions that revealed moderate, heterogeneous diversity with localized hotspots. D^2 and *J'* were not modeled due to their weak or non-significant correlations, enforcing the point that *S* and *H'* are the most significant diversity under these conditions (Aklilu Tesfaye & Gessesse Awoke, 2021; Conti et al., 2021; Gyamfi-Ampadu et al., 2021).

The systematic analysis of land cover legends and classification approaches revealed substantial inconsistencies between global and national datasets, often driven by semantic ambiguities, coarse spatial resolution, and differences in land cover class definitions. (Mushtaq et al., 2022). The study implemented an ISO-based national land cover legend to address these issues, relying on the WALCRS and the international standards described in ISO 19144-2. The process involved consultation with stakeholders and creating a land cover legend of 37 classes tailored to reflect Ghana's heterogeneous landscape, including plantations such as oil palm, rubber, specific agroforestry systems, mining sites, and salt pans, which are absent from global products. The subsequent RF classification of Sentinel-1 and Sentinel-2 imagery in GEE, supported by systematic hyperparameter tuning and validation, produced a 2023 national land cover dataset with an overall accuracy of 90%. Mining sites and built-up areas achieved the highest accuracy, while savanna and cultivated lands showed expected confusion due to spectral similarity. Importantly, this national product revealed significant discrepancies in global datasets: built-up areas reported 3.9% by the Environmental Systems Research Institute (ESRI) and 1.3% by MODIS, while the national dataset recorded 1.9% for built-up; cropland estimates by ESRI were 3.8% and 10.9% for MODIS, contrasted sharply with 46.5% for the national land cover (Njomaba, Mushtaq, et al., 2025). These divergence in land cover

percentages mirrors findings from Herold et al. (2006) and Tsendbazar et al. (2016), who have documented cropland differences of up to 30%, consistent with the overestimation of urban areas in coarse products. Incorporating the WALCRS, Ghana's national land cover achieved greater ecological relevance and interoperability, echoing the experience of the Gambia, where the adoption of the WALCRS reduced cropland estimation errors by 22% compared to MODIS (Gregorio et al., 2022). The results underscore the necessity of regionalized standards for REDD+, greenhouse gas reporting, and SDG monitoring. Nevertheless, adoption challenges remain for capacity building, language translation, and consistent documentation across institutions. As highlighted by stakeholder feedback and presented in Paper II, training and continuous engagement are required to ensure long-term sustainability and usability of standardized legends in West Africa.

The most important finding in paper III was the mapping of tree species distribution and the estimation of population abundance of tree species across Ghana. Screening of 1,756 species across 282 plots identified the three dominant species as *Napoleaonaea leonensis* (18.1% of plots, *Myrianthus serratus* (13.8%), and *Penianthus patulinervis* (6.4%) for modeling. MaxEnt models performed strongly (AUC 0.93 – 0.96; Kappa 0.72 – 0.82; TSS 0.76 – 0.85), with key predictors including soil texture, slope, forest cover, and bioclimatic variables (BIO6, BIO19, BIO3). Abundance models (ZIP) showed the best fit for *Penianthus patulinervis* (Pseudo R^2 = 0.632), with uncertainty lowest in core abundance regions. Species richness was concentrated in the south-western moist evergreen/transition belts, with higher richness inside PAs (mean = 0.102) than outside (0.019). A composite conservation index (suitability x abundance) mapped 23.3 Mha of hotspots, ~30% within current PAs and ~70% outside, indicating significant protection gaps.

The most important finding in Paper IV was the use of SEM to provide deeper insights into the causal pathways of aridity, fragmentation, biomass, and biodiversity. Results showed that aridity affected AGB directly (wetter conditions supported higher biomass, while drier conditions resulted in lower biomass) and indirectly, through fragmentation. Drier aridity zones were associated with higher fragmentation metrics, significantly reducing AGB. This highlights the mediating role of fragmentation in carbon loss, consistent with Brinck et al. (2017), who demonstrated that dry tropical forests are particularly vulnerable to fragmentation under climate and land-use pressures.

The GAMs also revealed nonlinear relationships between fragmentation metrics and AGB. Among the five fragmentation metrics, AREA_MN exhibited the strongest contributions with a unimodal response peaking at intermediate patch size. This suggests that moderately sized patches may maximize carbon storage by balancing interior habitat and edge effects, whereas large patches reduce AGB. Similar unimodal or hump-shaped relationships between patch size

and ecosystem functions have been observed in the tropical regions, where moderate fragmentation enhances heterogeneity before degradation dominates (Arroyo-Rodríguez & Fahrig, 2014)

6. International Collaborations and Achievements

A strong international collaboration was established as part of this Ph.D. study. Paper II was conducted in collaboration with consultants and researchers from the Geospatial Unit of FAO. This collaboration formed part of the SoilFER project, which aims to improve agricultural livelihoods and build the resilience of agrifood systems in Central America and Sub-Saharan Africa, specifically in Guatemala, Honduras, Zambia, Kenya, and Ghana. The Geospatial Unit of FAO is engaged in two main components of the SoilFER project: (i) Development of improved crop models to enhance agricultural productivity, (ii) Development of a global decision-support platform for localized decision-making.

For Ghana, and in alignment with one of the objectives of this thesis, collaboration with FAO led to the production of an ISO-based national land cover legend and dataset. This dataset is intended to serve as a core input for suitability modeling, which will, in turn, provide outputs required to support the project's decision-making and agricultural planning processes.

7. Conclusion and recommendations

This dissertation was premised on the need to define a standard set of biodiversity variables from the EBVs framework that can be monitored in Ghana by integrating satellite RS data and field-based observations. The work focused on two key EBV classes: Ecosystem structure (land cover, forest fragmentation, and above-ground biomass) and species populations (species diversity, distribution, and abundance). These variables were derived from multiple sources, including RS datasets (PlanetScope, Sentinel-1, Sentinel-2, ESA Biomass, and Copernicus Land Cover dataset), field inventories, global biodiversity repositories such as GBIF, and ancillary global datasets (AI, bioclimatic variables, soils, and topography). This thesis generated robust and nationally relevant biodiversity indicators by combining global datasets, field observations, RS, and statistical and ecological modeling approaches. The outcomes presented in papers I-IV demonstrate that RS and EBV-based monitoring can provide scalable, reproducible, and cost-effective tools to support biodiversity management, conservation planning, and national reporting obligations. The overall conclusion is that EBVs can be operationalized in Ghana by integrating satellite and field-based data, providing a scientifically sound pathway for long-term biodiversity monitoring and policy support.

In paper I, the study showed that high-resolution optical satellite data, such as PlanetScope, can predict three species diversity with significant correlations to the visible spectral bands,

particularly red and blue. The findings confirmed that optical spectral signals contain strong ecological information linked to pigment content and canopy structure.

Paper II demonstrated the operationalization of ISO-based land cover standards in Ghana by developing a national land cover legend and dataset based on the ISO 19144-2 framework and the WALCRS. Using Sentinel-1 and Sentinel-2 with a Random Forest classifier, the study achieved a higher classification accuracy (overall accuracy of 90% with robust user and producer accuracies), 1outperforming widely used global land cover products. Thus, it confirmed the suitability of ISO-based standards for generating reliable, nationally relevant land cover datasets. A structured stakeholder survey further complemented the technical assessment by engaging experts. The survey revealed key challenges to adoption, including a lack of proper documentation, cost implications, and complexity of standards, leading to inconsistent use of terminologies. Nonetheless, stakeholders highlighted several meaningful opportunities, notably the potential of standardized land cover products to support decision-making and policy development, enhance data accuracy and reliability, and strengthen Ghana's capacity for monitoring, reporting, and verification in line with international standards.

In Paper III, species distribution and abundance models were developed for three dominant forest tree species using GBIF and field occurrence data. MaxEnt models performed strongly, while ZIP regressions mapped abundance and identified uncertainty patterns. Richness and composite index revealed biodiversity hotspots in Ghana's moist semi-deciduous and transitional zones. This confirms the existence of major conservation gaps.

In paper IV, the analysis confirmed that climate change, represented as aridity, has both direct and indirect effects on AGB. Using a space-for-time substitution, the study demonstrated that biomass declines systematically from humid to semi-arid zones, with transitional forests showing the steepest declines. Fragmentation further mediated the indirect effects of aridity on AGB through increased patch density, reduced patch size, and irregular configuration. These findings highlight the importance of addressing both climatic and structural drivers of biomass loss.

This dissertation demonstrates that EBVs can be operationalized in Ghana by integrating RS data, field inventories, global repositories, and ecological modeling approaches and relying on a minimum set of key essential biodiversity variables. Collectively, the dissertation establishes one of the first nationally based EBV frameworks in Africa, producing scalable and reproducible indicators under Ghana's NBSAP and related international commitments. The framework is relevant for national and regional efforts in biodiversity protection and provides a transferable framework for other Sub-Saharan African countries to strengthen biodiversity monitoring systems. However, future works should consider the following recommendations:

i) Enhanced ground-based validation and field data integration: While the image interpretation approach using the CEO platform, combined with global biodiversity repositories like GBIF, proved effective for training and validation in this study, incorporating large-scale and long-term field data collection would enhance the reliability of land cover data and biodiversity indicators. Acquiring systematic ground-based inventories across ecological zones, including the establishment of permanent field plots to conduct species abundance surveys, would improve biomass estimation accuracy, strengthen species distribution and abundance models, and reduce uncertainties associated with spatial biases in existing datasets.

ii) Adoption of time-series analysis: extending beyond a single-year classification to multi-year or decadal datasets will capture seasonal variability and long-term biodiversity trends, including deforestation rates and land cover change trajectories.

iii) Integration of multi-sensor datasets: combining optical, SAR, and LiDAR datasets will help to reduce spectral confusion, improve biomass estimates, and better capture forest complexity.

iv) Strengthening stakeholder engagement: building local capacity, developing clear documentation, and removing the technical and financial barriers to adopting land cover standards will improve uptake by national agencies and practitioners.

v) Developing EBV translation protocols: creating protocols to harmonize national EBVs with global biodiversity monitoring initiatives will facilitate interoperability and ensure that the contributions of nations are aligned with international reporting systems.

vi) Prioritizing conservation gaps: Translating hotspot maps into policy actions by expanding protection and connectivity in under-protected moist semi-deciduous and transitional zones will redirect the focus of national biodiversity monitoring towards those hotspots, ensuring effective forest management practices.

8. References

Abbam, T., Johnson, F. A., Dash, J., & Padmadas, S. S. (2018). Spatiotemporal Variations in Rainfall and Temperature in Ghana Over the Twentieth Century, 1900–2014. *Earth and Space Science*, *5*(4), 120–132. https://doi.org/10.1002/2017EA000327

Addo-Fordjour, P., Anning, A. K., Larbi, J. A., & Akyeampong, S. (2009). Liana species richness, abundance, and relationship with trees in the Bobiri forest reserve, Ghana: Impact of management systems. *Forest Ecology and Management*, *257*(8), 1822–1828. https://doi.org/10.1016/j.foreco.2009.01.051

Addo-Fordjour, P., Obeng, S., Anning, A., & Addo, M. (2009). Floristic composition, structure, and natural regeneration in a moist semi-deciduous forest following anthropogenic disturbances and plant invasion. *International Journal of Biodiversity and Conservation*, *1*, 21–37.

Aiello-Lammens, M. E., Boria, R. A., Radosavljevic, A., Vilela, B., & Anderson, R. P. (2015). spThin: An R package for spatial thinning of species occurrence records for use in ecological niche models. *Ecography*, *38*(5), 541–545. https://doi.org/10.1111/ecog.01132

Aklilu Tesfaye, A., & Gessesse Awoke, B. (2021). Evaluation of the saturation property of vegetation indices derived from sentinel-2 in mixed crop-forest ecosystem. *Spatial Information Research*, *29*(1), 109–121. https://doi.org/10.1007/s41324-020-00339-5

Alberto, L., Isuhuaylas, V., & Torobeo, N. S. (2018). *Natural Forest Mapping in the Andes (Peru): A Comparison of the Performance of Machine-Learning Algorithms*. https://doi.org/10.3390/rs10050782

Arekhi, M., Yılmaz, O. Y., Yılmaz, H., & Akyüz, Y. F. (2017). Can tree species diversity be assessed with Landsat data in a temperate forest? *Environmental Monitoring and Assessment*, *189*(11). https://doi.org/10.1007/s10661-017-6295-6

Arroyo-Rodríguez, V., & Fahrig, L. (2014). Why is a landscape perspective important in studies of primates? *American Journal of Primatology*, *76*(10), 901–909. https://doi.org/10.1002/ajp.22282

Asare. (2021). *Plants of Ghana. Version 1.1*. Ghana Herbarium. Occurrence Dataset. https://doi.org/10.15468/e8rhqm

Asner, G. P., Martin, R. E., Knapp, D. E., Tupayachi, R., Anderson, C. B., Sinca, F., Vaughn, N. R., & Llactayo, W. (2017). Airborne laser-guided imaging spectroscopy to map forest trait diversity and guide conservation. *Science*, *355*(6323), 385–389. https://doi.org/10.1126/science.aaj1987

Azzari, G., & Lobell, D. B. (2017). Landsat-based classification in the cloud: An opportunity for a paradigm shift in land cover monitoring. *Remote Sensing of Environment*, *202*, 64–74. https://doi.org/10.1016/j.rse.2017.05.025

Bergen, K. M., Goetz, S. J., Dubayah, R. O., Henebry, G. M., Hunsaker, C. T., Imhoff, M. L., Nelson, R. F., Parker, G. G., & Radeloff, V. C. (2009). Remote sensing of vegetation 3-D structure for biodiversity and habitat: Review and implications for lidar and radar spaceborne missions. *Journal of Geophysical Research: Biogeosciences*, *114*(4), 1–13. https://doi.org/10.1029/2008JG000883

Blois, J. L., Williams, J. W., Fitzpatrick, M. C., Jackson, S. T., & Ferrier, S. (2013). Space can substitute for time in predicting climate-change effects on biodiversity. *Proceedings of the National Academy of Sciences of the United States of America*, *110*(23), 9374–9379. https://doi.org/10.1073/pnas.1220228110

Bonsu, K., & Bonin, O. (2023). Assessing landscape fragmentation and its implications for biodiversity conservation in Ghana's Greater Accra Metropolitan Area (GAMA). *Discover Environment*, *1*(1). https://doi.org/10.1007/s44274-023-00023-z

Booth, T. H. (2025). The Origins of Modern Species Distribution Modeling: Some Comments on the Vasconcelos et al. (2024) Review. *Earth (Switzerland)*, *6*(1), 12–15. https://doi.org/10.3390/earth6010012

Brinck, K., Fischer, R., Groeneveld, J., Lehmann, S., Dantas De Paula, M., Pütz, S., Sexton, J. O., Song, D., & Huth, A. (2017). High resolution analysis of tropical forest fragmentation and its impact on the global carbon cycle. *Nature Communications*, *8*. https://doi.org/10.1038/ncomms14855

Bruggisser, M., Dorigo, W., Dostálová, A., Hollaus, M., Navacchi, C., Schlaffer, S., & Pfeifer, N. (2021). Potential of sentinel-1 c-band time series to derive structural parameters of temperate deciduous forests. *Remote Sensing*, *13*(4), 1–30. https://doi.org/10.3390/rs13040798

Cardinale, B. J., Duffy, J. E., Gonzalez, A., Hooper, D. U., Perrings, C., Venail, P., Narwani, A., Mace, G. M., Tilman, D., Wardle, D. A., Kinzig, A. P., Daily, G. C., Loreau, M., Grace, J. B., Larigauderie, A., Srivastava, D. S., & Naeem, S. (2012). Biodiversity loss and its impact on humanity. *Nature*, *486*(7401), 59–67. https://doi.org/10.1038/nature11148

Carlo, H. R., Herman, P., & Soetaery, K. (1998). Indices of diversity and evenness. *Oceanis*, *24*(4), 61–87. https://doi.org/10.1016/j.hal.2004.08.006

Carranza, M. L., Frate, L., Acosta, A. T. R., Hoyos, L., Ricotta, C., & Cabido, M. (2014). Measuring forest fragmentation using multitemporal remotely sensed data: Three decades of change in the dry Chaco. *European Journal of Remote Sensing*, *47*(1), 793–804. https://doi.org/10.5721/EuJRS20144745

Cavender-Bares, J., Gamon, J. A., & Townsend, P. A. (2020). *Remote Sensing of Plant Biodiversity*.

CBD. (2016). *Fifth National Report to the Convention on Biological Diversity: Ghana*.

CEO. (2018). *Collect Earth Online*. https://collect.earth/

Chave, J., Condit, R., Lao, S., Caspersen, J. P., Foster, R. B., & Hubbell, S. P. (2003). Spatial and temporal variation of biomass in a tropical forest: Results from a large census plot in Panama. *Journal of Ecology*, *91*(2), 240–252. https://doi.org/10.1046/j.1365-2745.2003.00757.x

Chiang, S. H., Valdez, M., & Chen, C. F. (2016). Forest tree species distribution mapping using Landsat satellite imagery and topographic variables with the Maximum Entropy method in Mongolia. *International Archives of the Photogrammetry, Remote Sensing and Spatial Information Sciences - ISPRS Archives*, *41*(July), 593–596. https://doi.org/10.5194/isprsarchives-XLI-B8-593-2016

Conchedda, G., & Tubiello, F. N. (2021). *Land cover statistics Global , regional and country trends*. Food and Agricultural Organization of the United Nations.

Conti, L., Malavasi, M., Galland, T., Komárek, J., Lagner, O., Carmona, C. P., Bello, F. De, Rocchini, D., & Šímová, P. (2021). *The relationship between species and spectral diversity in grassland communities is mediated by their vertical complexity*. *June*, 1–8. https://doi.org/10.1111/avsc.12600

De Simone, L., Ouellette, W., & Gennari, P. (2022). Operational Use of EO Data for National Land Cover Official Statistics in Lesotho. *Remote Sensing*, *14*(14). https://doi.org/10.3390/rs14143294

Díaz, S., Settele, J., Brondízio, E. S., Ngo, H. T., Agard, J., Arneth, A., Balvanera, P., Brauman, K. A., Butchart, S. H. M., Chan, K. M. A., Garibaldi, L. A., Ichii, K., Liu, J., Subramanian, S. M., Midgley, G. F., Miloslavich, P., Molnár, Z., Obura, D., Pfaff, A., … Zayas, C. N. (2019). Pervasive human-driven decline of life on Earth points to the need for transformative change. *Science*, *366*(6471), eaax3100. https://doi.org/10.1126/science.aax3100

Djagbletey, G. (2014). *Impact of Selective Logging on Plant diversity, Natural Recovery, and Vegetation Carbon Stock: The case of Bobiri Forest Reserve*. Kwame Nkrumah University of Science and Technology.

Drusch, M., Del Bello, U., Carlier, S., Colin, O., Fernandez, V., Gascon, F., Hoersch, B., Isola, C., Laberinti, P., Martimort, P., Meygret, A., Spoto, F., Sy, O., Marchese, F., & Bargellini, P. (2012). Sentinel-2: ESA's Optical High-Resolution Mission for GMES Operational Services. *Remote Sensing of Environment*, *120*, 25–36. https://doi.org/10.1016/j.rse.2011.11.026

Elith, J., & Leathwick, J. R. (2009). Species distribution models: Ecological explanation and prediction across space and time. *Annual Review of Ecology, Evolution, and Systematics*, *40*, 677–697. https://doi.org/10.1146/annurev.ecolsys.110308.120159

Enaruvbe, G. O., & Atafo, O. P. (2018). A Long-Term Assessment of Habitat Fragmentation in Coastal Wetlands, Niger Delta, Nigeria. *Ife Social Sciences Review*, *26*(1), 36–47.

Fagua, J. C., Jantz, P., Burns, P., Massey, R., Buitrago, J. Y., Saatchi, S., Hakkenberg, C., & Goetz, S. J. (2021). Mapping tree diversity in the tropical forest region of Chocó-Colombia. *Environmental Research Letters*, *16*(5). https://doi.org/10.1088/1748-9326/abf58a

FAO. (2020a). Global forest resources assessment. In *Food and Agricultural Organization of the United Nations*. https://doi.org/10.4324/9781315184487-1

FAO. (2020b). *Global Forest Resources Assessment 2020: Main Report*. Food and Agriculture Organization of the United Nations. https://doi.org/10.4060/ca9825en

Fassnacht, F. E., Latifi, H., Stereńczak, K., Modzelewska, A., Lefsky, M., Waser, L. T., Straub, C., & Ghosh, A. (2016). Review of studies on tree species classification from remotely sensed data. In *Remote Sensing of Environment* (Vol. 186, pp. 64–87). Elsevier Inc. https://doi.org/10.1016/j.rse.2016.08.013

Fisher, R. (1935). *The Design of Experiments*. Hafner Press.

Forestry Commission. (2015). *Forestry Commission Ghana National REDD+ Strategy*. *January*, 61.

Freeman, E. A., & Moisen, G. G. (2008). A comparison of the performance of threshold criteria for binary classification in terms of predicted prevalence and kappa. *Ecological Modelling*, *217*(1–2), 48–58. https://doi.org/10.1016/j.ecolmodel.2008.05.015

Fynn, I. E. M., & Campbell, J. (2019). Forest fragmentation analysis from multiple imaging formats. *Journal of Landscape Ecology(Czech Republic)*, *12*(1), 1–15. https://doi.org/10.2478/jlecol-2019-0001

Gaston, K. J. (2010). Valuing Common Species. *Science*, *327*(5962), 154–155. https://doi.org/10.1126/science.1182818

Geijzendorffer, I. R., Regan, E. C., Pereira, H. M., Brotons, L., Brummitt, N., Gavish, Y., Haase, P., Martin, C. S., Mihoub, J. B., Secades, C., Schmeller, D. S., Stoll, S., Wetzel, F. T., & Walters, M. (2016). Bridging the gap between biodiversity data and policy reporting needs: An Essential Biodiversity Variables perspective. *Journal of Applied Ecology*, *53*(5), 1341–1350. https://doi.org/10.1111/1365-2664.12417

Ghana Forestry Commission. (2018). *Framework for National Forest Monitoring System*.

Gibbs, H. K., Brown, S., Niles, J. O., & Foley, J. A. (2007). *Monitoring and estimating tropical forest carbon stocks : making REDD a reality*. https://doi.org/10.1088/1748-9326/2/4/045023

GOFC-GOLD. (2017). A sourcebook of methods and procedures for monitoring and reporting anthropogenic greenhouse gas emissions and removals associated with deforestation, gains and losses of carbon stocks in forests remaining forests, and forestation. In *GOFC-GOLD Report version COP18-1, (GOFC-GOLD Land Cover Project Office, Wageningen University, The Netherlands)*.

Gregorio, A. Di, Mushtaq, F., Aw, M., Henry, M., Mamane, B., Mahamane, M., Assoumana, B. T., Mimouni, M., Aubee, E., Enaruvbe, G. O., Mensah, F., Services, G. I., & Bartel, P. (2022). West African Land Cover Reference System. In *FAO report*. https://doi.org/10.4060/cc0730en

Griffiths, P., Kuemmerle, T., Baumann, M., Radeloff, V. C., Abrudan, I. V., Lieskovsky, J., Munteanu, C., Ostapowicz, K., & Hostert, P. (2014). Forest disturbances, forest recovery, and changes in forest types across the carpathian ecoregion from 1985 to 2010 based on landsat image composites. *Remote Sensing of Environment*, *151*, 72–88. https://doi.org/10.1016/j.rse.2013.04.022

Gyamfi-Ampadu, E., Gebreslasie, M., & Mendoza-Ponce, A. (2021). Evaluating multi-sensors spectral and spatial resolutions for tree species diversity prediction. *Remote Sensing*, *13*(5). https://doi.org/10.3390/rs13051033

Haase, P., Tonkin, J. D., Stoll, S., Burkhard, B., Frenzel, M., Geijzendorffer, I. R., Häuser, C., Klotz, S., Kühn, I., McDowell, W. H., Mirtl, M., Müller, F., Musche, M., Penner, J., Zacharias, S., & Schmeller, D. S. (2018). The next generation of site-based long-term ecological monitoring: Linking essential biodiversity variables and ecosystem integrity. *Science of the Total Environment*, *613–614*, 1376–1384. https://doi.org/10.1016/j.scitotenv.2017.08.111

Haddad, N. M., Brudvig, L. A., Clobert, J., Davies, K. F., Gonzalez, A., Holt, R. D., Lovejoy,

T. E., Sexton, J. O., Austin, M. P., Collins, C. D., Cook, W. M., Damschen, E. I., Ewers, R. M., Foster, B. L., Jenkins, C. N., King, A. J., Laurance, W. F., Levey, D. J., Margules, C. R., … Townshend, J. R. (2015). Habitat fragmentation and its lasting impact on Earth's ecosystems. *Science Advances*, *1*(2), 1–9. https://doi.org/10.1126/sciadv.1500052

Hansen, M. C., Potapov, P. V, Moore, R., Hancher, M., Turubanova, S. A., & Tyukavina, A. (2013). High-Resolution Global Maps of 21st-century forst cover change. *Science*, *342*(6160), 850–853.

Haub, C., Kleinewillinghöfer, L., Garcia, V., Eftas, M., Di, A., Fao, G., Gallego, J., Leo, O., Jrc, E. C., & Vito, Q. D. (2015). *Protocol for land cover validation*.

Hemmerling, J., Pflugmacher, D., & Hostert, P. (2021). Remote Sensing of Environment Mapping temperate forest tree species using dense Sentinel-2 time series. *Remote Sensing of Environment*, *267*(August), 112743. https://doi.org/10.1016/j.rse.2021.112743

Herold, M., Latham, J. S., Di Gregorio, A., & Schmullius, C. C. (2006). Evolving standards in land cover characterization. *Journal of Land Use Science*, *1*(2–4), 157–168. https://doi.org/10.1080/17474230601079316

Herold, M., Mayaux, P., Woodcock, C. E., Baccini, A., & Schmullius, C. (2008). Some challenges in global land cover mapping: An assessment of agreement and accuracy in existing 1 km datasets. *Remote Sensing of Environment*, *112*(5), 2538–2556. https://doi.org/10.1016/j.rse.2007.11.013

Hoffmann, J., Muro, J., & Dubovyk, O. (2022). Predicting Species and Structural Diversity of Temperate Forests with Satellite Remote Sensing and Deep Learning. *Remote Sensing*, *14*(7). https://doi.org/10.3390/rs14071631

Hooper, D., Adair, C., & C.Bradley. (2012). A global synthesis reveals biodiversity loss as a major driver of ecosystem change. *Nature*, *486*.

Immitzer, M., Vuolo, F., & Atzberger, C. (2016). *First Experience with Sentinel-2 Data for Crop and Tree Species Classifications in Central Europe*. https://doi.org/10.3390/rs8030166

IPBES. (2019). Summary for policymakers of the global assessment report on biodiversity and ecosystem services of the Intergovernmental Science-Policy Platform on Biodiversity and Ecosystem Services. S. Díaz, J. Settele, E. S. Brondízio E.S., H. T. Ngo, M. Guèze, J. Aga. In *Intergovernmental Science-Policy Platform on Biodiversity and Ecosystem Services* (Vol. 45, Issue 3).

ISO/TC 211. (2022). *ISO/TC 211 Geographic information/Geomatics*. https://www.iso.org/committee/54904.html

ISO 19144-2. (2012). *Geographic Information—Classification Systems—Part 2: Land Cover Meta Language (LCML)*.

Jaureguiberry, P., Titeux, N., Wiemers, M., Bowler, D. E., Coscieme, L., Golden, A. S., Guerra, C. A., Jacob, U., Takahashi, Y., Settele, J., Díaz, S., Molnár, Z., & Purvis, A. (2022). The direct drivers of recent global anthropogenic biodiversity loss. *Science Advances*, *8*(45), 1–11. https://doi.org/10.1126/sciadv.abm9982

Jetz, W., Mcgeoch, M. A., Guralnick, R., Ferrier, S., Beck, J., Costello, M. J., Fernandez, M., Geller, G. N., Keil, P., Merow, C., Meyer, C., Muller-karger, F. E., Pereira, H. M., & Regan, E. C. (2019). monitoring species populations. *Nature Ecology & Evolution*, *3*(April). https://doi.org/10.1038/s41559-019-0826-1

Joppa, L. N., O'Connor, B., Visconti, P., Smith, C., Geldmann, J., Hoffmann, M., Watson, J. E. M., Butchart, S. H. M., Virah-Sawmy, M., Halpern, B. S., Ahmed, S. E., Balmford, A., Sutherland, W. J., Harfoot, M., Hilton-Taylor, C., Foden, W., Minin, E. Di, Pagad, S., Genovesi, P., … Burgess, N. D. (2016). Filling in biodiversity threat gaps. *Science*, *352*(6284), 416–418. https://doi.org/10.1126/science.aaf3565

Joppa, L. N., & Pfaff, A. (2009). High and far: Biases in the location of protected areas. *PLoS ONE*, *4*(12), 1–6. https://doi.org/10.1371/journal.pone.0008273

Keith, D. A., Rodríguez, J. P., Rodríguez-Clark, K. M., Nicholson, E., Aapala, K., Alonso, A., Asmussen, M., Bachman, S., Basset, A., Barrow, E. G., Benson, J. S., Bishop, M. J., Bonifacio, R., Brooks, T. M., Burgman, M. A., Comer, P., Comín, F. A., Essl, F., Faber-Langendoen, D., … Zambrano-Martínez, S. (2013). Scientific Foundations for an IUCN Red List of Ecosystems. *PLoS ONE*, *8*(5). https://doi.org/10.1371/journal.pone.0062111

Kissling, W. D., Ahumada, J. A., Bowser, A., Fernandez, M., Fernández, N., García, E. A., Guralnick, R. P., Isaac, N. J. B., Kelling, S., Los, W., McRae, L., Mihoub, J. B., Obst, M., Santamaria, M., Skidmore, A. K., Williams, K. J., Agosti, D., Amariles, D., Arvanitidis, C., … Hardisty, A. R. (2018). Building essential biodiversity variables (EBVs) of species distribution and abundance at a global scale. *Biological Reviews*, *93*(1), 600–625. https://doi.org/10.1111/brv.12359

Lambert, D. (1992). Zero-inflated poisson regression, with an application to defects in manufacturing. *Technometrics*, *34*(1), 1–14. https://doi.org/10.2307/1269547

Laurance, W. F., Carolina Useche, D., Rendeiro, J., Kalka, M., Bradshaw, C. J. A., Sloan, S. P., Laurance, S. G., Campbell, M., Abernethy, K., Alvarez, P., Arroyo-Rodriguez, V., Ashton, P., Benítez-Malvido, J., Blom, A., Bobo, K. S., Cannon, C. H., Cao, M., Carroll, R., Chapman, C., … Zamzani, F. (2012). Averting biodiversity collapse in tropical forest protected areas. *Nature*, *489*(7415), 290–294. https://doi.org/10.1038/nature11318

Lawer, E. A. (2024). Predicting the impact of climate change on the potential distribution of a critically endangered avian scavenger, Hooded Vulture Necrosyrtes monachus, in Ghana. *Global Ecology and Conservation*, *49*(January), e02804. https://doi.org/10.1016/j.gecco.2024.e02804

Liu, Y., Gong, W., Hu, X., & Gong, J. (2018). Forest Type Identification with Random Forest Using Sentinel-1A, Sentinel-2A, Multi-Temporal Landsat-8 and DEM Data. *Remote Sensing*, 1–25. https://doi.org/10.3390/rs10060946

Lucas, R., Bunting, P., Clewley, D., Armston, J., Fairfax, R., Fensham, R., Accad, A., Kelley, J., Laidlaw, M., Eyre, T., Bowen, M., Carreiras, J., Bray, S., Metcalfe, D., Dwyer, J., & Shimada, M. (2010). An Evaluation of the ALOS PALSAR L-Band Backscatter—Above Ground Biomass Relationship Queensland, Australia: Impacts of Surface Moisture Condition and Vegetation Structure. *IEEE Journal of Selected Topics in Applied Earth Observations and Remote Sensing*, *3*(4), 576–593. https://doi.org/10.1109/JSTARS.2010.2086436

Ma, J., Li, J., Wu, W., & Liu, J. (2023). Global forest fragmentation change from 2000 to

2020. *Nature Communications*, *14*(1), 1–10. https://doi.org/10.1038/s41467-023-39221-x

Makinde, O. (2016). *Landscapes of West Africa: A Window on a Changing World*. https://doi.org/10.5066/F7N014QZ

Malhi, Y., Adu-Bredu, S., Asare, R. A., Lewis, S. L., & Mayaux, P. (2013). African rainforests: Past, present, and future. *Philosophical Transactions of the Royal Society B: Biological Sciences*, *368*(1625). https://doi.org/10.1098/rstb.2012.0312

Mapfumo, R. B., Murwira, A., Masocha, M., & Andriani, R. (2016). The relationship between satellite-derived indices and species diversity across African savanna ecosystems. *International Journal of Applied Earth Observation and Geoinformation*, *52*, 306–317. https://doi.org/10.1016/j.jag.2016.06.025

Maxwell, A. E., Warner, T. A., & Fang, F. (2018). Implementation of machine-learning classification in remote sensing: An applied review. *International Journal of Remote Sensing*, *39*(9), 2784–2817. https://doi.org/10.1080/01431161.2018.1433343

McGargical, K., Cushman, S., & Ene, E. (2023). *Spatial Pattern Analysis Program for Categorical Maps*. https://www.fragstats.org

Mensah, F., Mushtaq, F., Bartel, P., Abramowitz, J., Cherrington, E., Mahamane, M., Mamane, B., Dieye, A. M., Sanou, P., & Enaruvbe, G. (2024). Land Cover Mapping in West Africa : A Collaborative Process. *Land*, *13*(1712).

Mensah, S., Veldtman, R., Assogbadjo, A. E., Ham, C., Glèlè Kakaï, R., & Seifert, T. (2017). Ecosystem service importance and use vary with socio-environmental factors: A study from household surveys in local communities of South Africa. *Ecosystem Services*, *23*(February 2016), 1–8. https://doi.org/10.1016/j.ecoser.2016.10.018

Ministry of Environment, S. and T. National Biodiversity Strategy and Action Plan (2016 - 2020).

Morris, E. K., Caruso, T., Buscot, F., Fischer, M., Hancock, C., Maier, T. S., Meiners, T., Müller, C., Obermaier, E., Prati, D., Socher, S. A., Sonnemann, I., Wäschke, N., Wubet, T., Wurst, S., & Rillig, M. C. (2014). Choosing and using diversity indices: Insights for ecological applications from the German Biodiversity Exploratories. *Ecology and Evolution*, *4*(18), 3514–3524. https://doi.org/10.1002/ece3.1155

Mushtaq, F., Brien, C. D. O., Parslow, P., Åhlin, M., Gregorio, A. Di, Latham, J. S., & Henry, M. (2024). Land Cover and Land Use Ontology—Evolution of International Standards, Challenges, and Opportunities. *Land*, *13*(1202), 1–13.

Mushtaq, F., Henry, M., O'Brien, C. D., Di Gregorio, A., Jalal, R., Latham, J., Muchoney, D., Hill, C. T., Mosca, N., Tefera, M. G., Morteo, K., Franceschini, G., Ghosh, A., Tchana, E., & Chen, Z. (2022). An International Library for Land Cover Legends: The Land Cover Legend Registry. *Land*, *11*(7), 1083. https://doi.org/10.3390/land11071083

Mutowo, G., & Murwira, A. (2012). Relationship between remotely sensed variables and tree species diversity in savanna woodlands of Southern Africa. *International Journal of Remote Sensing*, *33*(20), 6378–6402. https://doi.org/10.1080/01431161.2012.687472

Myers, N., Mittermeier, R. A., Mittermeier, C. G., da Fonseca, G. A. B., & Kent, J. (2000). Biodiversity hotspots for conservation priorities. *Nature*, *403*(6772), 853–858. https://doi.org/10.1038/35002501

Nagendra, H. (2001). Using remote sensing to assess biodiversity. *International Journal of Remote Sensing*, *22*(12), 2377–2400. https://doi.org/10.1080/01431160117096

Newbold, T., Hudson, L. N., Hill, S. L. L., Contu, S., Lysenko, I., Senior, R. A., Börger, L., Bennett, D. J., Choimes, A., Collen, B., Day, J., De Palma, A., Díaz, S., Echeverria-Londoño, S., Edgar, M. J., Feldman, A., Garon, M., Harrison, M. L. K., Alhusseini, T., … Purvis, A. (2015). Global effects of land use on local terrestrial biodiversity. *Nature*, *520*(7545), 45–50. https://doi.org/10.1038/nature14324

Njomaba, E. (2025). *Ghana Land Cover Classification with Google Earth Engine*. GitHub Repository. https://github.com/Elisha-Njomaba/Ghana_LandCover_GEE

Njomaba, E., Aikins, B. E., & Surovy, P. (2025). Mapping species distribution and estimating population abundance of dominant forest tree species in Ghana: implications for conservation prioritization. *Trees, Forests and People*, *22*, 101019. https://doi.org/https://doi.org/10.1016/j.tfp.2025.101019

Njomaba, E., Mushtaq, F., Nagbija, R. K., Yakalim, S., Aikins, B. E., & Surovy, P. (2025). Adopting Land Cover Standards for Sustainable Development in Ghana: Challenges and Opportunities. *Land*, *14*(3), 550. https://doi.org/10.3390/land14030550

Njomaba, E., Ofori, J. N., Guuroh, R. T., Aikins, B. E., Nagbija, R. K., & Surový, P. (2024). Assessing Forest Species Diversity in Ghana's Tropical Forest Using PlanetScope Data. *Remote Sensing*, *16*(3), 1–16. https://doi.org/10.3390/rs16030463

Ofori, S. A., Dwomoh, J., Yeboah, E. O., Martin, A. L., Nti, S., Philip, A., & Asante, C. (2024). An ecological study of galamsey activities in Ghana and their physiological toxicity. *Asian Journal of Toxicology, Environmental, and Occupational Health*, *2*(1), 53–72. https://doi.org/10.61511/ajteoh.v2i1.2024.395

Oli, B. N., & Subedi, M. R. (2015). Effects of management activities on vegetation diversity, dispersion pattern and stand structure of community-managed forest (Shorea robusta) in Nepal. *International Journal of Biodiversity Science, Ecosystem Services and Management*, *11*(2), 96–105. https://doi.org/10.1080/21513732.2014.984334

Oliver, T. H., Heard, M. S., Isaac, N. J. B., Roy, D. B., Procter, D., Eigenbrod, F., Freckleton, R., Hector, A., Orme, C. D. L., Petchey, O. L., Proença, V., Raffaelli, D., Suttle, K. B., Mace, G. M., Martín-López, B., Woodcock, B. A., & Bullock, J. M. (2015). Biodiversity and Resilience of Ecosystem Functions. *Trends in Ecology & Evolution*, *30*(11), 673–684. https://doi.org/10.1016/j.tree.2015.08.009

Pan, Y., Birdsey, R., Fang, J., Houghton, R., Kauppi, P., Kurz, W., Phillips, O., Shvidenko, A., Lewis, S., Canadell, J., Ciaias, P., Jackson, R., Pacala, S., Mcguire, D., Piao, S., Rautiainen, A., Sitch, S., & Hayes, D. (2011). A Large and Persistent Carbon Sink in the World's Forests. *Science*, *333*(6045), 988–993. https://doi.org/DOI: 10.1126/science.1201609

Pandit, R., Parrota, J., Anker, Y., Coudel, E., Diaz Morejón, C. F., Harris, J., Karlen, D. L., Kertész, Á., Mariño De Posada, J. L., Ntshotsho Simelane, P., Tamin, N. M., & Vieira, D. L. M. (2018). Responses to halt land degradation and to restore degraded land. *Assessment Report on Land Degradation and Restoration*, *September*, 435–528.

Pasetto, D., Arenas-Castro, S., Bustamante, J., Casagrandi, R., Chrysoulakis, N., Cord, A. F., Dittrich, A., Domingo-Marimon, C., El Serafy, G., Karnieli, A., Kordelas, G. A.,

Manakos, I., Mari, L., Monteiro, A., Palazzi, E., Poursanidis, D., Rinaldo, A., Terzago, S., Ziemba, A., & Ziv, G. (2018). Integration of satellite remote sensing data in ecosystem modeling at local scales: Practices and trends. *Methods in Ecology and Evolution*, *9*(8), 1810–1821. https://doi.org/10.1111/2041-210X.13018

Pereira, H. ., Bruford, M. W., Brummitt, N., Butchart, S. H. M., Cardoso, A. C., Coops, N. C., & Dulloo, E. (2013a). Essential Biodiversity Variables. *Science*, *339*(6117), 277–278.

Pereira, H. M., Bruford, M. W., Brummitt, N., Butchart, S. H. M., Cardoso, A. C., Coops, N. C., & Dulloo, E. (2013b). Essential Biodiversity Variables. *Science*, *339*(6117), 277–278.

Pereira, H. M., Ferrier, S., Walters, M., Geller, G. N., Jongman, R. H. G., Scholes, R. J., Bruford, M. W., Brummitt, N., Butchart, S. H. M., Cardoso, A. C., Coops, N. C., Dulloo, E., Faith, D. P., Freyhof, J., Gregory, R. D., Heip, C., Höft, R., Hurtt, G., Jetz, W., … Wegmann, M. (2013). Essential Biodiversity Variables. *Science*, *339*(6117), 277–278. https://doi.org/10.1126/science.1229931

Persson, M., & Lindberg, E. (2018). *Tree Species Classification with Multi-Temporal Sentinel-2 Data*. 1–17. https://doi.org/10.3390/rs10111794

Pettorelli, N. (2016). Agree on biodiversity metrics to track from space. *Nature*, *523*, 403–405.

Phillips, S. B., Aneja, V. P., Kang, D., & Arya, S. P. (2006). Maximum entropy modeling of species geographic distributions. *Ecological Modelling*, *190*, 231–259. https://doi.org/10.1016/j.ecolmodel.2005.03.026

Potapov, P., Hansen, M. C., Pickens, A., Hernandez-serna, A., Tyukavina, A., Turubanova, S., Zalles, V., Li, X., & Khan, A. (2022). *The Global 2000-2020 Land Cover and Land Use Change Dataset Derived From the Landsat Archive : First Results*. *3*(April), 1–22. https://doi.org/10.3389/frsen.2022.856903

Proença, V., Martin, L. J., Pereira, H. M., Fernandez, M., McRae, L., Belnap, J., Böhm, M., Brummitt, N., García-Moreno, J., Gregory, R. D., Honrado, J. P., Jürgens, N., Opige, M., Schmeller, D. S., Tiago, P., & van Swaay, C. A. M. (2017). Global biodiversity monitoring: From data sources to Essential Biodiversity Variables. *Biological Conservation*, *213*, 256–263. https://doi.org/10.1016/j.biocon.2016.07.014

Rampheri, M., Dube, T., & Dhau, I. (2022). Use of remotely sensed data to estimate tree species diversity as an indicator of biodiversity in Blouberg Nature Reserve, South Africa. *Geocarto International*, *37*(2), 526–542. https://doi.org/10.1080/10106049.2020.1723717

Reid, W., Mooney, H., Cropper, A., Capistrano, D., Carpenter, S., & Chopra, K. (2005). *Millennium Ecosystem Assessment. Ecosystems and human well-being: synthesis*.

Reyes-palomeque, G., Dupuy, J. M., Portillo-quintero, C. A., Andrade, J. L., & Tun-dzul, F. J. (2021). *Mapping forest age and characterizing vegetation structure and species composition in tropical dry forests*. *120*. https://doi.org/10.1016/j.ecolind.2020.106955

Riitters, K., Wickham, J., O'Neill, R., Jones, B., & Smith, E. (2000). Global-scale patterns of forest fragmentation. *Ecology and Society*, *4*(2). https://doi.org/10.5751/es-00209-

040203
Rocchini, D., Delucchi, L., Bacaro, G., Cavallini, P., Feilhauer, H., Foody, G. M., He, K. S., Nagendra, H., Porta, C., Ricotta, C., Schmidtlein, S., Spano, L. D., Wegmann, M., & Neteler, M. (2013). Calculating landscape diversity with information-theory-based indices: A GRASS GIS solution. *Ecological Informatics*, *17*, 82–93. https://doi.org/10.1016/j.ecoinf.2012.04.002

Santoro, M., & Cartus, O. (2024). *ESA Biomass Climate Change Initiative (Biomass_cci): Global datasets of forest above-ground biomass for the years 2010, 2015, 2016, 2017, 2018, 2019, 2020 and 2021, v5.01*. NERC EDS Centre for Environmental Data Analysis. https://doi.org/doi:10.5285/bf535053562141c6bb7ad831f5998d77.

Schmeller, D. S., Julliard, R., Bellingham, P. J., Böhm, M., Brummitt, N., Chiarucci, A., Couvet, D., Elmendorf, S., Forsyth, D. M., Moreno, J. G., Gregory, R. D., Magnusson, W. E., Martin, L. J., McGeoch, M. A., Mihoub, J. B., Pereira, H. M., Proença, V., van Swaay, C. A. M., Yahara, T., & Belnap, J. (2015). Towards a global terrestrial species monitoring program. *Journal for Nature Conservation*, *25*, 51–57. https://doi.org/10.1016/j.jnc.2015.03.003

Seebach, L. M., Strobl, P., San Miguel-Ayanz, J., Gallego, J., & Bastrup-Birk, A. (2011). Comparative analysis of harmonized forest area estimates for European countries. *Forestry*, *84*(3), 285–299. https://doi.org/10.1093/forestry/cpr013

Shannon, C. . (1948). A Mathematical Theory of Communication By c. E. SHANNON IXTRODUCTION. *The Bell System Technical Journal*, *27*(3), 519–520. https://doi.org/10.1016/s0016-0032(23)90506-5

Skidmore, A. K., Coops, N. C., Neinavaz, E., Ali, A., Schaepman, M. E., Paganini, M., Kissling, W. D., Vihervaara, P., Darvishzadeh, R., Feilhauer, H., Fernandez, M., Fernández, N., Gorelick, N., Geijzendorffer, I., Heiden, U., Heurich, M., Hobern, D., Holzwarth, S., Muller-Karger, F. E., … Wingate, V. (2021). Priority list of biodiversity metrics to observe from space. *Nature Ecology and Evolution*, *5*(7), 896–906. https://doi.org/10.1038/s41559-021-01451-x

Steinmann, K., Mandallaz, D., Ginzler, C., & Lanz, A. (2013). Small area estimations of proportion of forest and timber volume combining Lidar data and stereo aerial images with terrestrial data. *Scandinavian Journal of Forest Research*, *28*(4), 373–385. https://doi.org/10.1080/02827581.2012.754936

Toivonen, J., Kangas, A., Maltamo, M., Kukkonen, M., & Packalen, P. (2023). Assessing biodiversity using forest structure indicators based on airborne laser scanning data. *Forest Ecology and Management*, *546*(August), 121376. https://doi.org/10.1016/j.foreco.2023.121376

Tsendbazar, N. E., de Bruin, S., Mora, B., Schouten, L., & Herold, M. (2016). Comparative assessment of thematic accuracy of GLC maps for specific applications using existing reference data. *International Journal of Applied Earth Observation and Geoinformation*, *44*, 124–135. https://doi.org/10.1016/j.jag.2015.08.009

Wang, R., & Gamon, J. A. (2019a). Remote sensing of terrestrial plant biodiversity. *Remote Sensing of Environment*, *231*(May), 111218. https://doi.org/10.1016/j.rse.2019.111218

Wang, R., & Gamon, J. A. (2019b). Remote sensing of terrestrial plant biodiversity. *Remote Sensing of Environment*, *231*(December 2018).

https://doi.org/10.1016/j.rse.2019.111218

Weisse, M., & Goldman, E. (2019). *The world lost a Belgium-sized area of primary rainforest in 2018.* Global Forest Watch, World UnitResources Institute.

Weisse, M., & Goldman, E. (2020). *how much forest was lost in 2019*. World Resources Institute. https://gfr.wri.org/global-tree-cover-loss-data-2019

WFO. (2021). *World Flora Online*. Published on the Internet. https://www.worldfloraonline.org/

Wulder, M. A., Hall, R. J., Coops, N. C., & Franklin, S. E. (2004). High Spatial Resolution Remotely Sensed Data for Ecosystem Characterization. *BioScience*, *54*(6), 511–521. https://doi.org/10.1641/0006-3568(2004)054[0511:HSRRSD]2.0.CO;2

Wulder, M. A., Roy, D. P., Radeloff, V. C., Loveland, T. R., Anderson, M. C., Johnson, D. M., Healey, S., Zhu, Z., Scambos, T. A., Pahlevan, N., Hansen, M., Gorelick, N., Crawford, C. J., Masek, J. G., Hermosilla, T., White, J. C., Belward, A. S., Schaaf, C., Woodcock, C. E., … Cook, B. D. (2022). Fifty years of Landsat science and impacts. *Remote Sensing of Environment*, *280*(July), 113195. https://doi.org/10.1016/j.rse.2022.113195

Zomer, R. J., Xu, J., & Trabucco, A. (2022). Version 3 of the Global Aridity Index and Potential Evapotranspiration Database. *Scientific Data*, *9*(1), 1–15. https://doi.org/10.1038/s41597-022-01493-1